UNIVERSITY OF CALIFORNIA

Santa Barbara

# Evaluating Mechanisms for Rare Earth Element (REE) Mineralization in Proterozoic Gneiss, Music Valley, California

A Thesis submitted in partial satisfaction of the

requirements for the degree Master of Science

in Earth Science

by

Samuel Tyson McKinney

Committee in charge:

Professor John M. Cottle, Chair

Professor Bradley R. Hacker

Professor Frank J. Spera

June 2014

The thesis of Samuel Tyson McKinney is approved.

_____
Bradley R. Hacker

_____
Frank J. Spera

_____
John M. Cottle, Committee Chair

June 2014

Evaluating Mechanisms for Rare Earth Element (REE) Mineralization in Proterozoic Gneiss, Music Valley, California



by

Samuel Tyson McKinney

# ACKNOWLEDGEMENTS

First and foremost I thank my advisor, John Cottle. Without his guidance, this project would not have been possible. I thank Graham Lederer, who not only was a huge help with all aspects of the research conducted, but was also largely responsible for securing funding for this project, which was provided by the USGS Mineral Resources External Research Program (MRERP). I thank Bradley Hacker and Frank Spera for their assistance and insight as members of my thesis committee. I thank Andrew Kylander-Clark and Gareth Seward for their assistance with LA-ICP-MS and EPMA data collection. I thank Joshua Garber for his invaluable assistance in the field. I thank Paige Granneman for her contributions to the project while completing her undergraduate senior thesis.

I also thank all of my family and friends that have provided me with love and support throughout my journey of obtaining a graduate degree. I thank my mother, Margaret, my father, Leroy, my step-mother, Robin, my brothers, Travis and Wade, my aunt and uncle, Kem and Dave, my cousins, Hallie Rae and Cameron, and my grandparents, Chester and Linda.

ABSTRACT

Evaluating Mechanisms for Rare Earth Element (REE) Mineralization in Proterozoic Gneiss, Music Valley, California

by

Samuel Tyson McKinney

Monazite [(LREE)$PO_4$] and xenotime [(HREE,Y)$PO_4$] occur in ore-grade concentrations within the Pinto Gneiss in the Music Valley region (MVR) of southern California. However, both the age and petrogenesis of this potentially economically significant rare earth element (REE) deposit remain uncertain. A combined petrologic and geochronologic study yields insight into the textural and temporal relationships between REE mineralization and the host rock. Ore-forming monazite and xenotime are typically restricted to biotite folia within the host Pinto Gneiss with highest modal abundances occurring within a few meters of contacts between the host gneiss and a diorite/amphibolite intrusive unit, the latter of which is cross-cut by pegmatite veins that appear to have been generated by partial melting of the Pinto Gneiss. Ore-forming monazite and xenotime preserve complex internal elemental zoning. Textures inferred to be the result of dissolution re-precipitation reactions overprint relict oscillatory zoning with xenotime and uranothorite [(U,Th)$SiO_4$] forming from the breakdown of monazite and monazite and uranothorite forming from the breakdown of xenotime, suggesting late-stage fluid mediated alteration of the ore minerals. Localized breakdown of monazite, anorthite and biotite to apatite and allanite provides further

evidence for post-mineralization metasomatism of the ore bodies. In-situ monazite and xenotime U-Pb geochronology constrains REE mineralization to ~1.71 Ga, consistent with zircon dates obtained from the Pinto Gneiss. Zircon from the diorite/amphibolite are ~1.4 Ga, inferred to represent the emplacement age of this unit, whereas zircon in the pegmatite veins yield ages of ~165 Ma. Zircon from a porphyritic hornblende diorite pluton exposed in the northern part of the MVR also yield an age of 165 Ma, suggesting a genetic link between emplacement of this intrusive suite and melting of the Pinto Gneiss to form the pegmatite veins. Based on the similarity in ages between monazite, xenotime and zircon in the Pinto Gneiss, along with relict 'igneous' zoning in the ore-bearing phosphate minerals, REE mineralization is interpreted to have occurred during crystallization of the igneous protolith of the Pinto Gneiss. Diorite/amphibolite emplacement at ~1.4 Ga and pegmatite genesis at ~165 Ma post-date the main phase of REE mineralization, but likely played a role in fluid-assisted alteration of the ore bodies and partial resetting of monazite and xenotime ages in the Pinto Gneiss.

TABLE OF CONTENTS

1. Introduction....1
2. Geologic Background....4
3. Geologic Units in the MVR....7
3.1 Pinto Gneiss....7
3.2 Dog Wash Gneiss....7
3.3 Diorite/Amphibolite....9
3.4 Leucogranite Gneiss....9
3.5 Porphyritic Hornblende Diorite....10
3.6 Mafic Dikes....11
4. Methods....11
4.1 Sampling and Mapping....11
4.2 Electron Microbeam Analyses....12
4.3 Geochronology....13
5. Results....14
5.1 Field Relationships....14
5.2 Petrography/Mineralogy of Ore Bodies....16
5.3 Alteration Textures of Ore Minerals....17
5.4 Geochronology....21
5.4.1 Pinto Gneiss Zircon....21
5.4.2 Pinto Gneiss Monazite....23
5.4.3 Pinto Gneiss Xenotime....23
5.4.4 Geochronology of REE Ore Mineral Alteration....24

5.4.5 Dog Wash Gneiss Zircon ..... 26
5.4.6 Diorite/amphibolite Zircon ..... 27
5.4.7 Leucogranite Gneiss Zircon ..... 28
5.4.8 Pegmatite Veins Zircon ..... 29
5.4.9 Porphyritic Hornblende Diorite ..... 29
5.4.10 Summary of Geochronologic Data ..... 30
6. Discussion ..... 30
6.1 Field Relationships ..... 30
6.2 Petrography/Mineralogy ..... 31
6.3 Alteration Textures of Ore Minerals ..... 32
6.4 Geochronology ..... 34
6.4.1 U-Pb Geochronology – Pinto Gneiss ..... 34
6.4.2 Geochronology of REE Ore Mineral Alteration ..... 36
6.4.3 U-Pb Geochronology – Other Units ..... 37
6.5 Petrogenetic Model for REE-Mineralization in the MVR ..... 41
7. Conclusions ..... 41
References ..... 43

LIST OF FIGURES

Figure 1: Global Primary REE Deposits....1
Figure 2: Geologic Map of Music Valley....3
Figure 3: Regional Tectonic Map of Southern California....5
Figure 4: Geologic Map of UThor Deposit....8
Figure 5: Field Photographs of Petrologic Relationships....10
Figure 6: Radiation Profiles....15
Figure 7: Thin Section Micrographs of Pinto Gneiss Ore Rock....16
Figure 8: EPMA Elemental X-ray Maps....18
Figure 9: EPMA Compositional Data (Dissolution Re-precipitation Texture)....19
Figure 10: BSE Images of Monazite Breakdown Reaction....20
Figure 11: EPMA Compositional Data (Monazite Breakdown Reaction)....21
Figure 12: U-Pb Geochronology of Pinto Gneiss....22
Figure 13: Alteration Geochronology of Monazite....24
Figure 14: Alteration Geochronology of Xenotime....26
Figure 15: U-Pb Geochronology of Other Units....27
Figure 16: Field Photographs of Pegmatite Genesis....31
Figure 17: Summary of REE-Mineral Petrogenesis in the MVR....40

LIST OF APPENDICES

Appendix A: EPMA Operating Conditions (Dissolution-Re-precipitation Texture)....48

Appendix B: EPMA Operating Conditions (Monazite Breakdown Reaction).....50

Appendix C: EPMA Compositional Data (Dissolution-Re-precipitation Texture).....54

Appendix D: EPMA Compositional Data (Monazite Breakdown Reaction).....56

Appendix E: U-Pb Geochronologic Data.....58

Appendix F: Alteration Geochronology U-Pb and REE Data.....110

# 1. Introduction

Rare earth elements (REE) have recently become ubiquitous in modern industrial applications, making them a significant economic commodity. The increased use of REE in modern technology such as high-definition display units, medical instrumentation and high-powered magnets has led to a newfound demand for understanding how anomalous concentrations of REE-bearing minerals form.

REE deposits are broadly divided into two categories: primary (i.e., REE associated with igneous and/or hydrothermal processes) and secondary (i.e., REE concentrated by sedimentary processes and weathering). The majority of globally known primary REE deposits occur in alkaline silicate intrusions (e.g., Bokan Mountain in Alaska), carbonatites (e.g. Mountain Pass in southeastern California and Bayan Obo in China) and hydrothermal veins and pegmatites (e.g., Ytterby in Sweden) (Orris & Grauch, 2002; Figure 1). As a result, the mechanisms by which such deposits form have been relatively well constrained in a number of settings (e.g., Alexander & Williams-Jones, 2013; Chakhmouradian & Zaitsev, 2012; Lai & Yang, 2013; Long et al., 2010; Philpotts et al., 1998; Smith et al., 2000; Taylor & Pollard, 1996; Williams-Jones et al., 2012; Yang et al., 2009; and others). However, despite their widespread occurrence, much less research has been conducted on REE deposits in metamorphic rocks (but see e.g., Aleinikoff et al., 2012; Andreoli et al., 1994; Gibson, 1998; Holtstam & Broman, 2002).

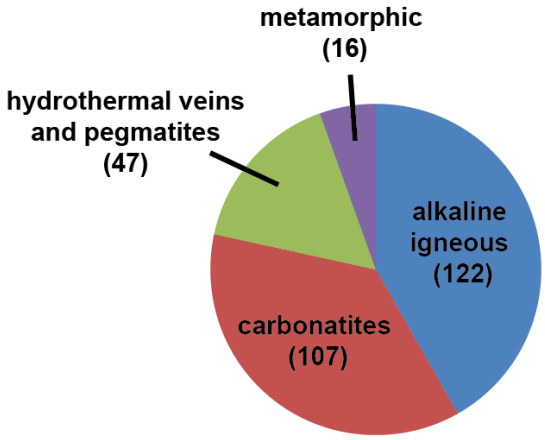


**Figure 1:** Pie chart showing the distribution of documented global primary REE deposits (Orris & Grauch, 2002).

Proposed mechanisms for such deposits are similar to those described for igneous rocks and include hydrothermal mobilization of REE during, or immediately following, metamorphism (Aleinikoff et al., 2012; Gibson, 1998) and/or protracted fractionation of a REE-enriched magma (Andreoli et al., 1994). An excellent exposure of a putative metamorphic-type REE deposit occurs within Proterozoic gneiss in the Music Valley region (MVR) of southern California (Figure 2). REE in this locality are contained primarily in monazite [(LREE)$PO_4$] and xenotime [(HREE)$PO_4$]. As such, this deposit has the potential to reveal further insight into the mechanisms by which REE mineralization occurs in metamorphic rocks.

REE-bearing ore bodies in the MVR were originally identified during airborne radioactive prospecting surveys in the Live Oak Tank-White Tank areas in Riverside County conducted by the U.S. Geological Survey in conjunction with the U.S. Atomic Energy Commission during 1949 and 1952 (Moxham, 1952). The only subsequent published work on the deposit described the occurrence of monazite and xenotime ores in biotite-rich pods and folia within the Pinto Gneiss and concluded that the REE phosphates were likely detrital in origin, being concentrated as a heavy mineral sand in the sedimentary protolith to the Pinto Gneiss (Evans, 1964). However, migmatitic textures observed in the Pinto Gneiss in the MVR suggest some degree of partial melting, providing a potential alternative mechanism by which monazite and xenotime may have been concentrated into an ore-grade deposit. The excellent exposure in this region and accessibility of this deposit offer an opportunity to differentiate between these competing hypotheses and understand the mechanisms by which REE mineralization occurred in these rocks. Furthermore, characterization of REE mineralization in the MVR places constraints on the chemical behavior of REE in a high-grade metamorphic/anatectic setting.

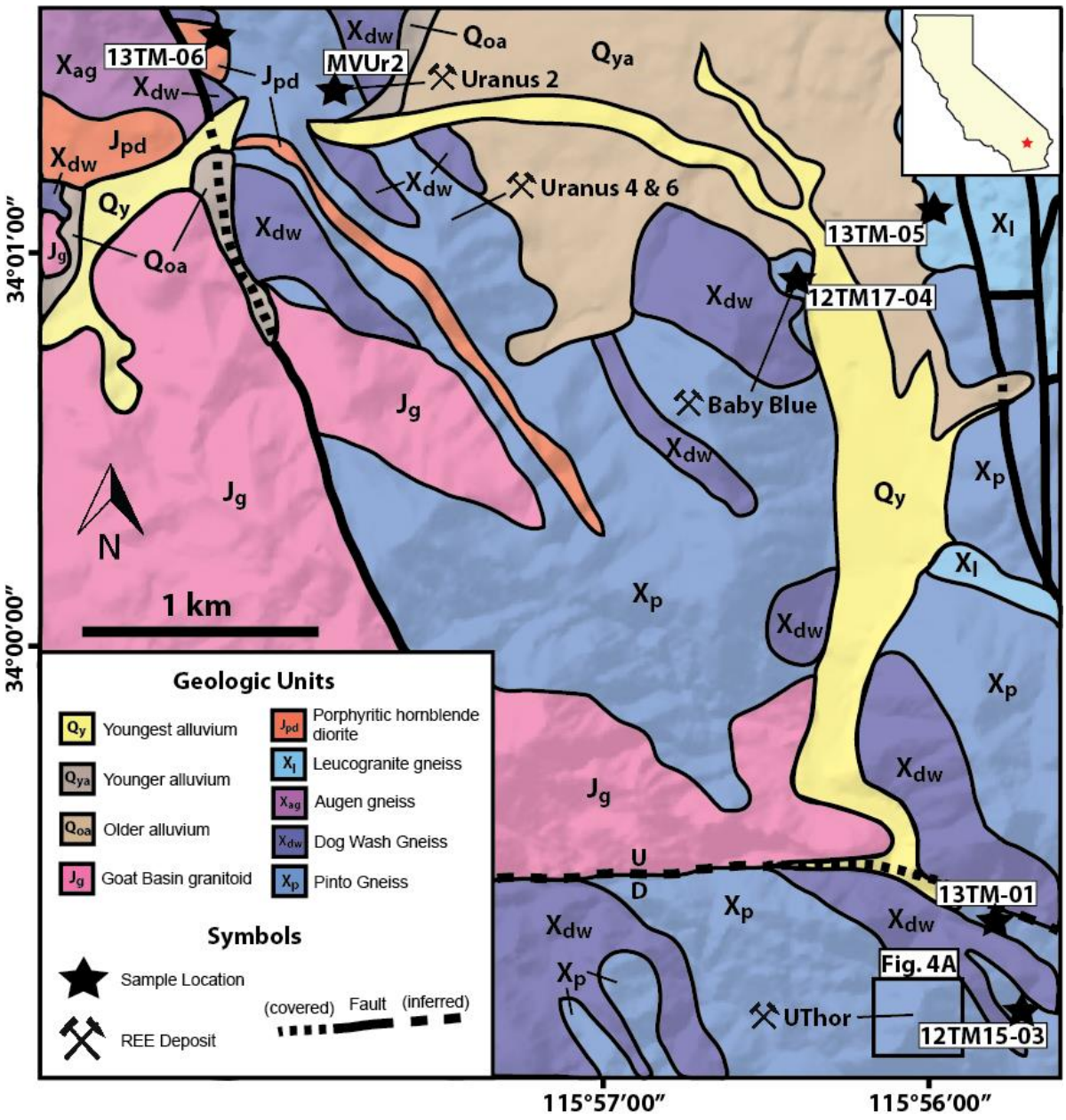


**Figure 2:** Regional geologic map of the Music Valley region (MVR) of southern California (modified from Howard et al., 2013; Dibblee, 2008). REE deposits and sample locations are labeled and location of the UThor deposit (Figure 4A) is marked.

This study combines U-Pb geochronology of zircon, monazite, and xenotime with electron microbeam techniques to characterize the nature of REE mineralization in the MVR and develop a petrogenetic model. U-Pb geochronology of zircon with igneous textures suggests that the ore-body Pinto Gneiss is an orthogneiss with a crystallization age of ~1.71

Ga. Ore-forming monazite from the same unit produce ages within uncertainty of the zircon dates, suggesting primary ore formation during igneous crystallization of the Pinto Gneiss protolith. U-Pb ratios of ore-forming xenotime have been intensely altered by Pb addition and/or Pb loss, but also suggest primary crystallization in an igneous setting at ~1.71 Ga. Electron microbeam imaging of ore monazite and xenotime reveal complex dissolution re-precipitation textures that overprint relict oscillatory zoning. In addition, monazite is observed to have broken down to form apatite and allanite, suggesting metasomatic alteration of the ore body. U-Pb geochronology of other igneous and meta-igneous units in the MVR provides temporal constraints on additional geologic processes that affected the region, including intrusion of a diorite/amphibolite unit at ~1.4 Ga, emplacement of a leucogranite gneiss unit at ~224 Ma and intrusion of a porphyritic hornblende diorite and generation of pegmatite veins at 165 Ma.

## 2. Geologic Background

The MVR is located within the Mojave province of southeastern California, which marks the southwestern edge of the North American craton, Laurentia (Figure 3). This region has experienced a complex tectonic and geologic history of several discrete magmatic and metamorphic episodes during the Proterozoic (Barth et al., 2009; Barth & Wooden, 2010; Bender, 1994; Coleman et al., 2002; Strickland et al., 2013; Wooden & Miller, 1990), multiple intrusive events during the Mesozoic (Barth et al, 1997; Haxel and Miller, 2007 and references therein) and extensive rifting and volcanism during the Tertiary (Miller and Rytuba, 2007 and references therein).

The geologic history of the Mojave tectonic province during the Proterozoic is dominated by plutonism and metamorphism. The major tectonic event that has been

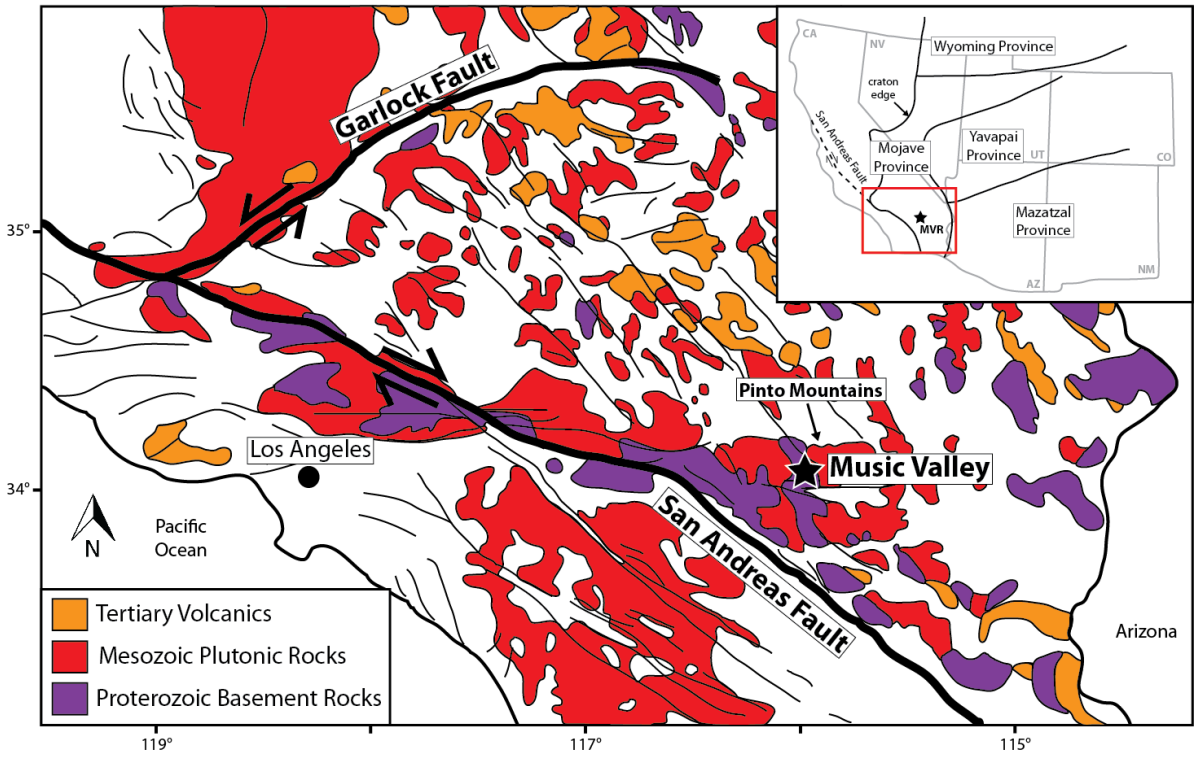


**Figure 3:** Regional tectonic map of southern California (modified from Jennings et al., 2010). Inset shows approximate boundaries of Laurentian provinces (after Coleman et al., 2002) and location of the Music Valley study area is marked.

described in the region is the Ivanpah orogeny, a 1.71-1.70 Ga granulite-facies metamorphic event associated with emplacement of pre-, syn- and post-tectonic granitoids (Wooden & Miller, 1990). Proterozoic basement rocks in the western Mojave Province include orthogneisses that range in age from 1.78 Ga to 1.68 Ga with a metamorphic signature at 1.74 Ga (Barth et al., 2000). Paragneisses in the region have detrital zircon populations of predominantly 2.15-1.80 Ga (with a minor component of 2.8-2.4 Ga). Overgrowths on detrital zircon indicate multiple metamorphic events at ~1.76, 1.74, 1.70 and 1.67 Ga (Strickland et al., 2013). There is also evidence for widespread anorogenic magmatism at 1.49-1.40 Ga resulting in the emplacement of potassium-rich granites along with gabbros, anorthosites and diabase dike swarms (Anderson & Bender, 1989).

In the Mesozoic, the Mojave Province experienced extensive plutonism, beginning with emplacement of a belt of Triassic plutons during the onset of North American Cordilleran magmatism. The plutonic belt extends from the western Mojave Desert through the Transverse Ranges to the Colorado River trough and consists primarily of quartz monzonites and monzonites. Exposed plutons define a general southward-younging trend from ~241-231 Ma to ~218-213 Ma (Barth et al., 1997). Additional plutonism occurred during the Jurassic, predominantly from ~170-160 Ma, and includes mafic, intermediate to silicic, and mixed/heterogeneous composition rocks (Haxel & Miller, 2007). Mesozoic plutonism was followed by a hiatus that lasted until the early to mid-Miocene, when intense volcanism and deformation occurred throughout the region (Miller & Rytuba, 2007).

Whereas the geologic history outlined above offers an overview of the complex tectonic and magmatic events that have affected the Mojave Province as a whole, relatively little research has been conducted in the MVR specifically. Exposed bedrock in the MVR consists primarily of Proterozoic quartzofeldspathic gneiss intruded by Mesozoic plutons. Based on initial geologic mapping of the MVR, metamorphic rocks were defined as the Pinto Gneiss and intrusive bodies were termed the Gold Park Diorite-Gabbro, Palms Granite, and White Tank Quartz Monzonite (Miller, 1938). The Pinto Gneiss consists of interlayered paragneiss and orthogneiss and has been interpreted as sedimentary and/or volcanic in origin (Evans, 1964; Powell, 1981). In the MVR and surrounding areas, the Pinto Gneiss has been described as both migmatitic (Matti et al., 1994; Powell, 1981) and non-migmatitic (Evans, 1964). Geochronology of the Pinto Gneiss is scarce, but detrital zircon from quartzites in the Pinto Mountains (Figure 3) yielded no concordant U-Pb dates younger than 1630 Ma, providing a maximum depositional age for the unit in this area, whereas

discordant zircons define a lower intercept of ~200 Ma, consistent with thermal disturbance during Mesozoic plutonism (Barth et al., 2009).

## 3. Geologic Units in the MVR

### 3.1 Pinto Gneiss

The Pinto Gneiss within the MVR is a widespread unit that consists primarily of quartzofeldspathic biotite gneiss (Figures 2 and 4). Quartz and feldspar occur in roughly equal proportions and biotite comprises ~30% of the rock, defining a compositional banding. Polysynthetic and Carlsbad twins are abundant in feldspar, and quartz typically displays undulatory extinction and is locally recrystallized with sutured grain boundaries. Monazite and xenotime occur in anomalous concentrations locally, and other accessory phases include zircon, apatite, allanite, rutile, ilmenite, titanite, iron oxides (primarily magnetite) and chlorite (as an alteration product of biotite). Although not observed in the MVR, sections of the Pinto Gneiss also contain garnet, cummingtonite and/or sillimanite (Howard et al., 2013). While no pressure and temperature constraints exist for this unit, metamorphism in the region is thought to have reached upper amphibolite to lower granulite facies (Barth et al., 2009; Wooden & Miller, 1990). The origin (sedimentary versus igneous) and mode of deposition and/or emplacement of this unit is widely debated, with possible explanations including sedimentary deposition, intercalated volcanic-sedimentary rocks and intrusive injection into a sedimentary protolith (Powell, 1981).

### 3.2 Dog Wash Gneiss

This unit is exposed throughout the MVR (Figures 2 and 4). It is distinguished from the Pinto Gneiss by a paler weathering color, no compositional banding and a more felsic

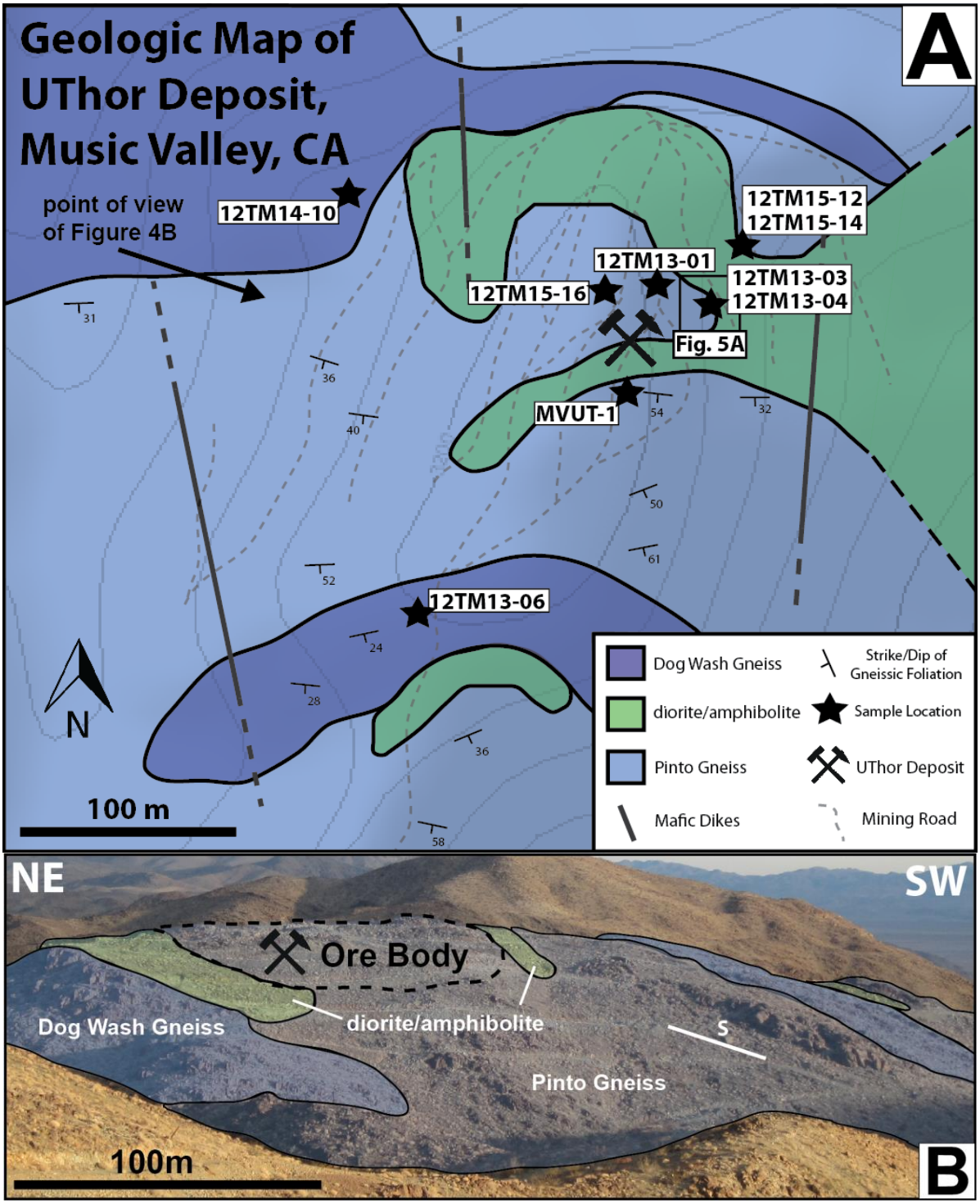


**Figure 4: (A)** Geologic map of UThor deposit with DEM overlay; **(B)** profile view of UThor deposit looking southeast from mining road. Pinto Gneiss (light blue), Dog Wash Gneiss (blue) and diorite/amphibolite (green) are marked as well as an approximate outline of the ore body.

mineralogy. The unit consists of medium-grained leucomonzogranite to leucosyenogranite gneiss that is locally trondhjemitic (Howard et al., 2013). Accessory minerals include allanite, clotted chlorite, muscovite, oxides and biotite. Detailed geologic mapping suggests that this unit intrudes the Pinto Gneiss and the diorite/amphibolite described below (Howard et al., 2013).

### 3.3 Diorite/Amphibolite

This unit encompasses compositionally heterogeneous diorite, foliated metadiorite, metagabbro and amphibolite and is spatially associated with the Pinto Gneiss (Howard et al., 2013). In the MVR, the diorite/amphibolite unit consists primarily of intergrown medium-grained black hornblende and plagioclase feldspar in roughly equal proportions, giving the rock a "salt and pepper" appearance on fresh surfaces. A few percent of quartz and biotite are present. The unit is generally massive, but locally is cut by pegmatite veins and/or has a weak foliation. Where present, the foliation is coplanar to that of the Pinto Gneiss. Within the MVR, this unit occurs as isolated bodies enclosed by the Pinto Gneiss that range in size from a few meters to 10's of meters (Figure 4). Locally, the contact between the diorite/amphibolite and the Pinto Gneiss is sharp, whereas in other localities the contact is characterized by either (or both) a biotite-rich layer and a pegmatitic leucosome (Figure 5A).

### 3.4 Leucogranite Gneiss

This unit is exposed on the eastern side of the MVR (Figure 2) and consists of leucomonzogranite and leucogranodiorite gneiss containing hornblende pseudomorphs, biotite, sphene, epidote and chlorite (Howard et al., 2013). Foliation is subtle to wavy and the unit has a possible gradational relationship to the Twenty-nine Palms Quartz Monzonite to the north, which has been dated via zircon U-Pb at 242 ± 30 Ma (Barth et al., 1997).

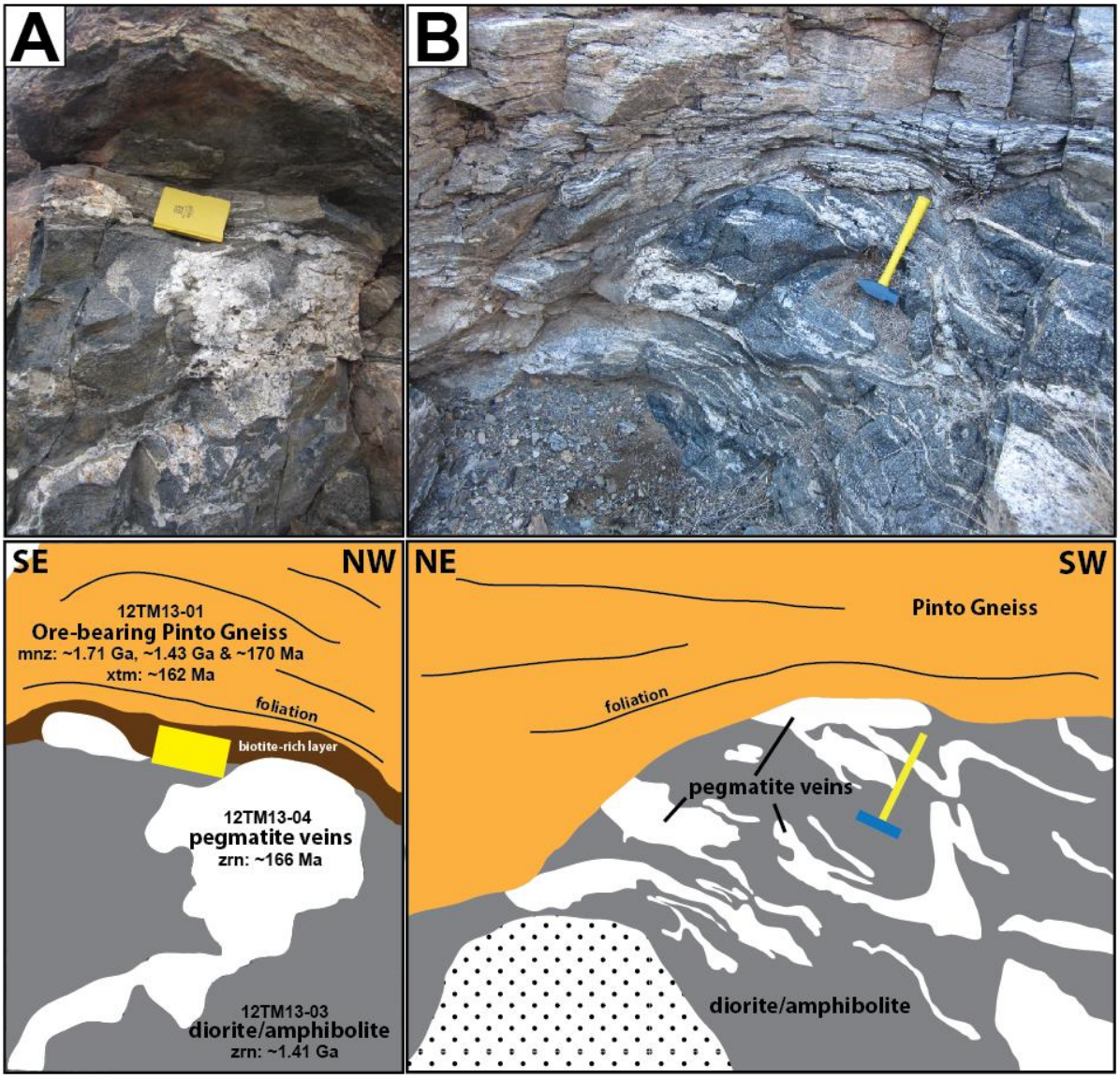


**Figure 5:** Field photographs showing relationship between the Pinto Gneiss, diorite/amphibolite and pegmatite veins at **(A)** the UThor deposit and **(B)** a non-ore rock outcrop in a wash ~200 m north of the UThor deposit. Units are outlined in bottom set of photographs and foliation of Pinto Gneiss is marked.

### 3.5 Porphyritic Hornblende Diorite

This unit is exposed in the northern section of the MVR (Figure 2) and consists of coarse-grained hornblende and medium- to fine-grained plagioclase. The unit intrudes the Pinto Gneiss and the Dog Wash Gneiss and was originally paired with the diorite/amphibolite and referred to collectively as the Gold Park Gabbro-Diorite (Evans,

1964). More recent geologic mapping that has differentiated the two units (Howard et al., 2013) is borne out by field observations and geochronology in this study.

### 3.6 Mafic Dikes

North-south striking, steeply dipping andesitic/basaltic dikes are present throughout the MVR and cross-cut all units described above (Figure 4A). The dikes are typically dm wide, have a very fine grain size and are dark grey to black. One such dike previously studied consists of fractured phenocrysts of olivine set in an intergranular matrix composed of hornblende, labradorite, and augite (Evans, 1964). Minor chlorite and epidote exist as alteration products of hornblende and olivine.

## 4. Methods

### 4.1 Sampling and Mapping

For clarity, the naming scheme developed by Evans (1964) for the various REE ore deposits (i.e. UThor, Baby Blue, etc., see Figure 2) is used throughout this paper. Ore body samples of Pinto Gneiss were targeted for collection using a Polimaster® PM1703M radiation detector to locate radiation anomalies resulting from elevated concentrations of U and Th. Diorite/amphibolite and pegmatite vein samples were collected near high-radiation Pinto Gneiss samples. Several other rock units, including the Dog Wash Gneiss, leucogranite gneiss and porphyritic hornblende diorite were sampled to develop a comprehensive understanding of the regional geology.

Heavy mineral separates were created using standard separation procedures including crushing, sieving, heavy liquid separation using methyl iodide ($\rho$~3.3 g/cm$^3$) and magnetic separation using a Frantz isodynamic magnetic barrier separator. Monazite, xenotime and

zircon were hand-picked from the final mineral separate, mounted in epoxy and polished for geochemical and geochronologic analyses. To establish petrographic and textural relationships, polished thin sections were also produced for Pinto Gneiss ore samples for additional in-situ analyses.

### 4.2 Electron Microbeam Analyses

To understand internal zoning and textures, electron microbeam techniques were employed to image accessory minerals using the electron imaging facility at the University of California, Santa Barbara (UCSB). Monazite and xenotime were first imaged using a back-scattered electron (BSE) detector mounted on an FEI Q400 FEG Scanning Electron Microscope (SEM) operated at an accelerating voltage of 20 keV, a beam current of 2-3 nA and a working distance of 10-15 mm. Zircon were imaged using a cathodoluminescence (CL) detector on the same instrument operated at an accelerating voltage of 10 keV, a beam current of 2-3 nA and a working distance of 20 mm. Based on BSE imaging of monazite and xenotime, representative crystals were selected for electron probe microanalyzer (EPMA) elemental x-ray mapping using a Cameca SX-100 Electron Microprobe. Monazite was mapped for the following elements (with the corresponding large-crystal wavelength spectrometer noted in parenthesis): Y Lα (LPET), Ce Lα (LLiF), Nd Lα (LPET), Th Mα (LPET) and U Mβ (LPET). Xenotime was mapped for Ce Lα (LPET), Nd Lα (LPET), Dy Lα (LLiF), Th Mα (LPET) and U Mβ (LPET). Analytical conditions included a beam current of 200 nA, accelerating voltage of 20 keV, dwell time of 40-100 msec and a spot size of 1-3 μm (with the latter two settings dependent on individual crystal size).

EPMA compositional analyses were performed on selected monazite and xenotime grains. Operating conditions for spot analyses were an accelerating voltage of 15 keV, beam

current of 55 nA and a focused beam (details on the elements analyzed, crystals used, standards and correction methodology are provided in Appendix A). In addition, compositional analyses were performed on monazite, apatite and allanite involved in a monazite breakdown reaction (discussed in the Results section). Details on the operating conditions, elements analyzed, crystals used, standards and correction methodology are provided in Appendix B.

### 4.3 Geochronology

U-Th/Pb and trace element data were collected simultaneously using the laser-ablation split-stream (LASS) inductively coupled plasma mass spectrometry (ICP-MS) facility located at UCSB. Methods follow those outlined in Cottle et al. (2012) and Kylander-Clark et al. (2013) and are briefly summarized here. Instrumentation consists of a Photon Machines 4 ns pulse duration 193 nm wavelength ArF excimer laser attached to a Nu Plasma HR multi-collector (MC) ICP-MS for measuring U, Th and Pb isotope ratios and an Agilent 7700S quadrupole ICP-MS for measuring major and trace element concentrations. Analytical conditions of the laser varied depending on the U-Th/Pb content of minerals for a given sample and ranged from a 5-31 μm spot size, laser energy of 3-4 mJ at 56-75% power, 3-4 Hz firing frequency, and 75-100 shots per analysis (see Appendix E for further details).

U-Th/Pb and trace element data reduction, including corrections for baseline, instrumental drift, mass bias, down-hole fractionation and uncorrected age calculations were carried out using Igor Pro and the plugin Iolite v. 2.1.3 (see Paton et al., 2010 for details on data reduction methodology). Primary reference zircon “91500” (1065 Ma Pb/U ID-TIMS age, Wiedenbeck et al., 1995) and primary reference monazite “44069” (424 Ma Pb/U ID-TIMS age, Aleinikoff et al., 2006) were used to monitor and correct for instrumental drift,

mass bias and down-hole inter-element fractionation for zircon and monazite/xenotime unknowns, respectively. A secondary reference zircon, "GJ1" (601.7 ± 1.3 Ma, D. Condon unpublished ID-TIMS age) and a secondary reference monazite, "Bananeira" (508.9 Ma Pb/U LA-ICP-MS age, Kylander-Clark et al., 2013) were analyzed concurrently and treated as unknowns to assess accuracy and precision within each analytical session. Bananeira served as the primary trace element reference standard for monazite and xenotime. During the analytical period, repeat analyses of GJ1 gave a weighted mean $^{206}Pb/^{238}U$ age of 601.3 ± 0.5 Ma (MSWD = 1.04) and repeat analyses of Bananeira gave a weighted mean $^{206}Pb/^{238}U$ age of 509.3 ± 1.5 Ma (MSWD = 1.11). All uncertainties are quoted at 2σ and include contributions from the reproducibility of the reference materials for $^{207}Pb/^{206}Pb$, $^{206}Pb/^{238}U$ and $^{207}Pb/^{235}U$. U-Pb data of zircon, monazite and xenotime were plotted using the Isoplot Excel plugin, version 3.75 (Ludwig, 2012).

# 5. Results

## 5.1 Field Relationships

Ore-grade concentrations of monazite and xenotime in the MVR occur solely within the Pinto Gneiss and are spatially associated with the diorite/amphibolite intrusive unit, which is commonly cross-cut by felsic pegmatite veins (Figure 5). Radiation levels in the Pinto Gneiss increase towards the contact with the diorite/amphibolite, with the highest radioactivity typically recorded just above the contact (Figure 6). The largest ore body of Pinto Gneiss (the UThor deposit) is ~100 m in diameter; the depth of the ore body is unknown, but is likely not more than a few 10's of meters deep based on down-slope mapping of the ore body (Figure 4). The spatial extent of other ore bodies (e.g., Baby Blue,

Uranus 2-6, etc., labeled in Figure 2) within the Pinto Gneiss have not been well constrained, but based on geologic mapping carried out during this study, are believed to be much smaller (~10's of meters in diameter; see also Evans, 1964).

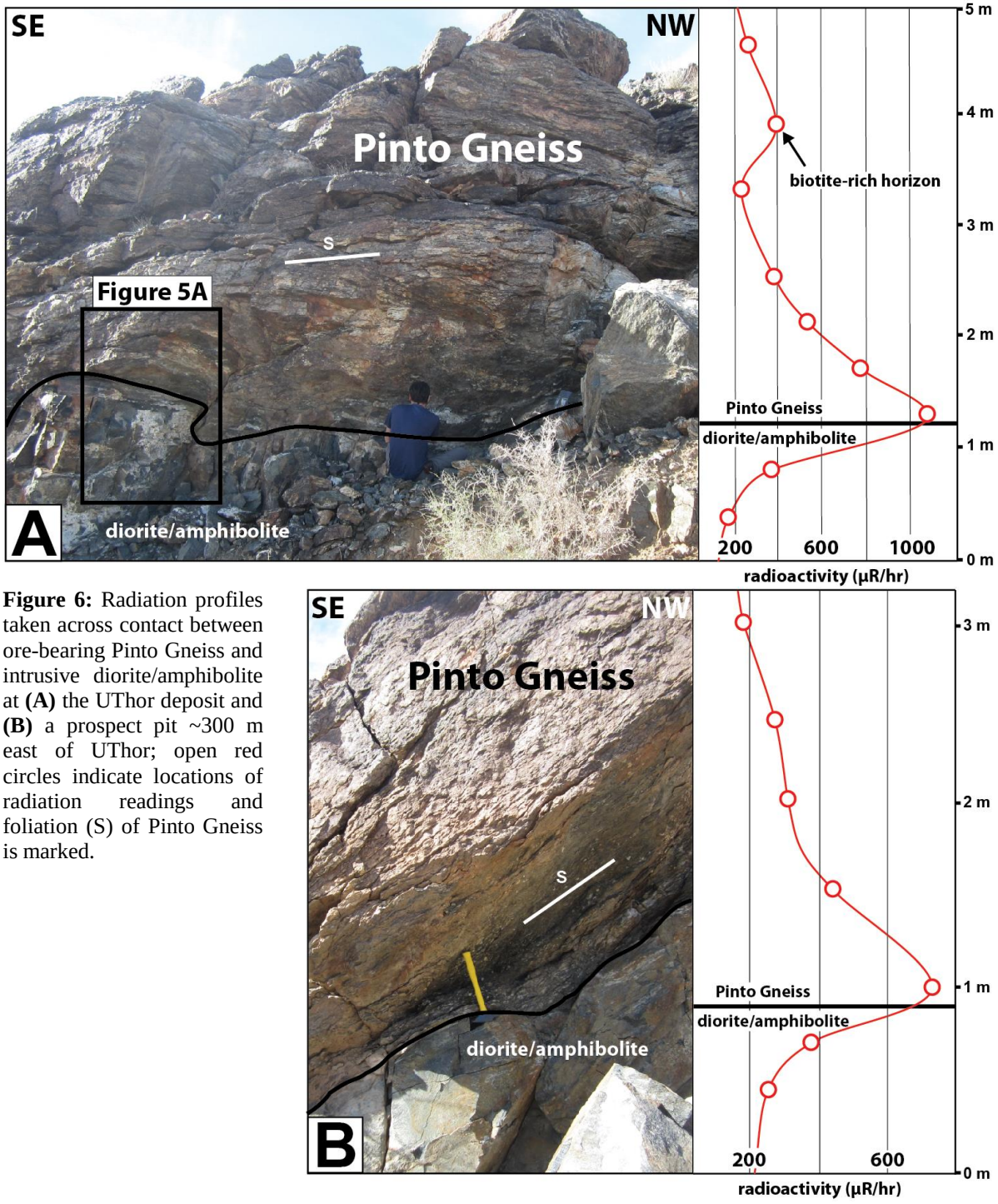


**Figure 6:** Radiation profiles taken across contact between ore-bearing Pinto Gneiss and intrusive diorite/amphibolite at **(A)** the UThor deposit and **(B)** a prospect pit ~300 m east of UThor; open red circles indicate locations of radiation readings and foliation (S) of Pinto Gneiss is marked.

## 5.2 Petrography/Mineralogy of Ore Bodies

Monazite and xenotime are the two dominant REE-bearing minerals in the MVR, although allanite [$(LREE,Ca)_2(Al,Fe^{3+})_3(SiO_4)_3(OH)$] is also present. Within the ore bodies, monazite and xenotime are typically restricted to biotite folia; they are less abundant within

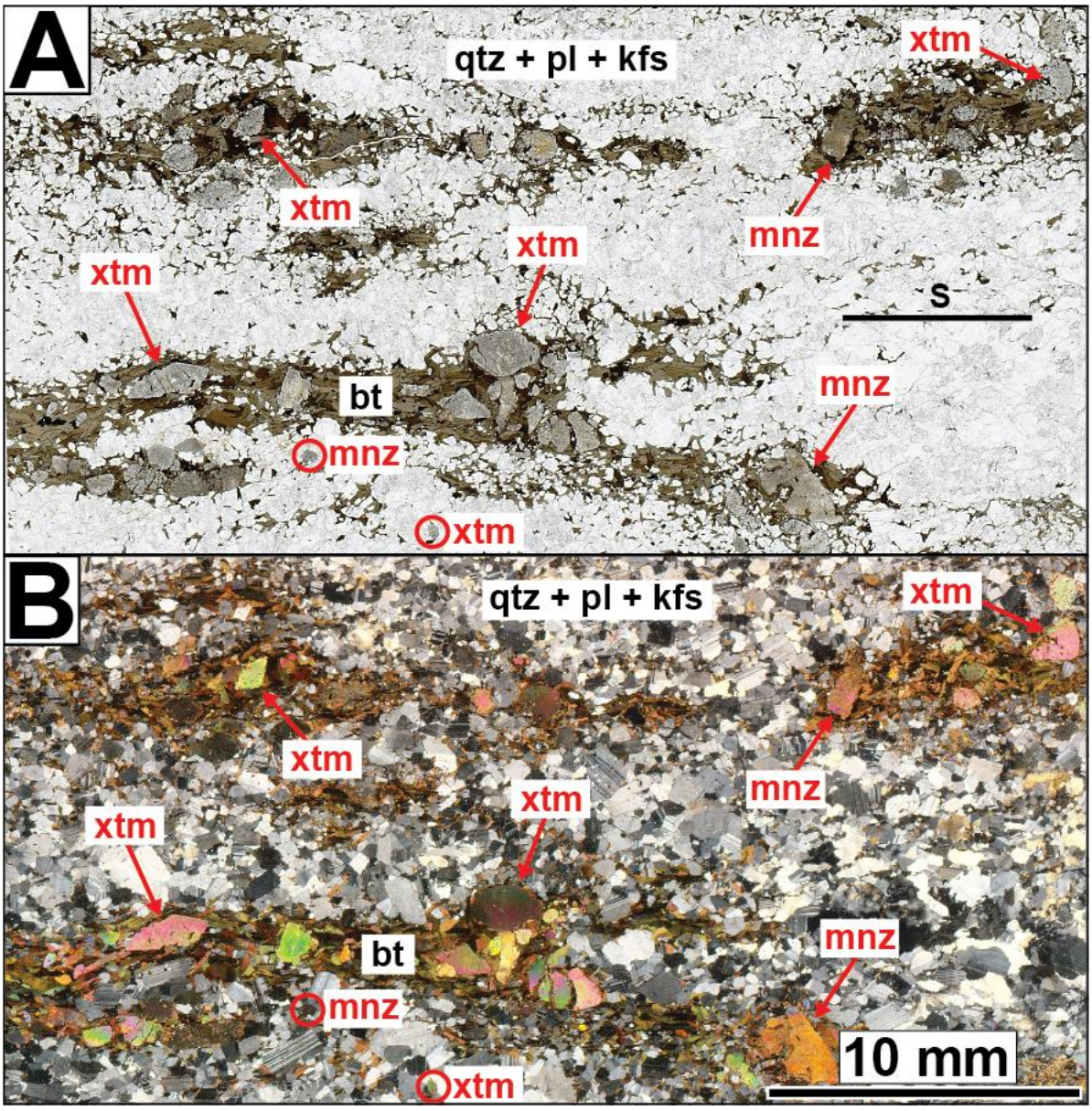


**Figure 7:** Thin section micrographs of Pinto Gneiss ore sample 12TM13-01 under **(A)** plane-polarized light and **(B)** cross-polarized light. Red arrows indicate monazite (mnz) and xenotime (xtm) grains present within biotite folia whereas red circles indicate mnz and xtm present in quartzofeldspathic (qtz + pl + kfs) layers (mineral abbreviations after Whitney & Evans, 2010); foliation (S) of Pinto Gneiss is marked.

quartzofeldspathic layers (Figure 7). Allanite occurs in several different forms, including brown, euhedral, tabular crystals within quartzofeldspathic layers (a few mm's long) and as a product of a monazite breakdown reaction (discussed below). Monazite in ore-grade Pinto Gneiss is yellow-orange and anhedral to subhedral. Xenotime is generally dark green-brown, although some are yellow-orange and virtually indistinguishable from monazite in hand sample. They are easily distinguished in thin section by higher birefringence (Figure 7). Xenotime grains are commonly subhedral to euhedral, prismatic and similar in appearance to zircon from the same rock. Ore-forming monazite and xenotime range in size from 10's of μm to several mm's, but are typically 100's of μm.

### 5.3 Alteration Textures of Ore Minerals

Figure 8 presents representative EPMA elemental Y, Th, and U x-ray maps of monazite and Nd, Th and U x-ray maps of xenotime. Two distinct textural domains can be identified in the REE phases. The first is an altered domain in which xenotime and uranothorite inclusions occur within monazite and vice versa (i.e., monazite and uranothorite inclusions within xenotime). In the monazite maps, Y serves as a proxy for xenotime inclusions, and in the xenotime maps, Nd serves as a proxy for monazite inclusions. Th and U serve as proxies for uranothorite inclusions in both phases. The inclusions are round, irregular in shape and range in size from a few microns to 10's of microns. The contact between the inclusions and the host mineral is sharp. The second textural domain is unaltered and displays relict oscillatory zoning (most easily identified in Th maps). The unaltered domain is typically in the center of the grain, although it also occurs on the periphery of some grains.

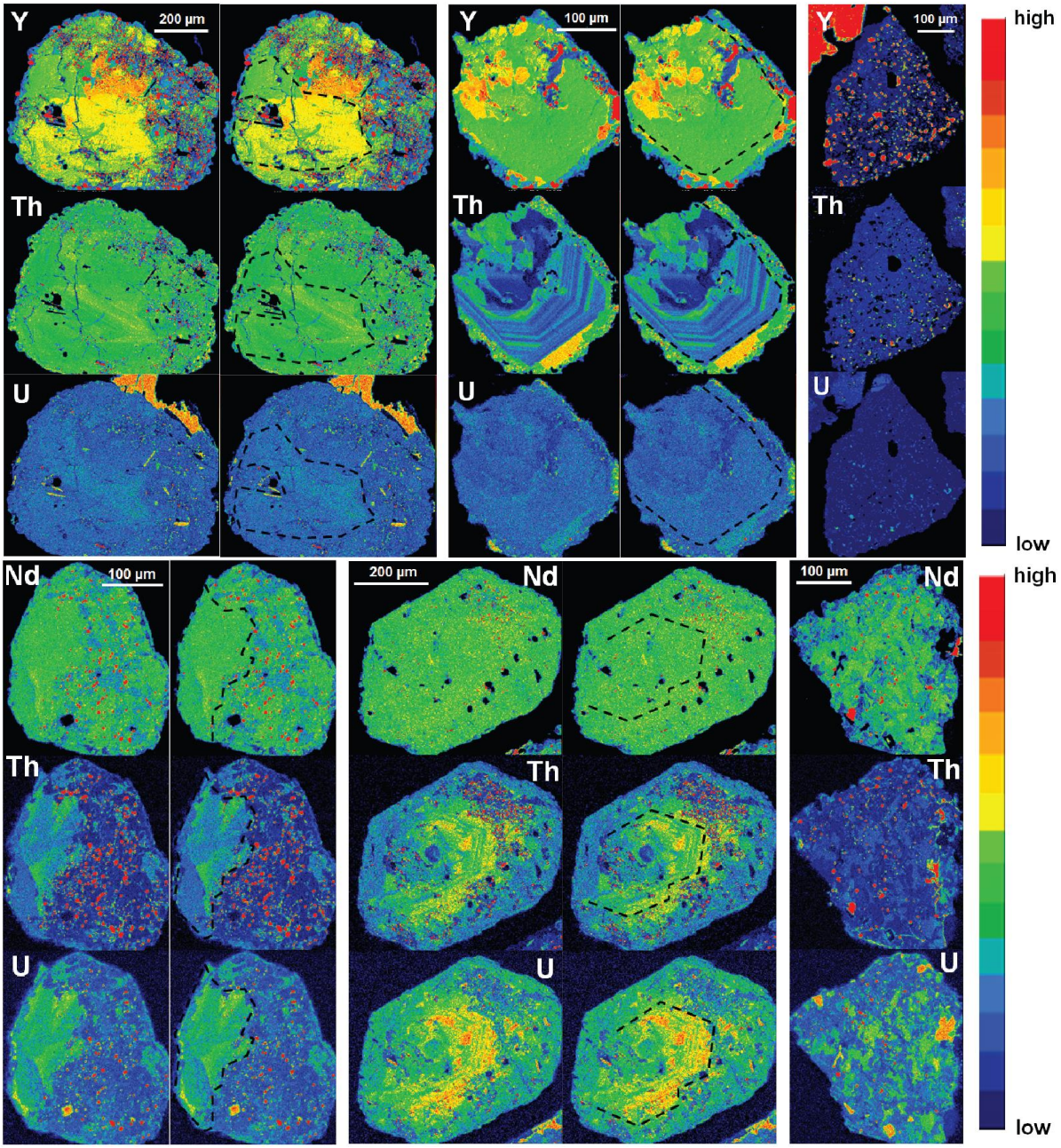


**Figure 8:** Electron probe microanalyzer (EPMA) elemental x-ray maps of 3 monazite grains (top) and 3 xenotime grains (bottom); dashed black lines outline relict zoning where evident.

Figure 9 presents quantitative EPMA compositional data for several ore-forming monazite and xenotime grains. Analyses were conducted on unaltered monazite and xenotime domains as well as monazite and xenotime within the altered domain of a monazite grain (i.e., xenotime inclusions and the altered monazite). The xenotime inclusions

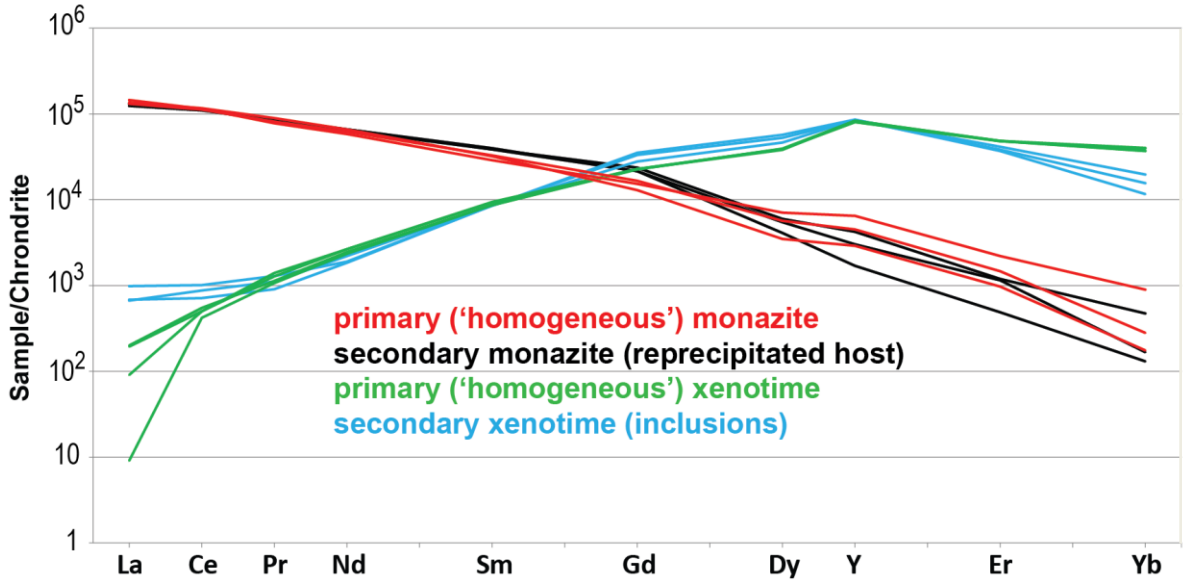


**Figure 9:** Trace element data (normalized to chondrite values from McDonough & Sun, 1995) for primary monazite (red), secondary (i.e. the re-precipitated host) monazite (black), primary xenotime (green) and secondary xenotime 'inclusions' (blue) within monazite (texture shown in top row of Figure 8) from Pinto Gneiss ore samples.

contain higher concentrations of La and Ce and lower concentrations of Er and Yb compared to unaltered xenotime. REE patterns of unaltered versus altered monazite are nearly identical, although the altered monazite contains more Sm and Gd.

A monazite breakdown reaction occurs to varying degrees in ore-body Pinto Gneiss throughout the MVR. Figure 10 presents BSE images of three monazite grains that, to varying degrees, preserve the breakdown reaction. All three grains are from the same hand sample, 12TM15-06. Figure 10A presents a nearly unaltered monazite, whereas Figure 10B presents a monazite grain that has almost completely broken down to form apatite and allanite. Figures 10C and 10D present a monazite grain at an intermediate stage in the breakdown reaction, with product grains of apatite and allanite surrounding the original monazite grain.

Figure 11 presents EPMA compositional data for monazite, apatite and allanite measured in three monazite breakdown occurrences (compositional data for unaltered

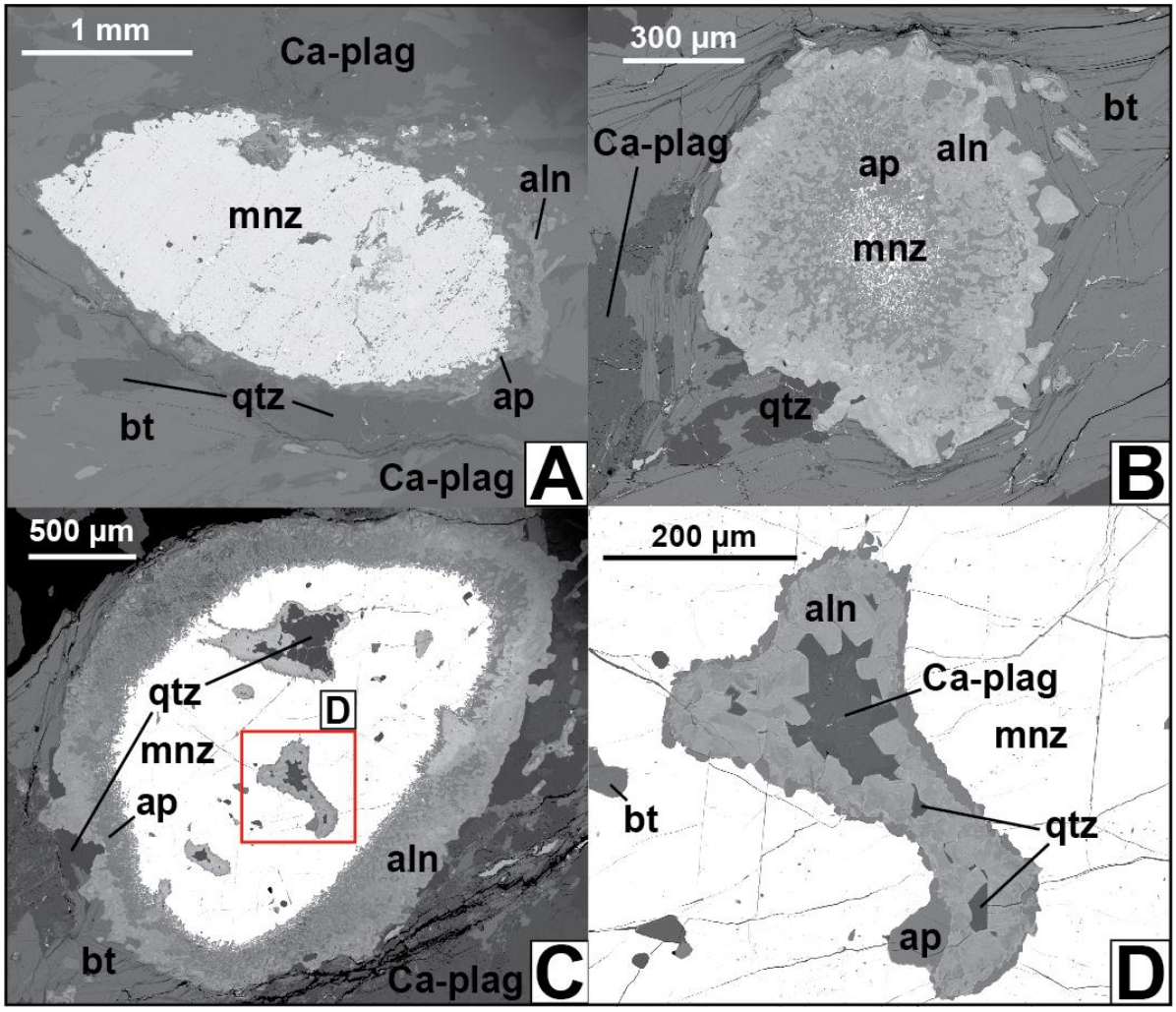


**Figure 10:** Back-scattered electron (BSE) images of monazite breakdown reaction in sample 12TM15-06 at various stages: **(A)** nearly unaltered grain, **(B)** completely altered grain, **(C)** moderately altered grain with apatite and allanite rims and **(D)** a zoomed-in look at the reaction boundary. Abbreviations as follows (after Whitney & Evans, 2010): biotite (bt), monazite (mnz), apatite (ap), allanite (aln), calcic plagioclase (Ca-plag) and quartz (qtz).

xenotime from Figure 9 is also provided for reference). The REE patterns of allanite closely mimic those of monazite with a general decrease from La to Y, although in lower concentrations. The REE concentrations of apatite are low, more variable and produce a slightly positive REE pattern.

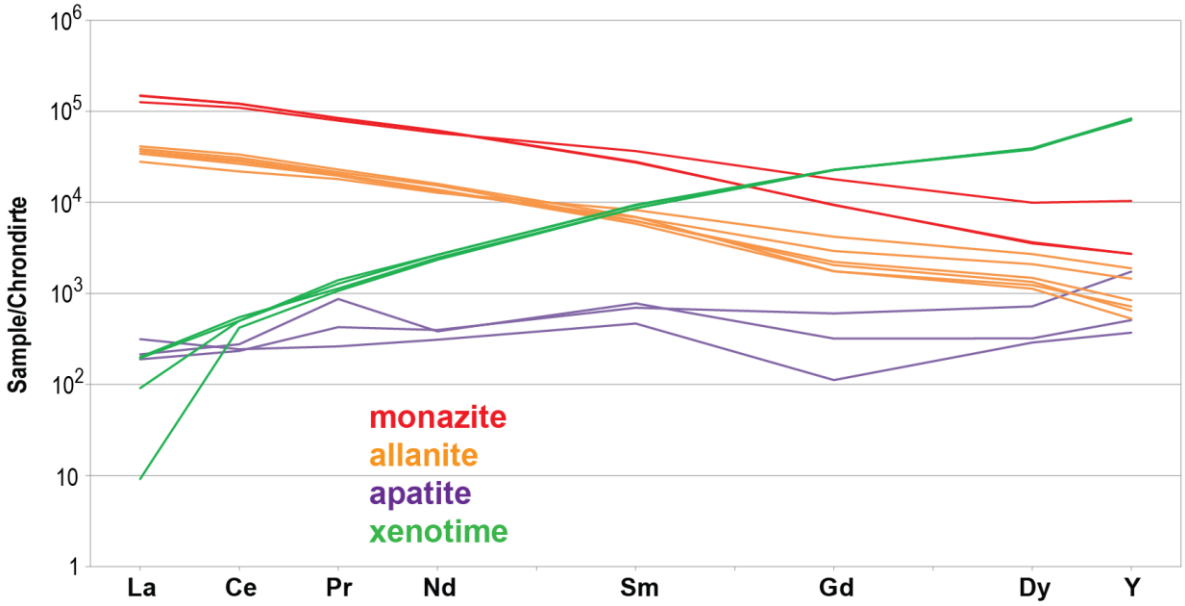


**Figure 11:** Trace element data (normalized to chondrite values from McDonough & Sun, 1995) for monazite (red), allanite (orange) and apatite (purple) measured in monazite breakdown reaction. Trace element data for xenotime (shown in Figure 9) is provided for reference.

## 5.4 Geochronology

### *5.4.1 Pinto Gneiss Zircon*

Zircon analyses of three representative ore-bearing Pinto Gneiss samples (12TM15-03, MVUr2 and MVUT-1) are presented in Figures 12A-C (sample locations are labeled in Figures 2 and 4A; data are presented in Appendix E). Zircon in Pinto Gneiss ore samples are generally euhedral and contain oscillatory zoned, embayed and locally metamict cores surrounded by irregular rim overgrowths (CL images of representative zircons are included with each concordia plot).

Zircon U-Pb data from these samples display variable normal discordance suggestive of radiogenic Pb loss. Ninety-nine analyses were conducted on 62 zircons from 12TM15-03. Eight analyses are younger than the main population, ranging in age from ~1.6-1.4 Ga. The remaining 91 analyses yield an upper intercept age of 1710 ± 7 Ma (MSWD = 3). The

elevated MSWD is inferred to reflect mixing of slightly different age domains in some grains. Ninety-eight analyses were conducted on 64 zircons from MVUr2. One analysis is younger than the main population (~1570 Ma) and the remaining ninety-seven analyses yield an upper intercept age of 1710 ± 11 Ma (MSWD = 1.1). In contrast, 83 analyses from MVUT-1 display a spread in near-concordant to discordant analyses and therefore a statistically valid upper intercept age cannot be calculated.

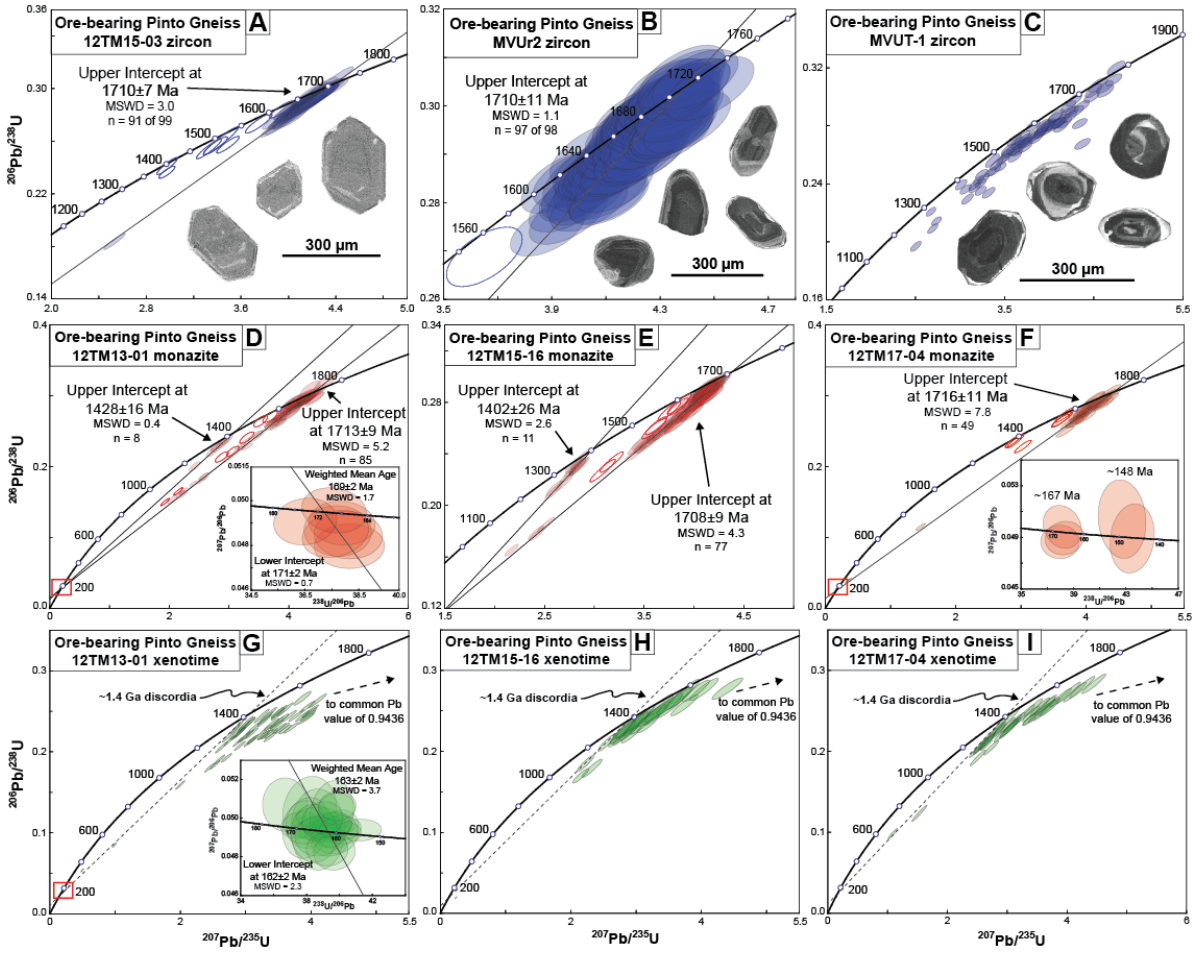


**Figure 12:** Wetherill concordia diagrams of **(A-C)** zircon (blue), **(D-F)** monazite (red) and **(G-I)** xenotime (green) in several ore-bearing Pinto Gneiss samples. Cathodoluminescence (CL) images of representative zircon are provided. Where applicable, an inset consisting of a Tera-Wasserburg concordia diagram is provided to highlight the younger age data (intercept lines are anchored at 1.71 Ga). Empty ellipses represent analyses assumed to be affected by Pb loss that are excluded from intercept age calculations. A dashed arrow is provided in the xenotime plots to show the direction of common Pb inclusion, calculated for an age of 1.4 Ga (after Stacey & Kramers, 1975).

### *5.4.2 Pinto Gneiss Monazite*

Figures 12D-F present Wetherill concordia diagrams of U-Pb monazite data for three representative ore-bearing Pinto Gneiss samples: 12TM13-01, 12TM15-16 and 12TM17-04 (sample locations are labeled in Figures 2 and 4A; data are presented in Appendix E). Where applicable, an inset consisting of a Tera-Wasserburg concordia diagram is presented to highlight Mesozoic data. Monazite from each sample consistently contain two distinct Proterozoic age populations. The older groups of analyses produce upper intercept ages of 1713 ± 9 Ma (MSWD = 5.2) (12TM13-01), 1708 ± 9 Ma (MSWD = 4.3) (12TM15-16) and 1716 ± 11 Ma (MSWD = 7.8) (12TM17-04). The younger Proterozoic population produces upper intercept ages of 1428 ± 16 Ma (MSWD = 0.4) (12TM13-01) and 1402 ± 26 Ma (MSWD = 2.6) (12TM15-16), and two analyses of 12TM17-04 yield sub-concordant ~1.4 Ga dates. In addition, seven analyses in 12TM13-01 produce a lower intercept age of 171 ± 2 Ma (MSWD = 0.7, upper intercept anchored at 1.71 Ga) and five analyses in 12TM17-04 produce concordant ages at ~148 Ma and ~167 Ma. The high MSWD of the older Proterozoic ages is inferred to reflect mixing of slightly different age domains and/or Pb loss over extended periods in some grains.

### *5.4.3 Pinto Gneiss Xenotime*

Figures 12G-I present Wetherill concordia diagrams of U-Pb data in xenotime for the same three ore-bearing Pinto Gneiss samples as presented above for monazite: 12TM13-01, 12TM15-16 and 12TM17-04 (sample locations are labeled in Figures 2 and 4A; data are presented in Appendix E). Similar to zircon from sample MVUT-1, xenotime in all ore-bearing Pinto Gneiss samples display a spread in near-concordant to discordant analyses for which statistically valid upper intercept ages cannot be calculated. However, thirty-one

analyses in sample 12TM13-01 produce a lower intercept age of 162 ± 2 Ma (MSWD = 2.3, upper intercept anchored at 1.71 Ga). A dashed arrow in each xenotime plot shows the approximate effect of common Pb (calculated using the Stacey and Kramers, 1975, two stage model at an age of 1.4 Ga). A dashed discordia is also provided to highlight the youngest Proterozoic ages recorded at ~1.4 Ga.

### *5.4.4 Geochronology of REE Ore Mineral Alteration*

Figures 13A and 13B present BSE images of a representative monazite grain from Pinto Gneiss sample 12TM13-01 and Figure 13C presents a corresponding EPMA Th map. Laser ablation spots are marked and labeled in both full grain images and the resulting

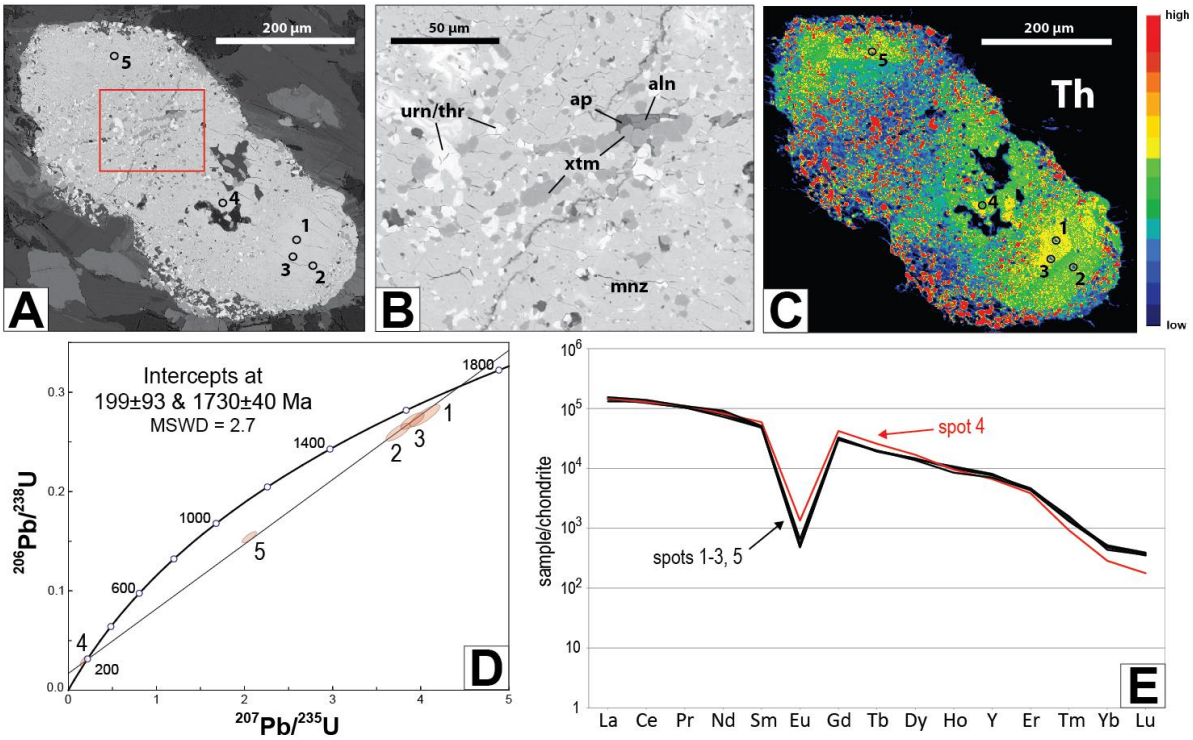


**Figure 13: (A)** BSE image of a monazite from ore Pinto Gneiss sample 12TM13-01 with distinct age domains; red box indicates area shown in **(B)** in which abbreviations are as follows: allanite (aln), apatite (ap), monazite (mnz), xenotime (xtm) and uranothorite (urn/thr) (Whitney & Evans, 2010); **(C)** Th map of the same grain; LASS spots are labeled in both (A) and (C) and correspond to data shown in **(D)** a Wetherill concordia diagram of U-Pb data showing spread in ages (error ellipse on spot 4 is exaggerated 5x for display purposes) and **(E)** trace element data corresponding to U-Pb analyses (normalized to chondrite values from McDonough & Sun, 1995).

Wetherill concordia diagram is shown in Figure 13D. In addition, a plot of the corresponding REE data (normalized to chondrite using values from McDonough & Sun, 1995) is provided in Figure 13E (sample location is marked in Figure 4A; data are presented in Appendix F). U-Pb and trace element data were collected simultaneously using the split-stream technique described in the methods section. Five analyses of the grain define a discordant array with poorly defined upper and lower intercepts of 1730 ± 40 Ma and 199 ± 93 Ma. The three analyses with the oldest ages (spots 1-3) are from a relict oscillatory-zoned core of the grain (see Figure 13C), whereas the intermediate and youngest analyses (spots 5 and 4, respectively) are within zones of partial alteration. The youngest analysis (spot 4) has a noticeably different REE pattern, with higher concentrations of Gd and Tb, lower concentrations of Er through Lu and a less prominent negative Eu anomaly relative to the core region (Figure 13E).

Figure 14 presents similar data for a representative xenotime grain from Pinto Gneiss sample 12TM13-01 (sample location is marked in Figure 4A; data are presented in Appendix F). Eight analyses performed on the grain define a discordant array with loosely defined upper and lower intercepts of 1488 ± 33 Ma and 166 ± 80 Ma (Figure 14D). The analyses that yield Proterozoic ages (spots 1-6) are located in a section of the grain where relict oscillatory zoning is preserved (see Figure 14C), and analyses with Jurassic ages (spots 7-8) are located within zones of alteration. The youngest analyses (spots 7-8) have noticeably different REE patterns than the remainder of the analyses, with lower La through Nd compared to the Proterozoic data (Figure 14E).

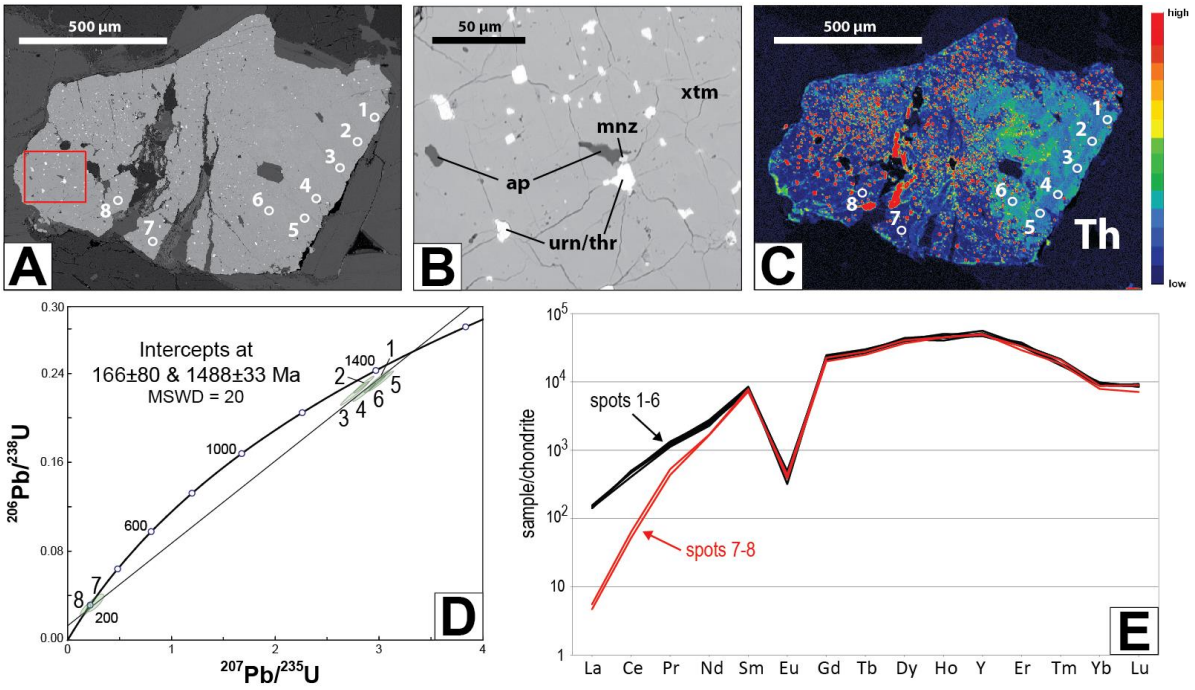


**Figure 14: (A)** BSE image of a xenotime from ore Pinto Gneiss sample 12TM13-01 with distinct age domains; red box indicates area shown in **(B)** in which abbreviations are as follows: allanite (aln), apatite (ap), monazite (mnz), xenotime (xtm) and uranothorite (urn/thr) (Whitney & Evans, 2010); **(C)** Th map of the same grain; LASS spots are labeled in both (A) and (C) and correspond to data shown in **(D)** a Wetherill concordia diagram of U-Pb data showing spread in ages (error ellipses on spots 7 and 8 are exaggerated 5x for display purposes) and **(E)** trace element data corresponding to U-Pb analyses (normalized to chondrite values from McDonough & Sun, 1995).

### *5.4.5 Dog Wash Gneiss Zircon*

Figures 15A and 15B present Wetherill concordia plots of zircon data from two Dog Wash Gneiss samples: 12TM13-06 and 12TM14-10 (sample locations are labeled in Figure 4A; data are presented in Appendix E). Zircon from the Dog Wash Gneiss are subhedral, sub- to well-rounded and contain complex internal zoning including metamict and/or embayed cores and multiple rim overgrowths (CL images of representative zircon are included with each concordia plot). Zircon data obtained from these two samples are consistently discordant. Upper intercepts forced through all data yield ages of 1872 ± 27 Ma (MSWD = 8) (12TM13-06) and 1891 ± 34 Ma (MSWD = 31) (12TM14-10). Given the high

MSWD, it is not possible to assign this unit a precise date, but the majority of data for both samples lies between ~1.8-1.5 Ga.

### *5.4.6 Diorite/amphibolite Zircon*

Figures 15C and 15D present Wetherill concordia diagrams of U-Pb zircon data obtained from two diorite/amphibolite samples: 12TM13-03 and 12TM15-14 (sample

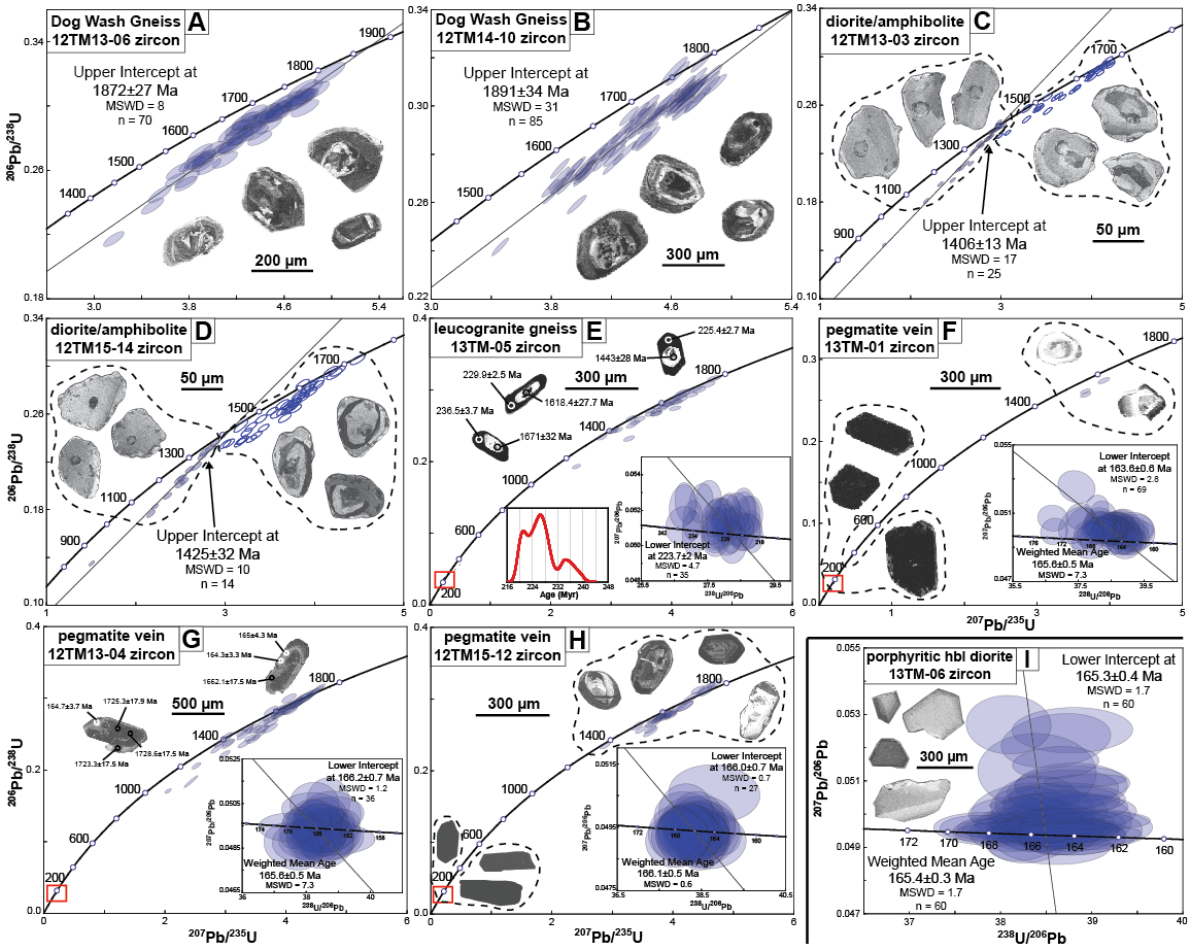


**Figure 15:** Concordia diagrams of zircon for various other units in the MVR including **(A-B)** Dog Wash Gneiss, **(C-D)** diorite/amphibolite, **(E)** leucogranite gneiss, **(F-H)** pegmatite veins and **(I)** porphyritic hornblende diorite. Cathodoluminescence (CL) images of representative zircon are provided. Where applicable, an inset consisting of a Tera-Wasserburg concordia diagram is provided to highlight the younger age data (intercept lines for pegmatite veins and leucogranite gneiss are anchored at 1.71 Ga; intercept line of porphyritic hornblende diorite is anchored at a common Pb value of 0.83 [after Stacey & Kramers, 1975]). Ages reported with zircon CL images in samples 12TM13-04 (pegmatite) and 13TM-05 (leucogranite gneiss) are $^{206}Pb/^{238}U$ (< 300 Ma) and $^{207}Pb/^{206}Pb$ (> 1000 Ma). A probability density function of Mesozoic ages is provided with 13TM-05 to highlight the spread in ages.

locations are labeled in Figure 4A; data are presented in Appendix E). There are two main populations of zircon in the diorite/amphibolite unit. The first population consists of rounded zircon with embayed cores and multiple rim overgrowths. The second population has nearly homogeneous cores with thin, bright CL rims (CL images of representative zircon are provided with each concordia plot). U-Pb data from the diorite/amphibolite produce a significant spread in sub-concordant to discordant analyses in the Proterozoic, although separate arrays exist at ~1.7 and 1.4 Ga. Calculating an upper intercept age is feasible only for the ~1.4 Ga arrays. Twenty-five analyses in 12TM13-03 yield an upper intercept age of 1406 ± 13 Ma (MSWD = 17) and 14 analyses in 12TM15-14 yield an upper intercept age of 1425 ± 32 Ma (MSWD = 10). The high MSWD of these intercept ages is inferred to reflect mixing of multiple age domains in some grains and the small sample size.

### *5.4.7 Leucogranite Gneiss Zircon*

Figure 15E presents a Wetherill concordia diagram of U-Pb data obtained from zircon in the leucogranite gneiss (sample location is labeled in Figure 2; data are presented in Appendix E). An inset consisting of a Tera-Wasserburg concordia plot is presented to highlight the younger data along with a probability density function of $^{206}Pb/^{238}U$ ages to emphasize the spread. Zircon from the leucogranite gneiss are characterized by rounded, bright CL cores with complex internal zoning enclosed by euhedral, dark CL rims (CL images of representative zircon with apparent ages are included with the concordia plot). Analyses of the bright cores yield a spread in Proterozoic ages from ~1.8-1.4 Ga while analyses on the dark rims produce a cluster of Triassic ages ranging from ~238-218 Ma. A discordia fit to the Triassic data (anchored at 1.71 Ga) produces a lower intercept age of

223.7 ± 2 Ma (MSWD = 4.7). The probability density function shows prominent age peaks at ~226 and 220 Ma and a less pronounced peak at ~234 Ma.

### *5.4.8 Pegmatite Veins Zircon*

Wetherill concordia diagrams of U-Pb zircon data from three representative pegmatite veins are displayed in Figures 15F-H (sample locations are labeled in Figures 2 and 4A; data are presented in Appendix E). A Tera-Wasserburg concordia diagram is also included for each sample to highlight the Mesozoic data. Zircon from the pegmatite veins display a wide range of grain morphologies and internal zoning. The majority of zircon have complex CL textures including oscillatory zoned, embayed and locally metamict cores surrounded by rim overgrowths. In addition, homogeneous, dark CL, euhedral zircon exist (CL images of representative zircon are included with each concordia plot). Zircon cores give sub-concordant Proterozoic ages ranging from ~1.7-1.4 Ga, whereas rims and euhedral, unaltered zircon produce lower intercept ages of 163.6 ± 0.6 Ma (MSWD = 2.8, anchored to 1.71 Ga) (13TM-01), 166.2 ± 0.7 Ma (MSWD = 1.2, anchored to 1.71 Ga) (12TM13-04) and 166.0 ± 0.7 Ma (MSWD = 0.7, anchored to 1.71 Ga) (12TM15-12). Weighted mean average $^{206}Pb/^{238}U$ ages are also provided and agree within uncertainty with lower intercept ages.

### *5.4.9 Porphyritic Hornblende Diorite*

Figure 15I presents a Terra-Wasserburg concordia diagram for zircon U-Pb data from a representative porphyritic hornblende diorite sample, 13TM-06 (sample location is labeled in Figure 2; data are presented in Appendix E). Zircon in the porphyritic hornblende diorite are gem quality, euhedral, and display simple oscillatory zoning, indicative of an igneous origin (CL images of representative zircons are included with the concordia plot). Sixty

analyses on 29 zircons yield a lower intercept age of 165.3 ± 0.4 Ma (MSWD = 1.7, anchored to a common Pb value of 0.83 ± 0.017 [Stacey & Kramers, 1975]), identical to the weighted mean average of the $^{206}Pb/^{238}U$ data (165.4 ± 0.3 Ma, MSWD = 1.7).

#### *5.4.10 Summary of Geochronologic Data*

Zircon and monazite from ore-bearing Pinto Gneiss record crystallization at ~1.71 Ga. Xenotime from the same rocks display a spread in Proterozoic ages, prohibiting a robust age calculation for this phase, although crystallization likely occurred ≥ 1.4 Ga. In addition, monazite from ore-bearing Pinto Gneiss samples record events at ~1.4 Ga and, along with xenotime, ~160-170 Ma. Zircon from the Dog Wash Gneiss are almost exclusively discordant, with dates ranging from ~1.8-1.6 Ga and tentative upper intercepts ~1.88 Ga. Zircon from the leucogranite gneiss produce a spread in Proterozoic ages from ~1.8-1.4 Ga as well as a distinct population of Triassic (~224 Ma) ages. Zircon from the diorite/amphibolite unit produce a large spread in Proterozoic ages from ~1.7-1.5 Ga as well as distinct younger Proterozoic ages of ~1.4 Ga. Zircon cores from pegmatite veins record a large spread in Proterozoic ages from ~1.7-1.4 Ga, whereas rims and homogeneous, euhedral zircon produce distinct populations of Jurassic (~165 Ma) dates. Zircon from the porphyritic hornblende diorite unit produce a single age population at 165 Ma.

## 6. Discussion

### 6.1 Field Relationships

At first appearance, the spatial association of ore-grade Pinto Gneiss with the diorite/amphibolite intrusive unit suggests a potential genetic link between intrusion of the diorite/amphibolite and REE mineralization. In addition, gamma radiation levels (and

therefore U- and Th-bearing REE-mineral concentrations) are greatest along the contact between the Pinto Gneiss and the diorite/amphibolite (Figure 6). However, there are locations within the MVR with this petrologic relationship where no anomalous concentrations of monazite and xenotime are found (Figure 5B), prohibiting direct correlation of the diorite/amphibolite to REE mineralization in the Pinto Gneiss based on field observations alone. In addition, the contact between the diorite/amphibolite and the Pinto Gneiss also appears to be the location of partial melting of the Pinto Gneiss to form pegmatite veins that emanate from the contact and cross-cut the diorite/amphibolite (Figure 16, see geochronology discussion for further detail).

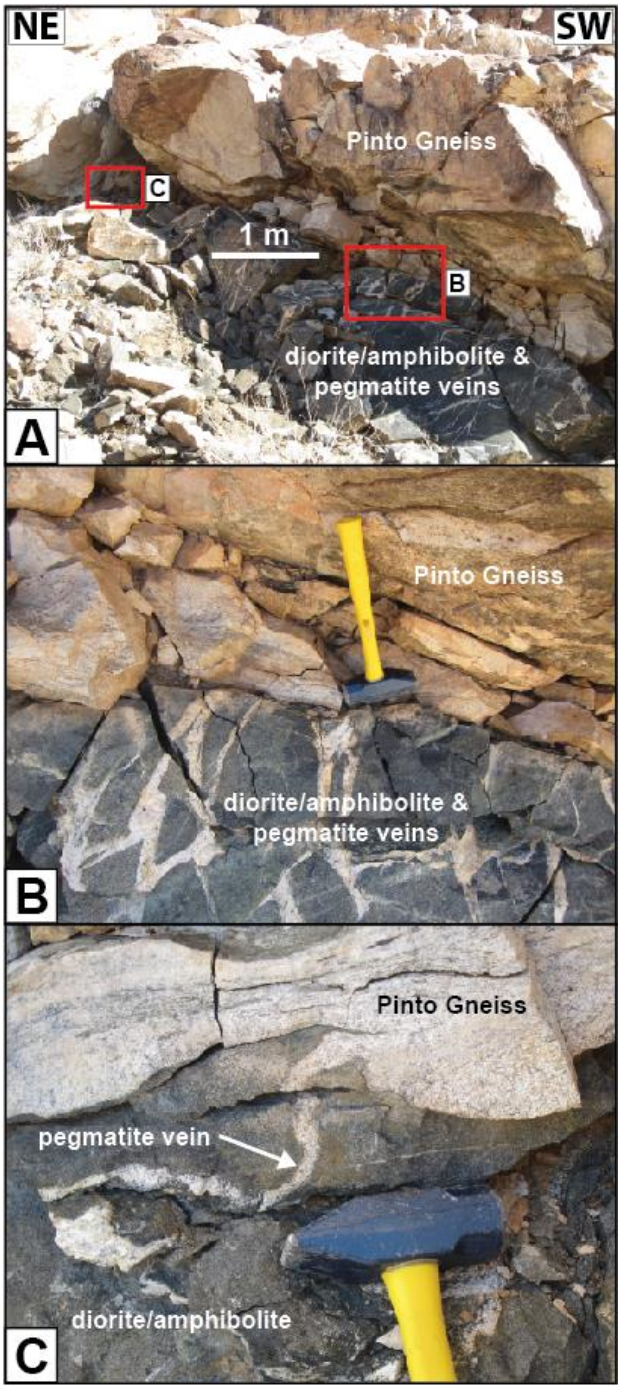


**Figure 16:** Field photographs showing pegmatite veins emanating from Pinto Gneiss and being injected into the diorite/amphibolite. Red boxes in **(A)** denote locations of close-up photographs shown in **(B)** and **(C)**.

### 6.2 Petrography/Mineralogy

The subhedral to euhedral morphology of ore monazite and xenotime is compatible with an igneous origin. In addition, the REE minerals commonly

preserve relict oscillatory zoning that is overprinted by an inclusion-rich texture (Figure 8). Oscillatory zoning in zircon is often interpreted to represent growth during igneous crystallization (Seyedolali et al., 1997). Similarly, we interpret the relict oscillatory zoning in monazite and xenotime in the MVR to reflect primary igneous crystallization and the inclusion-rich texture to reflect fluid-related alteration of those domains (discussed below). The restriction of monazite and xenotime to biotite folia in the Pinto Gneiss suggests interaction between the REE phases and fluids partially derived from the surrounding biotite, as addressed in the following section.

### 6.3 Alteration Textures of Ore Minerals

Evidence for fluid-induced alteration of monazite and xenotime in the MVR exists in the form of the inclusion-rich texture seen in Figure 8. This texture has been described in other igneous and metamorphic settings and has been replicated through experiments; it is interpreted to be the result of fluid-induced dissolution of the primary phase and re-precipitation of secondary phases (Dider et al., 2013; Harlov et al., 2005; Harlov et al., 2007; Harlov & Hetherington, 2010; Harlov et al, 2011; Hetherington & Harlov, 2008). In the MVR, original monazite was dissolved and re-precipitated as secondary xenotime (red in the Y x-ray map, Figure 8), uranothorite [$(U,Th)SiO_4$] (red in Th and U x-ray maps, Figure 8) and secondary monazite that is depleted in HREE, Th and U relative to the original monazite (blue regions in all three maps, Figure 8). Similarly, original xenotime was dissolved and re-precipitated as secondary monazite (red in Nd x-ray map, Figure 8), uranothorite (red in Th and U x-ray maps, Figure 8) and secondary xenotime that is depleted in LREE, Th and U relative to the original xenotime (blue regions in all three maps, Figure 8). REE can be mobilized in high-temperature fluids by a range of anionic species including $F^-$, $Cl^-$, $(CO_3)^{2-}$,

$(HCO_3)^-$, $(SO_4)^{2-}$ and $(OH)^-$ (Taylor & Fryer, 1983; Wood, 1990; Poitrasson et al., 2000). Furthermore, experimental studies have shown that the formation of dissolution re-precipitation textures is generally the result of interaction with alkali-bearing fluids (Harlov & Hetherington, 2010; Harlov et al., 2011). Given that monazite and xenotime are generally restricted to biotite folia within the Pinto Gneiss, it seems possible that $F^-$ and/or $(OH)^-$ played a significant role in the dissolution re-precipitation reaction. The absence of carbonate minerals such as calcite and bastnäsite suggests that $(CO_3)^{2-}$ and $(HCO_3)^-$ were not major components of the reacting fluid. Plagioclase and potassium feldspar make up a large proportion of the Pinto Gneiss, providing a viable source for alkali metals for such a fluid.

Further evidence for fluid-assisted alteration of the Pinto Gneiss ore bodies is present in the form of the monazite breakdown reaction shown in Figure 10. This reaction has been described in other metamorphic settings as a fluid-induced breakdown in which monazite, biotite and calcic plagioclase break down in the presence of an externally derived fluid to form apatite and allanite (Broska & Siman, 1998; Broska et al., 2005; Budzyn et al., 2011; Finger et al., 1998). A hypothetical representation of this reaction has been proposed by Broska and Siman (1998) as:

**monazite + annite (biotite) + anorthite + quartz + fluids =**

**apatite + allanite + muscovite (or K-feldspar)**

or in chemical form as:

$$\mathbf{3(LREE)PO_4 + KFe_3(Si_3AlO_{10})(OH,F)_2 + 4CaAl_2Si_2O_8 + 3SiO_2 + 4Ca^{2+} + 2H^+ \rightarrow}$$

$$\mathbf{Ca_5(PO_4)_3(OH,F) + 3Ca(LREE)FeAl_2Si_3O_{12}(OH,F) + KAl(Si_3AlO_{10})(OH)_2}$$

Presumably, the LREE from monazite are incorporated into allanite (essentially LREE epidote) while the leftover phosphate combines with calcium derived from plagioclase (and/or a fluid) to form apatite. It has been proposed that for such a reaction, the extent of

the apatite rim marks the boundary of the original monazite grain, whereas growth of allanite likely occurs peripheral to the original grain (Finger et al., 1998). Previous descriptions of monazite breakdown constrain the reaction to greenschist/amphibolite facies metamorphism, perhaps providing pressure-temperature constraints on the Pinto Gneiss during this reaction (Broska & Siman, 1998; Broska et al., 2005; Finger et al., 1998). However, experimental data suggest that the fluid composition and ratio of silicate minerals in a rock influence monazite stability more than pressure and temperature (Budzyn et al., 2011). Specifically, fluids with a high Ca content promote monazite dissolution and the formation of apatite and allanite, whereas fluids with a higher Na content decrease the solubility of monazite (Budzyn et al., 2011). These findings suggest that the fluid responsible for monazite breakdown in the MVR had a high concentration of Ca, possibly derived from anorthite in the Pinto Gneiss.

## 6.4 Geochronology

### *6.4.1 U-Pb Geochronology – Pinto Gneiss*

Given the widespread evidence for fluid interaction throughout the Pinto Gneiss, it is not surprising that the geochronologic data collected from zircon, monazite and xenotime in the MVR is complex. Despite this apparent complexity, several key observations support an igneous origin for the Pinto Gneiss and the REE-minerals it contains.

U-Pb data from zircon in two of the ore-bearing Pinto Gneiss samples (12TM15-03 and MVUr2) yield single age populations. The zircon are euhedral and preserve oscillatory zoning. We therefore interpret these zircon ages to record magmatic crystallization of a felsic igneous precursor to the Pinto Gneiss at ~1.71 Ga. The other Pinto Gneiss sample, MVUT-1, contains a wider range of ages (~1.7-1.4 Ga), perhaps reflecting variable Pb loss

in zircons that crystallized at ~1.71 Ga, or recrystallization during a tectonic/magmatic event at ~1.4 Ga.

Upper intercept ages of monazite from the three ore-bearing Pinto Gneiss samples are also ~1.71 Ga, within uncertainty of the upper intercept ages of zircon from the same unit. This suggests that monazite in the MVR may also be igneous. Further evidence for an igneous origin for the monazite is the relict oscillatory zoning present in unaltered regions of the grains (Figure 8). Together, these data and observations suggest that ore-forming monazite formed during crystallization of the igneous protolith of the Pinto Gneiss at ~1.71 Ga. The spread in Proterozoic age data for xenotime in the Pinto Gneiss makes it difficult to assess the primary concentration mechanism for this phase. However, the observation that xenotime yield a spread of Proterozoic ages similar to that seen in zircons from MVUT-1 rules out the possibility of primary crystallization of xenotime after ~1.4 Ga (the youngest concordant Proterozoic analyses for this phase). Furthermore, the presence of relict oscillatory zoning in the xenotime implies an igneous origin of this phase.

Together, the textural and geochronologic data refute the hypothesis put forward by Evans (1964) that monazite and xenotime in the MVR are detrital heavy mineral concentrates in a sedimentary protolith of the Pinto Gneiss. If the ore-bearing Pinto Gneiss were indeed a paragneiss, U-Pb zircon and monazite dates might stretch as far back as ~2.8 Ga, the age of the oldest detrital zircon in paragneisses present in the Mojave Province (Strickland et al., 2013). Rather, zircon and monazite in the Pinto Gneiss record a single crystallization event at ~1.71 Ga followed by Pb loss and/or recrystallization due to thermal disturbance and/or fluid-related alteration at ~1.4 Ga and again at ~165 Ma.

### *6.4.2 Geochronology of REE Ore Mineral Alteration*

The origin and extent of age resetting in monazite and xenotime of the Pinto Gneiss is evident from domains within single grains that have different ages and trace element profiles (Figures 13 & 14). For the monazite presented in Figure 13, spot number 4 produces an age ~175 Ma, while the remaining four spots are Proterozoic. The trace element data that corresponds to the U-Pb data used to calculate ages show that the younger domain is slightly depleted in the heaviest REE and enriched in Eu, suggesting the involvement of an external source (i.e., a fluid) in the alteration of this domain. Likewise, in the xenotime presented in Figure 14, spot numbers 7 and 8 produce young ages (~165 Ma) while the remaining spots produce a spread of Proterozoic ages (~1.55-1.45 Ga). The corresponding trace element data show that the younger domains are depleted in the lightest REE, again suggesting the involvement of an external source in the alteration of these domains. The occurrence of Jurassic ages in the altered, dissolution re-precipitation domains of monazite and xenotime suggests that this alteration occurred at ~165 Ma, concurrent with emplacement of the porphyritic hornblende diorite and genesis of pegmatite veins (discussed in the following section). This interpretation is supported by laboratory experiments that show resetting of U-Pb ages in fluid-altered domains of monazite in the presence of hydrous, alkalic, Ca-bearing fluids at temperatures well below the closure temperature of monazite (Williams et al., 2011).

By comparing U-Pb data from monazite and xenotime from ore-bearing Pinto Gneiss samples, the relative susceptibility of these phases to fluid-assisted alteration and U-Pb age resetting can be assessed. In all three ore-bearing samples analyzed, xenotime appears to be significantly more affected by Pb loss than monazite. This is evident in the large and fairly even spread in Proterozoic age data from ~1.7-1.4 Ga in all of the xenotime samples. In

contrast, monazite does record an episode of Pb loss at ~1.4 Ga, but the overall effect is much less pronounced. Previous studies have suggested that monazite and xenotime have similar U-Pb systematics (Aleinikoff & Grouch, 1990; Childe et al., 1993; Hawkins & Bowring, 1997; Sevigny & Hanson, 1995). However, the data presented here suggest that xenotime is more susceptible to Pb loss and age resetting during fluid-assisted alteration compared to monazite. This is important because it implies that within such ore-bodies, the heavy REE can be preferentially re-distributed relative to the light REE during fluid-assisted alteration.

### *6.4.3 U-Pb Geochronology – Other Units*

Based on cross-cutting relationships and detailed geologic mapping, the Dog Wash Gneiss is thought to be younger than the Pinto Gneiss (Howard et al., 2013). However, no conclusive evidence was observed in the field during this study to confirm or refute that claim. U-Pb data from two Dog Wash Gneiss samples produce virtually no concordant analyses and a spread in ages from ~1.8-1.5 Ga, making it difficult to place a firm age limit on this unit. The upper extent of this age range, though, suggests that the Dog Wash Gneiss may be older than the Pinto Gneiss.

Zircon from the diorite/amphibolite unit produce two arrays, one at ~1.7 Ga and the other at ~1.4 Ga. There are at least two possible interpretations for these two distinct Proterozoic arrays. Either the 1.7 Ga data reflect primary igneous zircon crystallization and the 1.4 Ga zircon record a recrystallization event, or the 1.7 Ga zircon are inherited from the host Pinto Gneiss and the 1.4 Ga zircon record igneous crystallization. The latter interpretation is favored based on the abundance of ~1.4 Ga data from the diorite/amphibolite samples compared to all other rock types analyzed. Therefore, the

tectonic/magmatic event thought to be responsible for the ~1.4 Ga signature seen in the zircon, monazite and xenotime data from the Pinto Gneiss is emplacement of the diorite/amphibolite unit, with samples 12TM13-03 and 12TM15-14 yielding upper intercept ages of 1406 ± 13 Ma and 1425 ± 32 Ma, respectively (Figure 15C and 15D). The spread in Proterozoic ages from ~1.7-1.5 Ga in this unit is interpreted to represent inheritance from the Pinto Gneiss into which the diorite/amphibolite intruded. This interpretation is supported by the two populations of zircon present in the diorite/amphibolite. The homogeneous population consistently produces ~1.4 Ga ages, while zircon with complex internal zoning produce ~1.7-1.5 ages. The increase in radioactivity in the Pinto Gneiss towards the contact with the diorite/amphibolite (Figure 6) suggests that the intrusion of this unit may have resulted in remobilization of REE, U and Th in the Pinto Gneiss, leading to increased concentrations near the contact.

The leucogranite gneiss on the eastern side of Music Valley contains a significant component of Proterozoic ages from ~1.8-1.4 Ga and a cluster of Triassic ages ~238-218 Ma. This unit is most likely related to the Triassic intrusive suite studied by Barth et al. (1997). We interpret the spread in Proterozoic ages to reflect inherited zircon entrained from surrounding units, including, but not limited to, the Pinto Gneiss, the Dog Wash Gneiss and the diorite/amphibolite. This interpretation is supported by the presence of zircon with rounded, complex cores with Proterozoic ages that are surrounded by euhedral, homogeneous rims with Triassic ages (Figure 15E). The spread in Triassic ages for this unit could be the result of protracted crystallization, or possibly mixing of multiple melt batches. Despite the close proximity of this unit to the ore bodies, there is no evidence for Triassic ages in any other unit. We attribute this to either an absence of significant fluid flow and/or limited heating of the surrounding rocks during intrusion of this unit. The lack of Triassic

alteration stands in contrast to emplacement of the porphyritic hornblende diorite, which caused extensive resetting of monazite and xenotime ages in the Pinto Gneiss.

A third tectonic/magmatic event at ~160-170 Ma was recorded by partially recrystallized monazite (Figures 12D and 12F) and xenotime (Figure 12G) in the Pinto Gneiss, as well as generation of the pegmatite veins (Figures 15F-H) that cross-cut the diorite/amphibolite in proximity to the ore bodies. Extensive plutonism occurred throughout the Mojave Province during this time, providing a tectonic framework for this event (Haxel & Miller, 2007). In addition to the ~165 Ma ages in the pegmatites, the ~1.7-1.4 Ga spread of ages is likely the result of inheritance from both the Pinto Gneiss and the diorite/amphibolite. This interpretation is supported by the existence of zircon with Proterozoic cores surrounded by Jurassic rims (Figure 15G). Additionally, rounded and irregular zircon from the pegmatite veins consistently produce Proterozoic ages while euhedral, homogeneous zircon produce ages ~165 Ma (Figures 15F and 15H).

The age of the porphyritic hornblende diorite (165.3 ± 0.4 Ma, MSWD = 1.7) is nearly identical to the age of the pegmatite veins (~165 Ma), suggesting a causal link between the two. One possibility is that the intrusion of the porphyritic hornblende diorite was associated with significant fluid activity, which, when injected into the Pinto Gneiss, may have induced partial melting. In this scenario, the contact between the diorite/amphibolite and the Pinto Gneiss acted as a fluid conduit that promoted localized partial melting. In addition, fluid activity at this time reset the U-Pb systematics of certain domains within monazite and xenotime in the Pinto Gneiss. The cluster of monazite and xenotime ages at ~165 Ma are interpreted to be the result of resetting during the ~165 Ma thermal/melting event as opposed to new crystallization of these phases, an interpretation that is supported by the distinct, fluid-altered age domains presented in Figures 13 and 14.

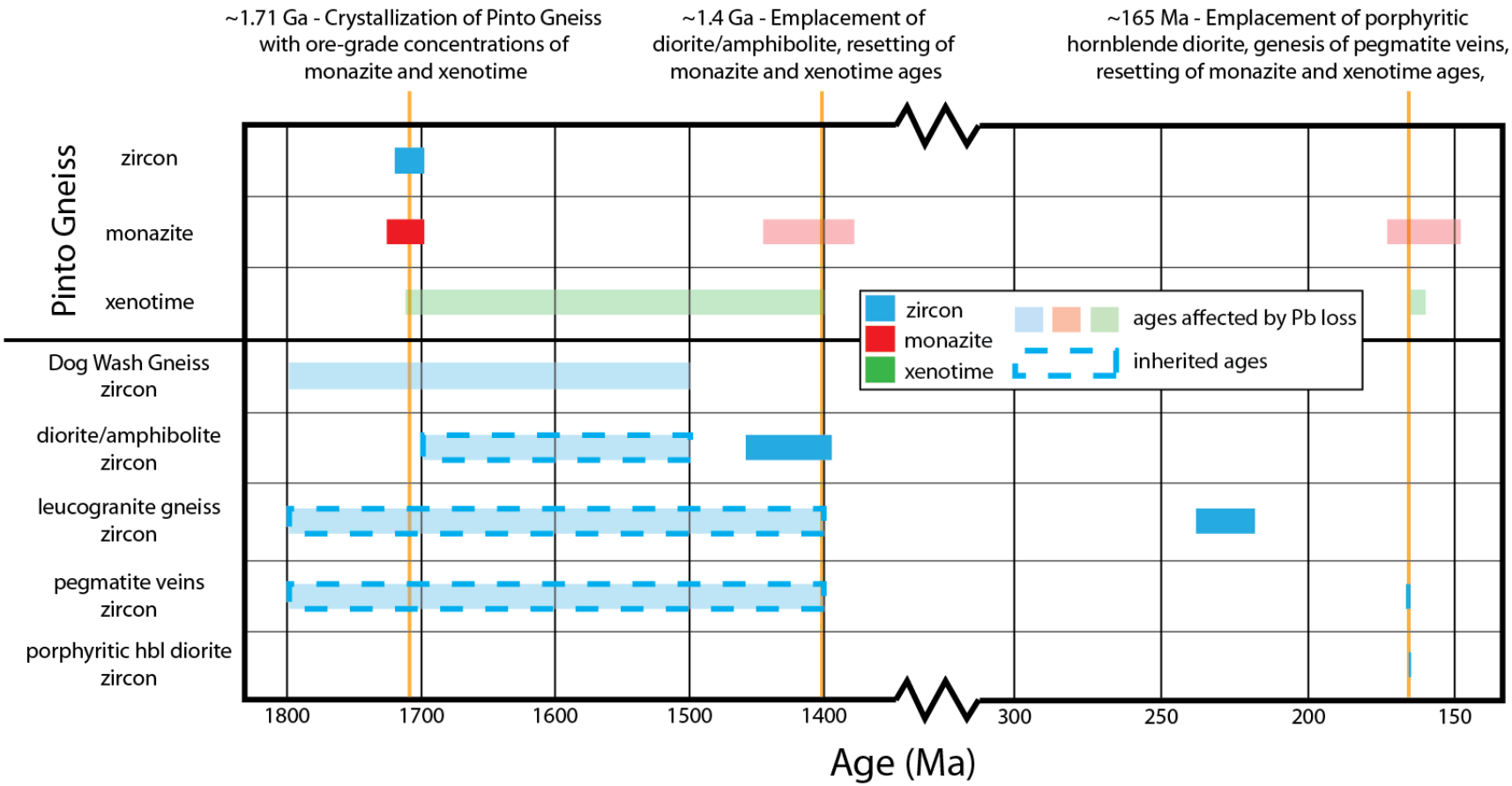


**Figure 17:** Summary of REE-mineral petrogenesis in the MVR based on the geochronologic results of this study; dashed boxes represent inherited components whereas faded boxes represent ages affected by Pb loss.

### 6.5 Petrogenetic Model for REE-Mineralization in the MVR

Figure 17 summarizes the textural and geochronologic data, and illustrates a petrogenetic model for REE-mineralization in the MVR. At ~1.71 Ga, the igneous protolith to the Pinto Gneiss crystallized with anomalous concentrations of monazite and xenotime. This was the primary mechanism for concentration of REE-bearing minerals in the MVR. At ~1.4 Ga, intrusion of the diorite/amphibolite unit remobilized REE, U and Th, leading to elevated concentrations of monazite and xenotime near the contact between the Pinto Gneiss and the diorite/amphibolite. At ~165 Ma, crystallization of porphyritic hornblende diorites and pegmatite veins occurred. Emplacement of the porphyritic hornblende diorites may have caused partial melting of the Pinto Gneiss to generate the pegmatites. Fluid activity during this period was responsible for further alteration of the REE ore bodies, and partial resetting of U-Pb systematics in monazite and xenotime.

## 7. Conclusions

In the MVR of southern California, ore grade concentrations of monazite and xenotime occur within the Pinto Gneiss. Anomalous concentrations of REE-bearing minerals are spatially associated with diorite/amphibolite intrusions that are cross-cut by pegmatite veins generated by partial melting of the Pinto Gneiss. Zircon, monazite and xenotime U-Pb geochronology of ore bodies indicates that initial REE ore formation occurred during igneous crystallization of the protolith of the Pinto Gneiss at ~1.71 Ga. Within the Pinto Gneiss, all three phases also show evidence for a tectonic/magmatic event at ~1.4 Ga and the latter two minerals also record ~165 Ma ages. Both the ~1.4 Ga and ~165 Ma events had a significant effect on ore-forming monazite and xenotime, with evidence of

fluid-assisted alteration in the form of dissolution re-precipitation textures and monazite breakdown to form apatite and allanite. Alteration was accompanied by partial resetting of U-Pb systematics and redistribution of certain REE and actinides.

## References


Aleinikoff, J.N. and Grauch, R.I., 1990. U-Pb geochronologic constraints on the origin of a unique monazite-xenotime gneiss, Hudson Highlands, New York. *American Journal of Science*, **290**, p. 522-546.

Aleinikoff, J.N., Schenck, W.S., Plank, M.O., Srogi, L., Fanning, C.M., Kamo, S.L. and Bosbyshell, H., 2006. Deciphering igneous and metamorphic events in high-grade rocks of the Wilmington Complex, Delaware: morphology, cathodoluminescence and backscattered electron zoning, and SHRIMP U-Pb geochronology of zircon and monazite. *GSA Bulletin*, **118(1-2)**, p. 39-64.

Aleinikoff, J.N., Grauch, R.I., Mazdab, F.K., Kwak, L., Fanning, C.M. and Kamo, S.L., 2012. Origin of an unusual monazite-xenotime gneiss, Hudson Highlands, New York: SHRIMP U-Pb geochronology and trace element geochemistry. *American Journal of Science*, **312**, p. 723-765.

Alexander, P.G. and Williams-Jones, A.E., 2013. Hydrothermal mobilization of pegmatite-hosted REE and Zr at Strange Lake, Canada: A reaction path model. *Geochimica et Cosmochimica Acta*, **122**, p. 324-352.

Anderson, J.L. and Bender, E.E., 1989. Nature and origin of Proterozoic A-type granitic magmatism in the southwestern United States of America. *Lithos*, **23**, p. 19-52.

Andreoli, M.A.G., Smith, C.B., Watkeys, M., Moore, J.M., Ashwal, L.D., and Hart, R.J., 1994. The geology of the Steenkampskraal monazite deposit, South Africa: Implications for REE-Th-Cu mineralization in charnockite-granulite terranes. *Economic Geology*, **89**, p. 994-1016.

Armstrong, J.T., 1988. Quantitative analysis of silicates and oxide minerals: Comparison of Monte-Carlo, ZAF and Phi-Rho-Z procedures. *Microbeam Analysis*, p. 239-246.

Barth, A.P., Tosdal, R.M., Wooden, J.L. and Howard, K.A., 1997. Triassic plutonism in southern California: Southward younging of arc initiation along a truncated continental margin. *Tectonics*, **16(2)**, p. 290-304.

Barth, A.P., Wooden, J.L., Coleman, D.S. and Fanning, C.M., 2000. Geochronology of the Proterozoic basement of southwesternmost North America, and the origin and evolution of the Mojave crustal province. *Tectonics*, **19**, p. 616-629.

Barth, A.P., Wooden, J.L., Coleman, D.S., and Vogel, M.B., 2009. Assembling and disassembling California: A zircon and monazite geochronologic framework for Proterozoic crustal evolution in southern California. *J. Geol.*, **117(3)**, p. 221-239.

Barth, A.P. and Wooden, J.L., 2010. Coupled elemental and isotopic analyses of polygenetic zircons from granitic rocks by ion microprobe, with impliications for melt evolution and the sources of granitic magmas. *Chemical Geology*, **277**, p. 149-159.

Bender, E.E., 1994. Petrology of Early Proterozoic granitoids from the southwestern United States: Implications for genesis and tectonics of the Mojave Crustal Province [Ph.D. thesis]: University of Southern California, 354 p.

Broska, I. and Siman, P., 1998. The breakdown of monazite in the west-Carpathian Veporic orthogneisses and Tatric granites. *Geologica Carpathica*, **49(3)**, p. 161-167. Broska, I., Williams, C.T., Janak, M. and Nagy, G., 2005. Alteration and breakdown of xenotime-(Y) and monazite-(Ce) in granitic rocks of the Western Carpathians, Slovakia. *Lithos*, **82**, p. 71-83.

Budzyn, B., Harvlov, D.E., Williams, M.L., and Jercinovic, M.J., 2011. Experimental determination of stability relations between monazite, fluorapatite, allanite, and REE-epidote as a function of pressure, temperature, and fluid composition. *American Mineralogist*, **96**, p. 1547-1567.

Chakhmouradian, A.R. and Zaitsev, A.N., 2012. Rare earth mineralization in igneous rocks: Sources and processes. *Elements*, **8.5**, p. 347-353.

Chile F., Doig, R., and Gariepy, C., 1993. Monazite as a metamorphic chronometer, south of the Grenville Front, western Quebec. *Candian Journal of Earth Sciences*, **30**, p. 1056-1065.

Coleman, D.S., Barth, A.P., and Wooden, J.L., 2002. Early to Middle Proterozoic construction of the Mojave Province, southern California. *Gondwana Research*, **5(1)**, p. 75-78.

Cottle, J.M., Burrows, A.J., Kylander-Clark, A.R.C., Freedman, P.A. and Cohen, R., 2013. Enhanced sensitivity in laser ablation multi-collector inductively coupled plasma mass spectrometry. *Journal of Analytical Atomic Spectrometry*, **28**, p. 1700-1706.

Cottle, J.M., Kylander-Clar, A.R.C., and Vrijmoed, J.C., 2012. U-Th/Pb geochronology of detrital zircon and monazite by single shot laser ablation inductively coupled plasma mass spectrometry (SS-LA-ICPMS). *Chemical Geology*, **332-333**, p. 136-147.

Didier, A., Bosse, V., Boulvais, P., Bouloton, J., Paquette, J.L., Montel, J.M. and Devidal, J.L., 2013. Disturbance versus preservation of U-Th-Pb ages in monazite during fluid-rock interaction: textural, chemical and isotopic in situ study in microgranites (Velay Dome, France). *Contrib Mineral Petrol*, **165**, p. 1051-1072.

Donovan, J.J., Snyder, D.A. and Rivers, M.L., 1993. An Improved Interference Correction for Trace Element Analysis in Microbeam Analyis, **2**, p. 23-28.

Donovan, J.J., Lowers, H.A., and Rusk, B.G., 2011. Improved electron probe microanalysis of trace elements in quartz. *American Mineralogist*, **96**, p. 274-282.

Evans, J.R., 1964. Xenotime mineralization in the southern Music Valley area, Riverside County, California: California Division of Mines and Geology Special Report **79**, 24 p.

Finger, F., Broska, I., Roberts, M.P. and Schermaier, A., 1998. Replacement of primary monazite by apatite-allanite-epidote coronas in an amphibolite facies granite gneiss from the eastern Alps. *American Mineralogist*, **83**, p. 248-258.

Gibson, P.E., 1998. Origin of the Lemhi Pass REE-Th deposits, Idaho/Montana; petrology, mineralogy, paragenesis, whole-rock chemistry and isotopic evidence [Master's Thesis]: University of Idaho, 350 p.

Harlov, D.E., Wirth, R., and Förster, H.J., 2005. An experimental study of dissolution-reprecipitation in fluorapatite: fluid inclusion and the formation of monazite. *Contributions to Mineralogy and Petrology*, **150**, p. 268-286.

Harlov, D.E., Wirth, R., Hetherington, C.J., 2007. The relative stability of monazite and huttonite at 300-900°C and 200-1000 MPa: metasomatism and the propagation of metastable mineral phases. *American Mineralogist*, **92**, p. 1652-1664.

Harlov, D.E., and Hetherington, C.J., 2010. Partial high-grade alteration of monazite using alkali-bearing fluids: experiment and nature. *American Mineralogist*, **87**, p. 245-261.

Harlov, D.E., Wirth, R., and Hetherington, C.J., 2011. Fluid-mediated partial alteration in monazite: the role of coupled dissolution-reprecipitation in element redistribution and mass transfer. *Contributions to Mineralogy and Petrology*, **162**, p. 329-348.

Hawkins, D.P. and Bowring, S.A., 1997. U-Pb systematics of monazite and xenotime: case studies from the Paleoproterozoic of the Grand Canyon, Arizona. *Contributions to Mineralogy and Petrology*, **127**, p. 87-103.

Haxel, G.B. and Miller, D.M., 2007. Mesozoic rocks. In T.G. Theodore (Ed.), Geology and mineral resources of the East Mojave National Scenic Area, San Bernardino County, California. *U.S. Geological Survey Bulletin*, **2160**, p. 59-66.

Hetherington, C.J. and Harlov, D.E., 2008. Metasomatic thorite and uraninite inclusions in xenotime and monazite from granitic pegmatites, Hidra anorthosite massif, southwestern Norway: Mechanics and fluid chemistry. *American Mineralogist*, **93**, p. 806-820.

Holstam, D. and Broman, C., 2003. Lanthanide mineralizations of Bastnas type: overview and new data. *Geological Society of Sweden*, **124(4)**, p. 230-231.

Howard, K.A., Bacheller, J., Fitzgibbon, T.T., Powell, R.E. and Allen, C.M., 2013. Geologic map of the Valley Mountain 15' quadrangle, San Bernardino and Riverside Counties, California. *U.S. Geological Survey Geological Quadrangle Map GQ-1767*. 19 p.

Jennings, C.W., Gutierrez, C., Bryant, W., Saucedo, G., and Wills, C., 2010. Geologic Map of California. *California Geologic Society,* **Geologic Data Map No. 2**.

Kylander-Clark, A.R.C., Hacker, B.R. and Cottle. J.M., 2013. Laser-ablation split-stream ICP petrochornology. *Chemical Geology*, **345**, p. 99-112.

Lai, X. and Yang, X., 2013. Geochemical characteristics of the Bayan Obo giant REE-Nb-Fe deposit: Constraints on its genesis. *Journal of South American Earth Sciences*, **41**, p. 99-112

Long, K.R., Van Gosen, B.S., Foley, N.K. and Cordier, D., 2010. The principal rare earth elements deposits of the United States: A summary of domestic deposits and a global perspective. *U.S. Geological Survey Scientific Investigations Report*, 2010-**5220**, 96 p.

Ludwig, K.R., 2012. User's manual for Isoplot 3.75: A geochronological toolkit for Microsoft Excel. *Berkeley Geochronology Center Special Publication*, **5**, 75 p.

Matti, J.C., Wooden. J.L., Powell, R.E., 1994. Late Cretaceous plutonic and metamorphic complex in the Little San Bernadino Mountains, southern California. *Absracts with Programs, Geol. Soc. of Amer.*, **26**, p. 70.

McDonough, W.F. and Sun, S., 1995. The composition of the Earth. *Chemical Geology*, **120**, p. 223-253.

Miller, W.J., 1938. Precambrian and associated rocks near Twenty-nine Palms, California. *Geol. Soc. Amer. Bull.,* **49**, 417-446.

Miller, R.J. and Rytuba, J.J., 2007. Tertiary rocks. In T.G. Theodore (Ed.), Geology and mineral resources of the East Mojave National Scenic Area, San Bernardino County, California. *U.S. Geological Survey Bulletin*, **2160**, p. 67-72.

Moxam, R.M., 1952. Airborne radioactivity surveys in the Mojave Desert region, Kern, Riverside, and San Bernardino Counties, California: U.S. Geological Survey Preliminary Report TEM-**360**, 34 p.

Orris, G.J. and Grauch, R.I., 2002. Rare earth element mines, deposits, and occurrences. *U.S. Geological Survey Open-File Report*, **02-189**.

Philpotts, J.A., Taylor, C.D., Tatsumoto, M., and Belkin, H.E., 1998. Petrogenesis of late-stage granites and Y-REE-Zr-Nb-enriched vein dikes of the Bokan Mountain stock, Prince of Wales Island, Southeastern Alaska. *U.S. Geological Survey Open-File Report*, **98-459**, 71 p.

Poitrasson, F., Chernery, S., and Shepherd, T.J., 2000. Electron microprobe and LA-ICP-MS study of monazite hydrothermal alteration: Implications for U-Th-Pb geochronology and nuclear ceramics. *Geochimica et Cosmochimica Acta*, **68**, p. 2207-2221.

Powell, R.E., 1981. Geology of the crystalline basement complex, eastern Transverse Ranges, southern California: constraints on regional tectonic interpretation [Ph.D. thesis]: California Institute of Technology, 441 p.

Sevigny, J.H. and Hanson, G.N., 1995. Late-Acadian and Pre-Acadian history of the New England Appalachians of southwestern Connecticut. *Geological Society of America Bulletin*, **107**, p. 487-498.

Seyedolali, A., Krinsley, D.H., Boggs Jr., S., O'Hara, P.F., Dypvik, H., and Goles, G.C., 1997. Provenance interpretation of quartz by scanning electron microscope-cathodoluminescence fabric analysis. *Geology*, **25(9)**, p. 787-790.

Smith, M.P., Henderson, P. and Campbell, L.S., 2000. Fractionation of the REE during hydrothermal processes: Constraints from the Bayan Obo Fe-REE-Nb deposit, Inner Mongolia, China. *Geochimica et Cosmochimica Acta*, **64**, p. 3141-3160.

Stacey, J.S. and Kramers, J.D., 1975. Approximation of terrestrial lead isotope evolution by a 2-stage model. *Earth and Planetary Science Letters*, **26(2)**, p. 207-221.

Strickland, A., Wooden, J.L., Mattinson, C.G., Ushikubo, T., Miller, D.M. and Valley, J.W., 2013. Proterozoic evolution of the Mojave crustal province as preserved in the Ivanpah Mountains, southeastern California. *Precambrian Research*, **224**, p. 222-241.

Taylor, R.P. and Fryer, B.J., 1983. Rare earth element lithogeochemistry of granitoids mineral deposits. *Canadian Mining and Metallurgical Bulletin*, **76(860)**, p. 74-84.

Taylor, R.P. and Pollard, P.J., 1996. Rare earth element mineralization in peralkaline systems: The T-zone-REE-Y-Be deposit, Thor Lake, Northwest Territories, Canada. *Mineralogical Society Series*, **7**, p. 167-192.

Walters, A., Lusty, P., Chetwyn, C., and Hill, A., 2011. Rare Earth Elements. *British Geological Survey: Mineral Profile Series*, 45 p.

Whitney, D.L. and Evans, B.W., 2010. Abbreviations for names of rock-forming minerals. *American Mineralogist*, **95**, p. 185-187.

Wiedenbeck, M., Alle, P., Corfu, F., Griffin, W.L., Meier, M., Oberli, F., Von Quadt, A., Roddick, J.C., and Spiegel, W., 1995. Three natural zircon standards for U-Th-Pb, Lu-Hf, trace element and REE analyses. *Geostandards Newsletter*, **19(1)**, 23 p.

Williams, M.L., Jercinovic, M.J., Harlov, D.E., Budzyn, B. and Hetherington, C.J., 2011. Resetting monazite ages during fluid-related alteration. *Chemical Geology*, **283**, p. 218-225.

Williams-Jones, A.E., Migdisov, A.A. and Samson, I.M., 2012. Hydrothermal mobilization of the rare earth elements – a tale of "ceria" and "yttria". *Elements*, **8.5**, p. 355-360.

Wood, S.A., 1990. The aqueous geochemistry of the rare earth elements and yttrium: 1. Review of available low-temperature data for inorganic complexes and the inorganic REE speciation of natural waters. *Chemical Geology*, **82**, p. 159-186.

Wooden, J.L. and Miller, D.M., 1990. Chronologic and isotopic framework for Early Proterozoic crustal evolution in the eastern Mojave Desert region, SE California. *Journal of Geophysical Research*, **95**, 20 p.

Yang, X.Y., Sun, W.D., Zhang, Y.X. and Zheng, Y.F., 2009. Geochemical constraints on the genesis of the Bayan Obo Fe-Nb-REE deposit in Inner Mongolia, China. *Geochimica et Cosmochimica Acta*, **73**, p. 1417-1435.

## Appendix A – EPMA Compositional Analyses (Dissolution Re-precipitation Texture)

### Monazite

Elements were acquired using analyzing crystals LLIF for Sm Lα, Gd Lα, Dy Lα, Nd Lα, Pr Lα, Yb Lα, Er Lα, LPET for Th Mα, Ca Kα, U Mβ, Ce Lα, Y Lα, La Lα, and TAP for Si Kα, P Kα.

The standards were $ThO_2$ for Th Mα, U-2 (10.00% $UO_2$ in diopside glass) for Si Kα, Ca Kα, U Mβ, $CePO_4$ (USNM 168484) for P Kα, Ce Lα, $DyPO_4$ (USNM 168485) for Dy Lα, $ErPO_4$ (USNM 168486) for Er Lα, $GdPO_4$ (USNM 168488) for Gd Lα, $LaPO_4$ (USNM 168490) for La Lα, $NdPO_4$ (USNM 168492) for Nd Lα, $PrPO_4$ (USNM 168493) for Pr Lα, SmPO4 (USNM 168494) for Sm Lα, $YbPO_4$ (USNM 168498) for Yb Lα, and $YPO_4$ (USNM 168499) for Y Lα.

The counting time was 40 seconds for Ce Lα, Nd Lα, 50 seconds for P Kα, 60 seconds for Sm Lα, Pr Lα, 80 seconds for Dy Lα, Er Lα, 100 seconds for Th Mα, Yb Lα, Ca Kα, 110 seconds for Y Lα, 120 seconds for La Lα, 160 seconds for U Mβ, 200 seconds for Gd Lα, and 280 seconds for Si Kα. The off peak counting time was 40 seconds for Ce Lα, Nd Lα, 50 seconds for P Kα, 60 seconds for Sm Lα, Pr Lα, 80 seconds for Dy Lα, Er Lα, 100 seconds for Th Mα, Yb Lα, Ca Kα, 110 seconds for Y Lα, 120 seconds for La Lα, 160 seconds for U Mβ, 200 seconds for Gd Lα, and 280 seconds for Si Kα. Off peak correction method was Linear for all elements.

Unknown and standard intensities were corrected for deadtime. Standard intensities were corrected for standard drift over time. Interference corrections were applied to Sm for interference by Ce, and to Gd for interference by Ce, La, Nd, and to P for interference by Y, and to Nd for interference by Ce, and to La for interference by Nd, and to Pr for interference by La, Y, and to Yb for interference by Dy, Y, and to Er for interference by Nd. See Donovan et al., (1993) for detail.

Results are the average of 5 points and detection limits ranged from .002 weight percent for Si Kα to .011 weight percent for Y Lα to .022 weight percent for U Mβ to .029 weight percent for Er Lα to .034 weight percent for Nd Lα. Analytical sensitivity (at the 99% confidence level) ranged from .138 percent relative for P Kα to .411 percent relative for Ca Kα to .840 percent relative for Gd Lα to 1.982 percent relative for Si Kα to 23.946 percent relative for Yb Lα.

Oxygen was calculated by cation stoichiometry and included in the matrix correction. The matrix correction method was ZAF or Phi-Rho-Z Calculations and the mass absorption coefficients dataset was LINEMU Henke (LBL, 1985) < 10KeV / CITZMU > 10KeV. The ZAF or Phi-Rho-Z algorithm utilized was Armstrong/Love Scott (Armstrong, 1988).

### Xenotime

Elements were acquired using analyzing crystals LLIF for Sm Lα, Gd Lα, Dy Lα, Nd Lα, Pr Lα, Yb Lα, Er Lα, LPET for Th Mα, Ca Kα, U Mβ, Ce Lα, Y Lα, La Lα, and TAP for Si Kα, P Kα.

The standards were $ThO_2$ for Th Mα, U-2 (10.00% UO2 in diopside glass) for Si Kα, Ca Kα, U Mβ, $CePO_4$ (USNM 168484) for P Kα, Ce Lα, $DyPO_4$ (USNM 168485) for Dy Lα, $ErPO_4$ (USNM 168486) for Er Lα, $GdPO_4$ (USNM 168488) for Gd Lα, $LaPO_4$ (USNM

168490) for La Lα, $NdPO_4$ (USNM 168492) for Nd Lα, $PrPO_4$ (USNM 168493) for Pr Lα, $SmPO_4$ (USNM 168494) for Sm Lα, $YbPO_4$ (USNM 168498) for Yb Lα, and $YPO_4$ (USNM 168499) for Y Lα.

The counting time was 40 seconds for Y Lα, 50 seconds for P Kα, 60 seconds for Dy Lα, Yb Lα, Er Lα, 80 seconds for Gd Lα, 100 seconds for Ce Lα, U Mβ, 120 seconds for Sm Lα, Pr Lα, Nd Lα, La Lα, 130 seconds for Th Mα, 140 seconds for Ca Kα, and 280 seconds for Si Kα. The off peak counting time was 40 seconds for Y Lα, 50 seconds for P Kα, 60 seconds for Dy Lα, Yb Lα, Er Lα, 80 seconds for Gd Lα, 100 seconds for Ce Lα, U Mβ, 120 seconds for Sm Lα, Pr Lα, Nd Lα, La Lα, 130 seconds for Th Mα, 140 seconds for Ca Kα, and 280 seconds for Si Kα. The off peak correction method was Linear for all elements.

Unknown and standard intensities were corrected for deadtime. Standard intensities were corrected for standard drift over time. Interference corrections were applied to Sm for interference by Ce, and to Gd for interference by Ce, La, Nd, and to P for interference by Y, and to Nd for interference by Ce, and to La for interference by Nd, and to Pr for interference by La, Y, and to Yb for interference by Dy, Y, and to Er for interference by Nd. See Donovan et al., (1993) for detail.

Results are the average of 5 points and detection limits ranged from .002 weight percent for Si Kα to .014 weight percent for La Lα to .017 weight percent for Sm Lα to .027 weight percent for U Mβ to .038 weight percent for Yb Lα. Analytical sensitivity (at the 99% confidence level) ranged from .123 percent relative for P Kα to .625 percent relative for Dy Lα to .915 percent relative for Yb Lα to 2.145 percent relative for Nd Lα to 43.429 percent relative for La Lα.

Oxygen was calculated by cation stoichiometry and included in the matrix correction. The matrix correction method was ZAF or Phi-Rho-Z Calculations and the mass absorption coefficients dataset was LINEMU Henke (LBL, 1985) < 10KeV / CITZMU > 10KeV. The ZAF or Phi-Rho-Z algorithm utilized was Armstrong/Love Scott (Armstrong 1988).

## Appendix B – EPMA Compositional Analyses (Monazite Breakdown Reaction)

### Monazite

Operating conditions were 40 degrees takeoff angle, beam energy of 15 keV, beam current of 80 nA and a beam diameter of 2 µm. Elements were acquired using analyzing crystals LLIF for La Lα, Pr Lα, Nd Lα, Sm Lα, Eu Lα, Gd Lα, Dy Lα, Er Lα, Ce Lα, Fe Kα, Mn Kα, LPET for Th ma, P Kα, Y Lα, Pb Mβ, U Mβ, Ti Kα, Cl Kα, Ca Kα, and TAP for Al Kα, Mg Kα, Sr Lα, Si Lα.

The standards were $ThO_2$ for Th Mα, MnO synthetic for Mn Kα, U-2 (10.00% $UO_2$ in diopside glass) for U Mβ, REE-4 glass for Al Kα, Er Lα, Dy Lα, REE-1 glass for Eu Lα, Gd Lα, REE-2 glass for Nd Lα, Sm Lα, REE-3 glass for Ce Lα, Y Lα, Strontium titanate ($SrTiO_3$) for Sr Lα, Ti Kα, $Ca_{10}(PO_4)_6Cl_2$ (halogen corrected) for Cl Kα, Diopside (Chesterman) for Mg Kα, Ca Kα, Si Kα, Magnetite U.C. #3380 for Fe Kα, $LaPO_4$ (USNM 168490) for La Lα, P Kα, $PrPO_4$ (USNM 168493) for Pr Lα, and Pyromorphite (Cameca) for Pb Mβ.

The counting time was 10 seconds for La Lα, P Kα, Ce Lα, 20 seconds for Th Mα, Pr Lα, Nd Lα, Fe Kα, Ti Kα, Sr Lα, Mn Kα, 40 seconds for Ca Kα, Eu Lα, Cl Kα, Dy Lα, Er Lα, 50 seconds for Al Kα, Mg Kα, 60 seconds for Gd Lα, Pb Mβ, U Mβ, Si Kα, Sm Lα, and 80 seconds for Y Lα. The off peak counting time was 10 seconds for La Lα, P Kα, Ce Lα, 20 seconds for Th Mα, Pr Lα, Nd Lα, Fe Kα, Ti Kα, Sr Lα, Mn Kα, 40 seconds for Ca Kα, Eu Lα, Cl Kα, Dy Lα, Er Lα, 50 seconds for Al Kα, Mg Kα, 60 seconds for Gd Lα, Pb Mβ, U Mβ, Si Kα, Sm Lα, and 80 seconds for Y Lα. The off peak correction method was Linear for all elements.

Unknown and standard intensities were corrected for deadtime. Standard intensities were corrected for standard drift over time. Interference corrections were applied to La for interference by Nd, and to Pr for interference by La, and to Nd for interference by Ce, and to Sm for interference by Ce, Pr, and to Eu for interference by Pr, Nd, and to Gd for interference by Nd, Ce, and to Dy for interference by Th, and to Er for interference by Nd, and to Pb for interference by Y, and to U for interference by Gd, Th, and to Si for interference by La, Th, and to Al for interference by Th, and to Ca for interference by Th. See Donovan et al., (1993) for detail.

Results are the average of 10 points and detection limits ranged from .000 weight percent for Fe Kα to .005 weight percent for Si Kα to .024 weight percent for Gd Lα to .032 weight percent for Dy Lα to .059 weight percent for Ce Lα. Analytical sensitivity (at the 99% confidence level) ranged from .000 percent relative for Fe Kα to .520 percent relative for Ce Lα to 1.094 percent relative for Ca Kα to 6.678 percent relative for Cl Kα to 787.779 percent relative for Er Lα.

Oxygen was calculated by cation stoichiometry and included in the matrix correction. Oxygen equivalent from halogens (F/Cl/Br/I), was not subtracted in the matrix correction. The matrix correction method was ZAF or Phi-Rho-Z Calculations and the mass absorption coefficients dataset was LINEMU Henke (LBL, 1985) < 10KeV / CITZMU > 10KeV. The ZAF or Phi-Rho-Z algorithm utilized was Armstrong/Love Scott (Armstrong, 1988).

**Apatite**

Operating conditions were 40 degrees takeoff angle, and beam energies of 7 keV for F Kα, and 15 keV for Pr Lα, Nd Lα, Sm Lα, Eu Lα, Gd Lα, Dy Lα, Er Lα, Pb Mβ, U Mβ, Si Kα, Al Kα, Ca Kα, Th Mα, P Kα, Y Lα, Ce Lα, Fe Kα, Ti Kα, Cl Kα, Mg Kα, Sr Lα, Mn Kα, La Lα. Beam current was 20 nA for F Kα, and 80 nA for Pr Lα, Nd Lα, Sm Lα, Eu Lα, Gd Lα, Dy Lα, Er Lα, Pb Mβ, U Mβ, Si Kα, Al Kα, Ca Kα, Th Mα, P Kα, Y Lα, Ce Lα, Fe Kα, Ti Kα, Cl Kα, Mg Kα, Sr Lα, Mn Kα, La Lα. Beam size was 2 microns for La Lα, Pr Lα, Nd Lα, Sm Lα, Eu Lα, Gd Lα, Dy Lα, Er Lα, Pb Mβ, U Mβ, Si Kα, Al Kα, Ca Kα, Th Mα, P Kα, Y Lα, Ce Lα, Fe Kα, Ti Kα, Cl Kα, Mg Kα, Sr Lα, Mn Kα, and 5 microns for F Kα. Elements were acquired using analyzing crystals LLIF for La Lα, Pr Lα, Nd Lα, Sm Lα, Eu Lα, Gd Lα, Dy Lα, Er Lα, Ce Lα, Fe Kα, Mn Kα, LPET for Th Mα, P Kα, Y Lα, Pb Mβ, U Mβ, Ti Kα, Cl Kα, Ca Kα, TAP for Al Kα, Mg Kα, Sr Lα, Si Kα, and PC0 for F Kα.

The standards were $ThO_2$ for Th Mα, MnO synthetic for Mn Kα, U-2 (10.00% $UO_2$ in diopside glass) for U Mβ, REE-4 glass for Al Kα, Er Lα, Dy Lα, REE-1 glass for Eu Lα, Gd Lα, REE-2 glass for Nd Lα, Sm Lα, REE-3 glass for Ce Lα, Y Lα, Strontium titanate ($SrTiO_3$) for Sr Lα, Ti Kα, $Ca_{10}(PO_4)_6Cl_2$ (halogen corrected) for Cl Kα, Topaz, F bearing (halogen corrected) for F Kα, Diopside (Chesterman) for Mg Kα, Si Kα, Magnetite U.C. #3380 for Fe Kα, Fluor-apatite USNM 104021 for P Kα, Ca Kα, LaPO4 (USNM 168490) for La Lα, $PrPO_4$ (USNM 168493) for Pr Lα, and Pyromorphite (Cameca) for Pb Mβ.

The counting time was 10 seconds for Ca Kα, P Kα, Fe Kα, 20 seconds for F Kα, 30 seconds for Er Lα, La Lα, Th Mα, Nd Lα, Ce Lα, Eu Lα, Dy Lα, 40 seconds for Ti Kα, Sr Lα, Mn Kα, Pr Lα, 50 seconds for Gd Lα, Sm Lα, 60 seconds for U Mβ, Mg Kα, Si Kα, Al Kα, Pb Mβ, and 80 seconds for Y Lα, Cl Kα. The off peak counting time was 10 seconds for Ca Kα, P Kα, Fe Kα, 20 seconds for F Kα, 30 seconds for Er Lα, La Lα, Th Mα, Nd Lα, Ce Lα, Eu Lα, Dy Lα, 40 seconds for Ti Kα, Sr Lα, Mn Kα, Pr Lα, 50 seconds for Gd Lα, Sm Lα, 60 seconds for U Mβ, Mg Kα, Si Kα, Al Kα, Pb Mβ, and 80 seconds for Y Lα, Cl Kα. Off Peak correction method was Linear for La Lα, Pr Lα, Nd Lα, Sm Lα, Eu Lα, Gd Lα, Dy Lα, Er Lα, Pb Mβ, U Mβ, Si Kα, Al Kα, Ca Kα, Th Mα, P Kα, Y Lα, Ce Lα, Fe Kα, Ti Kα, Cl Kα, Mg Kα, Sr Lα, Mn Kα, and Polynomial for F Kα.

Unknown and standard intensities were corrected for deadtime. Standard intensities were corrected for standard drift over time. Interference corrections were applied to La for interference by Nd, and to Pr for interference by La, and to Nd for interference by Ce, and to Sm for interference by Ce, Pr, and to Eu for interference by Pr, Nd, and to Gd for interference by Nd, Ce, and to Dy for interference by Th, and to Er for interference by Nd, and to Pb for interference by Y, and to U for interference by Gd, Th, and to Si for interference by La, Th, and to Al for interference by Th, and to Ca for interference by Th, and to F for interference by Ce. See Donovan et al., (1993) for detail.

Results are the average of 10 points and detection limits ranged from .000 weight percent for Fe Kα to .003 weight percent for Al Kα to .017 weight percent for Sm Lα to .023 weight percent for Pb Mβ to .049 weight percent for F Kα. Analytical sensitivity (at the 99% confidence level) ranged from .000 percent relative for Fe Kα to .297 percent relative for P Kα to 15.214 percent relative for Pb Mβ to 33.127 percent relative for Mg Kα to 1526.501 percent relative for Er Lα.

Oxygen was calculated by cation stoichiometry and included in the matrix correction. Oxygen equivalent from halogens (F/Cl/Br/I), was not subtracted in the matrix correction.

The exponential or polynomial background fit was utilized. See Donovan et al., (2011) for detail. The matrix correction method was ZAF or Phi-Rho-Z Calculations and the mass absorption coefficients dataset was LINEMU Henke (LBL, 1985) < 10KeV / CITZMU > 10KeV. The ZAF or Phi-Rho-Z algorithm utilized was Armstrong/Love Scott (Armstrong, 1988).

**Allanite**

Operating conditions were 40 degrees takeoff angle, and beam energies of 7 keV for F Kα, and 15 keV for Pr Lα, Nd Lα, Sm Lα, Eu Lα, Gd Lα, Dy Lα, Er Lα, Pb Mβ, U Mβ, Si Kα, Al Kα, Ca Kα, Th Mα, P Kα, Y Lα, Ce Lα, Fe Kα, Ti Kα, Cl Kα, Mg Kα, Sr Lα, Mn Kα, La Lα. Beam current was 20 nA for F Kα, and 80 nA for Pr Lα, Nd Lα, Sm Lα, Eu Lα, Gd Lα, Dy Lα, Er Lα, Pb Mβ, U Mβ, Si Kα, Al Kα, Ca Kα, Th Mα, P Kα, Y Lα, Ce Lα, Fe Kα, Ti Kα, Cl Kα, Mg Kα, Sr Lα, Mn Kα, La Lα. Beam size was 2 microns for La Lα, Pr Lα, Nd Lα, Sm Lα, Eu Lα, Gd Lα, Dy Lα, Er Lα, Pb Mβ, U Mβ, Si Kα, Al Kα, Ca Kα, Th Mα, P Kα, Y Lα, Ce Lα, Fe Kα, Ti Kα, Cl Kα, Mg Kα, Sr Lα, Mn Kα, and 5 microns for F Kα. Elements were acquired using analyzing crystals LLIF for La Lα, Pr Lα, Nd Lα, Sm Lα, Eu Lα, Gd Lα, Dy Lα, Er Lα, Ce Lα, Fe Kα, Mn Kα, LPET for Th Mα, P Kα, Y Lα, Pb Mβ, U Mβ, Ti Kα, Cl Kα, Ca Kα, TAP for Al Kα, Mg Kα, Sr Lα, Si Kα, and PC0 for F Kα.

The standards were $ThO_2$ for Th Mα, MnO synthetic for Mn Kα, U-2 (10.00% $UO_2$ in diopside glass) for U Mβ, REE-4 glass for Al Kα, Er Lα, Dy Lα, REE-1 glass for Eu Lα, Gd Lα, REE-2 glass for Nd Lα, Sm Lα, REE-3 glass for Ce Lα, Y Lα, Strontium titanate ($SrTiO_3$) for Sr Lα, Ti Kα, $Ca_{10}(PO_4)_6Cl_2$ (halogen corrected) for Cl Kα, Topaz, F bearing (halogen corrected) for F Kα, Diopside (Chesterman) for Ca Kα, Si Kα, Mg Kα, Magnetite U.C. #3380 for Fe Kα, $LaPO_4$ (USNM 168490) for P Kα, La Lα, $PrPO_4$ (USNM 168493) for Pr Lα, and Pyromorphite (Cameca) for Pb Mβ.

The counting time was 10 seconds for La Lα, Nd Lα, Si Kα, Ce Lα, Fe Kα, 20 seconds for Pr Lα, Al Kα, Ca Kα, P Kα, Sm Lα, Gd Lα, F Kα, 30 seconds for Eu Lα, Y Lα, Dy Lα, Er Lα, Cl Kα, Th Mα, 40 seconds for Sr Lα, Mn Kα, Ti Kα, and 60 seconds for Pb Mβ, U Mβ, Mg Kα. The off peak counting time was 10 seconds for La Lα, Nd Lα, Si Kα, Ce Lα, Fe Kα, 20 seconds for Pr Lα, Al Kα, Ca Kα, P Kα, Sm Lα, Gd Lα, F Kα, 30 seconds for Eu Lα, Y Lα, Dy Lα, Er Lα, Cl Kα, Th Mα, 40 seconds for Sr Lα, Mn Kα, Ti Kα, and 60 seconds for Pb Mβ, U Mβ, Mg Kα. Off Peak correction method was Linear for La Lα, Pr Lα, Nd Lα, Sm Lα, Eu Lα, Gd Lα, Pb Mβ, U Mβ, Si Kα, Al Kα, Ca Kα, Th Mα, P Kα, Y Lα, Ce Lα, Fe Kα, Ti Kα, Cl Kα, Mg Kα, Sr Lα, Mn Kα, F Kα, Low Only for Dy Lα, and Slope (Hi) for Er Lα.

Unknown and standard intensities were corrected for deadtime. Standard intensities were corrected for standard drift over time. Interference corrections were applied to La for interference by Nd, and to Pr for interference by La, and to Nd for interference by Ce, and to Sm for interference by Ce, Pr, and to Eu for interference by Pr, Nd, and to Gd for interference by Nd, Ce, and to Dy for interference by Th, and to Er for interference by Nd, and to Pb for interference by Y, and to U for interference by Gd, Th, and to Si for interference by La, Th, and to Al for interference by Th, and to Ca for interference by Th, and to F for interference by Ce. See Donovan et al., (1993) for detail.

Results are the average of 5 points and detection limits ranged from .000 weight percent for P Kα to .006 weight percent for Al Kα to .025 weight percent for U Mβ to .035

weight percent for Gd Lα to .049 weight percent for F Kα. Analytical sensitivity (at the 99% confidence level) ranged from .000 percent relative for P Kα to .695 percent relative for Ti Kα to 1.735 percent relative for La Lα to 5.582 percent relative for Dy Lα to 290.285 percent relative for Pb Mβ.

Oxygen was calculated by cation stoichiometry and included in the matrix correction. Oxygen equivalent from halogens (F/Cl/Br/I), was not subtracted in the matrix correction. The matrix correction method was ZAF or Phi-Rho-Z Calculations and the mass absorption coefficients dataset was LINEMU Henke (LBL, 1985) < 10KeV / CITZMU > 10KeV. The ZAF or Phi-Rho-Z algorithm utilized was Armstrong/Love Scott (Armstrong, 1988).

## Appendix C – EPMA Compositional Data (Dissolution-Re-precipitation Texture)

| | M5 | | M8 | | M9 | | X2 | | X4 | | X5 | |
|---|---|---|---|---|---|---|---|---|---|---|---|---|
| | **mean (n=5)** | **1 σ std** | **mean (n=5)** | **1 σ std** | **mean (n=5)** | **1 σ std** | **mean (n=4)** | **1 σ std** | **mean (n=5)** | **1 σ std** | **mean (n=10)** | **1 σ std** |
| $P_2O_5$ | 28.55 | 0.601 | 28.50 | 0.681 | 28.72 | 0.335 | 33.33 | 0.964 | 31.59 | 0.412 | 30.97 | 0.620 |
| $SiO_2$ | 0.25 | 0.097 | 0.45 | 0.288 | 0.13 | 0.037 | 0.67 | 0.411 | 1.13 | 0.143 | 1.60 | 0.342 |
| $ThO_2$ | 5.25 | 0.512 | 5.78 | 1.168 | 3.96 | 0.237 | 1.10 | 0.664 | 1.86 | 0.334 | 2.32 | 0.618 |
| $UO_2$ | 0.25 | 0.063 | 0.47 | 0.313 | 0.19 | 0.093 | 1.24 | 0.802 | 2.10 | 0.267 | 3.20 | 0.551 |
| $Y_2O_3$ | 1.27 | 1.094 | 1.99 | 1.147 | 2.84 | 0.216 | 42.16 | 0.918 | 41.00 | 0.424 | 39.24 | 0.735 |
| $La_2O_3$ | 12.89 | 0.665 | 12.55 | 0.473 | 13.87 | 0.304 | 0.01 | 0.008 | 0.02 | 0.009 | 0.02 | 0.010 |
| $Ce_2O_3$ | 28.93 | 0.742 | 27.95 | 0.600 | 28.52 | 0.537 | 0.14 | 0.059 | 0.15 | 0.006 | 0.14 | 0.006 |
| $Pr_2O_3$ | 3.37 | 0.156 | 3.08 | 0.192 | 2.95 | 0.210 | 0.05 | 0.009 | 0.05 | 0.007 | 0.06 | 0.008 |
| $Nd_2O_3$ | 12.53 | 0.540 | 11.80 | 0.634 | 11.05 | 0.257 | 0.54 | 0.030 | 0.52 | 0.018 | 0.56 | 0.020 |
| $Sm_2O_3$ | 2.05 | 0.117 | 2.10 | 0.153 | 1.84 | 0.059 | 0.64 | 0.028 | 0.62 | 0.008 | 0.66 | 0.026 |
| $Gd_2O_3$ | 1.15 | 0.201 | 1.48 | 0.166 | 1.37 | 0.117 | 2.33 | 0.088 | 2.26 | 0.058 | 2.26 | 0.050 |
| $Dy_2O_3$ | 0.40 | 0.303 | 0.65 | 0.248 | 0.80 | 0.039 | 5.11 | 0.144 | 5.01 | 0.106 | 4.91 | 0.121 |
| $Er_2O_3$ | 0.07 | 0.081 | 0.11 | 0.086 | 0.17 | 0.031 | 4.25 | 0.176 | 4.12 | 0.079 | 4.06 | 0.074 |
| $Yb_2O3$ | 0.01 | 0.028 | 0.02 | 0.036 | 0.07 | 0.020 | 3.37 | 0.371 | 3.27 | 0.281 | 3.49 | 0.101 |
| CaO | 1.06 | 0.067 | 1.06 | 0.173 | 0.82 | 0.068 | 0.03 | 0.012 | 0.04 | 0.006 | 0.05 | 0.007 |
| **SUM** | **98.04** | **0.483** | **97.99** | **0.430** | **97.31** | **0.734** | **94.97** | **0.771** | **93.75** | **0.455** | **93.54** | **0.225** |
| | | | | | | | | | | | | |
| P | 0.9763 | 0.00913 | 0.9720 | 0.01228 | 0.9815 | 0.00395 | 0.9856 | 0.01582 | 0.9607 | 0.00621 | 0.9503 | 0.01231 |
| Si | 0.0101 | 0.00398 | 0.0183 | 0.01179 | 0.0052 | 0.00150 | 0.0236 | 0.01451 | 0.0404 | 0.00530 | 0.0581 | 0.01291 |
| Th | 0.0483 | 0.00514 | 0.0531 | 0.01124 | 0.0364 | 0.00235 | 0.0088 | 0.00534 | 0.0152 | 0.00277 | 0.0192 | 0.00528 |
| U | 0.0022 | 0.00057 | 0.0042 | 0.00284 | 0.0017 | 0.00085 | 0.0097 | 0.00631 | 0.0168 | 0.00222 | 0.0258 | 0.00467 |
| Y | 0.0273 | 0.02332 | 0.0425 | 0.02408 | 0.0610 | 0.00448 | 0.7836 | 0.00886 | 0.7837 | 0.00377 | 0.7568 | 0.00978 |
| La | 0.1921 | 0.00869 | 0.1865 | 0.00518 | 0.2066 | 0.00457 | 0.0002 | 0.00011 | 0.0003 | 0.00012 | 0.0002 | 0.00014 |
| Ce | 0.4280 | 0.01360 | 0.4123 | 0.00832 | 0.4216 | 0.00804 | 0.0017 | 0.00076 | 0.0020 | 0.00006 | 0.0018 | 0.00007 |
| Pr | 0.0497 | 0.00269 | 0.0452 | 0.00311 | 0.0434 | 0.00287 | 0.0006 | 0.00012 | 0.0006 | 0.00009 | 0.0007 | 0.00010 |
| Nd | 0.1808 | 0.00954 | 0.1698 | 0.01073 | 0.1593 | 0.00350 | 0.0067 | 0.00042 | 0.0067 | 0.00024 | 0.0073 | 0.00027 |
| Sm | 0.0285 | 0.00180 | 0.0292 | 0.00240 | 0.0257 | 0.00084 | 0.0078 | 0.00036 | 0.0077 | 0.00012 | 0.0083 | 0.00029 |
| Gd | 0.0154 | 0.00260 | 0.0198 | 0.00225 | 0.0183 | 0.00159 | 0.0270 | 0.00103 | 0.0269 | 0.00065 | 0.0272 | 0.00047 |
| Dy | 0.0052 | 0.00391 | 0.0084 | 0.00313 | 0.0105 | 0.00048 | 0.0575 | 0.00145 | 0.0580 | 0.00099 | 0.0574 | 0.00114 |
| Er | 0.0009 | 0.00101 | 0.0014 | 0.00106 | 0.0021 | 0.00037 | 0.0462 | 0.00137 | 0.0461 | 0.00092 | 0.0458 | 0.00062 |
| Yb | 0.0002 | 0.00034 | 0.0003 | 0.00044 | 0.0009 | 0.00025 | 0.0359 | 0.00371 | 0.0358 | 0.00314 | 0.0385 | 0.00099 |
| Ca | 0.0457 | 0.00308 | 0.0458 | 0.00781 | 0.0357 | 0.00297 | 0.0010 | 0.00044 | 0.0015 | 0.00025 | 0.0019 | 0.00029 |
| **SUM** | **2.0108** | **0.00402** | **2.0087** | **0.00162** | **2.0098** | **0.00287** | **1.9959** | **0.00219** | **2.0026** | **0.00132** | **1.9994** | **0.00221** |

| | M1 (mnz) | | M4 (mnz) | | Mx3 (mnz) | | M1 (xtm) | | M4 (xtm) | | Mx3 (xtm) | |
|---|---|---|---|---|---|---|---|---|---|---|---|---|
| | **mean (n=5)** | **1 σ std** | **mean (n=5)** | **1 σ std** | **mean (n=5)** | **1 σ std** | **mean (n=5)** | **1 σ std** | **mean (n=5)** | **1 σ std** | **mean (n=5)** | **1 σ std** |
| $P_2O_5$ | 24.19 | 3.158 | 27.29 | 0.417 | 25.44 | 1.305 | 33.29 | 0.320 | 32.94 | 0.335 | 32.62 | 0.800 |
| $SiO_2$ | 1.27 | 0.389 | 0.86 | 0.190 | 1.84 | 0.578 | 0.41 | 0.217 | 0.28 | 0.173 | 0.66 | 0.278 |
| $ThO_2$ | 8.84 | 1.676 | 7.37 | 0.803 | 9.57 | 2.013 | 0.97 | 0.347 | 0.73 | 0.357 | 1.57 | 0.785 |
| $UO_2$ | 0.29 | 0.226 | 0.13 | 0.034 | 0.20 | 0.070 | 0.74 | 0.501 | 0.43 | 0.303 | 1.08 | 0.505 |
| $Y_2O_3$ | 1.72 | 0.939 | 0.73 | 0.317 | 1.25 | 0.394 | 42.72 | 0.391 | 43.13 | 0.440 | 42.74 | 1.019 |
| $La_2O_3$ | 11.30 | 0.624 | 12.38 | 0.522 | 11.32 | 1.007 | 0.08 | 0.020 | 0.11 | 0.012 | 0.07 | 0.020 |
| $Ce_2O_3$ | 25.10 | 1.245 | 27.59 | 0.897 | 26.02 | 1.360 | 0.20 | 0.040 | 0.29 | 0.035 | 0.25 | 0.039 |
| $Pr_2O_3$ | 2.95 | 0.118 | 3.19 | 0.088 | 3.03 | 0.163 | 0.04 | 0.011 | 0.06 | 0.006 | 0.05 | 0.017 |
| $Nd_2O_3$ | 11.44 | 0.544 | 12.32 | 0.267 | 11.61 | 0.822 | 0.40 | 0.053 | 0.41 | 0.066 | 0.48 | 0.056 |
| $Sm_2O_3$ | 2.26 | 0.081 | 2.49 | 0.052 | 2.34 | 0.114 | 0.63 | 0.028 | 0.62 | 0.058 | 0.62 | 0.044 |
| $Gd_2O_3$ | 1.92 | 0.111 | 1.89 | 0.130 | 1.83 | 0.162 | 3.41 | 0.474 | 3.60 | 0.278 | 2.84 | 0.275 |
| $Dy_2O_3$ | 0.63 | 0.207 | 0.46 | 0.130 | 0.59 | 0.079 | 6.85 | 0.756 | 7.41 | 0.396 | 6.02 | 0.374 |
| $Er_2O_3$ | 0.08 | 0.076 | 0.04 | 0.022 | 0.08 | 0.024 | 3.33 | 0.209 | 3.21 | 0.160 | 3.59 | 0.216 |
| $Yb_2O3$ | 0.04 | 0.036 | 0.01 | 0.017 | 0.01 | 0.016 | 1.41 | 0.487 | 1.04 | 0.347 | 1.76 | 0.440 |
| CaO | 0.85 | 0.180 | 0.92 | 0.152 | 0.53 | 0.082 | 0.04 | 0.022 | 0.04 | 0.019 | 0.05 | 0.037 |
| **SUM** | **92.89** | **4.582** | **97.66** | **0.523** | **95.67** | **2.131** | **94.52** | **0.312** | **94.30** | **0.331** | **94.39** | **0.889** |
| | | | | | | | | | | | | |
| P | 0.9030 | 0.04535 | 0.9500 | 0.01006 | 0.9121 | 0.02500 | 0.9880 | 0.00559 | 0.9836 | 0.00706 | 0.9747 | 0.01077 |
| Si | 0.0561 | 0.01568 | 0.0354 | 0.00799 | 0.0783 | 0.02573 | 0.0142 | 0.00764 | 0.0099 | 0.00611 | 0.0235 | 0.01012 |
| Th | 0.0896 | 0.01995 | 0.0690 | 0.00784 | 0.0926 | 0.02119 | 0.0077 | 0.00279 | 0.0058 | 0.00288 | 0.0126 | 0.00646 |
| U | 0.0028 | 0.00201 | 0.0012 | 0.00032 | 0.0019 | 0.00072 | 0.0058 | 0.00392 | 0.0034 | 0.00238 | 0.0085 | 0.00408 |
| Y | 0.0399 | 0.01953 | 0.0160 | 0.00697 | 0.0285 | 0.00956 | 0.7969 | 0.00476 | 0.8094 | 0.00500 | 0.8028 | 0.01004 |
| La | 0.1854 | 0.01874 | 0.1877 | 0.00731 | 0.1766 | 0.01125 | 0.0010 | 0.00025 | 0.0014 | 0.00017 | 0.0009 | 0.00026 |
| Ce | 0.4084 | 0.03415 | 0.4153 | 0.01204 | 0.4035 | 0.01516 | 0.0026 | 0.00051 | 0.0037 | 0.00046 | 0.0032 | 0.00052 |
| Pr | 0.0479 | 0.00524 | 0.0479 | 0.00121 | 0.0468 | 0.00146 | 0.0005 | 0.00013 | 0.0007 | 0.00007 | 0.0006 | 0.00023 |
| Nd | 0.1817 | 0.01779 | 0.1809 | 0.00329 | 0.1756 | 0.00808 | 0.0051 | 0.00067 | 0.0052 | 0.00085 | 0.0061 | 0.00075 |
| Sm | 0.0346 | 0.00255 | 0.0353 | 0.00067 | 0.0342 | 0.00156 | 0.0076 | 0.00032 | 0.0076 | 0.00074 | 0.0076 | 0.00051 |
| Gd | 0.0283 | 0.00247 | 0.0257 | 0.00187 | 0.0257 | 0.00177 | 0.0396 | 0.00536 | 0.0421 | 0.00331 | 0.0332 | 0.00296 |
| Dy | 0.0088 | 0.00242 | 0.0061 | 0.00174 | 0.0081 | 0.00129 | 0.0774 | 0.00824 | 0.0842 | 0.00450 | 0.0684 | 0.00367 |
| Er | 0.0011 | 0.00098 | 0.0005 | 0.00028 | 0.0011 | 0.00033 | 0.0364 | 0.00239 | 0.0352 | 0.00171 | 0.0394 | 0.00240 |
| Yb | 0.0005 | 0.00046 | 0.0001 | 0.00022 | 0.0002 | 0.00021 | 0.0151 | 0.00525 | 0.0112 | 0.00374 | 0.0190 | 0.00479 |
| Ca | 0.0406 | 0.01012 | 0.0407 | 0.00682 | 0.0239 | 0.00348 | 0.0015 | 0.00082 | 0.0017 | 0.00071 | 0.0020 | 0.00141 |
| **SUM** | **2.0287** | **0.02724** | **2.0118** | **0.00234** | **2.0090** | **0.00367** | **1.9993** | **0.00108** | **2.0051** | **0.00119** | **2.0026** | **0.00240** |

# Appendix D – EPMA Compositional Data (Monazite Breakdown Reaction)

| | M1 (mnz) | | M2 (mnz) | | M17 (mnz) | | M1 (ap) | | M2 (ap) | | M17 (ap) | | M1 (aln) | | M2 (aln) | | M17 (aln) | |
|---|---|---|---|---|---|---|---|---|---|---|---|---|---|---|---|---|---|---|
| | **mean (n=10)** | **1 σ std** | **mean (n=10)** | **1 σ std** | **mean (n=10)** | **1 σ std** | **mean (n=10)** | **1 σ std** | **mean (n=9)** | **1 σ std** | **mean (n=10)** | **1 σ std** | **mean (n=10)** | **1 σ std** | **mean (n=10)** | **1 σ std** | **mean (n=10)** | **1 σ std** |
| $SiO_2$ | 1.253 | 0.1593 | 1.325 | 0.3105 | 0.836 | 0.2082 | 0.286 | 0.1191 | 0.228 | 0.0663 | 0.761 | 0.3523 | 31.997 | 1.4159 | 31.576 | 0.9109 | 32.368 | 0.8181 |
| CaO | 0.347 | 0.1790 | 0.377 | 0.1495 | 0.438 | 0.1491 | 55.404 | 0.5720 | 56.054 | 0.3527 | 54.368 | 0.8619 | 9.855 | 0.6033 | 10.167 | 0.6157 | 9.442 | 0.3547 |
| $Al_2O_3$ | n.d. | n.d. | n.d. | n.d. | n.d. | n.d. | 0.147 | 0.3547 | 0.007 | 0.0143 | 0.013 | 0.0641 | 15.694 | 0.8320 | 15.610 | 1.0903 | 14.478 | 0.4877 |
| $P_2O_5$ | 27.317 | 0.3502 | 27.337 | 0.7099 | 28.307 | 0.4152 | 32.069 | 2.6929 | 32.786 | 2.9012 | 30.742 | 6.9370 | n.d. | n.d. | n.d. | n.d. | n.d. | n.d. |
| $La_2O_3$ | 14.177 | 0.5464 | 14.052 | 0.5359 | 12.160 | 0.4230 | 0.031 | 0.0223 | 0.046 | 0.0204 | 0.028 | 0.0180 | 5.109 | 0.6090 | 5.058 | 0.4912 | 4.131 | 0.5275 |
| $Ce_2O_3$ | 30.037 | 0.9419 | 29.883 | 1.1847 | 27.478 | 0.9347 | 0.105 | 0.0457 | 0.094 | 0.0278 | 0.089 | 0.0882 | 10.846 | 1.2124 | 10.535 | 0.9831 | 8.389 | 1.0806 |
| $Pr_2O_3$ | 3.177 | 0.0932 | 3.148 | 0.1430 | 3.022 | 0.0870 | 0.050 | 0.0191 | 0.015 | 0.0241 | 0.023 | 0.0275 | 1.148 | 0.1125 | 1.113 | 0.0882 | 0.989 | 0.0607 |
| $Nd_2O_3$ | 11.621 | 0.4573 | 11.552 | 0.6570 | 11.081 | 0.3962 | 0.111 | 0.0496 | 0.092 | 0.0267 | 0.114 | 0.0600 | 3.971 | 0.4086 | 3.901 | 0.2872 | 3.393 | 0.1453 |
| $Sm_2O_3$ | 1.773 | 0.1510 | 1.739 | 0.0766 | 2.358 | 0.0663 | 0.076 | 0.0342 | 0.046 | 0.0323 | 0.066 | 0.0328 | 0.593 | 0.0735 | 0.545 | 0.0343 | 0.667 | 0.0678 |
| $Eu_2O_3$ | 0.054 | 0.0310 | 0.045 | 0.0176 | 0.034 | 0.0146 | n.d. | n.d. | n.d. | n.d. | 0.012 | 0.0242 | n.d. | n.d. | n.d. | n.d. | n.d. | n.d. |
| $Gd_2O_3$ | 0.827 | 0.1519 | 0.839 | 0.0612 | 1.612 | 0.0715 | 0.043 | 0.0339 | 0.015 | 0.0445 | 0.088 | 0.1275 | 0.251 | 0.0730 | 0.239 | 0.0558 | 0.441 | 0.0865 |
| $Dy_2O_3$ | 0.412 | 0.0805 | 0.401 | 0.0765 | 1.138 | 0.1901 | 0.056 | 0.0231 | 0.051 | 0.0166 | 0.122 | 0.0663 | 0.210 | 0.0480 | 0.206 | 0.0299 | 0.379 | 0.0512 |
| $Er_2O_3$ | n.d. | n.d. | n.d. | n.d. | 0.223 | 0.0845 | 0.022 | 0.0163 | 0.015 | 0.0171 | 0.072 | 0.0895 | n.d. | n.d. | n.d. | n.d. | 0.028 | 0.0137 |
| $Y_2O_3$ | 1.185 | 0.3410 | 1.186 | 0.4177 | 4.584 | 1.2181 | 0.340 | 0.1444 | 0.252 | 0.0266 | 1.136 | 0.5011 | 0.426 | 0.1396 | 0.423 | 0.0867 | 1.014 | 0.1536 |
| $ThO_2$ | 5.794 | 1.4635 | 6.331 | 1.8352 | 3.960 | 0.7205 | 0.034 | 0.0971 | 0.030 | 0.0403 | 2.564 | 8.0964 | 1.364 | 0.7934 | 1.237 | 0.4033 | 1.878 | 0.3076 |
| $UO_2$ | 0.056 | 0.0356 | 0.054 | 0.0380 | 0.354 | 0.1362 | n.d. | n.d. | n.d. | n.d. | n.d. | n.d. | 0.006 | 0.0187 | 0.005 | 0.0118 | 0.040 | 0.0226 |
| PbO | 0.296 | 0.1759 | 0.178 | 0.0769 | 0.340 | 0.1201 | n.d. | n.d. | n.d. | n.d. | n.d. | n.d. | 0.047 | 0.0563 | 0.075 | 0.1162 | 0.029 | 0.0280 |
| FeO | n.d. | n.d. | n.d. | n.d. | n.d. | n.d. | n.d. | n.d. | n.d. | n.d. | n.d. | n.d. | 12.866 | 0.9758 | 12.916 | 1.1510 | 12.894 | 0.5432 |
| $TiO_2$ | n.d. | n.d. | n.d. | n.d. | n.d. | n.d. | n.d. | n.d. | n.d. | n.d. | n.d. | n.d. | 0.330 | 0.1801 | 0.521 | 0.0746 | 0.720 | 0.0521 |
| MgO | n.d. | n.d. | n.d. | n.d. | n.d. | n.d. | n.d. | n.d. | n.d. | n.d. | n.d. | n.d. | 0.851 | 0.2859 | 0.922 | 0.2103 | 0.898 | 0.1224 |
| MnO | n.d. | n.d. | n.d. | n.d. | n.d. | n.d. | n.d. | n.d. | n.d. | n.d. | n.d. | n.d. | 0.243 | 0.0561 | 0.262 | 0.0339 | 0.238 | 0.0146 |
| SrO | n.d. | n.d. | n.d. | n.d. | n.d. | n.d. | n.d. | n.d. | n.d. | n.d. | n.d. | n.d. | 0.120 | 0.0486 | 0.120 | 0.0371 | 0.201 | 0.0270 |
| Cl | 0.039 | 0.0176 | 0.044 | 0.0248 | 0.033 | 0.0075 | 0.033 | 0.0101 | 0.019 | 0.0108 | 0.015 | 0.0163 | 0.052 | 0.0400 | 0.087 | 0.1064 | 0.026 | 0.0037 |
| F | 0.036 | 0.0303 | 0.072 | 0.0336 | -0.043 | 0.0647 | 3.549 | 0.3295 | 3.874 | 0.2979 | 3.961 | 0.1855 | n.d. | n.d. | n.d. | n.d. | 0.302 | 0.8270 |
| **SUM** | **98.398** | **0.2449** | **98.560** | **0.5121** | **97.916** | **0.3468** | **92.281** | **2.8068** | **93.580** | **3.1829** | **94.177** | **1.5924** | **95.895** | **0.7086** | **95.408** | **1.0315** | **92.917** | **3.0511** |

| | M1 (mnz) | | M2 (mnz) | | M17 (mnz) | | M1 (ap) | | M2 (ap) | | M17 (ap) | | M1 (aln) | | M2 (aln) | | M17 (aln) | |
|---|---|---|---|---|---|---|---|---|---|---|---|---|---|---|---|---|---|---|
| | **mean (n=10)** | **1 σ std** | **mean (n=10)** | **1 σ std** | **mean (n=10)** | **1 σ std** | **mean (n=10)** | **1 σ std** | **mean (n=9)** | **1 σ std** | **mean (n=10)** | **1 σ std** | **mean (n=10)** | **1 σ std** | **mean (n=10)** | **1 σ std** | **mean (n=10)** | **1 σ std** |
| | **2 cations pfu** | | | | | | **8 cations pfu** | | | | | | **8 cations pfu** | | | | | |
| Si | 0.051 | 0.0066 | 0.054 | 0.0130 | 0.034 | 0.0086 | 0.025 | 0.0105 | 0.019 | 0.0051 | 0.067 | 0.0331 | 2.995 | 0.0906 | 2.970 | 0.0605 | 3.069 | 0.0810 |
| Ca | 0.015 | 0.0078 | 0.016 | 0.0066 | 0.019 | 0.0063 | 5.101 | 0.2195 | 5.063 | 0.2121 | 5.033 | 0.4659 | 0.989 | 0.0650 | 1.025 | 0.0529 | 0.959 | 0.0309 |
| Al | n.d. | n.d. | n.d. | n.d. | n.d. | n.d. | 0.014 | 0.0352 | 0.001 | 0.0014 | 0.001 | 0.0070 | 1.731 | 0.0656 | 1.730 | 0.0981 | 1.618 | 0.0448 |
| P | 0.940 | 0.0082 | 0.937 | 0.0157 | 0.961 | 0.0079 | 2.326 | 0.1018 | 2.332 | 0.1008 | 2.205 | 0.4044 | n.d. | n.d. | n.d. | n.d. | n.d. | n.d. |
| La | 0.213 | 0.0077 | 0.210 | 0.0063 | 0.180 | 0.0071 | 0.001 | 0.0007 | 0.001 | 0.0007 | 0.001 | 0.0006 | 0.177 | 0.0236 | 0.176 | 0.0192 | 0.144 | 0.0155 |
| Ce | 0.447 | 0.0129 | 0.443 | 0.0141 | 0.403 | 0.0161 | 0.003 | 0.0015 | 0.003 | 0.0009 | 0.003 | 0.0027 | 0.373 | 0.0473 | 0.363 | 0.0381 | 0.291 | 0.0307 |
| Pr | 0.047 | 0.0013 | 0.046 | 0.0018 | 0.044 | 0.0014 | 0.002 | 0.0006 | 0.000 | 0.0007 | 0.001 | 0.0010 | 0.039 | 0.0044 | 0.038 | 0.0036 | 0.034 | 0.0018 |
| Nd | 0.169 | 0.0061 | 0.167 | 0.0084 | 0.159 | 0.0067 | 0.003 | 0.0016 | 0.003 | 0.0008 | 0.004 | 0.0018 | 0.133 | 0.0154 | 0.131 | 0.0115 | 0.115 | 0.0047 |
| Sm | 0.025 | 0.0020 | 0.024 | 0.0009 | 0.033 | 0.0010 | 0.002 | 0.0010 | 0.001 | 0.0009 | 0.002 | 0.0012 | 0.019 | 0.0025 | 0.018 | 0.0013 | 0.022 | 0.0025 |
| Eu | 0.001 | 0.0004 | 0.001 | 0.0002 | 0.000 | 0.0002 | n.d. | n.d. | n.d. | n.d. | 0.000 | 0.0008 | n.d. | n.d. | n.d. | n.d. | n.d. | n.d. |
| Gd | 0.011 | 0.0020 | 0.011 | 0.0008 | 0.021 | 0.0009 | 0.001 | 0.0010 | 0.000 | 0.0012 | 0.002 | 0.0040 | 0.008 | 0.0021 | 0.007 | 0.0017 | 0.014 | 0.0028 |
| Dy | 0.005 | 0.0011 | 0.005 | 0.0010 | 0.015 | 0.0024 | 0.002 | 0.0006 | 0.001 | 0.0004 | 0.003 | 0.0019 | 0.006 | 0.0014 | 0.006 | 0.0009 | 0.012 | 0.0017 |
| Er | n.d. | n.d. | n.d. | n.d. | 0.003 | 0.0011 | 0.001 | 0.0005 | 0.000 | 0.0004 | 0.002 | 0.0031 | n.d. | n.d. | n.d. | n.d. | 0.001 | 0.0004 |
| Y | 0.026 | 0.0074 | 0.026 | 0.0091 | 0.098 | 0.0257 | 0.016 | 0.0068 | 0.011 | 0.0013 | 0.053 | 0.0262 | 0.021 | 0.0066 | 0.021 | 0.0041 | 0.051 | 0.0083 |
| Th | 0.054 | 0.0137 | 0.058 | 0.0173 | 0.036 | 0.0068 | 0.001 | 0.0020 | 0.001 | 0.0008 | 0.064 | 0.2036 | 0.029 | 0.0164 | 0.026 | 0.0086 | 0.041 | 0.0074 |
| U | 0.001 | 0.0003 | 0.000 | 0.0003 | 0.003 | 0.0012 | n.d. | n.d. | n.d. | n.d. | n.d. | n.d. | 0.000 | 0.0004 | 0.000 | 0.0002 | 0.001 | 0.0005 |
| Pb | 0.003 | 0.0019 | 0.002 | 0.0008 | 0.004 | 0.0013 | n.d. | n.d. | n.d. | n.d. | n.d. | n.d. | 0.001 | 0.0014 | 0.002 | 0.0029 | 0.001 | 0.0007 |
| Fe | n.d. | n.d. | n.d. | n.d. | n.d. | n.d. | n.d. | n.d. | n.d. | n.d. | n.d. | n.d. | 1.009 | 0.0924 | 1.018 | 0.1072 | 1.022 | 0.0367 |
| Ti | n.d. | n.d. | n.d. | n.d. | n.d. | n.d. | n.d. | n.d. | n.d. | n.d. | n.d. | n.d. | 0.023 | 0.0125 | 0.037 | 0.0058 | 0.051 | 0.0048 |
| Mg | n.d. | n.d. | n.d. | n.d. | n.d. | n.d. | n.d. | n.d. | n.d. | n.d. | n.d. | n.d. | 0.119 | 0.0392 | 0.129 | 0.0289 | 0.127 | 0.0150 |
| Mn | n.d. | n.d. | n.d. | n.d. | n.d. | n.d. | n.d. | n.d. | n.d. | n.d. | n.d. | n.d. | 0.019 | 0.0043 | 0.021 | 0.0026 | 0.019 | 0.0010 |
| Sr | 0.000 | 0.0000 | 0.000 | 0.0000 | 0.000 | 0.0000 | 0.000 | 0.0000 | 0.000 | 0.0000 | 0.000 | 0.0000 | 0.006 | 0.0025 | 0.007 | 0.0020 | 0.011 | 0.0017 |
| Cl | 0.003 | 0.0012 | 0.003 | 0.0017 | 0.002 | 0.0005 | 0.005 | 0.0015 | 0.003 | 0.0015 | 0.002 | 0.0024 | 0.008 | 0.0065 | 0.014 | 0.0167 | 0.004 | 0.0006 |
| F | 0.005 | 0.0039 | 0.009 | 0.0043 | n.d. | n.d. | 0.964 | 0.0918 | 1.032 | 0.0876 | 1.082 | 0.1038 | n.d. | n.d. | n.d. | n.d. | 0.085 | 0.2310 |
| **SUM** | **2.014** | **0.0028** | **2.014** | **0.0034** | **2.008** | **0.0049** | **8.464** | **0.1530** | **8.472** | **0.1519** | **8.525** | **0.3836** | **7.701** | **0.0762** | **7.722** | **0.0493** | **7.689** | **0.0958** |

# Appendix E – U-Pb Geochronologic Data

**12TM15-03** zircon (spot size: 7 μm, frequency: 3 Hz, 80 shot count, laser energy: 3 mJ at 75%)

| | | | | | ISOTOPIC RATIOS | | | | | | | | APPARENT AGES (Ma) | | | |
|---|---|---|---|---|---|---|---|---|---|---|---|---|---|---|---|---|
| | Pb (ppm) | U (ppm) | Th (ppm) | Th/U | $^{207}Pb/^{206}Pb$ | 2σ % | $^{207}Pb/^{235}U$ | 2σ % | $^{206}Pb/^{238}U$ | 2σ % | Rho | % disc.* | $^{207}Pb/^{206}Pb$ | 2σ abs | $^{206}Pb/^{238}U$ | 2σ abs |
| spot 1 | 249 | 1443 | 322 | 0.22 | 0.10493 | 0.922 | 4.194 | 1.838 | 0.2893 | 1.590 | 0.87 | 2.08 | 1713 | 16 | 1638 | 23 |
| spot 2 | 130 | 1129 | 172 | 0.15 | 0.10413 | 0.961 | 4.078 | 1.948 | 0.2832 | 1.695 | 0.87 | 2.61 | 1699 | 16 | 1607 | 24 |
| spot 3 | 66 | 552 | 85 | 0.15 | 0.10520 | 0.970 | 4.320 | 2.059 | 0.2973 | 1.816 | 0.88 | 1.13 | 1718 | 17 | 1677 | 27 |
| spot 4 | 98 | 994 | 123 | 0.12 | 0.10315 | 0.949 | 4.105 | 1.972 | 0.2892 | 1.729 | 0.88 | 1.34 | 1681 | 16 | 1637 | 25 |
| spot 5 | 60 | 514 | 76 | 0.15 | 0.10256 | 0.970 | 4.130 | 2.280 | 0.2907 | 2.064 | 0.91 | 0.91 | 1671 | 16 | 1644 | 30 |
| spot 6 | 113 | 1094 | 139 | 0.13 | 0.10338 | 0.925 | 4.069 | 1.951 | 0.2853 | 1.717 | 0.88 | 1.79 | 1686 | 16 | 1618 | 25 |
| spot 7 | 117 | 908 | 128 | 0.14 | 0.10372 | 0.940 | 3.995 | 1.928 | 0.2791 | 1.684 | 0.87 | 2.90 | 1692 | 16 | 1586 | 23 |
| spot 8 | 103 | 101 | 119 | 1.19 | 0.10428 | 1.195 | 4.320 | 1.977 | 0.2984 | 1.575 | 0.80 | 0.77 | 1701 | 21 | 1683 | 23 |
| spot 9 | 108 | 108 | 130 | 1.21 | 0.10308 | 1.082 | 4.159 | 2.478 | 0.2916 | 2.229 | 0.90 | 1.09 | 1680 | 19 | 1649 | 32 |
| spot 10 | 113 | 976 | 136 | 0.14 | 0.10452 | 0.939 | 4.119 | 1.899 | 0.2848 | 1.650 | 0.87 | 2.47 | 1706 | 16 | 1619 | 23 |
| spot 11 | 119 | 1122 | 142 | 0.13 | 0.10485 | 0.931 | 4.199 | 2.143 | 0.2901 | 1.930 | 0.90 | 1.89 | 1712 | 16 | 1641 | 28 |
| spot 12 | 135 | 1032 | 157 | 0.15 | 0.10508 | 0.931 | 4.305 | 2.097 | 0.2980 | 1.879 | 0.90 | 0.89 | 1716 | 16 | 1680 | 28 |
| spot 13 | 143 | 1116 | 181 | 0.16 | 0.10410 | 0.934 | 3.971 | 2.137 | 0.2757 | 1.922 | 0.90 | 3.70 | 1698 | 16 | 1569 | 27 |
| spot 14 | 76 | 227 | 91 | 0.40 | 0.10086 | 0.992 | 3.942 | 2.082 | 0.2841 | 1.830 | 0.88 | 0.74 | 1640 | 17 | 1612 | 26 |
| spot 15 | 105 | 928 | 120 | 0.13 | 0.10542 | 0.947 | 4.279 | 2.157 | 0.2941 | 1.938 | 0.90 | 1.63 | 1722 | 16 | 1661 | 28 |
| spot 16 | 140 | 849 | 124 | 0.15 | 0.10580 | 0.931 | 4.397 | 2.021 | 0.3010 | 1.794 | 0.89 | 0.83 | 1728 | 16 | 1696 | 27 |
| spot 17 | 100 | 981 | 138 | 0.14 | 0.09116 | 0.935 | 2.975 | 1.859 | 0.2364 | 1.607 | 0.86 | 2.41 | 1450 | 14 | 1368 | 20 |
| spot 18 | 82 | 888 | 98 | 0.11 | 0.10485 | 0.920 | 4.183 | 2.145 | 0.2890 | 1.938 | 0.90 | 2.02 | 1712 | 16 | 1636 | 28 |
| spot 19 | 136 | 207 | 165 | 0.80 | 0.10469 | 1.121 | 4.270 | 2.459 | 0.2970 | 2.189 | 0.89 | 0.84 | 1708 | 20 | 1675 | 33 |
| spot 20 | 132 | 1055 | 169 | 0.16 | 0.10519 | 0.933 | 4.072 | 2.076 | 0.2804 | 1.854 | 0.89 | 3.58 | 1718 | 16 | 1593 | 26 |
| spot 21 | 149 | 1051 | 187 | 0.18 | 0.10462 | 0.929 | 4.080 | 1.845 | 0.2822 | 1.595 | 0.86 | 2.93 | 1708 | 16 | 1602 | 23 |
| spot 22 | 85 | 916 | 103 | 0.11 | 0.10468 | 0.945 | 4.138 | 2.192 | 0.2882 | 1.978 | 0.90 | 2.21 | 1709 | 16 | 1632 | 29 |
| spot 23 | 138 | 1043 | 178 | 0.17 | 0.10515 | 0.941 | 4.041 | 2.359 | 0.2774 | 2.163 | 0.92 | 3.99 | 1717 | 16 | 1578 | 30 |
| spot 24 | 152 | 1027 | 190 | 0.19 | 0.10469 | 0.922 | 4.172 | 2.268 | 0.2896 | 2.072 | 0.91 | 2.01 | 1709 | 16 | 1639 | 30 |
| spot 25 | 117 | 837 | 145 | 0.17 | 0.10433 | 0.927 | 4.188 | 2.357 | 0.2907 | 2.167 | 0.92 | 1.70 | 1702 | 16 | 1644 | 32 |
| spot 26 | 137 | 872 | 172 | 0.20 | 0.10472 | 0.936 | 4.188 | 2.337 | 0.2896 | 2.141 | 0.92 | 1.89 | 1709 | 16 | 1639 | 31 |
| spot 27 | 123 | 1010 | 156 | 0.15 | 0.10515 | 0.924 | 4.192 | 2.197 | 0.2910 | 1.993 | 0.91 | 1.70 | 1717 | 16 | 1646 | 29 |
| spot 28 | 128 | 1238 | 171 | 0.14 | 0.10194 | 0.935 | 3.890 | 2.236 | 0.2757 | 2.031 | 0.91 | 2.61 | 1660 | 16 | 1569 | 28 |

**12TM15-03** zircon (spot size: 7 µm, frequency: 3 Hz, 80 shot count, laser energy: 3 mJ at 75%)

| | | | | | ISOTOPIC RATIOS | | | | | | | | APPARENT AGES (Ma) | | | |
|---|---|---|---|---|---|---|---|---|---|---|---|---|---|---|---|---|
| | Pb (ppm) | U (ppm) | Th (ppm) | Th/U | $^{207}Pb/^{206}Pb$ | 2σ % | $^{207}Pb/^{235}U$ | 2σ % | $^{206}Pb/^{238}U$ | 2σ % | Rho | % disc.* | $^{207}Pb/^{206}Pb$ | 2σ abs | $^{206}Pb/^{238}U$ | 2σ abs |
| spot 29 | 68 | 763 | 90 | 0.12 | 0.10386 | 0.972 | 4.149 | 2.378 | 0.2903 | 2.170 | 0.91 | 1.46 | 1694 | 17 | 1642 | 31 |
| spot 30 | 84 | 858 | 107 | 0.13 | 0.10407 | 0.934 | 4.148 | 2.093 | 0.2883 | 1.873 | 0.89 | 1.78 | 1698 | 16 | 1633 | 27 |
| spot 31 | 111 | 1143 | 162 | 0.14 | 0.09788 | 0.951 | 3.489 | 2.233 | 0.2573 | 2.021 | 0.90 | 3.18 | 1584 | 15 | 1476 | 27 |
| spot 32 | 112 | 954 | 157 | 0.16 | 0.09510 | 1.111 | 3.386 | 2.414 | 0.2566 | 2.143 | 0.89 | 1.56 | 1529 | 18 | 1476 | 29 |
| spot 33 | 145 | 1030 | 186 | 0.18 | 0.10483 | 0.944 | 4.296 | 2.233 | 0.2965 | 2.024 | 0.91 | 1.08 | 1711 | 16 | 1673 | 30 |
| spot 34 | 96 | 997 | 122 | 0.12 | 0.10510 | 0.939 | 4.358 | 2.268 | 0.3003 | 2.065 | 0.91 | 0.77 | 1717 | 16 | 1692 | 31 |
| spot 35 | 137 | 969 | 176 | 0.18 | 0.10499 | 0.920 | 4.304 | 2.284 | 0.2965 | 2.091 | 0.92 | 1.14 | 1714 | 16 | 1673 | 31 |
| spot 36 | 130 | 1232 | 167 | 0.14 | 0.10478 | 0.922 | 4.202 | 2.390 | 0.2902 | 2.205 | 0.92 | 1.95 | 1710 | 16 | 1641 | 32 |
| spot 37 | 123 | 1062 | 169 | 0.16 | 0.10452 | 0.939 | 3.999 | 2.466 | 0.2763 | 2.280 | 0.92 | 3.49 | 1706 | 16 | 1577 | 31 |
| spot 38 | 104 | 913 | 135 | 0.15 | 0.10497 | 0.947 | 4.190 | 2.219 | 0.2891 | 2.006 | 0.90 | 2.08 | 1714 | 16 | 1636 | 29 |
| spot 39 | 134 | 860 | 169 | 0.20 | 0.10527 | 0.944 | 4.273 | 2.001 | 0.2947 | 1.765 | 0.88 | 1.32 | 1719 | 16 | 1665 | 26 |
| spot 40 | 76 | 582 | 92 | 0.16 | 0.10511 | 0.997 | 4.306 | 2.107 | 0.2963 | 1.856 | 0.88 | 1.26 | 1716 | 17 | 1672 | 28 |
| spot 41 | 105 | 1016 | 127 | 0.12 | 0.10513 | 0.924 | 4.172 | 2.349 | 0.2871 | 2.160 | 0.92 | 2.52 | 1717 | 16 | 1626 | 31 |
| spot 42 | 79 | 239 | 99 | 0.42 | 0.10360 | 1.035 | 3.934 | 2.382 | 0.2750 | 2.145 | 0.90 | 3.83 | 1689 | 18 | 1565 | 30 |
| spot 43 | 114 | 1084 | 139 | 0.13 | 0.10395 | 0.942 | 4.037 | 2.270 | 0.2809 | 2.065 | 0.91 | 2.82 | 1696 | 16 | 1595 | 29 |
| spot 44 | 109 | 1022 | 128 | 0.13 | 0.10523 | 0.924 | 4.305 | 2.197 | 0.2960 | 1.993 | 0.91 | 1.07 | 1718 | 16 | 1675 | 30 |
| spot 45 | 69 | 238 | 85 | 0.36 | 0.10473 | 1.019 | 4.220 | 2.569 | 0.2926 | 2.358 | 0.92 | 1.27 | 1709 | 18 | 1654 | 34 |
| spot 46 | 64 | 419 | 79 | 0.19 | 0.10233 | 0.981 | 3.976 | 2.117 | 0.2825 | 1.876 | 0.89 | 1.56 | 1667 | 17 | 1603 | 27 |
| spot 47 | 107 | 982 | 133 | 0.14 | 0.10437 | 0.945 | 4.104 | 2.368 | 0.2856 | 2.171 | 0.92 | 2.29 | 1703 | 16 | 1619 | 31 |
| spot 48 | 79 | 940 | 97 | 0.10 | 0.10456 | 0.948 | 4.149 | 2.518 | 0.2872 | 2.333 | 0.93 | 2.21 | 1707 | 16 | 1626 | 34 |
| spot 49 | 129 | 1175 | 164 | 0.14 | 0.10420 | 0.927 | 4.084 | 2.118 | 0.2835 | 1.905 | 0.90 | 2.61 | 1700 | 16 | 1608 | 27 |
| spot 50 | 228 | 1322 | 282 | 0.21 | 0.10498 | 0.926 | 4.257 | 2.279 | 0.2930 | 2.082 | 0.91 | 1.81 | 1714 | 16 | 1656 | 31 |
| spot 51 | 127 | 987 | 154 | 0.16 | 0.10500 | 0.931 | 4.243 | 2.409 | 0.2925 | 2.222 | 0.92 | 1.69 | 1714 | 16 | 1653 | 32 |
| spot 52 | 132 | 656 | 196 | 0.30 | 0.08923 | 0.939 | 2.978 | 2.391 | 0.2411 | 2.198 | 0.92 | 0.65 | 1409 | 14 | 1392 | 28 |
| spot 53 | 88 | 309 | 103 | 0.33 | 0.10381 | 0.958 | 4.130 | 2.909 | 0.2876 | 2.747 | 0.94 | 2.03 | 1693 | 16 | 1628 | 39 |
| spot 54 | 88 | 942 | 107 | 0.11 | 0.10483 | 0.934 | 4.277 | 2.333 | 0.2946 | 2.138 | 0.92 | 1.56 | 1711 | 16 | 1664 | 31 |
| spot 55 | 140 | 1211 | 176 | 0.15 | 0.10328 | 0.937 | 4.110 | 2.902 | 0.2876 | 2.747 | 0.95 | 1.60 | 1684 | 16 | 1628 | 40 |
| spot 56 | 209 | 1511 | 253 | 0.17 | 0.10451 | 0.931 | 4.280 | 2.695 | 0.2965 | 2.530 | 0.94 | 1.08 | 1706 | 16 | 1672 | 37 |
| spot 57 | 38 | 426 | 46 | 0.11 | 0.10445 | 0.954 | 4.260 | 2.533 | 0.2941 | 2.346 | 0.93 | 1.32 | 1705 | 16 | 1661 | 34 |
| spot 58 | 94 | 952 | 121 | 0.13 | 0.10354 | 0.934 | 4.056 | 2.134 | 0.2815 | 1.918 | 0.90 | 2.88 | 1689 | 16 | 1598 | 27 |
| spot 59 | 238 | 1390 | 299 | 0.22 | 0.10464 | 0.929 | 4.178 | 2.413 | 0.2874 | 2.227 | 0.92 | 2.46 | 1708 | 16 | 1628 | 32 |

**12TM15-03** zircon (spot size: 7 µm, frequency: 3 Hz, 80 shot count, laser energy: 3 mJ at 75%)

| | | | | | ISOTOPIC RATIOS | | | | | | | | APPARENT AGES (Ma) | | | |
|---|---|---|---|---|---|---|---|---|---|---|---|---|---|---|---|---|
| | Pb (ppm) | U (ppm) | Th (ppm) | Th/U | $^{207}Pb/^{206}Pb$ | 2σ % | $^{207}Pb/^{235}U$ | 2σ % | $^{206}Pb/^{238}U$ | 2σ % | Rho | % disc.* | $^{207}Pb/^{206}Pb$ | 2σ abs | $^{206}Pb/^{238}U$ | 2σ abs |
| spot 60 | 136 | 1234 | 166 | 0.13 | 0.10457 | 0.922 | 4.238 | 2.475 | 0.2917 | 2.297 | 0.93 | 1.82 | 1707 | 16 | 1649 | 33 |
| spot 61 | 51 | 708 | 67 | 0.09 | 0.09427 | 0.948 | 3.329 | 2.581 | 0.2541 | 2.401 | 0.93 | 1.92 | 1513 | 15 | 1458 | 31 |
| spot 62 | 150 | 1061 | 193 | 0.18 | 0.10335 | 0.937 | 3.935 | 2.663 | 0.2728 | 2.493 | 0.94 | 4.18 | 1685 | 16 | 1554 | 35 |
| spot 63 | 109 | 445 | 138 | 0.31 | 0.10212 | 0.960 | 4.083 | 2.502 | 0.2856 | 2.311 | 0.92 | 1.92 | 1664 | 16 | 1618 | 33 |
| spot 64 | 81 | 409 | 105 | 0.26 | 0.09880 | 1.097 | 3.749 | 2.453 | 0.2735 | 2.194 | 0.89 | 1.41 | 1601 | 19 | 1558 | 30 |
| spot 65 | 92 | 895 | 116 | 0.13 | 0.10178 | 1.035 | 4.014 | 2.591 | 0.2820 | 2.376 | 0.92 | 2.19 | 1657 | 18 | 1600 | 33 |
| spot 66 | 135 | 1273 | 161 | 0.13 | 0.10410 | 0.939 | 4.300 | 2.604 | 0.2964 | 2.429 | 0.93 | 1.08 | 1698 | 16 | 1672 | 36 |
| spot 67 | 104 | 1051 | 123 | 0.12 | 0.10352 | 0.929 | 4.231 | 2.346 | 0.2924 | 2.155 | 0.92 | 1.51 | 1690 | 16 | 1653 | 32 |
| spot 68 | 146 | 1129 | 194 | 0.17 | 0.10258 | 0.930 | 3.951 | 2.234 | 0.2757 | 2.031 | 0.91 | 3.63 | 1671 | 16 | 1569 | 28 |
| spot 69 | 92 | 939 | 111 | 0.12 | 0.10277 | 0.940 | 4.217 | 2.462 | 0.2945 | 2.275 | 0.92 | 0.72 | 1675 | 16 | 1663 | 33 |
| spot 70 | 71 | 839 | 94 | 0.11 | 0.10368 | 0.948 | 3.910 | 2.984 | 0.2722 | 2.829 | 0.95 | 4.51 | 1691 | 16 | 1551 | 39 |
| spot 71 | 189 | 1377 | 234 | 0.17 | 0.10369 | 0.929 | 4.118 | 2.363 | 0.2854 | 2.172 | 0.92 | 2.35 | 1692 | 16 | 1618 | 31 |
| spot 72 | 127 | 1276 | 154 | 0.12 | 0.10408 | 0.922 | 4.250 | 2.714 | 0.2938 | 2.553 | 0.94 | 1.63 | 1698 | 16 | 1659 | 38 |
| spot 73 | 144 | 1078 | 189 | 0.18 | 0.10395 | 0.922 | 4.050 | 2.655 | 0.2812 | 2.489 | 0.94 | 3.26 | 1696 | 16 | 1596 | 35 |
| spot 74 | 163 | 1392 | 200 | 0.14 | 0.10399 | 0.918 | 4.240 | 2.683 | 0.2935 | 2.521 | 0.94 | 1.33 | 1696 | 16 | 1658 | 37 |
| spot 75 | 122 | 1024 | 149 | 0.15 | 0.10367 | 0.929 | 4.300 | 2.710 | 0.2985 | 2.546 | 0.94 | 0.48 | 1691 | 16 | 1683 | 38 |
| spot 76 | 62 | 646 | 80 | 0.12 | 0.10217 | 0.960 | 4.090 | 3.040 | 0.2877 | 2.885 | 0.95 | 1.23 | 1664 | 16 | 1629 | 42 |
| spot 77 | 88 | 443 | 117 | 0.26 | 0.10218 | 0.978 | 4.010 | 2.667 | 0.2821 | 2.481 | 0.93 | 2.12 | 1664 | 17 | 1601 | 35 |
| spot 78 | 109 | 860 | 147 | 0.17 | 0.10366 | 0.940 | 4.081 | 2.573 | 0.2839 | 2.395 | 0.93 | 2.36 | 1691 | 16 | 1610 | 34 |
| spot 79 | 98 | 993 | 124 | 0.12 | 0.10284 | 0.930 | 4.090 | 2.899 | 0.2877 | 2.746 | 0.95 | 1.72 | 1676 | 16 | 1629 | 39 |
| spot 80 | 60 | 185 | 89 | 0.48 | 0.09522 | 1.064 | 3.430 | 3.509 | 0.2602 | 3.344 | 0.95 | 1.21 | 1532 | 18 | 1489 | 44 |
| spot 81 | 104 | 746 | 133 | 0.18 | 0.10384 | 0.922 | 4.230 | 2.905 | 0.2941 | 2.754 | 0.95 | 1.27 | 1694 | 16 | 1660 | 40 |
| spot 82 | 85 | 821 | 115 | 0.14 | 0.10307 | 0.935 | 3.990 | 2.738 | 0.2798 | 2.573 | 0.94 | 2.83 | 1680 | 16 | 1589 | 36 |
| spot 83 | 112 | 1066 | 146 | 0.14 | 0.10210 | 0.944 | 4.050 | 2.643 | 0.2876 | 2.469 | 0.93 | 1.23 | 1663 | 16 | 1628 | 35 |
| spot 84 | 94 | 964 | 119 | 0.12 | 0.10293 | 0.949 | 4.137 | 2.157 | 0.2891 | 1.937 | 0.90 | 0.91 | 1677 | 16 | 1645 | 28 |
| spot 85 | 100 | 840 | 133 | 0.16 | 0.10330 | 0.937 | 4.080 | 2.633 | 0.2845 | 2.460 | 0.93 | 2.11 | 1684 | 16 | 1613 | 35 |
| spot 86 | 189 | 224 | 237 | 1.06 | 0.10315 | 1.093 | 4.279 | 2.544 | 0.3003 | 2.298 | 0.90 | 0.30 | 1681 | 19 | 1692 | 34 |
| spot 87 | 141 | 992 | 172 | 0.17 | 0.10444 | 0.936 | 4.310 | 2.844 | 0.2979 | 2.685 | 0.94 | 1.07 | 1705 | 16 | 1679 | 40 |
| spot 88 | 125 | 1126 | 155 | 0.14 | 0.10296 | 0.932 | 4.170 | 2.593 | 0.2934 | 2.420 | 0.93 | 0.12 | 1678 | 16 | 1671 | 36 |
| spot 89 | 83 | 122 | 103 | 0.85 | 0.10246 | 1.224 | 4.190 | 2.784 | 0.2960 | 2.500 | 0.90 | 0.00 | 1668 | 21 | 1670 | 37 |
| spot 90 | 110 | 1071 | 139 | 0.13 | 0.10424 | 0.927 | 4.190 | 2.570 | 0.2920 | 2.397 | 0.93 | 1.15 | 1701 | 16 | 1651 | 35 |

**12TM15-03** zircon (spot size: 7 µm, frequency: 3 Hz, 80 shot count, laser energy: 3 mJ at 75%)

| | | | | | ISOTOPIC RATIOS | | | | | | | | APPARENT AGES (Ma) | | | |
|---|---|---|---|---|---|---|---|---|---|---|---|---|---|---|---|---|
| | Pb (ppm) | U (ppm) | Th (ppm) | Th/U | $^{207}Pb/^{206}Pb$ | 2σ % | $^{207}Pb/^{235}U$ | 2σ % | $^{206}Pb/^{238}U$ | 2σ % | Rho | % disc.* | $^{207}Pb/^{206}Pb$ | 2σ abs | $^{206}Pb/^{238}U$ | 2σ abs |
| spot 91 | 83 | 918 | 106 | 0.12 | 0.10263 | 0.943 | 4.020 | 2.728 | 0.2852 | 2.560 | 0.94 | 1.61 | 1672 | 16 | 1616 | 37 |
| spot 92 | 109 | 929 | 129 | 0.14 | 0.10449 | 0.945 | 4.240 | 2.814 | 0.2943 | 2.650 | 0.94 | 1.02 | 1705 | 16 | 1662 | 39 |
| spot 93 | 114 | 1084 | 137 | 0.13 | 0.10302 | 0.930 | 4.182 | 2.455 | 0.2949 | 2.272 | 0.93 | 0.24 | 1679 | 16 | 1665 | 33 |
| spot 94 | 132 | 1013 | 157 | 0.15 | 0.10381 | 0.922 | 4.200 | 3.095 | 0.2945 | 2.954 | 0.95 | 0.54 | 1693 | 16 | 1662 | 43 |
| spot 95 | 72 | 728 | 82 | 0.11 | 0.10355 | 0.958 | 4.130 | 2.501 | 0.2900 | 2.310 | 0.92 | 1.40 | 1689 | 16 | 1641 | 33 |
| spot 96 | 128 | 939 | 132 | 0.14 | 0.10433 | 0.936 | 4.390 | 2.928 | 0.3064 | 2.774 | 0.95 | 0.58 | 1702 | 16 | 1721 | 42 |
| spot 97 | 221 | 1534 | 282 | 0.18 | 0.10366 | 0.925 | 4.004 | 2.321 | 0.2818 | 2.129 | 0.92 | 2.06 | 1691 | 16 | 1600 | 30 |
| spot 98 | 136 | 1099 | 161 | 0.15 | 0.10396 | 0.925 | 3.980 | 2.982 | 0.2787 | 2.835 | 0.95 | 2.97 | 1696 | 16 | 1583 | 40 |
| spot 99 | 116 | 1268 | 140 | 0.11 | 0.10108 | 0.933 | 2.535 | 2.884 | 0.1832 | 2.729 | 0.95 | 18.08 | 1644 | 15 | 1084 | 27 |

**MVUr2 zircon** (spot size: 19 µm, frequency: 4 Hz, 80 shot count, laser energy: 4 mJ at 75%)

| | | | | | ISOTOPIC RATIOS | | | | | | | | APPARENT AGES (Ma) | | | |
|---|---|---|---|---|---|---|---|---|---|---|---|---|---|---|---|---|
| | Pb (ppm) | U (ppm) | Th (ppm) | Th/U | $^{207}Pb/^{206}Pb$ | 2σ % | $^{207}Pb/^{235}U$ | 2σ % | $^{206}Pb/^{238}U$ | 2σ % | Rho | % disc.* | $^{207}Pb/^{206}Pb$ | 2σ abs | $^{206}Pb/^{238}U$ | 2σ abs |
| spot 1 | 183 | 1014 | 189 | 0.19 | 0.10597 | 2.417 | 4.322 | 3.018 | 0.2947 | 1.807 | 0.60 | 2.10 | 1732 | 42 | 1664 | 28 |
| spot 2 | 213 | 1008 | 216 | 0.21 | 0.10558 | 2.422 | 4.361 | 2.974 | 0.2990 | 1.727 | 0.58 | 1.16 | 1724 | 42 | 1686 | 28 |
| spot 3 | 165 | 886 | 159 | 0.18 | 0.10623 | 2.421 | 4.482 | 3.006 | 0.3035 | 1.782 | 0.59 | 0.88 | 1736 | 42 | 1713 | 29 |
| spot 4 | 256 | 1482 | 262 | 0.18 | 0.10464 | 2.413 | 4.269 | 2.922 | 0.2959 | 1.649 | 0.56 | 1.01 | 1708 | 41 | 1671 | 26 |
| spot 5 | 201 | 1017 | 204 | 0.20 | 0.10552 | 2.412 | 4.363 | 2.953 | 0.2995 | 1.704 | 0.58 | 0.86 | 1723 | 42 | 1690 | 27 |
| spot 6 | 256 | 1482 | 270 | 0.18 | 0.10587 | 2.411 | 4.312 | 2.909 | 0.2954 | 1.629 | 0.56 | 1.62 | 1729 | 42 | 1668 | 26 |
| spot 7 | 362 | 1689 | 398 | 0.24 | 0.10573 | 2.413 | 4.128 | 2.879 | 0.2833 | 1.571 | 0.55 | 3.19 | 1727 | 42 | 1609 | 24 |
| spot 8 | 167 | 978 | 177 | 0.18 | 0.10615 | 2.424 | 4.373 | 2.990 | 0.2987 | 1.750 | 0.59 | 1.31 | 1734 | 42 | 1684 | 28 |
| spot 9 | 199 | 992 | 213 | 0.21 | 0.10585 | 2.424 | 4.267 | 2.985 | 0.2930 | 1.743 | 0.58 | 1.81 | 1729 | 42 | 1656 | 27 |
| spot 10 | 32 | 948 | 17 | 0.02 | 0.10645 | 2.425 | 4.344 | 2.957 | 0.2951 | 1.693 | 0.57 | 1.92 | 1739 | 42 | 1669 | 27 |
| spot 11 | 202 | 1060 | 226 | 0.21 | 0.10589 | 2.418 | 4.245 | 2.942 | 0.2926 | 1.677 | 0.57 | 1.77 | 1730 | 42 | 1654 | 26 |
| spot 12 | 162 | 956 | 187 | 0.20 | 0.10369 | 2.426 | 4.052 | 2.975 | 0.2838 | 1.721 | 0.58 | 2.11 | 1692 | 41 | 1610 | 26 |
| spot 13 | 110 | 739 | 120 | 0.16 | 0.10610 | 2.424 | 4.341 | 2.994 | 0.2959 | 1.758 | 0.59 | 1.80 | 1733 | 42 | 1670 | 28 |
| spot 14 | 153 | 1545 | 181 | 0.12 | 0.10606 | 2.414 | 4.103 | 2.872 | 0.2809 | 1.556 | 0.54 | 3.72 | 1733 | 42 | 1596 | 24 |
| spot 15 | 179 | 954 | 199 | 0.21 | 0.10669 | 2.420 | 4.353 | 2.965 | 0.2958 | 1.713 | 0.58 | 1.96 | 1743 | 42 | 1670 | 27 |
| spot 16 | 313 | 1504 | 346 | 0.23 | 0.10804 | 2.419 | 4.399 | 2.989 | 0.2965 | 1.756 | 0.59 | 2.33 | 1767 | 43 | 1674 | 28 |
| spot 17 | 92 | 602 | 98 | 0.16 | 0.10535 | 2.439 | 4.206 | 2.977 | 0.2893 | 1.707 | 0.57 | 2.26 | 1720 | 42 | 1637 | 27 |
| spot 18 | 197 | 1121 | 232 | 0.21 | 0.10442 | 2.422 | 4.035 | 2.914 | 0.2795 | 1.620 | 0.56 | 3.31 | 1704 | 41 | 1589 | 25 |
| spot 19 | 113 | 1000 | 126 | 0.13 | 0.10695 | 2.415 | 4.335 | 2.915 | 0.2939 | 1.632 | 0.56 | 2.25 | 1748 | 42 | 1663 | 26 |
| spot 20 | 120 | 969 | 144 | 0.15 | 0.10645 | 2.426 | 4.110 | 2.916 | 0.2808 | 1.617 | 0.55 | 3.88 | 1739 | 42 | 1595 | 25 |
| spot 21 | 496 | 2475 | 591 | 0.24 | 0.10678 | 2.408 | 4.343 | 2.897 | 0.2949 | 1.610 | 0.56 | 2.23 | 1745 | 42 | 1666 | 26 |
| spot 22 | 243 | 1778 | 281 | 0.16 | 0.10626 | 2.413 | 4.251 | 2.981 | 0.2904 | 1.750 | 0.59 | 2.43 | 1736 | 42 | 1643 | 27 |
| spot 23 | 200 | 1075 | 228 | 0.21 | 0.10588 | 2.418 | 4.237 | 2.972 | 0.2898 | 1.728 | 0.58 | 2.44 | 1730 | 42 | 1640 | 27 |
| spot 24 | 132 | 953 | 159 | 0.17 | 0.10528 | 2.420 | 4.102 | 2.959 | 0.2823 | 1.702 | 0.58 | 3.26 | 1719 | 42 | 1603 | 26 |
| spot 25 | 80 | 1381 | 99 | 0.07 | 0.10506 | 2.426 | 4.151 | 2.956 | 0.2871 | 1.690 | 0.57 | 2.50 | 1715 | 42 | 1627 | 27 |
| spot 26 | 330 | 1748 | 394 | 0.23 | 0.10535 | 2.409 | 4.260 | 2.877 | 0.2938 | 1.573 | 0.55 | 1.52 | 1720 | 41 | 1660 | 25 |
| spot 27 | 275 | 1331 | 339 | 0.25 | 0.10540 | 2.417 | 4.203 | 2.921 | 0.2899 | 1.640 | 0.56 | 2.09 | 1722 | 42 | 1641 | 26 |
| spot 28 | 192 | 1048 | 232 | 0.22 | 0.10517 | 2.420 | 4.233 | 2.969 | 0.2930 | 1.720 | 0.58 | 1.50 | 1717 | 42 | 1656 | 27 |
| spot 29 | 263 | 1385 | 340 | 0.25 | 0.10391 | 2.418 | 4.030 | 3.044 | 0.2816 | 1.848 | 0.61 | 2.50 | 1695 | 41 | 1601 | 28 |
| spot 30 | 180 | 1087 | 237 | 0.22 | 0.10394 | 2.429 | 3.959 | 3.001 | 0.2772 | 1.763 | 0.59 | 3.04 | 1695 | 41 | 1577 | 26 |
| spot 31 | 83 | 515 | 100 | 0.19 | 0.10456 | 2.438 | 4.287 | 2.977 | 0.2978 | 1.708 | 0.57 | 0.60 | 1706 | 42 | 1680 | 27 |

**MVUr2 zircon** (spot size: 19 µm, frequency: 4 Hz, 80 shot count, laser energy: 4 mJ at 75%)

| | | | | | ISOTOPIC RATIOS | | | | | | | | APPARENT AGES (Ma) | | | |
|---|---|---|---|---|---|---|---|---|---|---|---|---|---|---|---|---|
| | Pb (ppm) | U (ppm) | Th (ppm) | Th/U | $^{207}Pb/^{206}Pb$ | 2σ % | $^{207}Pb/^{235}U$ | 2σ % | $^{206}Pb/^{238}U$ | 2σ % | Rho | % disc.* | $^{207}Pb/^{206}Pb$ | 2σ abs | $^{206}Pb/^{238}U$ | 2σ abs |
| spot 32 | 65 | 1598 | 84 | 0.05 | 0.10318 | 2.415 | 4.054 | 2.924 | 0.2860 | 1.649 | 0.56 | 1.33 | 1683 | 41 | 1623 | 25 |
| spot 33 | 146 | 761 | 180 | 0.24 | 0.10459 | 2.423 | 4.276 | 3.004 | 0.2975 | 1.776 | 0.59 | 0.42 | 1707 | 41 | 1681 | 28 |
| spot 34 | 151 | 1014 | 186 | 0.18 | 0.10474 | 2.424 | 4.196 | 2.914 | 0.2918 | 1.616 | 0.55 | 1.38 | 1710 | 42 | 1650 | 26 |
| spot 35 | 124 | 689 | 151 | 0.22 | 0.10428 | 2.432 | 4.308 | 2.968 | 0.3005 | 1.702 | 0.57 | 0.01 | 1701 | 41 | 1694 | 28 |
| spot 36 | 123 | 828 | 154 | 0.19 | 0.10502 | 2.432 | 4.230 | 3.017 | 0.2937 | 1.787 | 0.59 | 1.21 | 1714 | 42 | 1659 | 28 |
| spot 37 | 96 | 170 | 130 | 0.76 | 0.09869 | 2.511 | 3.651 | 3.129 | 0.2688 | 1.866 | 0.60 | 1.69 | 1599 | 41 | 1534 | 27 |
| spot 38 | 238 | 1153 | 290 | 0.25 | 0.10400 | 2.418 | 4.239 | 2.938 | 0.2968 | 1.668 | 0.57 | 0.35 | 1697 | 41 | 1675 | 27 |
| spot 39 | 287 | 1767 | 374 | 0.21 | 0.10381 | 2.414 | 4.092 | 2.959 | 0.2874 | 1.712 | 0.58 | 1.47 | 1693 | 41 | 1628 | 27 |
| spot 40 | 306 | 2166 | 367 | 0.17 | 0.10419 | 2.415 | 4.223 | 2.914 | 0.2950 | 1.630 | 0.56 | 0.78 | 1700 | 41 | 1666 | 26 |
| spot 41 | 156 | 805 | 193 | 0.24 | 0.10301 | 2.424 | 4.202 | 3.005 | 0.2972 | 1.777 | 0.59 | 0.24 | 1679 | 41 | 1677 | 28 |
| spot 42 | 206 | 1272 | 263 | 0.21 | 0.10331 | 2.419 | 4.138 | 2.984 | 0.2909 | 1.748 | 0.59 | 1.06 | 1685 | 41 | 1645 | 27 |
| spot 43 | 186 | 1004 | 240 | 0.24 | 0.10318 | 2.425 | 4.146 | 2.976 | 0.2908 | 1.726 | 0.58 | 1.06 | 1682 | 41 | 1645 | 27 |
| spot 44 | 82 | 698 | 108 | 0.16 | 0.10207 | 2.430 | 4.016 | 3.092 | 0.2856 | 1.911 | 0.62 | 1.17 | 1662 | 41 | 1619 | 29 |
| spot 45 | 264 | 1312 | 336 | 0.26 | 0.10319 | 2.416 | 4.166 | 2.954 | 0.2924 | 1.699 | 0.58 | 0.82 | 1682 | 41 | 1653 | 27 |
| spot 46 | 283 | 1963 | 339 | 0.17 | 0.10426 | 2.412 | 4.362 | 2.962 | 0.3024 | 1.719 | 0.58 | 0.08 | 1701 | 41 | 1703 | 28 |
| spot 47 | 78 | 452 | 99 | 0.22 | 0.10242 | 2.438 | 4.069 | 2.955 | 0.2862 | 1.670 | 0.57 | 1.57 | 1668 | 41 | 1622 | 26 |
| spot 48 | 124 | 697 | 162 | 0.23 | 0.10377 | 2.426 | 4.204 | 2.987 | 0.2929 | 1.743 | 0.58 | 1.09 | 1692 | 41 | 1656 | 27 |
| spot 49 | 209 | 1226 | 256 | 0.21 | 0.10483 | 2.419 | 4.396 | 3.005 | 0.3032 | 1.783 | 0.59 | 0.23 | 1711 | 41 | 1707 | 29 |
| spot 50 | 260 | 1313 | 339 | 0.26 | 0.10390 | 2.425 | 4.157 | 2.931 | 0.2873 | 1.646 | 0.56 | 2.29 | 1695 | 41 | 1630 | 26 |
| spot 51 | 132 | 866 | 169 | 0.19 | 0.10280 | 2.421 | 4.212 | 2.929 | 0.2959 | 1.649 | 0.56 | 0.41 | 1675 | 41 | 1670 | 26 |
| spot 52 | 225 | 1941 | 292 | 0.15 | 0.10359 | 2.409 | 4.199 | 2.934 | 0.2930 | 1.676 | 0.57 | 1.03 | 1690 | 41 | 1656 | 27 |
| spot 53 | 353 | 1755 | 441 | 0.25 | 0.10423 | 2.408 | 4.320 | 2.914 | 0.2996 | 1.641 | 0.56 | 0.44 | 1701 | 41 | 1689 | 27 |
| spot 54 | 217 | 1056 | 267 | 0.25 | 0.10385 | 2.418 | 4.378 | 3.014 | 0.3058 | 1.798 | 0.60 | 0.70 | 1694 | 41 | 1719 | 29 |
| spot 55 | 68 | 914 | 75 | 0.08 | 0.10396 | 2.423 | 4.380 | 3.019 | 0.3049 | 1.801 | 0.60 | 0.41 | 1696 | 41 | 1715 | 29 |
| spot 56 | 132 | 891 | 165 | 0.19 | 0.10276 | 2.428 | 4.170 | 2.925 | 0.2945 | 1.631 | 0.56 | 0.28 | 1675 | 41 | 1664 | 26 |
| spot 57 | 207 | 1134 | 263 | 0.23 | 0.10330 | 2.421 | 4.230 | 2.976 | 0.2975 | 1.731 | 0.58 | 0.14 | 1684 | 41 | 1678 | 28 |
| spot 58 | 119 | 687 | 157 | 0.23 | 0.10067 | 2.430 | 3.930 | 3.033 | 0.2840 | 1.816 | 0.60 | 0.50 | 1637 | 40 | 1611 | 28 |
| spot 59 | 308 | 1847 | 386 | 0.21 | 0.10444 | 2.414 | 4.255 | 2.984 | 0.2969 | 1.755 | 0.59 | 0.48 | 1704 | 41 | 1676 | 28 |
| spot 60 | 272 | 1798 | 342 | 0.19 | 0.10430 | 2.417 | 4.339 | 2.977 | 0.3033 | 1.738 | 0.58 | 0.41 | 1702 | 41 | 1707 | 28 |
| spot 61 | 145 | 777 | 185 | 0.24 | 0.10433 | 2.425 | 4.295 | 2.894 | 0.3007 | 1.580 | 0.55 | 0.18 | 1702 | 41 | 1695 | 26 |
| spot 62 | 176 | 1092 | 226 | 0.21 | 0.10417 | 2.420 | 4.236 | 2.975 | 0.2976 | 1.731 | 0.58 | 0.07 | 1700 | 41 | 1679 | 28 |

**MVUr2 zircon** (spot size: 19 µm, frequency: 4 Hz, 80 shot count, laser energy: 4 mJ at 75%)

| | | | | | ISOTOPIC RATIOS | | | | | | | | APPARENT AGES (Ma) | | | |
|---|---|---|---|---|---|---|---|---|---|---|---|---|---|---|---|---|
| | Pb (ppm) | U (ppm) | Th (ppm) | Th/U | $^{207}Pb/^{206}Pb$ | 2σ % | $^{207}Pb/^{235}U$ | 2σ % | $^{206}Pb/^{238}U$ | 2σ % | Rho | % disc.* | $^{207}Pb/^{206}Pb$ | 2σ abs | $^{206}Pb/^{238}U$ | 2σ abs |
| spot 63 | 160 | 856 | 199 | 0.23 | 0.10423 | 2.418 | 4.229 | 2.937 | 0.2971 | 1.667 | 0.57 | 0.13 | 1701 | 41 | 1677 | 27 |
| spot 64 | 214 | 1055 | 265 | 0.25 | 0.10430 | 2.423 | 4.318 | 2.995 | 0.3032 | 1.761 | 0.59 | 0.76 | 1702 | 41 | 1709 | 29 |
| spot 65 | 124 | 907 | 160 | 0.18 | 0.10266 | 2.418 | 4.039 | 3.013 | 0.2898 | 1.798 | 0.60 | 0.18 | 1673 | 41 | 1640 | 28 |
| spot 66 | 329 | 1280 | 396 | 0.31 | 0.10506 | 2.420 | 4.335 | 2.956 | 0.3025 | 1.697 | 0.57 | 0.34 | 1715 | 42 | 1705 | 27 |
| spot 67 | 140 | 762 | 171 | 0.22 | 0.10442 | 2.435 | 4.232 | 2.916 | 0.2977 | 1.605 | 0.55 | 0.02 | 1704 | 42 | 1680 | 26 |
| spot 68 | 186 | 921 | 224 | 0.24 | 0.10421 | 2.425 | 4.292 | 3.015 | 0.2999 | 1.792 | 0.59 | 0.06 | 1701 | 41 | 1690 | 28 |
| spot 69 | 187 | 987 | 241 | 0.24 | 0.10201 | 2.423 | 3.969 | 2.932 | 0.2848 | 1.651 | 0.56 | 0.84 | 1661 | 40 | 1615 | 26 |
| spot 70 | 280 | 1278 | 340 | 0.27 | 0.10375 | 2.422 | 4.185 | 2.995 | 0.2945 | 1.761 | 0.59 | 0.44 | 1692 | 41 | 1663 | 28 |
| spot 71 | 131 | 802 | 172 | 0.21 | 0.10381 | 2.432 | 3.994 | 2.932 | 0.2815 | 1.637 | 0.56 | 2.09 | 1693 | 41 | 1599 | 25 |
| spot 72 | 453 | 2712 | 552 | 0.20 | 0.10582 | 2.409 | 4.345 | 2.925 | 0.3005 | 1.660 | 0.57 | 0.43 | 1729 | 42 | 1694 | 27 |
| spot 73 | 193 | 1654 | 238 | 0.14 | 0.10486 | 2.409 | 4.265 | 2.883 | 0.2983 | 1.584 | 0.55 | 0.30 | 1712 | 41 | 1682 | 25 |
| spot 74 | 405 | 1618 | 483 | 0.30 | 0.10599 | 2.416 | 4.366 | 2.918 | 0.3018 | 1.636 | 0.56 | 0.31 | 1731 | 42 | 1700 | 27 |
| spot 75 | 126 | 841 | 158 | 0.19 | 0.10432 | 2.429 | 4.167 | 2.865 | 0.2929 | 1.519 | 0.53 | 0.74 | 1704 | 41 | 1656 | 25 |
| spot 76 | 160 | 902 | 207 | 0.23 | 0.10539 | 2.419 | 4.080 | 2.893 | 0.2859 | 1.587 | 0.55 | 1.84 | 1721 | 42 | 1621 | 25 |
| spot 77 | 100 | 762 | 130 | 0.17 | 0.10460 | 2.442 | 4.149 | 2.952 | 0.2907 | 1.660 | 0.56 | 1.12 | 1707 | 42 | 1645 | 26 |
| spot 78 | 212 | 1101 | 265 | 0.24 | 0.10516 | 2.426 | 4.325 | 2.874 | 0.3016 | 1.542 | 0.54 | 0.08 | 1718 | 42 | 1699 | 25 |
| spot 79 | 211 | 1614 | 263 | 0.16 | 0.10622 | 2.414 | 4.430 | 2.936 | 0.3054 | 1.670 | 0.57 | 0.02 | 1735 | 42 | 1718 | 27 |
| spot 80 | 199 | 1227 | 258 | 0.21 | 0.10513 | 2.418 | 4.220 | 2.941 | 0.2938 | 1.674 | 0.57 | 1.10 | 1717 | 42 | 1660 | 27 |
| spot 81 | 476 | 1927 | 602 | 0.31 | 0.10577 | 2.408 | 4.406 | 2.858 | 0.3040 | 1.538 | 0.54 | 0.12 | 1728 | 42 | 1711 | 25 |
| spot 82 | 390 | 1615 | 489 | 0.30 | 0.10550 | 2.412 | 4.378 | 2.881 | 0.3029 | 1.576 | 0.55 | 0.09 | 1723 | 42 | 1706 | 26 |
| spot 83 | 172 | 932 | 221 | 0.24 | 0.10507 | 2.429 | 4.287 | 2.879 | 0.2985 | 1.546 | 0.54 | 0.39 | 1715 | 42 | 1684 | 25 |
| spot 84 | 147 | 985 | 195 | 0.20 | 0.10396 | 2.426 | 4.204 | 2.902 | 0.2940 | 1.592 | 0.55 | 0.85 | 1696 | 41 | 1661 | 26 |
| spot 85 | 191 | 995 | 262 | 0.26 | 0.10335 | 2.428 | 3.954 | 2.919 | 0.2793 | 1.620 | 0.56 | 2.35 | 1685 | 41 | 1588 | 24 |
| spot 86 | 165 | 866 | 207 | 0.24 | 0.10474 | 2.429 | 4.320 | 2.887 | 0.3005 | 1.562 | 0.54 | 0.14 | 1710 | 42 | 1694 | 26 |
| spot 87 | 290 | 1176 | 356 | 0.30 | 0.10463 | 2.423 | 4.114 | 2.943 | 0.2861 | 1.670 | 0.57 | 2.11 | 1708 | 41 | 1622 | 26 |
| spot 88 | 263 | 1417 | 338 | 0.24 | 0.10382 | 2.417 | 4.247 | 2.891 | 0.2974 | 1.586 | 0.55 | 0.42 | 1693 | 41 | 1678 | 25 |
| spot 89 | 156 | 801 | 216 | 0.27 | 0.10260 | 2.427 | 3.882 | 2.912 | 0.2742 | 1.609 | 0.55 | 3.03 | 1671 | 41 | 1562 | 24 |
| spot 90 | 321 | 1384 | 429 | 0.31 | 0.10306 | 2.416 | 4.120 | 2.888 | 0.2886 | 1.582 | 0.55 | 1.39 | 1680 | 41 | 1636 | 25 |
| spot 91 | 301 | 1473 | 380 | 0.26 | 0.10346 | 2.414 | 4.277 | 2.840 | 0.2981 | 1.495 | 0.53 | 0.44 | 1688 | 41 | 1682 | 24 |
| spot 92 | 182 | 922 | 236 | 0.26 | 0.10244 | 2.433 | 4.106 | 2.960 | 0.2886 | 1.686 | 0.57 | 1.28 | 1669 | 41 | 1634 | 26 |
| spot 93 | 174 | 897 | 227 | 0.25 | 0.10309 | 2.438 | 4.161 | 2.987 | 0.2907 | 1.726 | 0.58 | 1.41 | 1681 | 41 | 1645 | 27 |

**MVUr2 zircon** (spot size: 19 µm, frequency: 4 Hz, 80 shot count, laser energy: 4 mJ at 75%)

| | | | | | ISOTOPIC RATIOS | | | | | | | | APPARENT AGES (Ma) | | | |
|---|---|---|---|---|---|---|---|---|---|---|---|---|---|---|---|---|
| | Pb (ppm) | U (ppm) | Th (ppm) | Th/U | $^{207}Pb/^{206}Pb$ | 2σ % | $^{207}Pb/^{235}U$ | 2σ % | $^{206}Pb/^{238}U$ | 2σ % | Rho | % disc.* | $^{207}Pb/^{206}Pb$ | 2σ abs | $^{206}Pb/^{238}U$ | 2σ abs |
| spot 94 | 175 | 922 | 230 | 0.25 | 0.10293 | 2.428 | 4.101 | 2.948 | 0.2857 | 1.671 | 0.57 | 1.97 | 1677 | 41 | 1622 | 26 |
| spot 95 | 189 | 965 | 239 | 0.25 | 0.10220 | 2.424 | 4.214 | 2.942 | 0.2968 | 1.668 | 0.57 | 0.06 | 1664 | 40 | 1675 | 26 |
| spot 96 | 90 | 581 | 115 | 0.20 | 0.10149 | 2.452 | 4.047 | 2.954 | 0.2869 | 1.647 | 0.56 | 1.13 | 1652 | 41 | 1626 | 26 |
| spot 97 | 87 | 678 | 114 | 0.17 | 0.10240 | 2.443 | 4.003 | 2.965 | 0.2821 | 1.680 | 0.57 | 2.08 | 1668 | 41 | 1602 | 26 |
| spot 98 | 325 | 1557 | 387 | 0.25 | 0.10393 | 2.414 | 4.347 | 2.865 | 0.3011 | 1.543 | 0.54 | 0.35 | 1695 | 41 | 1696 | 25 |

**MVUT-1 zircon** (spot size: 19 µm, frequency: 4 Hz, 80 shot count, laser energy: 4 mJ at 75%)

| | | | | | ISOTOPIC RATIOS | | | | | | | | APPARENT AGES | | | |
|---|---|---|---|---|---|---|---|---|---|---|---|---|---|---|---|---|
| | Pb (ppm) | U (ppm) | Th (ppm) | Th/U | $^{207}Pb/^{206}Pb$ | 2σ % | $^{207}Pb/^{235}U$ | 2σ % | $^{206}Pb/^{238}U$ | 2σ % | Rho | % disc.* | $^{207}Pb/^{206}Pb$ | 2σ abs | $^{206}Pb/^{238}U$ | 2σ abs |
| spot 1 | 6 | 1042 | 8 | 0.01 | 0.10177 | 1.139 | 3.756 | 1.573 | 0.2683 | 1.085 | 0.69 | 3.33 | 1656 | 19 | 1532 | 15 |
| spot 2 | 56 | 525 | 83 | 0.16 | 0.09813 | 1.173 | 3.483 | 1.682 | 0.2567 | 1.205 | 0.72 | 3.37 | 1588 | 19 | 1473 | 17 |
| spot 3 | 11 | 576 | 17 | 0.03 | 0.09730 | 1.201 | 3.263 | 1.733 | 0.2432 | 1.249 | 0.72 | 4.85 | 1572 | 20 | 1403 | 16 |
| spot 4 | 40 | 263 | 67 | 0.26 | 0.09195 | 1.232 | 2.739 | 1.677 | 0.2138 | 1.137 | 0.68 | 7.18 | 1466 | 20 | 1249 | 13 |
| spot 5 | 92 | 909 | 139 | 0.15 | 0.09843 | 1.144 | 3.498 | 1.595 | 0.2573 | 1.111 | 0.70 | 3.40 | 1594 | 19 | 1476 | 15 |
| spot 6 | 58 | 483 | 66 | 0.14 | 0.11051 | 1.200 | 4.632 | 1.653 | 0.3040 | 1.137 | 0.69 | 2.53 | 1809 | 22 | 1711 | 18 |
| spot 7 | 34 | 1248 | 29 | 0.02 | 0.10292 | 1.149 | 3.894 | 1.570 | 0.2745 | 1.071 | 0.68 | 3.13 | 1678 | 19 | 1564 | 16 |
| spot 8 | 15 | 547 | 22 | 0.04 | 0.09592 | 1.180 | 3.211 | 1.565 | 0.2422 | 1.028 | 0.66 | 4.37 | 1546 | 19 | 1398 | 14 |
| spot 9 | 53 | 1111 | 62 | 0.06 | 0.10694 | 1.140 | 4.253 | 1.542 | 0.2900 | 1.039 | 0.67 | 2.78 | 1748 | 20 | 1642 | 16 |
| spot 10 | 55 | 587 | 79 | 0.13 | 0.10038 | 1.170 | 3.624 | 1.566 | 0.2626 | 1.041 | 0.66 | 3.53 | 1631 | 19 | 1503 | 15 |
| spot 11 | 9 | 871 | 12 | 0.01 | 0.10021 | 1.133 | 3.703 | 1.531 | 0.2678 | 1.030 | 0.67 | 2.79 | 1628 | 19 | 1530 | 15 |
| spot 12 | 152 | 1173 | 198 | 0.17 | 0.10575 | 1.129 | 4.102 | 1.546 | 0.2818 | 1.055 | 0.68 | 3.26 | 1727 | 20 | 1602 | 16 |
| spot 13 | 3 | 850 | 3 | 0.00 | 0.10107 | 1.153 | 3.642 | 1.486 | 0.2616 | 0.937 | 0.63 | 4.05 | 1644 | 19 | 1498 | 13 |
| spot 14 | 39 | 474 | 52 | 0.11 | 0.09859 | 1.398 | 3.654 | 1.720 | 0.2688 | 1.002 | 0.58 | 1.71 | 1596 | 24 | 1534 | 14 |
| spot 15 | 22 | 783 | 25 | 0.03 | 0.10156 | 1.159 | 3.745 | 1.531 | 0.2692 | 1.001 | 0.65 | 2.88 | 1653 | 19 | 1536 | 15 |
| spot 16 | 42 | 356 | 51 | 0.14 | 0.09951 | 1.231 | 3.820 | 1.642 | 0.2798 | 1.086 | 0.66 | 0.48 | 1614 | 20 | 1590 | 16 |
| spot 17 | 10 | 704 | 13 | 0.02 | 0.10204 | 1.189 | 3.945 | 1.627 | 0.2808 | 1.111 | 0.68 | 1.72 | 1661 | 20 | 1595 | 16 |
| spot 18 | 389 | 1674 | 489 | 0.29 | 0.11202 | 1.121 | 4.342 | 1.522 | 0.2814 | 1.030 | 0.68 | 6.45 | 1832 | 21 | 1598 | 15 |
| spot 19 | 22 | 613 | 32 | 0.05 | 0.09748 | 1.164 | 3.234 | 1.556 | 0.2400 | 1.033 | 0.66 | 5.64 | 1576 | 19 | 1387 | 13 |
| spot 20 | 6 | 1575 | 10 | 0.01 | 0.10067 | 1.118 | 3.675 | 1.506 | 0.2652 | 1.009 | 0.67 | 3.30 | 1636 | 18 | 1516 | 14 |
| spot 21 | 12 | 687 | 16 | 0.02 | 0.10155 | 1.142 | 3.617 | 1.656 | 0.2585 | 1.200 | 0.72 | 4.76 | 1653 | 19 | 1482 | 17 |
| spot 22 | 64 | 286 | 92 | 0.32 | 0.09741 | 1.261 | 3.612 | 1.802 | 0.2699 | 1.288 | 0.71 | 0.71 | 1575 | 21 | 1540 | 19 |
| spot 23 | 27 | 487 | 39 | 0.08 | 0.09652 | 1.191 | 3.169 | 1.692 | 0.2369 | 1.203 | 0.71 | 5.85 | 1560 | 19 | 1370 | 15 |
| spot 24 | 192 | 712 | 220 | 0.31 | 0.10830 | 1.163 | 4.478 | 1.597 | 0.3000 | 1.095 | 0.69 | 2.09 | 1771 | 21 | 1691 | 18 |
| spot 25 | 12 | 980 | 16 | 0.02 | 0.09907 | 1.194 | 3.649 | 1.561 | 0.2668 | 1.006 | 0.64 | 2.32 | 1606 | 20 | 1524 | 15 |
| spot 26 | 7 | 681 | 7 | 0.01 | 0.10265 | 1.152 | 3.911 | 1.535 | 0.2754 | 1.016 | 0.66 | 2.96 | 1672 | 19 | 1569 | 15 |
| spot 27 | 37 | 641 | 42 | 0.07 | 0.10317 | 1.154 | 3.993 | 1.604 | 0.2796 | 1.114 | 0.69 | 2.73 | 1683 | 20 | 1589 | 16 |
| spot 28 | 150 | 700 | 147 | 0.21 | 0.10286 | 1.164 | 4.067 | 1.566 | 0.2854 | 1.048 | 0.67 | 1.87 | 1677 | 20 | 1618 | 16 |
| spot 29 | 19 | 1291 | 23 | 0.02 | 0.10351 | 1.133 | 3.965 | 1.556 | 0.2766 | 1.066 | 0.69 | 3.33 | 1688 | 19 | 1574 | 16 |
| spot 30 | 30 | 370 | 41 | 0.11 | 0.10548 | 1.183 | 4.214 | 1.610 | 0.2894 | 1.092 | 0.68 | 2.40 | 1724 | 21 | 1638 | 17 |
| spot 31 | 21 | 678 | 23 | 0.03 | 0.10431 | 1.156 | 4.049 | 1.603 | 0.2810 | 1.111 | 0.69 | 2.98 | 1702 | 20 | 1596 | 17 |

**MVUT-1 zircon** (spot size: 19 µm, frequency: 4 Hz, 80 shot count, laser energy: 4 mJ at 75%)

| | | | | | ISOTOPIC RATIOS | | | | | | | | APPARENT AGES | | | |
|---|---|---|---|---|---|---|---|---|---|---|---|---|---|---|---|---|
| | Pb (ppm) | U (ppm) | Th (ppm) | Th/U | $^{207}Pb/^{206}Pb$ | 2σ % | $^{207}Pb/^{235}U$ | 2σ % | $^{206}Pb/^{238}U$ | 2σ % | Rho | % disc.* | $^{207}Pb/^{206}Pb$ | 2σ abs | $^{206}Pb/^{238}U$ | 2σ abs |
| spot 32 | 23 | 586 | 31 | 0.05 | 0.10203 | 1.165 | 3.836 | 1.624 | 0.2725 | 1.131 | 0.70 | 2.94 | 1662 | 20 | 1554 | 16 |
| spot 33 | 40 | 453 | 57 | 0.13 | 0.09422 | 1.199 | 3.069 | 1.677 | 0.2359 | 1.172 | 0.70 | 4.34 | 1512 | 19 | 1365 | 15 |
| spot 34 | 29 | 1020 | 44 | 0.04 | 0.09822 | 1.134 | 3.346 | 1.584 | 0.2478 | 1.106 | 0.70 | 4.58 | 1591 | 18 | 1427 | 15 |
| spot 35 | 26 | 1187 | 37 | 0.03 | 0.09986 | 1.138 | 3.456 | 1.485 | 0.2512 | 0.954 | 0.64 | 5.00 | 1622 | 19 | 1445 | 13 |
| spot 36 | 17 | 510 | 19 | 0.04 | 0.10125 | 1.202 | 3.805 | 1.690 | 0.2729 | 1.188 | 0.70 | 2.46 | 1647 | 20 | 1555 | 17 |
| spot 37 | 250 | 1018 | 300 | 0.29 | 0.10986 | 1.136 | 4.625 | 1.603 | 0.3068 | 1.131 | 0.71 | 1.64 | 1797 | 20 | 1725 | 18 |
| spot 38 | 23 | 1094 | 34 | 0.03 | 0.10301 | 1.122 | 3.736 | 1.651 | 0.2652 | 1.210 | 0.73 | 4.12 | 1679 | 19 | 1516 | 17 |
| spot 39 | 9 | 467 | 12 | 0.03 | 0.09904 | 1.215 | 3.527 | 1.585 | 0.2603 | 1.018 | 0.64 | 2.80 | 1607 | 20 | 1491 | 14 |
| spot 40 | 20 | 1015 | 27 | 0.03 | 0.10002 | 1.130 | 3.611 | 1.537 | 0.2626 | 1.041 | 0.68 | 3.22 | 1624 | 19 | 1503 | 15 |
| spot 41 | 326 | 1357 | 416 | 0.31 | 0.10613 | 1.186 | 4.142 | 1.740 | 0.2839 | 1.273 | 0.73 | 2.98 | 1734 | 21 | 1613 | 19 |
| spot 42 | 30 | 515 | 50 | 0.10 | 0.08861 | 1.173 | 2.678 | 1.644 | 0.2204 | 1.152 | 0.70 | 2.95 | 1395 | 17 | 1284 | 14 |
| spot 43 | 11 | 986 | 18 | 0.02 | 0.10395 | 1.137 | 3.988 | 1.650 | 0.2808 | 1.195 | 0.72 | 2.33 | 1696 | 19 | 1595 | 17 |
| spot 44 | 10 | 734 | 14 | 0.02 | 0.10049 | 1.130 | 3.729 | 1.623 | 0.2706 | 1.165 | 0.72 | 2.22 | 1633 | 19 | 1544 | 17 |
| spot 45 | 166 | 809 | 191 | 0.24 | 0.10485 | 1.139 | 4.217 | 1.628 | 0.2932 | 1.163 | 0.71 | 1.19 | 1712 | 20 | 1657 | 18 |
| spot 46 | 110 | 324 | 139 | 0.43 | 0.11125 | 1.185 | 4.725 | 1.614 | 0.3118 | 1.095 | 0.68 | 1.15 | 1820 | 22 | 1751 | 18 |
| spot 47 | 60 | 838 | 86 | 0.10 | 0.10149 | 1.139 | 3.721 | 1.536 | 0.2679 | 1.030 | 0.67 | 2.97 | 1651 | 19 | 1530 | 15 |
| spot 48 | 68 | 223 | 106 | 0.48 | 0.09568 | 1.310 | 3.247 | 1.781 | 0.2461 | 1.206 | 0.68 | 3.37 | 1544 | 21 | 1420 | 16 |
| spot 49 | 30 | 499 | 51 | 0.10 | 0.09421 | 1.175 | 2.698 | 1.791 | 0.2087 | 1.351 | 0.75 | 8.60 | 1512 | 18 | 1222 | 16 |
| spot 50 | 67 | 378 | 131 | 0.35 | 0.09293 | 1.287 | 2.506 | 1.945 | 0.1963 | 1.458 | 0.75 | 10.20 | 1487 | 21 | 1157 | 16 |
| spot 51 | 12 | 718 | 18 | 0.03 | 0.09887 | 1.159 | 3.600 | 1.677 | 0.2644 | 1.213 | 0.72 | 2.50 | 1604 | 19 | 1512 | 17 |
| spot 52 | 62 | 1127 | 86 | 0.08 | 0.10714 | 1.123 | 4.132 | 1.582 | 0.2792 | 1.115 | 0.70 | 4.61 | 1751 | 20 | 1587 | 16 |
| spot 53 | 21 | 1010 | 33 | 0.03 | 0.09851 | 1.144 | 3.389 | 1.729 | 0.2490 | 1.296 | 0.75 | 4.83 | 1596 | 19 | 1433 | 17 |
| spot 54 | 7 | 717 | 16 | 0.02 | 0.09714 | 1.164 | 3.085 | 1.746 | 0.2292 | 1.301 | 0.75 | 7.32 | 1570 | 19 | 1331 | 16 |
| spot 55 | 38 | 460 | 47 | 0.10 | 0.10309 | 1.183 | 4.078 | 1.775 | 0.2867 | 1.323 | 0.75 | 1.48 | 1680 | 20 | 1625 | 20 |
| spot 56 | 76 | 277 | 109 | 0.40 | 0.09762 | 1.291 | 3.548 | 1.817 | 0.2634 | 1.278 | 0.70 | 1.99 | 1578 | 22 | 1507 | 18 |
| spot 57 | 72 | 174 | 82 | 0.47 | 0.10664 | 1.258 | 4.549 | 1.837 | 0.3081 | 1.340 | 0.73 | 0.40 | 1742 | 22 | 1733 | 21 |
| spot 58 | 120 | 1250 | 120 | 0.10 | 0.10538 | 1.170 | 4.119 | 1.631 | 0.2820 | 1.136 | 0.70 | 3.39 | 1721 | 20 | 1603 | 17 |
| spot 59 | 8 | 948 | 11 | 0.01 | 0.10346 | 1.138 | 3.999 | 1.592 | 0.2794 | 1.114 | 0.70 | 2.87 | 1687 | 19 | 1588 | 16 |
| spot 60 | 48 | 922 | 69 | 0.08 | 0.10257 | 1.152 | 3.905 | 1.715 | 0.2753 | 1.270 | 0.74 | 2.93 | 1671 | 19 | 1568 | 18 |
| spot 61 | 744 | 1317 | 908 | 0.69 | 0.10773 | 1.132 | 4.367 | 1.585 | 0.2935 | 1.109 | 0.70 | 2.80 | 1761 | 20 | 1659 | 18 |
| spot 62 | 55 | 593 | 75 | 0.13 | 0.09974 | 1.201 | 3.236 | 1.613 | 0.2347 | 1.077 | 0.67 | 7.81 | 1619 | 20 | 1359 | 14 |

**MVUT-1 zircon** (spot size: 19 µm, frequency: 4 Hz, 80 shot count, laser energy: 4 mJ at 75%)

| | | | | | ISOTOPIC RATIOS | | | | | | | | APPARENT AGES | | | |
|---|---|---|---|---|---|---|---|---|---|---|---|---|---|---|---|---|
| | Pb (ppm) | U (ppm) | Th (ppm) | Th/U | $^{207}Pb/^{206}Pb$ | 2σ % | $^{207}Pb/^{235}U$ | 2σ % | $^{206}Pb/^{238}U$ | 2σ % | Rho | % disc.* | $^{207}Pb/^{206}Pb$ | 2σ abs | $^{206}Pb/^{238}U$ | 2σ abs |
| spot 63 | 45 | 788 | 60 | 0.08 | 0.10731 | 1.145 | 4.305 | 1.599 | 0.2900 | 1.117 | 0.70 | 3.22 | 1754 | 20 | 1641 | 17 |
| spot 64 | 4 | 780 | 8 | 0.01 | 0.10298 | 1.173 | 3.324 | 1.767 | 0.2334 | 1.321 | 0.75 | 9.91 | 1678 | 20 | 1352 | 17 |
| spot 65 | 33 | 986 | 41 | 0.04 | 0.10505 | 1.147 | 4.062 | 1.700 | 0.2801 | 1.255 | 0.74 | 3.46 | 1715 | 20 | 1591 | 19 |
| spot 66 | 230 | 1157 | 294 | 0.25 | 0.10682 | 1.162 | 4.171 | 1.644 | 0.2821 | 1.163 | 0.71 | 4.17 | 1747 | 20 | 1602 | 17 |
| spot 67 | 402 | 1481 | 510 | 0.34 | 0.10660 | 1.123 | 4.228 | 1.630 | 0.2861 | 1.181 | 0.72 | 3.51 | 1742 | 20 | 1622 | 17 |
| spot 68 | 303 | 1650 | 409 | 0.25 | 0.10482 | 1.124 | 4.101 | 1.618 | 0.2817 | 1.164 | 0.72 | 3.38 | 1711 | 19 | 1600 | 17 |
| spot 69 | 186 | 389 | 217 | 0.56 | 0.10705 | 1.156 | 4.750 | 1.685 | 0.3199 | 1.227 | 0.73 | 0.69 | 1750 | 20 | 1789 | 20 |
| spot 70 | 71 | 300 | 109 | 0.36 | 0.09462 | 1.216 | 3.367 | 1.910 | 0.2556 | 1.473 | 0.77 | 1.98 | 1521 | 19 | 1467 | 20 |
| spot 71 | 48 | 446 | 68 | 0.15 | 0.09696 | 1.198 | 3.412 | 1.754 | 0.2531 | 1.281 | 0.73 | 3.58 | 1566 | 19 | 1454 | 17 |
| spot 72 | 8 | 768 | 11 | 0.01 | 0.10132 | 1.144 | 3.925 | 1.683 | 0.2774 | 1.234 | 0.73 | 2.54 | 1648 | 19 | 1578 | 18 |
| spot 73 | 18 | 645 | 26 | 0.04 | 0.09508 | 1.163 | 3.167 | 1.719 | 0.2388 | 1.265 | 0.74 | 5.04 | 1529 | 18 | 1380 | 16 |
| spot 74 | 8 | 832 | 12 | 0.01 | 0.10168 | 1.156 | 3.861 | 1.703 | 0.2717 | 1.251 | 0.73 | 3.68 | 1655 | 19 | 1549 | 18 |
| spot 75 | 252 | 664 | 303 | 0.46 | 0.10598 | 1.141 | 4.499 | 1.727 | 0.3042 | 1.297 | 0.75 | 1.13 | 1732 | 20 | 1712 | 20 |
| spot 76 | 13 | 740 | 18 | 0.02 | 0.10120 | 1.150 | 3.947 | 1.704 | 0.2794 | 1.258 | 0.74 | 2.27 | 1646 | 19 | 1588 | 19 |
| spot 77 | 59 | 219 | 92 | 0.42 | 0.09028 | 1.291 | 3.016 | 1.760 | 0.2391 | 1.196 | 0.68 | 2.19 | 1434 | 20 | 1382 | 16 |
| spot 78 | 169 | 1147 | 191 | 0.17 | 0.11761 | 1.142 | 4.376 | 1.617 | 0.2673 | 1.145 | 0.71 | 11.81 | 1920 | 22 | 1527 | 16 |
| spot 79 | 53 | 229 | 79 | 0.35 | 0.09830 | 1.316 | 3.700 | 1.950 | 0.2715 | 1.440 | 0.74 | 1.42 | 1591 | 22 | 1548 | 20 |
| spot 80 | 41 | 482 | 59 | 0.12 | 0.09722 | 1.174 | 3.544 | 1.590 | 0.2617 | 1.071 | 0.67 | 2.59 | 1571 | 19 | 1499 | 15 |
| spot 81 | 54 | 468 | 69 | 0.15 | 0.10360 | 1.183 | 4.278 | 1.670 | 0.2976 | 1.179 | 0.71 | 0.57 | 1690 | 20 | 1679 | 18 |

**12TM13-01 monazite** (spot size: 7 µm, frequency: 3 Hz, 75 shot count, laser energy: 3 mJ at 75%)

| | | | | | ISOTOPIC RATIOS | | | | | | | | APPARENT AGES | | | |
|---|---|---|---|---|---|---|---|---|---|---|---|---|---|---|---|---|
| | Pb (ppm) | U (ppm) | Th (ppm) | Th/U | $^{207}Pb/^{206}Pb$ | 2σ % | $^{207}Pb/^{235}U$ | 2σ % | $^{206}Pb/^{238}U$ | 2σ % | Rho | % disc.* | $^{207}Pb/^{206}Pb$ | 2σ abs | $^{206}Pb/^{238}U$ | 2σ abs |
| spot 1 | 5740 | 1721 | 43300 | 25.16 | 0.10409 | 1.225 | 4.640 | 0.160 | 0.3212 | 3.233 | 0.83 | 1.84 | 1699 | 21 | 1792 | 52 |
| spot 2 | 6700 | 1896 | 52800 | 27.85 | 0.10147 | 1.258 | 4.360 | 0.140 | 0.3104 | 2.954 | 0.79 | 2.12 | 1650 | 21 | 1745 | 46 |
| spot 3 | 3650 | 1820 | 59700 | 32.80 | 0.09728 | 1.309 | 2.879 | 0.089 | 0.2137 | 2.819 | 0.77 | 10.02 | 1571 | 22 | 1247 | 33 |
| spot 4 | 7390 | 3080 | 62600 | 20.32 | 0.10207 | 1.204 | 4.092 | 0.127 | 0.2907 | 2.866 | 0.79 | 0.61 | 1663 | 20 | 1643 | 43 |
| spot 5 | 9330 | 4430 | 81300 | 18.35 | 0.10410 | 1.159 | 4.302 | 0.113 | 0.2969 | 2.358 | 0.69 | 0.54 | 1698 | 20 | 1682 | 37 |
| spot 6 | 8420 | 3930 | 73000 | 18.58 | 0.10345 | 1.173 | 4.280 | 0.110 | 0.2985 | 2.299 | 0.68 | 0.18 | 1687 | 20 | 1686 | 36 |
| spot 7 | 8790 | 4410 | 78000 | 17.69 | 0.10250 | 1.181 | 4.108 | 0.122 | 0.2903 | 2.724 | 0.77 | 0.55 | 1669 | 20 | 1645 | 42 |
| spot 8 | 9340 | 3820 | 82300 | 21.54 | 0.10359 | 1.176 | 4.279 | 0.126 | 0.2995 | 2.693 | 0.76 | 0.18 | 1689 | 20 | 1695 | 42 |
| spot 9 | 11260 | 7350 | 133800 | 18.20 | 0.09015 | 1.146 | 2.881 | 0.076 | 0.2315 | 2.387 | 0.70 | 2.61 | 1428 | 17 | 1341 | 31 |
| spot 10 | 12010 | 7390 | 142400 | 19.27 | 0.09029 | 1.146 | 2.934 | 0.073 | 0.2362 | 2.200 | 0.65 | 1.68 | 1431 | 17 | 1366 | 29 |
| spot 11 | 11210 | 6950 | 128900 | 18.55 | 0.09067 | 1.143 | 2.971 | 0.080 | 0.2381 | 2.446 | 0.72 | 1.60 | 1439 | 17 | 1379 | 32 |
| spot 12 | 9920 | 6320 | 127700 | 20.21 | 0.08968 | 1.164 | 2.715 | 0.067 | 0.2197 | 2.188 | 0.64 | 4.06 | 1419 | 17 | 1280 | 27 |
| spot 13 | 10290 | 6290 | 124700 | 19.83 | 0.09020 | 1.140 | 2.805 | 0.073 | 0.2265 | 2.351 | 0.69 | 3.12 | 1430 | 17 | 1315 | 29 |
| spot 14 | 7910 | 4380 | 117200 | 26.76 | 0.08866 | 1.177 | 2.785 | 0.074 | 0.2278 | 2.377 | 0.70 | 1.89 | 1397 | 17 | 1325 | 30 |
| spot 15 | 9410 | 4680 | 119400 | 25.51 | 0.10027 | 1.163 | 3.064 | 0.085 | 0.2218 | 2.523 | 0.73 | 10.31 | 1630 | 19 | 1290 | 31 |
| spot 16 | 7880 | 3911 | 121500 | 31.07 | 0.09882 | 1.207 | 2.254 | 0.060 | 0.1649 | 2.358 | 0.69 | 21.54 | 1601 | 20 | 984 | 23 |
| spot 17 | 13370 | 3298 | 134600 | 40.81 | 0.10148 | 1.156 | 4.068 | 0.116 | 0.2910 | 2.606 | 0.75 | 0.30 | 1652 | 19 | 1645 | 40 |
| spot 18 | 15300 | 4070 | 143900 | 35.36 | 0.10516 | 1.152 | 4.483 | 0.118 | 0.3070 | 2.362 | 0.69 | 0.23 | 1719 | 20 | 1724 | 38 |
| spot 19 | 15970 | 5820 | 155900 | 26.79 | 0.10489 | 1.152 | 4.298 | 0.116 | 0.2951 | 2.446 | 0.71 | 1.56 | 1712 | 20 | 1668 | 38 |
| spot 20 | 16850 | 5950 | 166000 | 27.90 | 0.10475 | 1.142 | 4.286 | 0.113 | 0.2943 | 2.370 | 0.70 | 1.38 | 1710 | 20 | 1665 | 36 |
| spot 21 | 16200 | 5990 | 164400 | 27.45 | 0.10430 | 1.135 | 4.088 | 0.108 | 0.2821 | 2.377 | 0.70 | 2.93 | 1702 | 19 | 1604 | 35 |
| spot 22 | 11390 | 6970 | 173600 | 24.91 | 0.10056 | 1.160 | 2.592 | 0.067 | 0.1853 | 2.328 | 0.68 | 18.40 | 1635 | 19 | 1098 | 24 |
| spot 23 | 13760 | 9160 | 240900 | 26.30 | 0.09991 | 1.208 | 2.219 | 0.070 | 0.1600 | 2.915 | 0.79 | 24.16 | 1622 | 20 | 956 | 26 |
| spot 24 | 1699 | 6730 | 154000 | 22.88 | 0.04864 | 1.894 | 0.180 | 0.006 | 0.0265 | 2.715 | 0.68 | 0.53 | 129 | 34 | 169 | 5 |
| spot 25 | 1534 | 7590 | 139800 | 18.42 | 0.04956 | 1.666 | 0.180 | 0.006 | 0.0266 | 2.615 | 0.69 | 0.41 | 171 | 28 | 169 | 4 |
| spot 26 | 1639 | 8150 | 149100 | 18.29 | 0.04796 | 1.697 | 0.176 | 0.006 | 0.0262 | 2.801 | 0.72 | 1.26 | 98 | 28 | 167 | 5 |
| spot 27 | 1679 | 8760 | 153200 | 17.49 | 0.05182 | 1.611 | 0.199 | 0.006 | 0.0278 | 2.779 | 0.73 | 4.30 | 278 | 27 | 177 | 5 |
| spot 28 | 1646 | 8430 | 151800 | 18.01 | 0.04899 | 1.631 | 0.178 | 0.006 | 0.0264 | 2.660 | 0.70 | 0.95 | 144 | 27 | 168 | 4 |
| spot 29 | 1549 | 6590 | 145300 | 22.05 | 0.05587 | 1.806 | 0.229 | 0.008 | 0.0298 | 2.900 | 0.73 | 10.40 | 447 | 31 | 189 | 5 |
| spot 30 | 1298 | 5750 | 118900 | 20.68 | 0.04851 | 1.766 | 0.179 | 0.006 | 0.0266 | 2.680 | 0.69 | 1.36 | 123 | 30 | 169 | 4 |
| spot 31 | 1425 | 5740 | 129400 | 22.54 | 0.04846 | 1.799 | 0.179 | 0.006 | 0.0262 | 2.735 | 0.70 | 0.18 | 121 | 31 | 167 | 4 |

**12TM13-01 monazite** (spot size: 7 µm, frequency: 3 Hz, 75 shot count, laser energy: 3 mJ at 75%)

| | | | | | ISOTOPIC RATIOS | | | | | | | | APPARENT AGES | | | |
|---|---|---|---|---|---|---|---|---|---|---|---|---|---|---|---|---|
| | Pb (ppm) | U (ppm) | Th (ppm) | Th/U | $^{207}Pb/^{206}Pb$ | 2σ % | $^{207}Pb/^{235}U$ | 2σ % | $^{206}Pb/^{238}U$ | 2σ % | Rho | % disc.* | $^{207}Pb/^{206}Pb$ | 2σ abs | $^{206}Pb/^{238}U$ | 2σ abs |
| spot 32 | 12940 | 4050 | 138700 | 34.25 | 0.09740 | 1.157 | 3.528 | 0.095 | 0.2641 | 2.445 | 0.71 | 1.52 | 1575 | 19 | 1509 | 34 |
| spot 33 | 14110 | 4220 | 143500 | 34.00 | 0.10158 | 1.172 | 3.997 | 0.123 | 0.2864 | 2.838 | 0.78 | 0.37 | 1653 | 20 | 1626 | 43 |
| spot 34 | 13500 | 3910 | 134200 | 34.32 | 0.10353 | 1.160 | 4.162 | 0.117 | 0.2946 | 2.557 | 0.74 | 0.12 | 1688 | 20 | 1663 | 39 |
| spot 35 | 13020 | 3940 | 129100 | 32.77 | 0.10249 | 1.158 | 3.978 | 0.107 | 0.2833 | 2.426 | 0.71 | 1.43 | 1669 | 20 | 1606 | 36 |
| spot 36 | 8360 | 4020 | 129500 | 32.21 | 0.08840 | 1.198 | 2.432 | 0.077 | 0.1995 | 2.921 | 0.79 | 6.11 | 1391 | 18 | 1179 | 32 |
| spot 37 | 11670 | 3326 | 119200 | 35.84 | 0.10332 | 1.163 | 3.973 | 0.114 | 0.2802 | 2.614 | 0.75 | 2.39 | 1685 | 20 | 1591 | 38 |
| spot 38 | 12660 | 3670 | 131400 | 35.80 | 0.09984 | 1.149 | 3.689 | 0.099 | 0.2704 | 2.439 | 0.71 | 1.48 | 1621 | 19 | 1551 | 35 |
| spot 39 | 10410 | 3780 | 120200 | 31.80 | 0.10017 | 1.145 | 3.299 | 0.098 | 0.2409 | 2.732 | 0.77 | 6.26 | 1627 | 19 | 1390 | 36 |
| spot 40 | 11380 | 3544 | 117900 | 33.27 | 0.10350 | 1.157 | 4.038 | 0.110 | 0.2859 | 2.467 | 0.72 | 1.23 | 1688 | 20 | 1623 | 37 |
| spot 41 | 11860 | 3660 | 121600 | 33.22 | 0.10414 | 1.162 | 3.909 | 0.119 | 0.2741 | 2.806 | 0.78 | 3.46 | 1699 | 20 | 1560 | 40 |
| spot 42 | 5980 | 3900 | 70200 | 18.00 | 0.10485 | 1.155 | 3.830 | 0.121 | 0.2653 | 2.937 | 0.80 | 5.13 | 1711 | 20 | 1519 | 41 |
| spot 43 | 8780 | 5820 | 80100 | 13.76 | 0.10780 | 1.147 | 4.428 | 0.127 | 0.2976 | 2.622 | 0.75 | 2.21 | 1762 | 20 | 1677 | 41 |
| spot 44 | 10350 | 3503 | 113400 | 32.37 | 0.10271 | 1.174 | 3.735 | 0.108 | 0.2615 | 2.646 | 0.75 | 5.13 | 1673 | 20 | 1500 | 38 |
| spot 45 | 11350 | 4280 | 116300 | 27.17 | 0.10415 | 1.150 | 4.080 | 0.128 | 0.2830 | 2.923 | 0.80 | 2.36 | 1700 | 20 | 1613 | 43 |
| spot 46 | 8350 | 4440 | 110700 | 24.93 | 0.10305 | 1.154 | 3.443 | 0.100 | 0.2426 | 2.650 | 0.76 | 8.43 | 1680 | 20 | 1399 | 34 |
| spot 47 | 978 | 4640 | 75300 | 16.23 | 0.06895 | 1.674 | 0.351 | 0.011 | 0.0366 | 2.653 | 0.70 | 31.72 | 896 | 28 | 231 | 6 |
| spot 48 | 951 | 5770 | 80200 | 13.90 | 0.05918 | 1.730 | 0.253 | 0.009 | 0.0310 | 2.987 | 0.75 | 16.17 | 571 | 30 | 197 | 6 |
| spot 49 | 17930 | 10240 | 194600 | 19.00 | 0.10687 | 1.138 | 4.050 | 0.140 | 0.2763 | 3.261 | 0.84 | 4.78 | 1747 | 20 | 1570 | 47 |
| spot 50 | 14850 | 8040 | 189200 | 23.53 | 0.10503 | 1.155 | 3.747 | 0.114 | 0.2599 | 2.818 | 0.78 | 6.39 | 1715 | 20 | 1487 | 39 |
| spot 51 | 18570 | 9530 | 203400 | 21.34 | 0.10649 | 1.138 | 3.908 | 0.108 | 0.2710 | 2.524 | 0.73 | 5.12 | 1741 | 20 | 1544 | 36 |
| spot 52 | 2229 | 9170 | 192800 | 21.03 | 0.04906 | 1.738 | 0.180 | 0.006 | 0.0274 | 2.625 | 0.68 | 3.67 | 148 | 30 | 174 | 5 |
| spot 53 | 9010 | 7780 | 188500 | 24.23 | 0.10034 | 1.208 | 2.059 | 0.068 | 0.1536 | 3.062 | 0.81 | 23.26 | 1630 | 20 | 920 | 27 |
| spot 54 | 13820 | 4890 | 135100 | 27.63 | 0.10253 | 1.048 | 3.887 | 2.146 | 0.2705 | 1.873 | 0.87 | 4.54 | 1671 | 18 | 1542 | 26 |
| spot 55 | 16660 | 6020 | 158300 | 26.30 | 0.10297 | 1.058 | 4.132 | 2.216 | 0.2861 | 1.947 | 0.88 | 2.34 | 1679 | 18 | 1621 | 29 |
| spot 56 | 17920 | 9860 | 192800 | 19.55 | 0.10505 | 1.023 | 3.875 | 1.933 | 0.2622 | 1.639 | 0.85 | 6.99 | 1716 | 18 | 1502 | 22 |
| spot 57 | 5920 | 3550 | 142700 | 40.20 | 0.10048 | 1.169 | 2.550 | 2.628 | 0.1801 | 2.354 | 0.90 | 20.34 | 1632 | 20 | 1067 | 24 |
| spot 58 | 12580 | 6260 | 148400 | 23.71 | 0.10287 | 1.047 | 3.313 | 2.203 | 0.2279 | 1.938 | 0.88 | 12.08 | 1676 | 18 | 1325 | 23 |
| spot 59 | 7030 | 6600 | 110600 | 16.76 | 0.09614 | 1.095 | 2.218 | 1.976 | 0.1632 | 1.645 | 0.83 | 21.97 | 1550 | 18 | 974 | 15 |
| spot 60 | 6790 | 6740 | 100300 | 14.88 | 0.09750 | 1.088 | 2.408 | 2.114 | 0.1754 | 1.813 | 0.86 | 19.40 | 1576 | 18 | 1041 | 18 |
| spot 61 | 5950 | 2392 | 53100 | 22.20 | 0.10493 | 1.149 | 4.350 | 2.868 | 0.2971 | 2.627 | 0.92 | 1.91 | 1713 | 20 | 1674 | 39 |
| spot 62 | 6330 | 2455 | 57200 | 23.30 | 0.10495 | 1.159 | 4.370 | 2.797 | 0.2992 | 2.545 | 0.91 | 1.42 | 1712 | 20 | 1685 | 37 |

**12TM13-01 monazite** (spot size: 7 µm, frequency: 3 Hz, 75 shot count, laser energy: 3 mJ at 75%)

| | | | | | ISOTOPIC RATIOS | | | | | | | | APPARENT AGES | | | |
|---|---|---|---|---|---|---|---|---|---|---|---|---|---|---|---|---|
| | Pb (ppm) | U (ppm) | Th (ppm) | Th/U | $^{207}Pb/^{206}Pb$ | 2σ % | $^{207}Pb/^{235}U$ | 2σ % | $^{206}Pb/^{238}U$ | 2σ % | Rho | % disc.* | $^{207}Pb/^{206}Pb$ | 2σ abs | $^{206}Pb/^{238}U$ | 2σ abs |
| spot 63 | 4760 | 3330 | 64400 | 19.34 | 0.09951 | 1.084 | 2.574 | 2.874 | 0.1851 | 2.662 | 0.93 | 17.50 | 1615 | 18 | 1097 | 28 |
| spot 64 | 4660 | 2947 | 58500 | 19.85 | 0.10229 | 1.118 | 3.186 | 3.079 | 0.2246 | 2.868 | 0.93 | 10.44 | 1665 | 19 | 1312 | 34 |
| spot 65 | 5770 | 3139 | 65500 | 20.87 | 0.10373 | 1.092 | 3.528 | 2.555 | 0.2466 | 2.310 | 0.90 | 7.89 | 1692 | 19 | 1420 | 29 |
| spot 66 | 6750 | 2421 | 67400 | 27.84 | 0.10323 | 1.154 | 3.940 | 2.723 | 0.2801 | 2.466 | 0.91 | 2.26 | 1682 | 20 | 1590 | 35 |
| spot 67 | 5800 | 2407 | 72600 | 30.16 | 0.10161 | 1.110 | 3.233 | 3.271 | 0.2320 | 3.076 | 0.94 | 8.98 | 1654 | 19 | 1347 | 37 |
| spot 68 | 4830 | 4030 | 80500 | 19.98 | 0.09623 | 1.119 | 2.150 | 2.845 | 0.1650 | 2.615 | 0.92 | 18.70 | 1551 | 18 | 984 | 24 |
| spot 69 | 3371 | 3074 | 75300 | 24.50 | 0.09421 | 1.180 | 1.929 | 3.037 | 0.1500 | 2.798 | 0.92 | 20.71 | 1515 | 19 | 903 | 24 |
| spot 70 | 8370 | 4340 | 87300 | 20.12 | 0.10603 | 1.047 | 4.120 | 2.679 | 0.2885 | 2.466 | 0.92 | 1.22 | 1733 | 18 | 1636 | 36 |
| spot 71 | 1020 | 3720 | 89500 | 24.06 | 0.06190 | 1.713 | 0.274 | 3.540 | 0.0329 | 3.098 | 0.88 | 17.66 | 666 | 31 | 209 | 6 |
| spot 72 | 7850 | 2917 | 80800 | 27.70 | 0.10494 | 1.041 | 4.157 | 2.453 | 0.2900 | 2.221 | 0.91 | 1.59 | 1714 | 18 | 1640 | 33 |
| spot 73 | 8240 | 3037 | 81900 | 26.97 | 0.10454 | 1.070 | 4.140 | 2.728 | 0.2873 | 2.509 | 0.92 | 1.47 | 1708 | 19 | 1634 | 36 |
| spot 74 | 7340 | 2860 | 83900 | 29.34 | 0.10278 | 1.047 | 3.692 | 2.290 | 0.2621 | 2.036 | 0.89 | 4.73 | 1675 | 18 | 1500 | 28 |
| spot 75 | 7310 | 3770 | 70200 | 18.62 | 0.10643 | 1.043 | 4.224 | 2.219 | 0.2897 | 1.958 | 0.88 | 2.44 | 1739 | 18 | 1639 | 29 |
| spot 76 | 7000 | 2379 | 69000 | 29.00 | 0.10276 | 1.058 | 4.109 | 2.551 | 0.2899 | 2.321 | 0.91 | 1.03 | 1674 | 18 | 1644 | 34 |
| spot 77 | 5630 | 3310 | 52400 | 15.83 | 0.10674 | 1.039 | 4.410 | 2.447 | 0.3001 | 2.215 | 0.91 | 1.36 | 1744 | 18 | 1694 | 33 |
| spot 78 | 9090 | 2595 | 91700 | 35.34 | 0.10407 | 1.033 | 4.253 | 2.237 | 0.2961 | 1.984 | 0.89 | 0.78 | 1698 | 18 | 1674 | 30 |
| spot 79 | 9480 | 3440 | 94800 | 27.56 | 0.10588 | 1.028 | 4.291 | 2.396 | 0.2934 | 2.164 | 0.90 | 1.99 | 1729 | 18 | 1657 | 32 |
| spot 80 | 8270 | 2579 | 91400 | 35.44 | 0.10386 | 1.053 | 3.845 | 2.652 | 0.2671 | 2.434 | 0.92 | 4.85 | 1695 | 18 | 1527 | 33 |
| spot 81 | 8850 | 3355 | 88900 | 26.50 | 0.10565 | 1.038 | 4.254 | 2.319 | 0.2921 | 2.074 | 0.89 | 1.87 | 1725 | 18 | 1657 | 31 |
| spot 82 | 8950 | 2872 | 91900 | 32.00 | 0.10511 | 1.048 | 4.160 | 2.970 | 0.2874 | 2.780 | 0.94 | 2.02 | 1716 | 18 | 1630 | 39 |
| spot 83 | 9170 | 2903 | 91700 | 31.59 | 0.10558 | 1.035 | 4.320 | 2.594 | 0.2954 | 2.379 | 0.92 | 1.50 | 1724 | 18 | 1667 | 35 |
| spot 84 | 8610 | 2909 | 92400 | 31.76 | 0.10331 | 1.065 | 3.857 | 2.562 | 0.2709 | 2.330 | 0.91 | 3.95 | 1684 | 18 | 1544 | 32 |
| spot 85 | 8930 | 2073 | 89200 | 43.03 | 0.10424 | 1.075 | 4.290 | 2.907 | 0.3000 | 2.701 | 0.93 | 0.30 | 1701 | 19 | 1688 | 40 |
| spot 86 | 8760 | 2471 | 88900 | 35.98 | 0.10545 | 1.041 | 4.107 | 2.523 | 0.2839 | 2.299 | 0.91 | 2.92 | 1723 | 18 | 1610 | 32 |
| spot 87 | 8580 | 2776 | 86200 | 31.05 | 0.10522 | 1.058 | 4.230 | 2.817 | 0.2913 | 2.610 | 0.93 | 2.07 | 1719 | 18 | 1646 | 38 |
| spot 88 | 7770 | 2209 | 76800 | 34.77 | 0.10438 | 1.052 | 4.210 | 2.659 | 0.2915 | 2.442 | 0.92 | 1.64 | 1703 | 18 | 1647 | 35 |
| spot 89 | 9120 | 3047 | 90200 | 29.60 | 0.10593 | 1.047 | 4.320 | 3.103 | 0.2938 | 2.921 | 0.94 | 2.11 | 1730 | 18 | 1658 | 43 |
| spot 90 | 9100 | 2610 | 89900 | 34.44 | 0.10447 | 1.056 | 4.271 | 2.382 | 0.2976 | 2.136 | 0.90 | 0.83 | 1706 | 18 | 1678 | 32 |
| spot 91 | 9150 | 2474 | 88000 | 35.57 | 0.10572 | 1.044 | 4.450 | 2.783 | 0.3029 | 2.580 | 0.93 | 0.94 | 1727 | 18 | 1707 | 38 |
| spot 92 | 9300 | 1894 | 91800 | 48.47 | 0.10396 | 1.071 | 4.370 | 2.829 | 0.3021 | 2.618 | 0.93 | 0.12 | 1696 | 18 | 1703 | 40 |
| spot 93 | 9890 | 2168 | 98200 | 45.30 | 0.10468 | 1.052 | 4.310 | 2.873 | 0.2955 | 2.674 | 0.93 | 1.62 | 1708 | 18 | 1666 | 39 |

**12TM13-01 monazite** (spot size: 7 µm, frequency: 3 Hz, 75 shot count, laser energy: 3 mJ at 75%)

| | | | | | ISOTOPIC RATIOS | | | | | | | | APPARENT AGES | | | |
|---|---|---|---|---|---|---|---|---|---|---|---|---|---|---|---|---|
| | Pb (ppm) | U (ppm) | Th (ppm) | Th/U | $^{207}Pb/^{206}Pb$ | 2σ % | $^{207}Pb/^{235}U$ | 2σ % | $^{206}Pb/^{238}U$ | 2σ % | Rho | % disc.* | $^{207}Pb/^{206}Pb$ | 2σ abs | $^{206}Pb/^{238}U$ | 2σ abs |
| spot 94 | 9410 | 1979 | 92000 | 46.49 | 0.10444 | 1.042 | 4.410 | 2.670 | 0.3020 | 2.458 | 0.92 | 0.47 | 1705 | 18 | 1703 | 37 |
| spot 95 | 6430 | 3960 | 76400 | 19.29 | 0.10209 | 1.055 | 3.023 | 3.070 | 0.2128 | 2.883 | 0.94 | 13.73 | 1663 | 18 | 1245 | 32 |
| spot 96 | 8800 | 3330 | 86400 | 25.95 | 0.10162 | 1.071 | 3.780 | 3.003 | 0.2664 | 2.805 | 0.93 | 4.13 | 1653 | 18 | 1524 | 38 |
| spot 97 | 8010 | 3270 | 78600 | 24.04 | 0.10227 | 1.066 | 3.860 | 3.096 | 0.2708 | 2.906 | 0.94 | 4.02 | 1666 | 18 | 1542 | 40 |
| spot 98 | 8310 | 3710 | 82700 | 22.29 | 0.10608 | 1.053 | 4.048 | 2.693 | 0.2745 | 2.478 | 0.92 | 5.44 | 1733 | 18 | 1562 | 34 |
| spot 99 | 9190 | 3840 | 84000 | 21.88 | 0.10729 | 1.036 | 4.440 | 2.995 | 0.2951 | 2.810 | 0.94 | 2.94 | 1754 | 18 | 1668 | 41 |
| spot 100 | 8430 | 3960 | 90000 | 22.73 | 0.10569 | 1.041 | 3.824 | 2.641 | 0.2593 | 2.428 | 0.92 | 7.68 | 1726 | 18 | 1485 | 33 |

**12TM15-16 monazite** (spot size: 6 µm, frequency: 3 Hz, 75 shot count, laser energy: 4 mJ at 56%)

| | | | | | ISOTOPIC RATIOS | | | | | | | | APPARENT AGES | | | |
|---|---|---|---|---|---|---|---|---|---|---|---|---|---|---|---|---|
| | Pb (ppm) | U (ppm) | Th (ppm) | Th/U | $^{207}Pb/^{206}Pb$ | 2σ % | $^{207}Pb/^{235}U$ | 2σ % | $^{206}Pb/^{238}U$ | 2σ % | Rho | % disc.* | $^{207}Pb/^{206}Pb$ | 2σ abs | $^{206}Pb/^{238}U$ | 2σ abs |
| spot 1 | 14030 | 4260 | 149400 | 35.07 | 0.10282 | 1.080 | 3.981 | 2.526 | 0.2831 | 2.284 | 0.90 | 1.49 | 1676 | 18 | 1606 | 34 |
| spot 2 | 16070 | 5340 | 170000 | 31.84 | 0.10365 | 1.062 | 4.051 | 2.496 | 0.2874 | 2.259 | 0.90 | 1.11 | 1690 | 18 | 1627 | 34 |
| spot 3 | 14870 | 5260 | 164100 | 31.20 | 0.10069 | 1.072 | 3.754 | 2.464 | 0.2733 | 2.219 | 0.90 | 1.60 | 1637 | 18 | 1563 | 33 |
| spot 4 | 14950 | 6620 | 172700 | 26.09 | 0.10476 | 1.070 | 3.849 | 2.785 | 0.2682 | 2.572 | 0.92 | 4.22 | 1710 | 19 | 1542 | 35 |
| spot 5 | 17770 | 7180 | 189800 | 26.43 | 0.10325 | 1.059 | 3.935 | 2.521 | 0.2772 | 2.288 | 0.91 | 2.79 | 1683 | 18 | 1576 | 33 |
| spot 6 | 15710 | 5370 | 159900 | 29.78 | 0.10422 | 1.064 | 4.117 | 2.412 | 0.2886 | 2.165 | 0.90 | 1.47 | 1701 | 18 | 1633 | 33 |
| spot 7 | 18080 | 6890 | 186700 | 27.10 | 0.10506 | 1.048 | 4.146 | 2.461 | 0.2880 | 2.226 | 0.90 | 1.71 | 1715 | 18 | 1637 | 33 |
| spot 8 | 14490 | 6080 | 151400 | 24.90 | 0.10167 | 1.068 | 3.840 | 2.236 | 0.2765 | 1.964 | 0.88 | 1.65 | 1655 | 18 | 1573 | 29 |
| spot 9 | 10570 | 5880 | 133600 | 22.72 | 0.08954 | 1.109 | 2.595 | 2.767 | 0.2105 | 2.535 | 0.92 | 5.69 | 1415 | 17 | 1231 | 29 |
| spot 10 | 11440 | 6210 | 137000 | 22.06 | 0.08925 | 1.087 | 2.800 | 2.789 | 0.2290 | 2.568 | 0.92 | 2.18 | 1409 | 16 | 1328 | 31 |
| spot 11 | 15740 | 5140 | 153000 | 29.77 | 0.10414 | 1.064 | 4.121 | 2.494 | 0.2881 | 2.255 | 0.90 | 1.59 | 1699 | 18 | 1631 | 33 |
| spot 12 | 17760 | 5990 | 173100 | 28.90 | 0.10417 | 1.058 | 4.132 | 2.604 | 0.2871 | 2.380 | 0.91 | 2.40 | 1700 | 18 | 1626 | 35 |
| spot 13 | 15480 | 6000 | 165100 | 27.52 | 0.10156 | 1.172 | 3.599 | 2.734 | 0.2594 | 2.470 | 0.90 | 4.03 | 1653 | 20 | 1488 | 33 |
| spot 14 | 14470 | 4850 | 140500 | 28.97 | 0.10405 | 1.068 | 4.143 | 2.682 | 0.2886 | 2.461 | 0.92 | 1.53 | 1697 | 18 | 1636 | 36 |
| spot 15 | 11300 | 4960 | 122700 | 24.74 | 0.10353 | 1.053 | 3.546 | 2.766 | 0.2479 | 2.558 | 0.92 | 7.57 | 1688 | 18 | 1426 | 34 |
| spot 16 | 17270 | 7130 | 176400 | 24.74 | 0.10478 | 1.051 | 3.939 | 2.783 | 0.2719 | 2.577 | 0.93 | 4.71 | 1710 | 18 | 1549 | 36 |
| spot 17 | 18310 | 4810 | 181300 | 37.69 | 0.10416 | 1.058 | 4.133 | 2.316 | 0.2867 | 2.060 | 0.89 | 2.15 | 1700 | 18 | 1628 | 32 |
| spot 18 | 12990 | 4900 | 130300 | 26.59 | 0.10392 | 1.065 | 3.955 | 2.628 | 0.2738 | 2.403 | 0.91 | 3.91 | 1695 | 18 | 1562 | 34 |
| spot 19 | 16650 | 7830 | 185500 | 23.69 | 0.10228 | 1.057 | 3.507 | 2.511 | 0.2480 | 2.277 | 0.91 | 6.94 | 1666 | 18 | 1427 | 30 |
| spot 20 | 15830 | 5850 | 148200 | 25.33 | 0.10489 | 1.046 | 4.172 | 2.649 | 0.2880 | 2.434 | 0.92 | 2.20 | 1712 | 18 | 1633 | 37 |
| spot 21 | 17720 | 8830 | 203100 | 23.00 | 0.10264 | 1.047 | 3.418 | 2.521 | 0.2405 | 2.293 | 0.91 | 8.65 | 1673 | 18 | 1388 | 29 |
| spot 22 | 17930 | 8720 | 199800 | 22.91 | 0.10348 | 1.039 | 3.664 | 2.832 | 0.2558 | 2.635 | 0.93 | 6.27 | 1687 | 18 | 1467 | 36 |
| spot 23 | 18370 | 8950 | 200000 | 22.35 | 0.10430 | 1.043 | 3.773 | 2.665 | 0.2618 | 2.453 | 0.92 | 6.01 | 1702 | 18 | 1498 | 34 |
| spot 24 | 16340 | 6710 | 167400 | 24.95 | 0.10083 | 1.052 | 3.854 | 2.538 | 0.2787 | 2.310 | 0.91 | 1.52 | 1639 | 17 | 1584 | 33 |
| spot 25 | 17510 | 6930 | 170600 | 24.62 | 0.10406 | 1.052 | 4.133 | 2.691 | 0.2862 | 2.476 | 0.92 | 2.22 | 1698 | 18 | 1621 | 37 |
| spot 26 | 14500 | 4980 | 137700 | 27.65 | 0.10422 | 1.061 | 4.234 | 2.438 | 0.2939 | 2.195 | 0.90 | 1.02 | 1700 | 18 | 1667 | 34 |
| spot 27 | 13960 | 4850 | 132500 | 27.32 | 0.10393 | 1.075 | 4.191 | 2.535 | 0.2912 | 2.296 | 0.91 | 1.64 | 1695 | 18 | 1646 | 34 |
| spot 28 | 15140 | 8850 | 144500 | 16.33 | 0.10551 | 1.037 | 4.176 | 2.388 | 0.2857 | 2.151 | 0.90 | 3.09 | 1724 | 18 | 1619 | 32 |
| spot 29 | 17340 | 9150 | 171700 | 18.77 | 0.10544 | 1.040 | 4.174 | 2.444 | 0.2852 | 2.212 | 0.91 | 2.90 | 1722 | 18 | 1619 | 33 |
| spot 30 | 11700 | 7540 | 128100 | 16.99 | 0.10326 | 1.095 | 3.583 | 2.986 | 0.2514 | 2.778 | 0.93 | 6.79 | 1683 | 19 | 1444 | 36 |
| spot 31 | 19560 | 9740 | 218500 | 22.43 | 0.10515 | 1.063 | 3.830 | 2.665 | 0.2631 | 2.443 | 0.92 | 6.25 | 1717 | 18 | 1504 | 33 |

**12TM15-16 monazite** (spot size: 6 µm, frequency: 3 Hz, 75 shot count, laser energy: 4 mJ at 56%)

| | | | | | ISOTOPIC RATIOS | | | | | | | | APPARENT AGES | | | |
|---|---|---|---|---|---|---|---|---|---|---|---|---|---|---|---|---|
| | Pb (ppm) | U (ppm) | Th (ppm) | Th/U | $^{207}Pb/^{206}Pb$ | 2σ % | $^{207}Pb/^{235}U$ | 2σ % | $^{206}Pb/^{238}U$ | 2σ % | Rho | % disc.* | $^{207}Pb/^{206}Pb$ | 2σ abs | $^{206}Pb/^{238}U$ | 2σ abs |
| spot 32 | 14910 | 9340 | 154400 | 16.53 | 0.10539 | 1.030 | 3.983 | 2.453 | 0.2719 | 2.227 | 0.91 | 5.23 | 1722 | 18 | 1549 | 32 |
| spot 33 | 12910 | 5790 | 139000 | 24.01 | 0.10256 | 1.070 | 3.670 | 2.736 | 0.2575 | 2.518 | 0.92 | 5.76 | 1673 | 18 | 1476 | 34 |
| spot 34 | 12860 | 7350 | 153800 | 20.93 | 0.08911 | 1.066 | 2.834 | 2.461 | 0.2305 | 2.218 | 0.90 | 2.10 | 1406 | 16 | 1336 | 28 |
| spot 35 | 12660 | 6980 | 149800 | 21.46 | 0.08903 | 1.063 | 2.865 | 2.831 | 0.2357 | 2.624 | 0.93 | 0.95 | 1405 | 16 | 1363 | 33 |
| spot 36 | 9190 | 6640 | 172500 | 25.98 | 0.10012 | 1.077 | 2.430 | 2.638 | 0.1772 | 2.408 | 0.91 | 19.07 | 1626 | 18 | 1054 | 25 |
| spot 37 | 15080 | 5450 | 143700 | 26.37 | 0.10416 | 1.068 | 4.131 | 2.612 | 0.2913 | 2.384 | 0.91 | 1.15 | 1701 | 18 | 1647 | 36 |
| spot 38 | 15270 | 5430 | 144900 | 26.69 | 0.10431 | 1.058 | 4.210 | 2.838 | 0.2944 | 2.633 | 0.93 | 0.90 | 1702 | 18 | 1662 | 40 |
| spot 39 | 13330 | 6560 | 123700 | 18.86 | 0.10544 | 1.060 | 4.220 | 3.022 | 0.2926 | 2.830 | 0.94 | 1.39 | 1722 | 18 | 1652 | 43 |
| spot 40 | 13740 | 7340 | 145300 | 19.80 | 0.10455 | 1.040 | 3.764 | 2.803 | 0.2641 | 2.603 | 0.93 | 5.09 | 1706 | 18 | 1513 | 36 |
| spot 41 | 14570 | 7370 | 138600 | 18.81 | 0.10557 | 1.045 | 4.214 | 2.785 | 0.2931 | 2.582 | 0.93 | 1.21 | 1725 | 18 | 1655 | 39 |
| spot 42 | 13360 | 7050 | 128800 | 18.27 | 0.10541 | 1.057 | 4.080 | 3.340 | 0.2830 | 3.169 | 0.95 | 2.74 | 1722 | 18 | 1604 | 46 |
| spot 43 | 11400 | 4250 | 137200 | 32.28 | 0.09950 | 1.124 | 3.084 | 3.379 | 0.2270 | 3.186 | 0.94 | 7.95 | 1616 | 19 | 1321 | 38 |
| spot 44 | 11860 | 4350 | 141300 | 32.48 | 0.09946 | 1.110 | 3.174 | 3.009 | 0.2336 | 2.796 | 0.93 | 7.17 | 1613 | 18 | 1352 | 35 |
| spot 45 | 17240 | 10400 | 169100 | 16.26 | 0.10633 | 1.039 | 4.109 | 2.740 | 0.2821 | 2.535 | 0.93 | 3.06 | 1738 | 18 | 1603 | 36 |
| spot 46 | 15960 | 10050 | 167700 | 16.69 | 0.10569 | 1.050 | 3.944 | 2.694 | 0.2717 | 2.481 | 0.92 | 5.04 | 1727 | 18 | 1548 | 35 |
| spot 47 | 15520 | 9470 | 155600 | 16.43 | 0.10573 | 1.039 | 4.051 | 2.669 | 0.2797 | 2.458 | 0.92 | 3.59 | 1727 | 18 | 1588 | 36 |
| spot 48 | 14670 | 9410 | 159900 | 16.99 | 0.10369 | 1.052 | 3.518 | 2.704 | 0.2474 | 2.491 | 0.92 | 7.30 | 1691 | 18 | 1424 | 33 |
| spot 49 | 10180 | 8760 | 152200 | 17.37 | 0.09895 | 1.071 | 2.417 | 2.668 | 0.1785 | 2.444 | 0.92 | 17.53 | 1604 | 18 | 1061 | 25 |
| spot 50 | 10170 | 9160 | 146000 | 15.94 | 0.09956 | 1.063 | 2.521 | 2.784 | 0.1845 | 2.573 | 0.92 | 16.83 | 1616 | 17 | 1093 | 27 |
| spot 51 | 20200 | 9850 | 229900 | 23.34 | 0.10458 | 1.067 | 4.034 | 2.326 | 0.2793 | 2.067 | 0.89 | 3.14 | 1707 | 18 | 1590 | 31 |
| spot 52 | 18510 | 13390 | 212100 | 15.84 | 0.10541 | 1.048 | 3.982 | 2.269 | 0.2723 | 2.013 | 0.89 | 5.02 | 1721 | 18 | 1554 | 29 |
| spot 53 | 17520 | 11260 | 229300 | 20.36 | 0.10469 | 1.071 | 3.694 | 2.406 | 0.2570 | 2.155 | 0.90 | 6.65 | 1709 | 19 | 1474 | 29 |
| spot 54 | 20080 | 10540 | 223100 | 21.17 | 0.10517 | 1.054 | 4.119 | 2.281 | 0.2824 | 2.023 | 0.89 | 3.31 | 1717 | 18 | 1603 | 30 |
| spot 55 | 20140 | 10300 | 230000 | 22.33 | 0.10534 | 1.060 | 4.056 | 2.505 | 0.2802 | 2.270 | 0.91 | 3.71 | 1720 | 18 | 1591 | 33 |
| spot 56 | 20880 | 10410 | 222500 | 21.37 | 0.10490 | 1.081 | 4.077 | 2.413 | 0.2845 | 2.157 | 0.89 | 2.29 | 1712 | 19 | 1616 | 32 |
| spot 57 | 18650 | 11740 | 212500 | 18.10 | 0.10573 | 1.045 | 4.093 | 2.038 | 0.2827 | 1.750 | 0.86 | 2.80 | 1727 | 18 | 1607 | 27 |
| spot 58 | 21960 | 12700 | 232300 | 18.29 | 0.10584 | 1.056 | 4.197 | 2.278 | 0.2896 | 2.018 | 0.89 | 1.83 | 1729 | 18 | 1641 | 31 |
| spot 59 | 20240 | 9130 | 209500 | 22.95 | 0.10481 | 1.054 | 4.236 | 2.322 | 0.2967 | 2.069 | 0.89 | 0.30 | 1711 | 18 | 1677 | 32 |
| spot 60 | 20670 | 9300 | 217000 | 23.33 | 0.10491 | 1.043 | 4.175 | 2.310 | 0.2924 | 2.061 | 0.89 | 1.03 | 1712 | 18 | 1652 | 31 |
| spot 61 | 15200 | 7140 | 194200 | 27.20 | 0.10475 | 1.067 | 4.085 | 2.372 | 0.2863 | 2.119 | 0.89 | 1.85 | 1710 | 18 | 1622 | 32 |
| spot 62 | 19190 | 9440 | 206700 | 21.90 | 0.10391 | 1.055 | 4.046 | 2.268 | 0.2858 | 2.008 | 0.89 | 1.36 | 1695 | 18 | 1619 | 30 |

**12TM15-16 monazite** (spot size: 6 µm, frequency: 3 Hz, 75 shot count, laser energy: 4 mJ at 56%)

| | | | | | ISOTOPIC RATIOS | | | | | | | | APPARENT AGES | | | |
|---|---|---|---|---|---|---|---|---|---|---|---|---|---|---|---|---|
| | Pb (ppm) | U (ppm) | Th (ppm) | Th/U | $^{207}Pb/^{206}Pb$ | 2σ % | $^{207}Pb/^{235}U$ | 2σ % | $^{206}Pb/^{238}U$ | 2σ % | Rho | % disc.* | $^{207}Pb/^{206}Pb$ | 2σ abs | $^{206}Pb/^{238}U$ | 2σ abs |
| spot 63 | 18570 | 9070 | 194800 | 21.48 | 0.10510 | 1.057 | 4.101 | 2.358 | 0.2886 | 2.108 | 0.89 | 1.22 | 1716 | 18 | 1634 | 32 |
| spot 64 | 18890 | 11160 | 193500 | 17.34 | 0.10523 | 1.057 | 4.114 | 2.281 | 0.2889 | 2.022 | 0.89 | 1.53 | 1719 | 18 | 1635 | 31 |
| spot 65 | 12110 | 6610 | 132900 | 20.11 | 0.10210 | 1.101 | 3.623 | 2.452 | 0.2618 | 2.191 | 0.89 | 3.40 | 1662 | 19 | 1501 | 30 |
| spot 66 | 13530 | 6060 | 135800 | 22.41 | 0.10406 | 1.058 | 4.105 | 2.554 | 0.2914 | 2.324 | 0.91 | 0.55 | 1697 | 18 | 1647 | 35 |
| spot 67 | 13740 | 5860 | 136900 | 23.36 | 0.10406 | 1.068 | 4.110 | 2.253 | 0.2911 | 1.984 | 0.88 | 0.49 | 1698 | 18 | 1646 | 30 |
| spot 68 | 13860 | 5750 | 136700 | 23.77 | 0.10391 | 1.072 | 4.117 | 2.483 | 0.2908 | 2.240 | 0.90 | 0.67 | 1695 | 18 | 1644 | 33 |
| spot 69 | 12480 | 5670 | 123600 | 21.80 | 0.10426 | 1.097 | 4.078 | 2.456 | 0.2879 | 2.197 | 0.89 | 1.29 | 1702 | 19 | 1630 | 33 |
| spot 70 | 14170 | 5490 | 140800 | 25.65 | 0.10397 | 1.065 | 4.112 | 2.539 | 0.2897 | 2.305 | 0.91 | 0.98 | 1696 | 18 | 1639 | 34 |
| spot 71 | 13650 | 5060 | 134000 | 26.48 | 0.10405 | 1.071 | 4.126 | 2.508 | 0.2911 | 2.267 | 0.90 | 0.49 | 1697 | 18 | 1649 | 34 |
| spot 72 | 15900 | 8080 | 188500 | 23.33 | 0.08841 | 1.052 | 2.792 | 2.387 | 0.2310 | 2.142 | 0.90 | 0.97 | 1391 | 15 | 1339 | 26 |
| spot 73 | 25200 | 8930 | 254000 | 28.44 | 0.10404 | 1.041 | 4.119 | 2.405 | 0.2880 | 2.168 | 0.90 | 1.66 | 1697 | 18 | 1630 | 33 |
| spot 74 | 13610 | 7340 | 172400 | 23.49 | 0.08845 | 1.132 | 2.598 | 2.536 | 0.2129 | 2.269 | 0.89 | 4.33 | 1392 | 17 | 1247 | 26 |
| spot 75 | 19880 | 7690 | 199700 | 25.97 | 0.10383 | 1.058 | 4.065 | 2.329 | 0.2837 | 2.074 | 0.89 | 2.30 | 1693 | 18 | 1612 | 31 |
| spot 76 | 23650 | 6320 | 241400 | 38.20 | 0.10369 | 1.075 | 4.079 | 2.697 | 0.2866 | 2.474 | 0.92 | 1.60 | 1691 | 18 | 1623 | 37 |
| spot 77 | 19030 | 6290 | 188500 | 29.97 | 0.10413 | 1.052 | 4.122 | 2.443 | 0.2865 | 2.205 | 0.90 | 2.09 | 1699 | 18 | 1625 | 33 |
| spot 78 | 19450 | 7930 | 208100 | 26.24 | 0.10448 | 1.043 | 3.819 | 2.337 | 0.2627 | 2.091 | 0.89 | 5.98 | 1705 | 18 | 1506 | 29 |
| spot 79 | 19040 | 5590 | 186000 | 33.27 | 0.10368 | 1.047 | 4.170 | 2.381 | 0.2881 | 2.139 | 0.90 | 1.96 | 1691 | 18 | 1634 | 33 |
| spot 80 | 16340 | 5270 | 163600 | 31.04 | 0.10242 | 1.051 | 3.896 | 2.540 | 0.2731 | 2.313 | 0.91 | 3.79 | 1669 | 18 | 1555 | 33 |
| spot 81 | 11750 | 4560 | 196900 | 43.18 | 0.09466 | 1.107 | 2.172 | 2.585 | 0.1647 | 2.336 | 0.90 | 19.14 | 1523 | 18 | 982 | 22 |
| spot 82 | 18080 | 4210 | 190900 | 45.34 | 0.10254 | 1.084 | 3.820 | 2.993 | 0.2660 | 2.790 | 0.93 | 4.79 | 1670 | 18 | 1524 | 38 |
| spot 83 | 14420 | 6530 | 144400 | 22.11 | 0.10376 | 1.041 | 3.963 | 2.446 | 0.2743 | 2.213 | 0.90 | 4.04 | 1692 | 18 | 1561 | 32 |
| spot 84 | 16680 | 4360 | 174400 | 40.00 | 0.10245 | 1.113 | 3.836 | 2.888 | 0.2689 | 2.665 | 0.92 | 4.30 | 1669 | 19 | 1534 | 37 |
| spot 85 | 18410 | 5990 | 201400 | 33.62 | 0.10045 | 1.056 | 3.488 | 2.591 | 0.2501 | 2.366 | 0.91 | 5.84 | 1632 | 18 | 1438 | 31 |
| spot 86 | 15630 | 5920 | 189800 | 32.06 | 0.08865 | 1.059 | 2.736 | 2.441 | 0.2225 | 2.199 | 0.90 | 3.40 | 1396 | 15 | 1294 | 27 |
| spot 87 | 20850 | 4250 | 202400 | 47.62 | 0.10381 | 1.062 | 4.163 | 2.595 | 0.2891 | 2.367 | 0.91 | 1.77 | 1693 | 18 | 1636 | 36 |
| spot 88 | 19810 | 6840 | 240600 | 35.18 | 0.08966 | 1.066 | 2.836 | 2.369 | 0.2295 | 2.116 | 0.89 | 2.63 | 1418 | 16 | 1331 | 26 |
| spot 89 | 19520 | 6810 | 238400 | 35.01 | 0.08984 | 1.069 | 2.851 | 2.845 | 0.2300 | 2.637 | 0.93 | 2.40 | 1422 | 16 | 1333 | 32 |
| spot 90 | 17590 | 6730 | 219700 | 32.64 | 0.08997 | 1.054 | 2.702 | 2.760 | 0.2177 | 2.551 | 0.92 | 5.21 | 1426 | 16 | 1268 | 30 |
| spot 91 | 16680 | 6330 | 200600 | 31.69 | 0.08927 | 1.059 | 2.839 | 2.844 | 0.2297 | 2.639 | 0.93 | 2.25 | 1410 | 16 | 1332 | 32 |
| spot 92 | 16710 | 4660 | 166900 | 35.82 | 0.10409 | 1.089 | 4.012 | 2.458 | 0.2814 | 2.203 | 0.90 | 2.57 | 1698 | 19 | 1597 | 32 |
| spot 93 | 16100 | 4620 | 168700 | 36.52 | 0.10406 | 1.065 | 3.848 | 2.652 | 0.2699 | 2.429 | 0.92 | 4.35 | 1698 | 18 | 1539 | 34 |

**12TM15-16 monazite** (spot size: 6 µm, frequency: 3 Hz, 75 shot count, laser energy: 4 mJ at 56%)

| | | | | | ISOTOPIC RATIOS | | | | | | | | APPARENT AGES | | | |
|---|---|---|---|---|---|---|---|---|---|---|---|---|---|---|---|---|
| | Pb (ppm) | U (ppm) | Th (ppm) | Th/U | $^{207}Pb/^{206}Pb$ | 2σ % | $^{207}Pb/^{235}U$ | 2σ % | $^{206}Pb/^{238}U$ | 2σ % | Rho | % disc.* | $^{207}Pb/^{206}Pb$ | 2σ abs | $^{206}Pb/^{238}U$ | 2σ abs |
| spot 94 | 14370 | 4530 | 160400 | 35.41 | 0.10198 | 1.089 | 3.450 | 2.692 | 0.2466 | 2.462 | 0.91 | 6.54 | 1662 | 18 | 1423 | 33 |
| spot 95 | 12710 | 4650 | 162000 | 34.84 | 0.10277 | 1.066 | 3.657 | 2.919 | 0.2584 | 2.717 | 0.93 | 5.06 | 1675 | 18 | 1483 | 37 |

**12TM17-04 monazite** (spot size: 6 µm, frequency: 3 Hz, 75 shot count, laser energy: 4 mJ at 56%)

| | | | | | ISOTOPIC RATIOS | | | | | | | | APPARENT AGES | | | |
|---|---|---|---|---|---|---|---|---|---|---|---|---|---|---|---|---|
| | Pb (ppm) | U (ppm) | Th (ppm) | Th/U | $^{207}Pb/^{206}Pb$ | 2σ % | $^{207}Pb/^{235}U$ | 2σ % | $^{206}Pb/^{238}U$ | 2σ % | Rho | % disc.* | $^{207}Pb/^{206}Pb$ | 2σ abs | $^{206}Pb/^{238}U$ | 2σ abs |
| spot 1 | 3326 | 4870 | 32200 | 6.61 | 0.10336 | 1.362 | 3.901 | 2.820 | 0.2699 | 2.469 | 0.88 | 4.87 | 1685 | 23 | 1540 | 36 |
| spot 2 | 4900 | 9280 | 45900 | 4.95 | 0.10619 | 1.346 | 4.279 | 2.808 | 0.2882 | 2.464 | 0.88 | 3.43 | 1735 | 23 | 1631 | 38 |
| spot 3 | 3520 | 6000 | 31020 | 5.17 | 0.10516 | 1.355 | 4.207 | 2.654 | 0.2866 | 2.283 | 0.86 | 3.26 | 1717 | 23 | 1624 | 35 |
| spot 4 | 499 | 4870 | 36400 | 7.47 | 0.06680 | 2.098 | 0.327 | 3.190 | 0.0352 | 2.403 | 0.75 | 28.91 | 835 | 34 | 223 | 5 |
| spot 5 | 207 | 3640 | 16060 | 4.41 | 0.04980 | 2.738 | 0.181 | 4.181 | 0.0262 | 3.160 | 0.76 | 1.02 | 180 | 54 | 167 | 5 |
| spot 6 | 171 | 2152 | 12040 | 5.59 | 0.05160 | 3.542 | 0.195 | 4.802 | 0.0275 | 3.242 | 0.68 | 3.21 | 277 | 71 | 175 | 6 |
| spot 7 | 1487 | 2498 | 11220 | 4.49 | 0.10455 | 1.395 | 4.360 | 3.286 | 0.2992 | 2.975 | 0.91 | 0.89 | 1706 | 24 | 1689 | 46 |
| spot 8 | 311 | 5400 | 27370 | 5.07 | 0.05145 | 2.087 | 0.181 | 3.293 | 0.0254 | 2.547 | 0.77 | 4.08 | 253 | 37 | 162 | 4 |
| spot 9 | 285 | 4847 | 27580 | 5.69 | 0.05774 | 2.016 | 0.201 | 3.169 | 0.0252 | 2.445 | 0.77 | 16.09 | 519 | 34 | 160 | 4 |
| spot 10 | 3062 | 3980 | 27140 | 6.82 | 0.10306 | 1.365 | 4.058 | 2.848 | 0.2859 | 2.499 | 0.88 | 1.54 | 1681 | 23 | 1620 | 38 |
| spot 11 | 3014 | 4230 | 26710 | 6.31 | 0.10375 | 1.356 | 4.000 | 2.806 | 0.2785 | 2.456 | 0.88 | 3.22 | 1692 | 23 | 1583 | 37 |
| spot 12 | 2898 | 3480 | 25290 | 7.27 | 0.10317 | 1.359 | 3.949 | 2.906 | 0.2767 | 2.568 | 0.88 | 2.99 | 1682 | 23 | 1574 | 39 |
| spot 13 | 2454 | 3196 | 24830 | 7.77 | 0.10405 | 1.345 | 3.878 | 2.725 | 0.2691 | 2.370 | 0.87 | 4.62 | 1697 | 23 | 1536 | 35 |
| spot 14 | 2145 | 2635 | 18180 | 6.90 | 0.10595 | 1.371 | 4.220 | 3.158 | 0.2898 | 2.845 | 0.90 | 2.50 | 1732 | 24 | 1639 | 44 |
| spot 15 | 1843 | 1924 | 16460 | 8.56 | 0.10513 | 1.391 | 4.010 | 3.346 | 0.2772 | 3.043 | 0.91 | 3.75 | 1716 | 24 | 1575 | 45 |
| spot 16 | 1680 | 1946 | 17530 | 9.01 | 0.10504 | 1.381 | 3.758 | 3.115 | 0.2620 | 2.792 | 0.90 | 5.74 | 1715 | 24 | 1499 | 39 |
| spot 17 | 1833 | 2006 | 15650 | 7.80 | 0.10447 | 1.403 | 3.910 | 3.351 | 0.2731 | 3.043 | 0.91 | 3.72 | 1708 | 24 | 1559 | 44 |
| spot 18 | 1201 | 1965 | 9770 | 4.97 | 0.10482 | 1.395 | 4.000 | 3.742 | 0.2767 | 3.473 | 0.93 | 3.30 | 1711 | 24 | 1577 | 51 |
| spot 19 | 220 | 868 | 19710 | 22.71 | 0.05040 | 4.936 | 0.160 | 6.052 | 0.0234 | 3.502 | 0.58 | 0.94 | 222 | 96 | 149 | 5 |
| spot 20 | 234 | 1052 | 21260 | 20.21 | 0.04890 | 4.487 | 0.155 | 5.499 | 0.0230 | 3.178 | 0.58 | 0.20 | 139 | 86 | 147 | 5 |
| spot 21 | 2703 | 6290 | 21880 | 3.48 | 0.10593 | 1.349 | 3.838 | 2.943 | 0.2623 | 2.616 | 0.89 | 6.30 | 1731 | 23 | 1507 | 37 |
| spot 22 | 2713 | 5950 | 21890 | 3.68 | 0.10526 | 1.340 | 3.845 | 3.322 | 0.2655 | 3.040 | 0.92 | 5.94 | 1719 | 23 | 1516 | 42 |
| spot 23 | 3730 | 8150 | 33000 | 4.05 | 0.10686 | 1.336 | 3.682 | 3.033 | 0.2492 | 2.723 | 0.90 | 9.42 | 1748 | 23 | 1433 | 37 |
| spot 24 | 3890 | 7870 | 32100 | 4.08 | 0.10653 | 1.348 | 3.993 | 3.191 | 0.2692 | 2.893 | 0.91 | 6.19 | 1741 | 24 | 1535 | 41 |
| spot 25 | 3131 | 6280 | 26800 | 4.27 | 0.10551 | 1.346 | 3.883 | 3.060 | 0.2643 | 2.748 | 0.90 | 6.69 | 1723 | 23 | 1510 | 39 |
| spot 26 | 3213 | 6010 | 27520 | 4.58 | 0.10518 | 1.347 | 3.917 | 2.939 | 0.2682 | 2.612 | 0.89 | 5.75 | 1717 | 23 | 1530 | 37 |
| spot 27 | 425 | 3090 | 32500 | 10.52 | 0.06050 | 2.372 | 0.253 | 3.965 | 0.0302 | 3.178 | 0.80 | 20.31 | 611 | 43 | 192 | 6 |
| spot 28 | 3220 | 3750 | 29420 | 7.85 | 0.09728 | 1.439 | 3.614 | 2.971 | 0.2653 | 2.600 | 0.87 | 2.51 | 1572 | 24 | 1516 | 37 |
| spot 29 | 379 | 2579 | 26420 | 10.24 | 0.06560 | 3.036 | 0.359 | 5.470 | 0.0381 | 4.550 | 0.83 | 28.63 | 795 | 61 | 241 | 11 |
| spot 30 | 298 | 3740 | 24560 | 6.57 | 0.04864 | 2.178 | 0.177 | 3.856 | 0.0263 | 3.182 | 0.83 | 1.01 | 125 | 38 | 168 | 5 |
| spot 31 | 299 | 2142 | 22830 | 10.66 | 0.05580 | 2.214 | 0.225 | 3.719 | 0.0293 | 2.988 | 0.80 | 10.37 | 432 | 41 | 186 | 6 |

**12TM17-04 monazite** (spot size: 6 µm, frequency: 3 Hz, 75 shot count, laser energy: 4 mJ at 56%)

| | | | | | ISOTOPIC RATIOS | | | | | | | | APPARENT AGES | | | |
|---|---|---|---|---|---|---|---|---|---|---|---|---|---|---|---|---|
| | Pb (ppm) | U (ppm) | Th (ppm) | Th/U | $^{207}Pb/^{206}Pb$ | 2σ % | $^{207}Pb/^{235}U$ | 2σ % | $^{206}Pb/^{238}U$ | 2σ % | Rho | % disc.* | $^{207}Pb/^{206}Pb$ | 2σ abs | $^{206}Pb/^{238}U$ | 2σ abs |
| spot 32 | 2322 | 2810 | 18410 | 6.55 | 0.10164 | 1.353 | 4.120 | 3.368 | 0.2953 | 3.084 | 0.92 | 0.00 | 1654 | 23 | 1670 | 46 |
| spot 33 | 2623 | 3090 | 20930 | 6.77 | 0.10325 | 1.362 | 4.360 | 3.290 | 0.3045 | 2.995 | 0.91 | 0.29 | 1683 | 23 | 1711 | 48 |
| spot 34 | 2354 | 2590 | 19260 | 7.44 | 0.10178 | 1.390 | 4.110 | 3.447 | 0.2934 | 3.154 | 0.92 | 0.36 | 1656 | 23 | 1660 | 48 |
| spot 35 | 2307 | 3500 | 19120 | 5.46 | 0.10162 | 1.364 | 4.020 | 3.409 | 0.2859 | 3.124 | 0.92 | 0.86 | 1653 | 23 | 1619 | 47 |
| spot 36 | 271 | 2770 | 21840 | 7.88 | 0.04893 | 2.170 | 0.174 | 3.815 | 0.0261 | 3.138 | 0.82 | 1.87 | 144 | 39 | 166 | 5 |
| spot 37 | 292 | 2528 | 23220 | 9.19 | 0.05530 | 2.376 | 0.203 | 3.731 | 0.0267 | 2.877 | 0.77 | 10.36 | 419 | 42 | 170 | 5 |
| spot 38 | 567 | 978 | 22620 | 23.13 | 0.09300 | 1.758 | 1.470 | 4.087 | 0.1139 | 3.690 | 0.90 | 31.85 | 1484 | 30 | 697 | 24 |
| spot 39 | 417 | 2039 | 26000 | 12.75 | 0.07170 | 1.907 | 0.398 | 3.569 | 0.0407 | 3.017 | 0.85 | 32.02 | 971 | 32 | 257 | 8 |
| spot 40 | 375 | 1733 | 24600 | 14.20 | 0.06860 | 2.179 | 0.357 | 3.839 | 0.0380 | 3.160 | 0.82 | 28.98 | 885 | 37 | 240 | 7 |
| spot 41 | 2801 | 3140 | 24390 | 7.77 | 0.10304 | 1.351 | 3.970 | 3.309 | 0.2803 | 3.020 | 0.91 | 1.88 | 1679 | 23 | 1595 | 44 |
| spot 42 | 2640 | 2649 | 28360 | 10.71 | 0.10638 | 1.359 | 4.075 | 3.137 | 0.2792 | 2.827 | 0.90 | 4.16 | 1739 | 24 | 1586 | 42 |
| spot 43 | 3237 | 2715 | 27530 | 10.14 | 0.10482 | 1.340 | 4.190 | 3.281 | 0.2921 | 2.995 | 0.91 | 1.52 | 1711 | 23 | 1650 | 45 |
| spot 44 | 3550 | 3040 | 30000 | 9.87 | 0.10510 | 1.349 | 4.120 | 3.126 | 0.2849 | 2.820 | 0.90 | 2.48 | 1717 | 23 | 1614 | 43 |
| spot 45 | 3470 | 2810 | 30400 | 10.82 | 0.10436 | 1.350 | 4.032 | 3.251 | 0.2811 | 2.957 | 0.91 | 2.57 | 1703 | 23 | 1595 | 43 |
| spot 46 | 4570 | 2575 | 39500 | 15.34 | 0.10545 | 1.337 | 4.305 | 3.050 | 0.2985 | 2.742 | 0.90 | 0.77 | 1722 | 23 | 1682 | 43 |
| spot 47 | 4324 | 2418 | 38100 | 15.76 | 0.10566 | 1.342 | 4.230 | 3.363 | 0.2914 | 3.084 | 0.92 | 2.00 | 1726 | 23 | 1646 | 47 |
| spot 48 | 2909 | 2007 | 29490 | 14.69 | 0.10554 | 1.360 | 4.213 | 3.132 | 0.2936 | 2.822 | 0.90 | 1.45 | 1723 | 24 | 1657 | 43 |
| spot 49 | 3156 | 1496 | 33200 | 22.19 | 0.10803 | 1.380 | 4.330 | 3.240 | 0.2934 | 2.931 | 0.90 | 2.78 | 1766 | 24 | 1656 | 45 |
| spot 50 | 3720 | 1960 | 34900 | 17.81 | 0.10343 | 1.343 | 3.895 | 3.364 | 0.2757 | 3.084 | 0.92 | 2.48 | 1686 | 23 | 1572 | 45 |
| spot 51 | 2817 | 1850 | 30000 | 16.22 | 0.08943 | 1.368 | 2.880 | 3.442 | 0.2358 | 3.158 | 0.92 | 1.17 | 1414 | 20 | 1363 | 41 |
| spot 52 | 2300 | 1165 | 28540 | 24.50 | 0.09706 | 1.391 | 3.031 | 3.451 | 0.2282 | 3.158 | 0.92 | 6.56 | 1568 | 22 | 1327 | 39 |
| spot 53 | 3341 | 1373 | 31800 | 23.16 | 0.09862 | 1.371 | 3.630 | 3.619 | 0.2662 | 3.349 | 0.93 | 1.44 | 1598 | 22 | 1533 | 47 |
| spot 54 | 3380 | 1300 | 31000 | 23.85 | 0.09840 | 1.375 | 3.679 | 3.422 | 0.2731 | 3.134 | 0.92 | 0.90 | 1595 | 22 | 1555 | 45 |
| spot 55 | 3018 | 2095 | 30800 | 14.70 | 0.08993 | 1.357 | 2.915 | 3.602 | 0.2358 | 3.337 | 0.93 | 1.32 | 1424 | 20 | 1366 | 43 |

**12TM13-01 xenotime** (spot size: 7 µm, frequency: 3 Hz, 75 shot count, laser energy: 3 mJ at 75%)

| | | | | | ISOTOPIC RATIOS | | | | | | | | APPARENT AGES | | | |
|---|---|---|---|---|---|---|---|---|---|---|---|---|---|---|---|---|
| | Pb (ppm) | U (ppm) | Th (ppm) | Th/U | $^{207}Pb/^{206}Pb$ | 2σ % | $^{207}Pb/^{235}U$ | 2σ % | $^{206}Pb/^{238}U$ | 2σ % | Rho | % disc.* | $^{207}Pb/^{206}Pb$ | 2σ abs | $^{206}Pb/^{238}U$ | 2σ abs |
| spot 1 | 793 | 11340 | 6750 | 0.60 | 0.11120 | 0.742 | 3.949 | 2.353 | 0.2553 | 2.233 | 0.95 | 11.00 | 1818 | 13 | 1464 | 29 |
| spot 2 | 453 | 6440 | 3950 | 0.61 | 0.10294 | 0.671 | 3.510 | 2.854 | 0.2487 | 2.774 | 0.97 | 7.07 | 1677 | 12 | 1429 | 35 |
| spot 3 | 417 | 5410 | 3560 | 0.66 | 0.10477 | 1.019 | 3.870 | 2.858 | 0.2659 | 2.670 | 0.93 | 5.45 | 1708 | 18 | 1522 | 36 |
| spot 4 | 943 | 7250 | 7910 | 1.09 | 0.11297 | 0.698 | 4.100 | 2.791 | 0.2627 | 2.703 | 0.97 | 9.63 | 1847 | 13 | 1506 | 37 |
| spot 5 | 475 | 5860 | 7070 | 1.21 | 0.09099 | 0.624 | 1.989 | 2.970 | 0.1584 | 2.904 | 0.98 | 17.76 | 1447 | 10 | 946 | 26 |
| spot 6 | 537 | 2932 | 5170 | 1.76 | 0.09626 | 0.670 | 3.246 | 2.906 | 0.2440 | 2.828 | 0.97 | 4.06 | 1552 | 11 | 1405 | 36 |
| spot 7 | 27 | 1516 | 813 | 0.54 | 0.06650 | 1.585 | 0.482 | 3.932 | 0.0528 | 3.598 | 0.92 | 20.24 | 820 | 31 | 331 | 11 |
| spot 8 | 263 | 5360 | 7240 | 1.35 | 0.08460 | 0.774 | 0.976 | 2.849 | 0.0839 | 2.741 | 0.96 | 33.14 | 1305 | 13 | 519 | 14 |
| spot 9 | 1458 | 9890 | 13450 | 1.36 | 0.10809 | 0.848 | 3.520 | 3.229 | 0.2375 | 3.116 | 0.96 | 11.20 | 1768 | 16 | 1375 | 39 |
| spot 10 | 1085 | 7520 | 10220 | 1.36 | 0.10633 | 0.719 | 3.469 | 2.566 | 0.2355 | 2.463 | 0.96 | 11.38 | 1737 | 13 | 1362 | 30 |
| spot 11 | 1323 | 9030 | 11660 | 1.29 | 0.11566 | 0.696 | 3.990 | 2.692 | 0.2500 | 2.600 | 0.97 | 13.75 | 1890 | 13 | 1440 | 33 |
| spot 12 | 796 | 7440 | 9490 | 1.28 | 0.09937 | 0.746 | 2.523 | 2.562 | 0.1836 | 2.451 | 0.96 | 17.40 | 1613 | 13 | 1086 | 25 |
| spot 13 | 24 | 3910 | 1801 | 0.46 | 0.05224 | 1.776 | 0.175 | 3.220 | 0.0238 | 2.686 | 0.83 | 7.64 | 286 | 38 | 152 | 4 |
| spot 14 | 12 | 1472 | 775 | 0.53 | 0.05160 | 2.379 | 0.193 | 4.011 | 0.0276 | 3.229 | 0.81 | 2.63 | 261 | 52 | 175 | 6 |
| spot 15 | 11 | 1721 | 873 | 0.51 | 0.05020 | 2.442 | 0.190 | 3.615 | 0.0270 | 2.666 | 0.74 | 2.79 | 195 | 53 | 172 | 5 |
| spot 16 | 22 | 3112 | 1520 | 0.49 | 0.05210 | 2.357 | 0.216 | 4.053 | 0.0300 | 3.298 | 0.81 | 4.14 | 285 | 52 | 191 | 6 |
| spot 17 | 14 | 2350 | 1205 | 0.51 | 0.04940 | 2.480 | 0.181 | 3.829 | 0.0264 | 2.918 | 0.76 | 0.71 | 168 | 55 | 168 | 5 |
| spot 18 | 41 | 6500 | 3340 | 0.51 | 0.05047 | 1.308 | 0.174 | 2.655 | 0.0251 | 2.311 | 0.87 | 2.07 | 213 | 28 | 160 | 4 |
| spot 19 | 84 | 14080 | 7060 | 0.50 | 0.04948 | 1.020 | 0.172 | 2.760 | 0.0250 | 2.564 | 0.93 | 2.08 | 168 | 21 | 159 | 4 |
| spot 20 | 126 | 13720 | 11120 | 0.81 | 0.04924 | 0.989 | 0.169 | 2.641 | 0.0249 | 2.449 | 0.93 | 0.13 | 159 | 20 | 159 | 4 |
| spot 21 | 62 | 13330 | 5210 | 0.39 | 0.04961 | 1.089 | 0.173 | 2.510 | 0.0252 | 2.261 | 0.90 | 1.06 | 174 | 22 | 160 | 4 |
| spot 22 | 95 | 13250 | 7860 | 0.59 | 0.04862 | 0.998 | 0.171 | 2.456 | 0.0254 | 2.244 | 0.91 | 1.18 | 129 | 20 | 162 | 4 |
| spot 23 | 627 | 6700 | 6060 | 0.90 | 0.09423 | 0.677 | 3.056 | 2.433 | 0.2354 | 2.336 | 0.96 | 4.34 | 1512 | 12 | 1361 | 28 |
| spot 24 | 729 | 7070 | 6740 | 0.95 | 0.10176 | 0.708 | 3.487 | 2.326 | 0.2482 | 2.216 | 0.95 | 6.57 | 1657 | 12 | 1431 | 29 |
| spot 25 | 581 | 10760 | 5510 | 0.51 | 0.09806 | 0.620 | 3.113 | 2.869 | 0.2285 | 2.801 | 0.98 | 8.15 | 1588 | 11 | 1325 | 33 |
| spot 26 | 733 | 12860 | 7280 | 0.57 | 0.09332 | 0.606 | 2.882 | 3.033 | 0.2221 | 2.972 | 0.98 | 5.62 | 1494 | 10 | 1299 | 35 |
| spot 27 | 1017 | 10860 | 9510 | 0.88 | 0.09873 | 0.771 | 3.300 | 2.884 | 0.2411 | 2.779 | 0.96 | 6.17 | 1601 | 14 | 1394 | 34 |
| spot 28 | 912 | 9770 | 8640 | 0.88 | 0.09973 | 0.708 | 3.288 | 2.654 | 0.2385 | 2.558 | 0.96 | 6.97 | 1619 | 13 | 1377 | 32 |
| spot 29 | 931 | 11930 | 9730 | 0.82 | 0.09317 | 0.619 | 2.742 | 2.426 | 0.2132 | 2.345 | 0.97 | 7.21 | 1491 | 10 | 1248 | 27 |
| spot 30 | 912 | 13260 | 9170 | 0.69 | 0.09422 | 0.599 | 2.915 | 2.438 | 0.2243 | 2.363 | 0.97 | 6.22 | 1512 | 10 | 1303 | 28 |
| spot 31 | 912 | 9920 | 8330 | 0.84 | 0.09888 | 0.663 | 3.350 | 3.042 | 0.2459 | 2.969 | 0.98 | 5.16 | 1603 | 11 | 1415 | 38 |

**12TM13-01 xenotime** (spot size: 7 µm, frequency: 3 Hz, 75 shot count, laser energy: 3 mJ at 75%)

| | | | | | ISOTOPIC RATIOS | | | | | | | | APPARENT AGES | | | |
|---|---|---|---|---|---|---|---|---|---|---|---|---|---|---|---|---|
| | Pb (ppm) | U (ppm) | Th (ppm) | Th/U | $^{207}Pb/^{206}Pb$ | 2σ % | $^{207}Pb/^{235}U$ | 2σ % | $^{206}Pb/^{238}U$ | 2σ % | Rho | % disc.* | $^{207}Pb/^{206}Pb$ | 2σ abs | $^{206}Pb/^{238}U$ | 2σ abs |
| spot 32 | 113 | 9470 | 7770 | 0.82 | 0.05603 | 1.102 | 0.232 | 3.252 | 0.0304 | 3.059 | 0.94 | 9.84 | 456 | 21 | 193 | 6 |
| spot 33 | 27 | 2847 | 1855 | 0.65 | 0.05470 | 1.895 | 0.225 | 3.163 | 0.0300 | 2.532 | 0.80 | 7.97 | 392 | 42 | 191 | 5 |
| spot 34 | 25 | 3083 | 2170 | 0.70 | 0.04985 | 1.990 | 0.178 | 3.384 | 0.0263 | 2.738 | 0.81 | 0.78 | 183 | 42 | 167 | 5 |
| spot 35 | 10 | 1382 | 684 | 0.49 | 0.05100 | 3.759 | 0.200 | 5.097 | 0.0282 | 3.442 | 0.68 | 3.74 | 227 | 80 | 179 | 6 |
| spot 36 | 23 | 2480 | 1668 | 0.67 | 0.05120 | 2.396 | 0.204 | 4.249 | 0.0285 | 3.509 | 0.83 | 3.53 | 239 | 53 | 181 | 6 |
| spot 37 | 9 | 970 | 605 | 0.62 | 0.05160 | 7.188 | 0.201 | 9.038 | 0.0292 | 5.479 | 0.61 | 0.54 | 270 | 150 | 186 | 10 |
| spot 38 | 9 | 1077 | 788 | 0.73 | 0.04940 | 3.477 | 0.176 | 4.921 | 0.0259 | 3.482 | 0.71 | 0.36 | 169 | 74 | 164 | 6 |
| spot 39 | 18 | 2244 | 1582 | 0.70 | 0.04920 | 2.490 | 0.174 | 3.899 | 0.0260 | 3.000 | 0.77 | 1.87 | 154 | 51 | 166 | 5 |
| spot 40 | 10 | 1519 | 898 | 0.59 | 0.05020 | 2.833 | 0.176 | 3.933 | 0.0253 | 2.728 | 0.69 | 1.74 | 188 | 61 | 161 | 4 |
| spot 41 | 15 | 1821 | 1160 | 0.64 | 0.05070 | 2.226 | 0.187 | 3.772 | 0.0273 | 3.045 | 0.81 | 0.40 | 223 | 47 | 173 | 5 |
| spot 42 | 582 | 4270 | 5760 | 1.35 | 0.09348 | 0.651 | 3.002 | 3.049 | 0.2350 | 2.979 | 0.98 | 3.46 | 1497 | 11 | 1358 | 36 |
| spot 43 | 461 | 3585 | 4550 | 1.27 | 0.09095 | 0.638 | 2.858 | 2.855 | 0.2300 | 2.783 | 0.97 | 2.40 | 1445 | 10 | 1336 | 33 |
| spot 44 | 477 | 3101 | 4930 | 1.59 | 0.09264 | 0.768 | 2.770 | 4.084 | 0.2219 | 4.011 | 0.98 | 5.12 | 1481 | 13 | 1290 | 47 |
| spot 45 | 438 | 3960 | 4500 | 1.14 | 0.09406 | 0.714 | 2.862 | 3.132 | 0.2230 | 3.049 | 0.97 | 5.31 | 1510 | 12 | 1300 | 37 |
| spot 46 | 456 | 3750 | 4520 | 1.21 | 0.09502 | 0.640 | 3.025 | 3.281 | 0.2331 | 3.218 | 0.98 | 4.82 | 1528 | 11 | 1348 | 39 |
| spot 47 | 527 | 4070 | 5190 | 1.28 | 0.09405 | 0.623 | 2.964 | 2.806 | 0.2303 | 2.736 | 0.98 | 4.65 | 1509 | 10 | 1334 | 33 |
| spot 48 | 8 | 930 | 370 | 0.40 | 0.05930 | 3.243 | 0.271 | 5.130 | 0.0327 | 3.976 | 0.77 | 17.28 | 551 | 73 | 207 | 8 |
| spot 49 | 11 | 1499 | 863 | 0.58 | 0.05030 | 3.024 | 0.179 | 4.635 | 0.0262 | 3.513 | 0.76 | 0.18 | 203 | 64 | 167 | 6 |
| spot 50 | 480 | 7750 | 4350 | 0.56 | 0.10885 | 0.699 | 3.324 | 2.403 | 0.2215 | 2.299 | 0.96 | 15.52 | 1781 | 13 | 1289 | 28 |
| spot 51 | 473 | 5970 | 4590 | 0.77 | 0.09902 | 0.583 | 2.882 | 2.329 | 0.2117 | 2.255 | 0.97 | 11.13 | 1606 | 10 | 1240 | 26 |
| spot 52 | 644 | 8960 | 5790 | 0.65 | 0.10872 | 0.657 | 3.269 | 2.259 | 0.2201 | 2.161 | 0.96 | 15.38 | 1779 | 12 | 1281 | 26 |
| spot 53 | 451 | 5910 | 4273 | 0.72 | 0.09917 | 0.626 | 2.970 | 2.598 | 0.2176 | 2.521 | 0.97 | 10.17 | 1608 | 11 | 1268 | 30 |
| spot 54 | 404 | 6290 | 3746 | 0.60 | 0.10041 | 0.618 | 3.012 | 2.853 | 0.2192 | 2.785 | 0.98 | 10.58 | 1631 | 11 | 1276 | 33 |
| spot 55 | 671 | 7640 | 6040 | 0.79 | 0.10594 | 0.598 | 3.302 | 2.236 | 0.2270 | 2.154 | 0.96 | 12.44 | 1731 | 11 | 1318 | 26 |
| spot 56 | 905 | 8140 | 8110 | 1.00 | 0.10879 | 0.712 | 3.470 | 2.374 | 0.2319 | 2.265 | 0.95 | 12.78 | 1779 | 13 | 1346 | 28 |
| spot 57 | 1157 | 10200 | 9490 | 0.93 | 0.11851 | 0.725 | 3.930 | 2.455 | 0.2407 | 2.346 | 0.96 | 16.59 | 1933 | 13 | 1392 | 31 |
| spot 58 | 1114 | 9030 | 9150 | 1.01 | 0.11683 | 0.730 | 3.985 | 2.257 | 0.2478 | 2.136 | 0.95 | 14.51 | 1909 | 14 | 1427 | 29 |
| spot 59 | 1123 | 9210 | 9360 | 1.02 | 0.11603 | 0.657 | 3.874 | 2.320 | 0.2436 | 2.225 | 0.96 | 14.14 | 1896 | 12 | 1407 | 29 |
| spot 60 | 1214 | 11770 | 11620 | 0.99 | 0.10505 | 0.609 | 3.103 | 2.171 | 0.2150 | 2.083 | 0.96 | 14.02 | 1715 | 11 | 1255 | 25 |
| spot 61 | 1534 | 14390 | 14200 | 0.99 | 0.11203 | 0.660 | 3.368 | 2.310 | 0.2177 | 2.213 | 0.96 | 18.28 | 1834 | 12 | 1269 | 27 |
| spot 62 | 1525 | 14350 | 13610 | 0.95 | 0.11704 | 0.711 | 3.695 | 2.495 | 0.2291 | 2.392 | 0.96 | 18.21 | 1911 | 13 | 1329 | 30 |

**12TM13-01 xenotime** (spot size: 7 µm, frequency: 3 Hz, 75 shot count, laser energy: 3 mJ at 75%)

| | | | | | ISOTOPIC RATIOS | | | | | | | | APPARENT AGES | | | |
|---|---|---|---|---|---|---|---|---|---|---|---|---|---|---|---|---|
| | Pb (ppm) | U (ppm) | Th (ppm) | Th/U | $^{207}Pb/^{206}Pb$ | 2σ % | $^{207}Pb/^{235}U$ | 2σ % | $^{206}Pb/^{238}U$ | 2σ % | Rho | % disc.* | $^{207}Pb/^{206}Pb$ | 2σ abs | $^{206}Pb/^{238}U$ | 2σ abs |
| spot 63 | 1308 | 13180 | 12800 | 0.97 | 0.10430 | 0.674 | 3.055 | 2.317 | 0.2116 | 2.217 | 0.96 | 14.34 | 1702 | 12 | 1241 | 26 |
| spot 64 | 689 | 8800 | 6040 | 0.69 | 0.10976 | 0.721 | 3.666 | 2.467 | 0.2438 | 2.359 | 0.96 | 11.74 | 1796 | 13 | 1405 | 31 |
| spot 65 | 992 | 13240 | 9210 | 0.70 | 0.11020 | 0.648 | 3.385 | 2.384 | 0.2221 | 2.295 | 0.96 | 16.18 | 1803 | 12 | 1292 | 28 |
| spot 66 | 813 | 9850 | 7060 | 0.72 | 0.11208 | 0.633 | 3.775 | 2.540 | 0.2442 | 2.460 | 0.97 | 12.72 | 1833 | 12 | 1407 | 32 |
| spot 67 | 760 | 7260 | 7130 | 0.98 | 0.10548 | 0.906 | 3.395 | 2.771 | 0.2331 | 2.619 | 0.95 | 11.33 | 1723 | 17 | 1350 | 33 |
| spot 68 | 416 | 5030 | 4720 | 0.94 | 0.09372 | 0.658 | 2.626 | 2.923 | 0.2052 | 2.848 | 0.97 | 9.15 | 1503 | 11 | 1202 | 32 |
| spot 69 | 429 | 4189 | 4004 | 0.96 | 0.10387 | 0.688 | 3.492 | 2.445 | 0.2457 | 2.347 | 0.96 | 7.84 | 1694 | 12 | 1415 | 31 |
| spot 70 | 458 | 4202 | 4198 | 1.00 | 0.10353 | 0.676 | 3.605 | 2.794 | 0.2522 | 2.711 | 0.97 | 6.69 | 1688 | 12 | 1451 | 35 |
| spot 71 | 1307 | 14230 | 12950 | 0.91 | 0.10625 | 0.651 | 3.117 | 2.472 | 0.2151 | 2.385 | 0.96 | 14.90 | 1736 | 11 | 1255 | 28 |
| spot 72 | 683 | 9020 | 6550 | 0.73 | 0.10095 | 0.628 | 3.092 | 2.595 | 0.2226 | 2.518 | 0.97 | 10.28 | 1641 | 11 | 1294 | 30 |
| spot 73 | 1297 | 12820 | 12390 | 0.97 | 0.11364 | 0.734 | 3.564 | 2.400 | 0.2288 | 2.285 | 0.95 | 16.20 | 1858 | 13 | 1327 | 28 |
| spot 74 | 1739 | 17370 | 15870 | 0.91 | 0.11595 | 0.817 | 3.602 | 2.144 | 0.2272 | 1.982 | 0.92 | 17.56 | 1896 | 15 | 1321 | 25 |
| spot 75 | 1529 | 14820 | 13070 | 0.88 | 0.11807 | 0.835 | 3.956 | 2.405 | 0.2442 | 2.255 | 0.94 | 15.42 | 1926 | 16 | 1407 | 29 |
| spot 76 | 674 | 6470 | 6790 | 1.05 | 0.09473 | 0.556 | 2.896 | 2.287 | 0.2225 | 2.219 | 0.97 | 6.47 | 1523 | 9 | 1299 | 27 |
| spot 77 | 965 | 14000 | 11450 | 0.82 | 0.09922 | 0.768 | 2.443 | 2.599 | 0.1796 | 2.483 | 0.96 | 17.86 | 1609 | 14 | 1064 | 25 |
| spot 78 | 1478 | 18090 | 13710 | 0.76 | 0.10777 | 0.735 | 3.274 | 2.249 | 0.2201 | 2.125 | 0.95 | 15.37 | 1762 | 13 | 1282 | 25 |
| spot 79 | 1492 | 17100 | 13460 | 0.79 | 0.11118 | 0.668 | 3.517 | 2.313 | 0.2287 | 2.214 | 0.96 | 15.30 | 1818 | 12 | 1327 | 27 |
| spot 80 | 923 | 15450 | 10050 | 0.65 | 0.09903 | 0.690 | 2.596 | 2.612 | 0.1900 | 2.519 | 0.96 | 15.70 | 1606 | 12 | 1121 | 26 |
| spot 81 | 1250 | 16510 | 12230 | 0.74 | 0.10184 | 0.615 | 2.909 | 2.372 | 0.2067 | 2.291 | 0.97 | 14.29 | 1658 | 11 | 1211 | 26 |
| spot 82 | 1569 | 21460 | 16490 | 0.77 | 0.10209 | 0.735 | 2.703 | 2.436 | 0.1922 | 2.323 | 0.95 | 17.56 | 1662 | 13 | 1133 | 25 |
| spot 83 | 20 | 3425 | 1512 | 0.44 | 0.04964 | 1.147 | 0.181 | 2.756 | 0.0266 | 2.506 | 0.91 | 0.41 | 175 | 24 | 169 | 4 |
| spot 84 | 8 | 1674 | 698 | 0.42 | 0.04923 | 1.800 | 0.170 | 3.465 | 0.0252 | 2.960 | 0.85 | 0.62 | 157 | 38 | 160 | 5 |
| spot 85 | 16 | 2765 | 1344 | 0.49 | 0.05062 | 1.218 | 0.175 | 2.644 | 0.0251 | 2.347 | 0.89 | 2.69 | 220 | 25 | 160 | 4 |
| spot 86 | 13 | 2083 | 1025 | 0.49 | 0.04989 | 1.568 | 0.178 | 3.013 | 0.0257 | 2.573 | 0.85 | 2.08 | 189 | 34 | 163 | 4 |
| spot 87 | 7 | 2029 | 601 | 0.30 | 0.04824 | 1.597 | 0.167 | 3.059 | 0.0252 | 2.610 | 0.85 | 2.55 | 108 | 33 | 161 | 4 |
| spot 88 | 48 | 7130 | 4270 | 0.60 | 0.04937 | 0.940 | 0.164 | 2.746 | 0.0242 | 2.580 | 0.94 | 0.06 | 163 | 18 | 154 | 4 |
| spot 89 | 9 | 2137 | 716 | 0.34 | 0.04904 | 1.690 | 0.173 | 3.448 | 0.0258 | 3.006 | 0.87 | 1.76 | 152 | 36 | 165 | 5 |
| spot 90 | 10 | 1859 | 848 | 0.46 | 0.04942 | 1.659 | 0.171 | 3.072 | 0.0251 | 2.585 | 0.84 | 0.13 | 165 | 35 | 160 | 4 |
| spot 91 | 13 | 2415 | 1154 | 0.48 | 0.04838 | 1.456 | 0.168 | 3.029 | 0.0255 | 2.656 | 0.88 | 2.65 | 117 | 30 | 162 | 4 |
| spot 92 | 50 | 15280 | 4300 | 0.28 | 0.04951 | 0.718 | 0.173 | 2.956 | 0.0254 | 2.868 | 0.97 | 0.12 | 172 | 12 | 162 | 5 |
| spot 93 | 52 | 12790 | 4451 | 0.35 | 0.04963 | 0.731 | 0.172 | 2.709 | 0.0252 | 2.608 | 0.96 | 0.50 | 178 | 12 | 161 | 4 |

**12TM13-01 xenotime** (spot size: 7 μm, frequency: 3 Hz, 75 shot count, laser energy: 3 mJ at 75%)

| | | | | | ISOTOPIC RATIOS | | | | | | | | APPARENT AGES | | | |
|---|---|---|---|---|---|---|---|---|---|---|---|---|---|---|---|---|
| | Pb (ppm) | U (ppm) | Th (ppm) | Th/U | $^{207}Pb/^{206}Pb$ | 2σ % | $^{207}Pb/^{235}U$ | 2σ % | $^{206}Pb/^{238}U$ | 2σ % | Rho | % disc.* | $^{207}Pb/^{206}Pb$ | 2σ abs | $^{206}Pb/^{238}U$ | 2σ abs |
| spot 94 | 18 | 12070 | 1541 | 0.13 | 0.04930 | 0.794 | 0.176 | 2.813 | 0.0258 | 2.699 | 0.96 | 0.06 | 161 | 14 | 164 | 4 |
| spot 95 | 20 | 14250 | 1684 | 0.12 | 0.04969 | 0.760 | 0.176 | 2.709 | 0.0258 | 2.600 | 0.96 | 0.24 | 181 | 13 | 164 | 4 |
| spot 96 | 11 | 6650 | 892 | 0.13 | 0.04936 | 0.841 | 0.178 | 2.842 | 0.0260 | 2.715 | 0.96 | 0.24 | 163 | 16 | 166 | 4 |
| spot 97 | 18 | 13070 | 1545 | 0.12 | 0.04964 | 0.760 | 0.178 | 2.889 | 0.0260 | 2.787 | 0.96 | 0.30 | 178 | 14 | 165 | 5 |
| spot 98 | 55 | 13340 | 5150 | 0.39 | 0.05004 | 0.850 | 0.179 | 2.889 | 0.0259 | 2.761 | 0.96 | 1.34 | 200 | 16 | 165 | 4 |
| spot 99 | 81 | 20210 | 6850 | 0.34 | 0.04985 | 0.674 | 0.173 | 2.553 | 0.0253 | 2.463 | 0.96 | 0.43 | 187 | 11 | 161 | 4 |
| spot 100 | 45 | 12460 | 3737 | 0.30 | 0.04921 | 0.779 | 0.175 | 2.629 | 0.0256 | 2.511 | 0.96 | 0.37 | 160 | 13 | 163 | 4 |
| spot 101 | 55 | 14940 | 4630 | 0.31 | 0.04942 | 0.664 | 0.174 | 2.938 | 0.0255 | 2.862 | 0.97 | 0.31 | 167 | 10 | 162 | 5 |

**12TM15-16 xenotime** (spot size: 6 µm, frequency: 3 Hz, 75 shot count, laser energy: 4 mJ at 56%)

| | | | | | ISOTOPIC RATIOS | | | | | | | | APPARENT AGES | | | |
|---|---|---|---|---|---|---|---|---|---|---|---|---|---|---|---|---|
| | Pb (ppm) | U (ppm) | Th (ppm) | Th/U | $^{207}Pb/^{206}Pb$ | 2σ % | $^{207}Pb/^{235}U$ | 2σ % | $^{206}Pb/^{238}U$ | 2σ % | Rho | % disc.* | $^{207}Pb/^{206}Pb$ | 2σ abs | $^{206}Pb/^{238}U$ | 2σ abs |
| spot 1 | 1006 | 10400 | 8970 | 0.86 | 0.10447 | 1.749 | 3.740 | 4.602 | 0.2567 | 4.256 | 0.92 | 7.11 | 1705 | 30 | 1476 | 59 |
| spot 2 | 868 | 11630 | 9040 | 0.78 | 0.09590 | 1.761 | 2.922 | 4.397 | 0.2206 | 4.029 | 0.92 | 8.00 | 1546 | 28 | 1287 | 50 |
| spot 3 | 1626 | 16770 | 13080 | 0.78 | 0.11495 | 1.735 | 4.400 | 4.367 | 0.2771 | 4.007 | 0.92 | 8.36 | 1879 | 33 | 1579 | 59 |
| spot 4 | 560 | 5730 | 5870 | 1.02 | 0.09274 | 1.780 | 2.947 | 4.474 | 0.2295 | 4.104 | 0.92 | 4.66 | 1482 | 27 | 1330 | 52 |
| spot 5 | 1234 | 19850 | 12010 | 0.61 | 0.09984 | 1.726 | 3.183 | 4.275 | 0.2335 | 3.911 | 0.91 | 7.31 | 1621 | 28 | 1355 | 50 |
| spot 6 | 940 | 8390 | 7820 | 0.93 | 0.10682 | 1.741 | 4.040 | 4.450 | 0.2763 | 4.095 | 0.92 | 4.65 | 1746 | 30 | 1571 | 61 |
| spot 7 | 563 | 7840 | 4840 | 0.62 | 0.09947 | 1.814 | 3.520 | 4.828 | 0.2548 | 4.475 | 0.93 | 5.13 | 1615 | 30 | 1461 | 62 |
| spot 8 | 475 | 4310 | 3800 | 0.88 | 0.10012 | 1.796 | 3.760 | 4.781 | 0.2740 | 4.430 | 0.93 | 1.73 | 1626 | 30 | 1558 | 65 |
| spot 9 | 249 | 4230 | 2167 | 0.51 | 0.09289 | 1.807 | 3.080 | 5.187 | 0.2409 | 4.862 | 0.94 | 2.31 | 1486 | 28 | 1388 | 63 |
| spot 10 | 353 | 4370 | 2950 | 0.68 | 0.09667 | 1.813 | 3.350 | 5.319 | 0.2502 | 5.001 | 0.94 | 3.40 | 1560 | 29 | 1443 | 68 |
| spot 11 | 151 | 3670 | 1663 | 0.45 | 0.09386 | 1.902 | 2.320 | 5.546 | 0.1786 | 5.210 | 0.94 | 15.33 | 1504 | 30 | 1057 | 52 |
| spot 12 | 1517 | 16760 | 16970 | 1.01 | 0.09351 | 1.750 | 2.791 | 4.455 | 0.2183 | 4.097 | 0.92 | 6.60 | 1498 | 27 | 1272 | 49 |
| spot 13 | 696 | 10770 | 7860 | 0.73 | 0.09104 | 1.759 | 2.719 | 4.499 | 0.2159 | 4.141 | 0.92 | 5.71 | 1447 | 26 | 1262 | 49 |
| spot 14 | 657 | 9740 | 6480 | 0.67 | 0.09561 | 1.798 | 3.200 | 4.478 | 0.2423 | 4.101 | 0.92 | 4.01 | 1540 | 28 | 1397 | 54 |
| spot 15 | 689 | 10300 | 7180 | 0.70 | 0.09332 | 1.756 | 2.959 | 4.303 | 0.2299 | 3.928 | 0.91 | 4.49 | 1494 | 27 | 1337 | 50 |
| spot 16 | 1020 | 7070 | 9620 | 1.36 | 0.10051 | 1.798 | 3.648 | 4.259 | 0.2645 | 3.861 | 0.91 | 3.37 | 1633 | 30 | 1512 | 55 |
| spot 17 | 735 | 7010 | 6620 | 0.94 | 0.10356 | 1.735 | 3.917 | 4.378 | 0.2745 | 4.020 | 0.92 | 3.39 | 1689 | 29 | 1565 | 59 |
| spot 18 | 683 | 6660 | 6830 | 1.03 | 0.09820 | 1.813 | 3.291 | 4.497 | 0.2440 | 4.115 | 0.92 | 5.19 | 1589 | 30 | 1406 | 55 |
| spot 19 | 701 | 5950 | 7300 | 1.23 | 0.09633 | 1.845 | 3.090 | 4.852 | 0.2335 | 4.487 | 0.92 | 5.85 | 1553 | 29 | 1350 | 57 |
| spot 20 | 781 | 9230 | 7910 | 0.86 | 0.09382 | 1.753 | 2.889 | 4.330 | 0.2239 | 3.960 | 0.91 | 5.67 | 1504 | 27 | 1304 | 49 |
| spot 21 | 781 | 9170 | 7240 | 0.79 | 0.09696 | 1.789 | 3.270 | 4.595 | 0.2453 | 4.232 | 0.92 | 4.04 | 1566 | 28 | 1412 | 57 |
| spot 22 | 783 | 6720 | 6940 | 1.03 | 0.09713 | 1.827 | 3.380 | 4.675 | 0.2571 | 4.303 | 0.92 | 1.63 | 1569 | 30 | 1473 | 59 |
| spot 23 | 840 | 13380 | 8420 | 0.63 | 0.09074 | 1.741 | 2.750 | 4.668 | 0.2210 | 4.331 | 0.93 | 4.28 | 1441 | 26 | 1286 | 53 |
| spot 24 | 571 | 5560 | 5810 | 1.04 | 0.09154 | 1.789 | 2.758 | 4.801 | 0.2205 | 4.455 | 0.93 | 4.04 | 1458 | 27 | 1286 | 55 |
| spot 25 | 627 | 5740 | 6120 | 1.07 | 0.09086 | 1.774 | 2.826 | 4.461 | 0.2272 | 4.093 | 0.92 | 3.03 | 1443 | 26 | 1322 | 51 |
| spot 26 | 683 | 10480 | 6420 | 0.61 | 0.09398 | 1.769 | 3.043 | 4.580 | 0.2388 | 4.225 | 0.92 | 2.54 | 1507 | 27 | 1379 | 55 |
| spot 27 | 704 | 10510 | 6440 | 0.61 | 0.09367 | 1.779 | 3.024 | 4.547 | 0.2371 | 4.184 | 0.92 | 2.99 | 1502 | 27 | 1370 | 54 |
| spot 28 | 620 | 9630 | 6510 | 0.68 | 0.08977 | 1.737 | 2.555 | 4.691 | 0.2109 | 4.357 | 0.93 | 4.30 | 1420 | 25 | 1232 | 51 |
| spot 29 | 635 | 8380 | 5960 | 0.71 | 0.09308 | 1.764 | 2.958 | 4.439 | 0.2345 | 4.073 | 0.92 | 2.43 | 1489 | 27 | 1360 | 53 |
| spot 30 | 734 | 10230 | 6690 | 0.65 | 0.09818 | 1.912 | 3.320 | 4.718 | 0.2485 | 4.313 | 0.91 | 3.35 | 1588 | 31 | 1433 | 58 |
| spot 31 | 595 | 9600 | 5730 | 0.60 | 0.09305 | 1.759 | 2.841 | 4.411 | 0.2266 | 4.045 | 0.92 | 3.65 | 1488 | 27 | 1315 | 51 |

**12TM15-16 xenotime** (spot size: 6 µm, frequency: 3 Hz, 75 shot count, laser energy: 4 mJ at 56%)

| | | | | | ISOTOPIC RATIOS | | | | | | | | APPARENT AGES | | | |
|---|---|---|---|---|---|---|---|---|---|---|---|---|---|---|---|---|
| | Pb (ppm) | U (ppm) | Th (ppm) | Th/U | $^{207}Pb/^{206}Pb$ | 2σ % | $^{207}Pb/^{235}U$ | 2σ % | $^{206}Pb/^{238}U$ | 2σ % | Rho | % disc.* | $^{207}Pb/^{206}Pb$ | 2σ abs | $^{206}Pb/^{238}U$ | 2σ abs |
| spot 32 | 702 | 10320 | 6630 | 0.64 | 0.09508 | 1.756 | 3.000 | 4.756 | 0.2347 | 4.420 | 0.93 | 3.46 | 1529 | 27 | 1357 | 56 |
| spot 33 | 296 | 4010 | 9340 | 2.33 | 0.09332 | 1.904 | 2.145 | 4.820 | 0.1693 | 4.429 | 0.92 | 15.25 | 1492 | 30 | 1010 | 42 |
| spot 34 | 318 | 4420 | 3910 | 0.88 | 0.08872 | 1.762 | 2.218 | 4.816 | 0.1846 | 4.482 | 0.93 | 8.71 | 1398 | 25 | 1091 | 47 |
| spot 35 | 241 | 16900 | 63200 | 3.74 | 0.09170 | 2.081 | 0.224 | 6.484 | 0.0182 | 6.141 | 0.95 | 76.88 | 1460 | 33 | 116 | 7 |
| spot 36 | 514 | 5720 | 4390 | 0.77 | 0.10117 | 1.782 | 3.650 | 4.907 | 0.2654 | 4.572 | 0.93 | 2.71 | 1646 | 30 | 1514 | 65 |
| spot 37 | 569 | 5180 | 5070 | 0.98 | 0.09964 | 1.790 | 3.510 | 4.564 | 0.2581 | 4.199 | 0.92 | 3.38 | 1618 | 29 | 1478 | 59 |
| spot 38 | 497 | 6330 | 4960 | 0.78 | 0.09110 | 1.759 | 2.803 | 4.741 | 0.2265 | 4.402 | 0.93 | 3.27 | 1450 | 26 | 1314 | 54 |

**12TM17-04 xenotime** (spot size: 6 µm, frequency: 3 Hz, 75 shot count, laser energy: 4 mJ at 56%)

| | | | | | ISOTOPIC RATIOS | | | | | | | | APPARENT AGES | | | |
|---|---|---|---|---|---|---|---|---|---|---|---|---|---|---|---|---|
| | Pb (ppm) | U (ppm) | Th (ppm) | Th/U | $^{207}Pb/^{206}Pb$ | 2σ % | $^{207}Pb/^{235}U$ | 2σ % | $^{206}Pb/^{238}U$ | 2σ % | Rho | % disc.* | $^{207}Pb/^{206}Pb$ | 2σ abs | $^{206}Pb/^{238}U$ | 2σ abs |
| spot 1 | 31 | 1796 | 674 | 0.38 | 0.08030 | 1.667 | 1.073 | 5.789 | 0.0974 | 5.544 | 0.96 | 23.24 | 1205 | 28 | 598 | 32 |
| spot 2 | 335 | 8370 | 4051 | 0.48 | 0.09017 | 1.030 | 2.447 | 2.910 | 0.1984 | 2.722 | 0.94 | 8.04 | 1430 | 16 | 1169 | 30 |
| spot 3 | 219 | 5510 | 2394 | 0.43 | 0.09020 | 1.073 | 2.690 | 4.083 | 0.2183 | 3.940 | 0.96 | 4.17 | 1430 | 17 | 1270 | 45 |
| spot 4 | 224 | 4960 | 2214 | 0.45 | 0.09176 | 1.055 | 2.858 | 3.478 | 0.2263 | 3.314 | 0.95 | 4.65 | 1462 | 16 | 1312 | 39 |
| spot 5 | 156 | 3230 | 1645 | 0.51 | 0.08956 | 1.131 | 2.895 | 3.356 | 0.2342 | 3.160 | 0.94 | 1.48 | 1418 | 18 | 1354 | 38 |
| spot 6 | 29 | 9010 | 3010 | 0.33 | 0.04991 | 1.727 | 0.162 | 3.997 | 0.0239 | 3.604 | 0.90 | 0.26 | 186 | 33 | 152 | 5 |
| spot 7 | 201 | 5240 | 2256 | 0.43 | 0.09067 | 1.104 | 2.560 | 3.851 | 0.2060 | 3.689 | 0.96 | 6.98 | 1440 | 18 | 1204 | 41 |
| spot 8 | 212 | 5250 | 2333 | 0.44 | 0.09057 | 1.062 | 2.632 | 3.298 | 0.2114 | 3.122 | 0.95 | 6.56 | 1438 | 16 | 1234 | 35 |
| spot 9 | 133 | 3720 | 1228 | 0.33 | 0.09117 | 1.131 | 2.800 | 4.509 | 0.2245 | 4.365 | 0.97 | 3.83 | 1449 | 18 | 1306 | 51 |
| spot 10 | 223 | 7290 | 2149 | 0.29 | 0.09455 | 1.131 | 2.910 | 3.839 | 0.2208 | 3.668 | 0.96 | 7.25 | 1518 | 19 | 1283 | 42 |
| spot 11 | 214 | 6100 | 1723 | 0.28 | 0.10207 | 1.144 | 3.650 | 3.352 | 0.2571 | 3.151 | 0.94 | 6.05 | 1661 | 20 | 1472 | 42 |
| spot 12 | 59 | 5040 | 526 | 0.10 | 0.09552 | 1.075 | 3.170 | 3.321 | 0.2387 | 3.142 | 0.95 | 4.93 | 1538 | 17 | 1378 | 39 |
| spot 13 | 141 | 8040 | 1184 | 0.15 | 0.10348 | 1.057 | 3.660 | 3.323 | 0.2539 | 3.151 | 0.95 | 6.64 | 1689 | 18 | 1461 | 42 |
| spot 14 | 96 | 7510 | 858 | 0.11 | 0.10114 | 1.085 | 3.390 | 3.145 | 0.2405 | 2.952 | 0.94 | 7.47 | 1646 | 18 | 1392 | 37 |
| spot 15 | 97 | 7760 | 882 | 0.11 | 0.10107 | 1.085 | 3.366 | 2.851 | 0.2390 | 2.636 | 0.92 | 8.33 | 1643 | 18 | 1380 | 33 |
| spot 16 | 294 | 4320 | 2696 | 0.62 | 0.09526 | 1.101 | 3.090 | 3.997 | 0.2342 | 3.843 | 0.96 | 5.40 | 1534 | 18 | 1353 | 47 |
| spot 17 | 165 | 4840 | 1417 | 0.29 | 0.09788 | 1.148 | 3.430 | 3.728 | 0.2537 | 3.547 | 0.95 | 3.15 | 1585 | 19 | 1459 | 46 |
| spot 18 | 289 | 8360 | 3240 | 0.39 | 0.09064 | 1.043 | 2.515 | 3.233 | 0.2026 | 3.060 | 0.95 | 7.50 | 1440 | 16 | 1187 | 33 |
| spot 19 | 301 | 9410 | 3190 | 0.34 | 0.09232 | 1.027 | 2.645 | 3.065 | 0.2078 | 2.887 | 0.94 | 7.46 | 1474 | 16 | 1220 | 33 |
| spot 20 | 137 | 4310 | 1457 | 0.34 | 0.09011 | 1.117 | 2.650 | 4.384 | 0.2123 | 4.239 | 0.97 | 5.79 | 1429 | 17 | 1244 | 49 |
| spot 21 | 157 | 5500 | 1692 | 0.31 | 0.09157 | 1.080 | 2.650 | 4.213 | 0.2112 | 4.072 | 0.97 | 7.22 | 1458 | 17 | 1232 | 46 |
| spot 22 | 154 | 4500 | 1764 | 0.39 | 0.09765 | 1.131 | 2.723 | 3.710 | 0.2038 | 3.533 | 0.95 | 11.82 | 1579 | 19 | 1193 | 38 |
| spot 23 | 151 | 5290 | 1645 | 0.31 | 0.09580 | 1.132 | 2.500 | 4.379 | 0.1915 | 4.230 | 0.97 | 12.17 | 1543 | 18 | 1126 | 43 |
| spot 24 | 268 | 7180 | 2890 | 0.40 | 0.09046 | 1.078 | 2.550 | 3.831 | 0.2067 | 3.677 | 0.96 | 6.29 | 1435 | 17 | 1208 | 41 |
| spot 25 | 224 | 5920 | 2040 | 0.34 | 0.10394 | 1.159 | 3.530 | 4.211 | 0.2470 | 4.049 | 0.96 | 7.51 | 1695 | 20 | 1424 | 54 |
| spot 26 | 268 | 7220 | 2500 | 0.35 | 0.09798 | 1.098 | 3.070 | 4.227 | 0.2303 | 4.082 | 0.97 | 6.68 | 1588 | 19 | 1332 | 49 |
| spot 27 | 232 | 5570 | 1978 | 0.36 | 0.09856 | 1.180 | 3.270 | 4.660 | 0.2440 | 4.508 | 0.97 | 4.90 | 1599 | 20 | 1407 | 55 |
| spot 28 | 301 | 7380 | 2410 | 0.33 | 0.10527 | 1.160 | 3.650 | 4.901 | 0.2520 | 4.762 | 0.97 | 7.51 | 1719 | 20 | 1451 | 62 |
| spot 29 | 117 | 2290 | 1117 | 0.49 | 0.09199 | 1.245 | 3.000 | 6.013 | 0.2380 | 5.882 | 0.98 | 2.12 | 1466 | 20 | 1366 | 70 |
| spot 30 | 284 | 7490 | 2560 | 0.34 | 0.09707 | 1.076 | 3.053 | 3.217 | 0.2309 | 3.032 | 0.94 | 5.66 | 1568 | 18 | 1342 | 37 |
| spot 31 | 36 | 1910 | 515 | 0.27 | 0.09011 | 1.403 | 1.520 | 6.908 | 0.1227 | 6.764 | 0.98 | 25.61 | 1428 | 23 | 742 | 48 |

**12TM17-04 xenotime** (spot size: 6 µm, frequency: 3 Hz, 75 shot count, laser energy: 4 mJ at 56%)

| | | | | | ISOTOPIC RATIOS | | | | | | | | APPARENT AGES | | | |
|---|---|---|---|---|---|---|---|---|---|---|---|---|---|---|---|---|
| | Pb (ppm) | U (ppm) | Th (ppm) | Th/U | $^{207}Pb/^{206}Pb$ | 2σ % | $^{207}Pb/^{235}U$ | 2σ % | $^{206}Pb/^{238}U$ | 2σ % | Rho | % disc.* | $^{207}Pb/^{206}Pb$ | 2σ abs | $^{206}Pb/^{238}U$ | 2σ abs |
| spot 32 | 530 | 8590 | 3930 | 0.46 | 0.11394 | 1.086 | 4.450 | 3.697 | 0.2830 | 3.534 | 0.96 | 7.23 | 1863 | 20 | 1604 | 52 |
| spot 33 | 320 | 7860 | 2742 | 0.35 | 0.10420 | 1.234 | 3.710 | 3.681 | 0.2537 | 3.469 | 0.94 | 7.91 | 1702 | 21 | 1454 | 45 |
| spot 34 | 312 | 6990 | 2630 | 0.38 | 0.10420 | 1.180 | 3.640 | 4.066 | 0.2570 | 3.891 | 0.96 | 6.20 | 1699 | 21 | 1468 | 52 |
| spot 35 | 223 | 6750 | 2128 | 0.32 | 0.09746 | 1.167 | 3.020 | 4.226 | 0.2265 | 4.062 | 0.96 | 7.62 | 1575 | 20 | 1312 | 48 |
| spot 36 | 272 | 5320 | 2634 | 0.50 | 0.09652 | 1.171 | 3.030 | 4.154 | 0.2283 | 3.986 | 0.96 | 6.81 | 1557 | 20 | 1322 | 48 |
| spot 37 | 200 | 3900 | 1726 | 0.44 | 0.10112 | 1.080 | 3.540 | 3.809 | 0.2546 | 3.653 | 0.96 | 4.73 | 1644 | 18 | 1458 | 48 |
| spot 38 | 205 | 3860 | 2045 | 0.53 | 0.09210 | 1.111 | 2.854 | 3.355 | 0.2243 | 3.165 | 0.94 | 4.99 | 1470 | 18 | 1302 | 37 |
| spot 39 | 206 | 4640 | 1845 | 0.40 | 0.10059 | 1.143 | 3.390 | 3.375 | 0.2456 | 3.176 | 0.94 | 6.23 | 1634 | 20 | 1413 | 40 |
| spot 40 | 185 | 4600 | 1951 | 0.42 | 0.09138 | 1.046 | 2.664 | 3.600 | 0.2119 | 3.445 | 0.96 | 5.88 | 1454 | 16 | 1242 | 40 |
| spot 41 | 577 | 5230 | 5560 | 1.06 | 0.09384 | 1.041 | 3.004 | 3.314 | 0.2320 | 3.147 | 0.95 | 4.31 | 1504 | 16 | 1347 | 38 |
| spot 42 | 519 | 5950 | 4090 | 0.69 | 0.10952 | 1.101 | 4.130 | 3.825 | 0.2730 | 3.663 | 0.96 | 6.58 | 1791 | 20 | 1550 | 52 |
| spot 43 | 507 | 5300 | 3880 | 0.73 | 0.11039 | 1.137 | 4.250 | 4.103 | 0.2790 | 3.943 | 0.96 | 6.14 | 1808 | 20 | 1580 | 53 |
| spot 44 | 215 | 3340 | 1732 | 0.52 | 0.10540 | 1.112 | 3.890 | 3.813 | 0.2660 | 3.647 | 0.96 | 5.98 | 1722 | 19 | 1523 | 49 |
| spot 45 | 262 | 4100 | 2039 | 0.50 | 0.10693 | 1.055 | 4.020 | 4.179 | 0.2720 | 4.044 | 0.97 | 5.17 | 1748 | 19 | 1548 | 54 |

**12TM13-06 zircon** (spot size: 24 µm, frequency: 4 Hz, 100 shot count, laser energy: 4 mJ at 75%)

| | | | | | ISOTOPIC RATIOS | | | | | | | | APPARENT AGES | | | |
|---|---|---|---|---|---|---|---|---|---|---|---|---|---|---|---|---|
| | Pb (ppm) | U (ppm) | Th (ppm) | Th/U | $^{207}Pb/^{206}Pb$ | 2σ % | $^{207}Pb/^{235}U$ | 2σ % | $^{206}Pb/^{238}U$ | 2σ % | Rho | % disc.* | $^{207}Pb/^{206}Pb$ | 2σ abs | $^{206}Pb/^{238}U$ | 2σ abs |
| spot 1 | 83 | 681 | 93 | 0.14 | 0.10672 | 1.332 | 4.165 | 2.398 | 0.2840 | 1.994 | 0.83 | 3.29 | 1744 | 23 | 1613 | 29 |
| spot 2 | 309 | 920 | 342 | 0.37 | 0.10996 | 1.336 | 4.510 | 2.106 | 0.2974 | 1.628 | 0.77 | 3.27 | 1799 | 24 | 1680 | 24 |
| spot 3 | 128 | 1284 | 166 | 0.13 | 0.10463 | 1.327 | 3.856 | 2.147 | 0.2662 | 1.688 | 0.79 | 5.33 | 1708 | 23 | 1521 | 23 |
| spot 4 | 32 | 527 | 49 | 0.09 | 0.10482 | 1.375 | 3.156 | 2.238 | 0.2168 | 1.766 | 0.79 | 14.13 | 1712 | 24 | 1267 | 20 |
| spot 5 | 520 | 1236 | 559 | 0.45 | 0.11308 | 1.336 | 4.983 | 2.164 | 0.3202 | 1.702 | 0.79 | 1.51 | 1849 | 25 | 1789 | 27 |
| spot 6 | 483 | 1219 | 570 | 0.47 | 0.11107 | 1.324 | 4.551 | 1.980 | 0.2975 | 1.472 | 0.74 | 3.64 | 1817 | 24 | 1678 | 22 |
| spot 7 | 382 | 1350 | 427 | 0.32 | 0.11119 | 1.322 | 4.644 | 1.983 | 0.3038 | 1.477 | 0.74 | 2.75 | 1819 | 24 | 1709 | 22 |
| spot 8 | 78 | 677 | 74 | 0.11 | 0.10607 | 1.356 | 4.257 | 2.024 | 0.2904 | 1.502 | 0.74 | 2.43 | 1733 | 24 | 1643 | 22 |
| spot 9 | 160 | 1128 | 202 | 0.18 | 0.10917 | 1.337 | 4.453 | 2.040 | 0.2960 | 1.541 | 0.76 | 2.99 | 1786 | 24 | 1671 | 23 |
| spot 10 | 351 | 1327 | 404 | 0.30 | 0.11170 | 1.351 | 4.548 | 2.222 | 0.2953 | 1.764 | 0.79 | 4.25 | 1827 | 25 | 1670 | 26 |
| spot 11 | 59 | 1142 | 68 | 0.06 | 0.10886 | 1.331 | 4.359 | 2.030 | 0.2907 | 1.533 | 0.76 | 3.71 | 1780 | 24 | 1644 | 22 |
| spot 12 | 35 | 659 | 37 | 0.06 | 0.10678 | 1.336 | 4.270 | 2.157 | 0.2904 | 1.694 | 0.79 | 2.68 | 1746 | 23 | 1643 | 25 |
| spot 13 | 275 | 882 | 357 | 0.40 | 0.11021 | 1.321 | 4.421 | 2.070 | 0.2913 | 1.593 | 0.77 | 4.07 | 1803 | 24 | 1647 | 23 |
| spot 14 | 527 | 1373 | 644 | 0.47 | 0.11222 | 1.350 | 4.559 | 1.896 | 0.2946 | 1.331 | 0.70 | 4.57 | 1835 | 25 | 1664 | 21 |
| spot 15 | 56 | 451 | 67 | 0.15 | 0.10691 | 1.364 | 4.343 | 2.037 | 0.2951 | 1.513 | 0.74 | 2.04 | 1748 | 24 | 1666 | 23 |
| spot 16 | 58 | 934 | 76 | 0.08 | 0.10777 | 1.326 | 4.301 | 1.893 | 0.2891 | 1.351 | 0.71 | 3.42 | 1762 | 23 | 1636 | 21 |
| spot 17 | 76 | 1221 | 101 | 0.08 | 0.10734 | 1.322 | 4.194 | 1.931 | 0.2828 | 1.407 | 0.73 | 3.98 | 1755 | 23 | 1607 | 20 |
| spot 18 | 88 | 2066 | 117 | 0.06 | 0.10972 | 1.321 | 4.160 | 1.932 | 0.2746 | 1.409 | 0.73 | 6.65 | 1795 | 24 | 1563 | 20 |
| spot 19 | 61 | 1109 | 88 | 0.08 | 0.10461 | 1.331 | 3.807 | 2.105 | 0.2638 | 1.631 | 0.77 | 5.50 | 1707 | 23 | 1509 | 23 |
| spot 20 | 71 | 706 | 98 | 0.14 | 0.10409 | 1.348 | 3.884 | 2.224 | 0.2704 | 1.769 | 0.80 | 4.34 | 1698 | 23 | 1544 | 24 |
| spot 21 | 269 | 1048 | 323 | 0.31 | 0.10957 | 1.329 | 4.464 | 2.037 | 0.2951 | 1.545 | 0.76 | 3.48 | 1792 | 24 | 1666 | 23 |
| spot 22 | 275 | 1393 | 352 | 0.25 | 0.10898 | 1.333 | 4.144 | 2.112 | 0.2755 | 1.638 | 0.78 | 5.66 | 1782 | 24 | 1572 | 23 |
| spot 23 | 123 | 1415 | 180 | 0.13 | 0.10771 | 1.345 | 3.780 | 2.244 | 0.2540 | 1.796 | 0.80 | 8.92 | 1761 | 24 | 1458 | 24 |
| spot 24 | 149 | 658 | 180 | 0.27 | 0.10724 | 1.387 | 4.257 | 2.148 | 0.2882 | 1.640 | 0.76 | 3.06 | 1753 | 25 | 1634 | 24 |
| spot 25 | 644 | 1590 | 739 | 0.46 | 0.11262 | 1.331 | 4.686 | 1.996 | 0.3013 | 1.487 | 0.75 | 3.89 | 1842 | 24 | 1697 | 22 |
| spot 26 | 367 | 1015 | 393 | 0.39 | 0.11126 | 1.333 | 4.754 | 2.106 | 0.3102 | 1.630 | 0.77 | 2.01 | 1821 | 24 | 1741 | 25 |
| spot 27 | 46 | 1360 | 53 | 0.04 | 0.10923 | 1.333 | 4.237 | 2.222 | 0.2809 | 1.778 | 0.80 | 5.06 | 1786 | 24 | 1600 | 25 |
| spot 28 | 37 | 1202 | 46 | 0.04 | 0.10818 | 1.327 | 4.053 | 2.017 | 0.2723 | 1.519 | 0.75 | 6.12 | 1769 | 24 | 1552 | 21 |
| spot 29 | 217 | 3058 | 242 | 0.08 | 0.11307 | 1.362 | 4.393 | 1.900 | 0.2796 | 1.324 | 0.70 | 7.54 | 1849 | 25 | 1591 | 19 |
| spot 30 | 677 | 1815 | 747 | 0.41 | 0.11225 | 1.358 | 4.467 | 2.034 | 0.2877 | 1.514 | 0.74 | 5.63 | 1836 | 25 | 1634 | 21 |
| spot 31 | 114 | 1429 | 141 | 0.10 | 0.10780 | 1.326 | 4.080 | 1.989 | 0.2729 | 1.483 | 0.75 | 6.05 | 1762 | 23 | 1555 | 21 |

**12TM13-06 zircon** (spot size: 24 µm, frequency: 4 Hz, 100 shot count, laser energy: 4 mJ at 75%)

| | | | | | ISOTOPIC RATIOS | | | | | | | | APPARENT AGES | | | |
|---|---|---|---|---|---|---|---|---|---|---|---|---|---|---|---|---|
| | Pb (ppm) | U (ppm) | Th (ppm) | Th/U | $^{207}Pb/^{206}Pb$ | 2σ % | $^{207}Pb/^{235}U$ | 2σ % | $^{206}Pb/^{238}U$ | 2σ % | Rho | % disc.* | $^{207}Pb/^{206}Pb$ | 2σ abs | $^{206}Pb/^{238}U$ | 2σ abs |
| spot 32 | 197 | 1468 | 237 | 0.16 | 0.10695 | 1.330 | 3.907 | 1.918 | 0.2651 | 1.382 | 0.72 | 6.60 | 1748 | 23 | 1515 | 19 |
| spot 33 | 181 | 1408 | 214 | 0.15 | 0.10622 | 1.341 | 3.840 | 2.088 | 0.2628 | 1.601 | 0.77 | 6.31 | 1735 | 23 | 1506 | 22 |
| spot 34 | 395 | 1229 | 413 | 0.34 | 0.11066 | 1.352 | 4.552 | 2.068 | 0.2975 | 1.565 | 0.76 | 3.69 | 1810 | 24 | 1678 | 23 |
| spot 35 | 307 | 793 | 324 | 0.41 | 0.11005 | 1.334 | 4.582 | 1.888 | 0.3016 | 1.336 | 0.71 | 2.89 | 1801 | 24 | 1698 | 21 |
| spot 36 | 464 | 1485 | 483 | 0.32 | 0.10935 | 1.323 | 4.317 | 1.902 | 0.2853 | 1.366 | 0.72 | 4.94 | 1788 | 24 | 1618 | 20 |
| spot 37 | 555 | 1633 | 588 | 0.36 | 0.11092 | 1.326 | 4.490 | 1.926 | 0.2932 | 1.397 | 0.73 | 4.28 | 1814 | 24 | 1659 | 21 |
| spot 38 | 625 | 1851 | 695 | 0.38 | 0.11168 | 1.342 | 4.537 | 1.847 | 0.2949 | 1.270 | 0.69 | 4.44 | 1827 | 24 | 1665 | 19 |
| spot 39 | 94 | 1332 | 113 | 0.08 | 0.10602 | 1.328 | 3.920 | 2.038 | 0.2668 | 1.546 | 0.76 | 6.04 | 1732 | 23 | 1524 | 21 |
| spot 40 | 161 | 1969 | 195 | 0.10 | 0.10735 | 1.338 | 3.909 | 1.930 | 0.2630 | 1.391 | 0.72 | 7.31 | 1755 | 24 | 1504 | 19 |
| spot 41 | 317 | 1231 | 344 | 0.28 | 0.10957 | 1.329 | 4.341 | 1.951 | 0.2853 | 1.429 | 0.73 | 5.26 | 1793 | 24 | 1617 | 20 |
| spot 42 | 127 | 1948 | 209 | 0.11 | 0.10654 | 1.358 | 3.485 | 2.215 | 0.2373 | 1.750 | 0.79 | 11.08 | 1741 | 24 | 1372 | 22 |
| spot 43 | 80 | 1553 | 101 | 0.07 | 0.10476 | 1.327 | 3.676 | 1.876 | 0.2537 | 1.326 | 0.71 | 7.55 | 1710 | 23 | 1457 | 17 |
| spot 44 | 50 | 872 | 53 | 0.06 | 0.10625 | 1.330 | 4.202 | 1.973 | 0.2861 | 1.457 | 0.74 | 3.21 | 1736 | 23 | 1621 | 21 |
| spot 45 | 73 | 1461 | 88 | 0.06 | 0.10633 | 1.343 | 3.921 | 2.019 | 0.2676 | 1.507 | 0.75 | 5.89 | 1737 | 23 | 1528 | 21 |
| spot 46 | 672 | 2020 | 714 | 0.35 | 0.11288 | 1.345 | 4.740 | 2.116 | 0.3029 | 1.633 | 0.77 | 4.05 | 1846 | 25 | 1705 | 25 |
| spot 47 | 65 | 1453 | 77 | 0.05 | 0.10591 | 1.329 | 3.988 | 2.042 | 0.2726 | 1.551 | 0.76 | 4.96 | 1730 | 23 | 1553 | 22 |
| spot 48 | 321 | 1548 | 379 | 0.24 | 0.10838 | 1.329 | 3.765 | 2.017 | 0.2513 | 1.517 | 0.75 | 9.76 | 1772 | 24 | 1444 | 20 |
| spot 49 | 185 | 1595 | 218 | 0.14 | 0.10896 | 1.346 | 4.309 | 2.110 | 0.2847 | 1.625 | 0.77 | 4.96 | 1782 | 24 | 1614 | 24 |
| spot 50 | 163 | 1258 | 187 | 0.15 | 0.10763 | 1.347 | 4.184 | 1.976 | 0.2813 | 1.446 | 0.73 | 4.63 | 1759 | 24 | 1597 | 21 |
| spot 51 | 593 | 1554 | 636 | 0.41 | 0.11114 | 1.338 | 4.620 | 2.121 | 0.3002 | 1.646 | 0.78 | 3.55 | 1818 | 24 | 1692 | 25 |
| spot 52 | 207 | 2686 | 255 | 0.09 | 0.10894 | 1.356 | 3.961 | 2.101 | 0.2620 | 1.605 | 0.76 | 8.40 | 1781 | 24 | 1500 | 22 |
| spot 53 | 153 | 1312 | 188 | 0.14 | 0.10559 | 1.327 | 3.880 | 2.151 | 0.2654 | 1.692 | 0.79 | 5.93 | 1724 | 23 | 1517 | 23 |
| spot 54 | 415 | 1777 | 506 | 0.28 | 0.11159 | 1.356 | 4.098 | 2.085 | 0.2661 | 1.584 | 0.76 | 8.82 | 1825 | 25 | 1520 | 22 |
| spot 55 | 859 | 1775 | 934 | 0.53 | 0.11340 | 1.322 | 4.784 | 1.848 | 0.3058 | 1.292 | 0.70 | 3.74 | 1855 | 25 | 1719 | 20 |
| spot 56 | 140 | 1196 | 163 | 0.14 | 0.10477 | 1.327 | 3.547 | 2.220 | 0.2447 | 1.780 | 0.80 | 9.01 | 1710 | 23 | 1410 | 23 |
| spot 57 | 506 | 1265 | 574 | 0.45 | 0.11045 | 1.338 | 4.496 | 2.046 | 0.2945 | 1.547 | 0.76 | 3.97 | 1807 | 24 | 1663 | 23 |
| spot 58 | 668 | 1560 | 736 | 0.47 | 0.11278 | 1.329 | 4.762 | 2.005 | 0.3050 | 1.502 | 0.75 | 3.62 | 1844 | 24 | 1715 | 23 |
| spot 59 | 617 | 1467 | 692 | 0.47 | 0.11280 | 1.350 | 4.724 | 1.981 | 0.3030 | 1.450 | 0.73 | 3.57 | 1846 | 25 | 1710 | 22 |
| spot 60 | 418 | 1137 | 463 | 0.41 | 0.11182 | 1.333 | 4.806 | 1.993 | 0.3102 | 1.481 | 0.74 | 2.47 | 1829 | 24 | 1741 | 23 |
| spot 61 | 419 | 1223 | 494 | 0.40 | 0.10899 | 1.346 | 4.405 | 2.083 | 0.2920 | 1.590 | 0.76 | 3.76 | 1782 | 24 | 1651 | 24 |
| spot 62 | 234 | 995 | 284 | 0.29 | 0.10857 | 1.337 | 4.143 | 2.013 | 0.2753 | 1.505 | 0.75 | 6.13 | 1775 | 24 | 1567 | 21 |

**12TM13-06 zircon** (spot size: 24 µm, frequency: 4 Hz, 100 shot count, laser energy: 4 mJ at 75%)

| | | | | | ISOTOPIC RATIOS | | | | | | | | APPARENT AGES | | | |
|---|---|---|---|---|---|---|---|---|---|---|---|---|---|---|---|---|
| | Pb (ppm) | U (ppm) | Th (ppm) | Th/U | $^{207}Pb/^{206}Pb$ | 2σ % | $^{207}Pb/^{235}U$ | 2σ % | $^{206}Pb/^{238}U$ | 2σ % | Rho | % disc.* | $^{207}Pb/^{206}Pb$ | 2σ abs | $^{206}Pb/^{238}U$ | 2σ abs |
| spot 63 | 474 | 1235 | 541 | 0.44 | 0.11186 | 1.326 | 4.721 | 2.002 | 0.3053 | 1.501 | 0.75 | 3.20 | 1830 | 24 | 1717 | 23 |
| spot 64 | 207 | 1557 | 258 | 0.17 | 0.10993 | 1.371 | 4.253 | 1.905 | 0.2801 | 1.322 | 0.69 | 5.78 | 1798 | 25 | 1592 | 19 |
| spot 65 | 481 | 1235 | 541 | 0.44 | 0.11235 | 1.327 | 4.741 | 2.027 | 0.3049 | 1.533 | 0.76 | 3.32 | 1838 | 24 | 1718 | 24 |
| spot 66 | 76 | 1606 | 91 | 0.06 | 0.10856 | 1.322 | 4.226 | 2.086 | 0.2805 | 1.613 | 0.77 | 5.27 | 1775 | 23 | 1593 | 23 |
| spot 67 | 45 | 1098 | 58 | 0.05 | 0.10328 | 1.343 | 3.697 | 2.105 | 0.2590 | 1.621 | 0.77 | 5.73 | 1684 | 23 | 1484 | 22 |
| spot 68 | 837 | 2214 | 950 | 0.43 | 0.11548 | 1.343 | 4.774 | 1.990 | 0.2984 | 1.469 | 0.74 | 5.70 | 1887 | 25 | 1683 | 22 |
| spot 69 | 491 | 1773 | 599 | 0.34 | 0.11221 | 1.346 | 4.361 | 1.946 | 0.2831 | 1.406 | 0.72 | 6.04 | 1836 | 25 | 1606 | 20 |
| spot 70 | 724 | 1676 | 759 | 0.45 | 0.11361 | 1.328 | 4.857 | 2.083 | 0.3091 | 1.605 | 0.77 | 3.34 | 1858 | 25 | 1735 | 24 |

**12TM14-10 zircon** (spot size: 24 µm, frequency: 4 Hz, 100 shot count, laser energy: 4 mJ at 75%)

| | | | | | ISOTOPIC RATIOS | | | | | | | | APPARENT AGES | | | |
|---|---|---|---|---|---|---|---|---|---|---|---|---|---|---|---|---|
| | Pb (ppm) | U (ppm) | Th (ppm) | Th/U | $^{207}Pb/^{206}Pb$ | 2σ % | $^{207}Pb/^{235}U$ | 2σ % | $^{206}Pb/^{238}U$ | 2σ % | Rho | % disc.* | $^{207}Pb/^{206}Pb$ | 2σ abs | $^{206}Pb/^{238}U$ | 2σ abs |
| spot 1 | 418 | 1151 | 459 | 0.40 | 0.11086 | 0.381 | 4.749 | 1.461 | 0.3104 | 1.411 | 0.97 | 1.84 | 1814 | 7 | 1742 | 22 |
| spot 2 | 596 | 1444 | 677 | 0.47 | 0.11232 | 0.379 | 4.748 | 1.533 | 0.3076 | 1.485 | 0.97 | 2.84 | 1837 | 7 | 1728 | 23 |
| spot 3 | 125 | 1231 | 157 | 0.13 | 0.10482 | 0.415 | 3.875 | 1.668 | 0.2683 | 1.616 | 0.97 | 5.03 | 1711 | 7 | 1531 | 22 |
| spot 4 | 681 | 1649 | 766 | 0.46 | 0.11266 | 0.401 | 4.731 | 1.520 | 0.3048 | 1.466 | 0.96 | 3.20 | 1843 | 7 | 1717 | 22 |
| spot 5 | 136 | 1216 | 171 | 0.14 | 0.10454 | 0.415 | 3.944 | 1.640 | 0.2735 | 1.587 | 0.97 | 3.97 | 1706 | 7 | 1560 | 22 |
| spot 6 | 1112 | 1859 | 1250 | 0.67 | 0.11324 | 0.400 | 4.832 | 1.533 | 0.3088 | 1.480 | 0.97 | 3.23 | 1852 | 7 | 1734 | 22 |
| spot 7 | 785 | 1883 | 871 | 0.46 | 0.11365 | 0.436 | 4.833 | 1.552 | 0.3067 | 1.489 | 0.96 | 3.83 | 1858 | 8 | 1723 | 22 |
| spot 8 | 260 | 2564 | 311 | 0.12 | 0.11103 | 0.435 | 4.286 | 1.511 | 0.2804 | 1.447 | 0.96 | 6.14 | 1816 | 8 | 1595 | 20 |
| spot 9 | 37 | 1121 | 45 | 0.04 | 0.10622 | 0.406 | 4.023 | 1.393 | 0.2753 | 1.333 | 0.96 | 4.72 | 1736 | 7 | 1567 | 19 |
| spot 10 | 85 | 1054 | 84 | 0.08 | 0.10813 | 0.396 | 4.402 | 1.627 | 0.2947 | 1.578 | 0.97 | 2.76 | 1768 | 7 | 1664 | 24 |
| spot 11 | 371 | 1140 | 427 | 0.37 | 0.10958 | 0.516 | 4.525 | 1.486 | 0.2996 | 1.394 | 0.94 | 2.54 | 1793 | 9 | 1691 | 21 |
| spot 12 | 35 | 944 | 40 | 0.04 | 0.10673 | 0.431 | 4.272 | 1.535 | 0.2892 | 1.473 | 0.96 | 3.05 | 1744 | 8 | 1637 | 21 |
| spot 13 | 563 | 1442 | 623 | 0.43 | 0.11228 | 0.446 | 4.734 | 1.681 | 0.3055 | 1.621 | 0.96 | 3.08 | 1836 | 8 | 1720 | 24 |
| spot 14 | 678 | 2544 | 912 | 0.36 | 0.11242 | 0.414 | 4.443 | 1.479 | 0.2863 | 1.420 | 0.96 | 5.98 | 1839 | 8 | 1622 | 20 |
| spot 15 | 49 | 780 | 64 | 0.08 | 0.10337 | 0.411 | 3.844 | 1.521 | 0.2698 | 1.464 | 0.96 | 4.16 | 1685 | 7 | 1539 | 20 |
| spot 16 | 378 | 1378 | 423 | 0.31 | 0.10960 | 0.371 | 4.473 | 1.429 | 0.2952 | 1.380 | 0.97 | 3.54 | 1793 | 7 | 1667 | 20 |
| spot 17 | 742 | 1837 | 818 | 0.45 | 0.11184 | 0.397 | 4.633 | 1.062 | 0.2997 | 0.986 | 0.93 | 3.87 | 1829 | 7 | 1689 | 15 |
| spot 18 | 222 | 1346 | 439 | 0.33 | 0.10671 | 0.424 | 3.994 | 1.061 | 0.2706 | 0.973 | 0.92 | 5.71 | 1744 | 8 | 1544 | 13 |
| spot 19 | 803 | 2230 | 950 | 0.43 | 0.11136 | 0.593 | 4.401 | 1.243 | 0.2853 | 1.092 | 0.88 | 5.65 | 1822 | 11 | 1620 | 15 |
| spot 20 | 72 | 1175 | 88 | 0.07 | 0.10634 | 0.418 | 4.093 | 1.067 | 0.2790 | 0.981 | 0.92 | 4.17 | 1738 | 7 | 1586 | 14 |
| spot 21 | 551 | 1617 | 591 | 0.37 | 0.11162 | 0.380 | 4.693 | 1.127 | 0.3052 | 1.061 | 0.94 | 2.86 | 1826 | 7 | 1718 | 16 |
| spot 22 | 225 | 766 | 263 | 0.34 | 0.10664 | 0.405 | 4.384 | 1.217 | 0.2974 | 1.148 | 0.94 | 1.81 | 1743 | 7 | 1678 | 17 |
| spot 23 | 204 | 837 | 227 | 0.27 | 0.10912 | 0.426 | 4.799 | 1.190 | 0.3182 | 1.112 | 0.93 | 0.15 | 1786 | 8 | 1781 | 18 |
| spot 24 | 735 | 2007 | 808 | 0.40 | 0.11296 | 0.425 | 4.683 | 1.099 | 0.3006 | 1.014 | 0.92 | 4.10 | 1848 | 8 | 1694 | 16 |
| spot 25 | 377 | 1156 | 423 | 0.37 | 0.11057 | 0.393 | 4.575 | 1.061 | 0.2996 | 0.986 | 0.93 | 3.43 | 1809 | 7 | 1689 | 16 |
| spot 26 | 394 | 1326 | 430 | 0.32 | 0.10945 | 0.466 | 4.381 | 1.261 | 0.2905 | 1.172 | 0.93 | 4.00 | 1790 | 8 | 1643 | 17 |
| spot 27 | 79 | 487 | 57 | 0.12 | 0.10645 | 0.511 | 4.619 | 1.541 | 0.3147 | 1.454 | 0.94 | 0.68 | 1739 | 9 | 1763 | 23 |
| spot 28 | 829 | 2685 | 930 | 0.35 | 0.11339 | 0.383 | 4.673 | 1.179 | 0.2979 | 1.115 | 0.95 | 4.65 | 1855 | 7 | 1683 | 17 |
| spot 29 | 112 | 765 | 115 | 0.15 | 0.10536 | 0.420 | 4.314 | 1.169 | 0.2956 | 1.091 | 0.93 | 1.56 | 1720 | 7 | 1669 | 16 |
| spot 30 | 109 | 998 | 200 | 0.20 | 0.10739 | 0.386 | 4.145 | 1.145 | 0.2796 | 1.078 | 0.94 | 4.63 | 1755 | 7 | 1589 | 15 |
| spot 31 | 134 | 1196 | 416 | 0.35 | 0.10589 | 0.388 | 3.982 | 1.267 | 0.2723 | 1.207 | 0.95 | 4.99 | 1730 | 7 | 1552 | 16 |

**12TM14-10 zircon** (spot size: 24 µm, frequency: 4 Hz, 100 shot count, laser energy: 4 mJ at 75%)

| | | | | | ISOTOPIC RATIOS | | | | | | | | APPARENT AGES | | | |
|---|---|---|---|---|---|---|---|---|---|---|---|---|---|---|---|---|
| | Pb (ppm) | U (ppm) | Th (ppm) | Th/U | $^{207}Pb/^{206}Pb$ | 2σ % | $^{207}Pb/^{235}U$ | 2σ % | $^{206}Pb/^{238}U$ | 2σ % | Rho | % disc.* | $^{207}Pb/^{206}Pb$ | 2σ abs | $^{206}Pb/^{238}U$ | 2σ abs |
| spot 32 | 288 | 1416 | 343 | 0.24 | 0.10886 | 0.372 | 4.239 | 1.133 | 0.2820 | 1.070 | 0.94 | 5.05 | 1781 | 7 | 1601 | 15 |
| spot 33 | 324 | 1097 | 385 | 0.35 | 0.10927 | 0.407 | 4.464 | 1.194 | 0.2954 | 1.123 | 0.94 | 3.32 | 1787 | 7 | 1668 | 16 |
| spot 34 | 22 | 803 | 27 | 0.03 | 0.10458 | 0.402 | 3.951 | 1.136 | 0.2744 | 1.062 | 0.94 | 3.86 | 1708 | 7 | 1563 | 15 |
| spot 35 | 637 | 1517 | 722 | 0.48 | 0.11097 | 0.375 | 4.688 | 1.211 | 0.3057 | 1.151 | 0.95 | 2.62 | 1815 | 7 | 1719 | 17 |
| spot 36 | 49 | 1094 | 57 | 0.05 | 0.10620 | 0.453 | 4.026 | 1.253 | 0.2732 | 1.169 | 0.93 | 5.29 | 1735 | 8 | 1556 | 16 |
| spot 37 | 196 | 1082 | 270 | 0.25 | 0.10394 | 0.403 | 3.839 | 1.096 | 0.2668 | 1.019 | 0.93 | 5.00 | 1696 | 7 | 1524 | 14 |
| spot 38 | 1119 | 2507 | 1306 | 0.52 | 0.11403 | 0.455 | 4.756 | 1.137 | 0.3015 | 1.042 | 0.92 | 4.61 | 1864 | 8 | 1699 | 16 |
| spot 39 | 536 | 1465 | 651 | 0.44 | 0.11013 | 0.366 | 4.493 | 1.123 | 0.2947 | 1.062 | 0.95 | 3.96 | 1802 | 7 | 1664 | 16 |
| spot 40 | 532 | 1446 | 652 | 0.45 | 0.10986 | 0.394 | 4.512 | 1.068 | 0.2972 | 0.993 | 0.93 | 3.30 | 1798 | 7 | 1677 | 15 |
| spot 41 | 217 | 2187 | 280 | 0.13 | 0.10816 | 0.368 | 4.188 | 1.198 | 0.2809 | 1.140 | 0.95 | 4.82 | 1769 | 7 | 1597 | 16 |
| spot 42 | 136 | 1758 | 171 | 0.10 | 0.10713 | 0.398 | 4.039 | 1.271 | 0.2721 | 1.207 | 0.95 | 5.67 | 1751 | 7 | 1555 | 17 |
| spot 43 | 504 | 1338 | 625 | 0.47 | 0.11104 | 0.381 | 4.627 | 1.139 | 0.3013 | 1.073 | 0.94 | 3.38 | 1816 | 7 | 1697 | 16 |
| spot 44 | 558 | 1459 | 694 | 0.48 | 0.11043 | 0.399 | 4.444 | 1.292 | 0.2926 | 1.229 | 0.95 | 3.93 | 1806 | 7 | 1654 | 18 |
| spot 45 | 214 | 660 | 260 | 0.39 | 0.10764 | 0.485 | 4.355 | 1.436 | 0.2942 | 1.352 | 0.94 | 2.53 | 1760 | 9 | 1662 | 20 |
| spot 46 | 620 | 1453 | 768 | 0.53 | 0.11171 | 0.374 | 4.628 | 1.261 | 0.2994 | 1.204 | 0.95 | 4.03 | 1827 | 7 | 1688 | 18 |
| spot 47 | 757 | 1663 | 859 | 0.52 | 0.11251 | 0.445 | 4.865 | 1.241 | 0.3127 | 1.159 | 0.93 | 2.40 | 1840 | 8 | 1753 | 18 |
| spot 48 | 459 | 986 | 554 | 0.56 | 0.11053 | 0.387 | 4.688 | 1.236 | 0.3081 | 1.174 | 0.95 | 1.96 | 1808 | 7 | 1731 | 18 |
| spot 49 | 1015 | 2372 | 1201 | 0.51 | 0.11460 | 0.454 | 4.892 | 1.257 | 0.3087 | 1.172 | 0.93 | 3.68 | 1873 | 8 | 1738 | 17 |
| spot 50 | 732 | 1646 | 914 | 0.56 | 0.11161 | 0.380 | 4.614 | 1.260 | 0.3002 | 1.201 | 0.95 | 3.61 | 1826 | 7 | 1692 | 18 |
| spot 51 | 261 | 852 | 308 | 0.36 | 0.10981 | 0.425 | 4.568 | 1.509 | 0.3019 | 1.448 | 0.96 | 2.47 | 1796 | 8 | 1703 | 22 |
| spot 52 | 99 | 729 | 140 | 0.19 | 0.10209 | 0.413 | 3.850 | 1.302 | 0.2739 | 1.235 | 0.95 | 2.72 | 1664 | 7 | 1560 | 17 |
| spot 53 | 413 | 1134 | 509 | 0.45 | 0.10821 | 0.384 | 4.429 | 1.364 | 0.2969 | 1.309 | 0.96 | 2.69 | 1769 | 7 | 1675 | 19 |
| spot 54 | 226 | 1683 | 286 | 0.17 | 0.10757 | 0.391 | 4.271 | 1.247 | 0.2870 | 1.185 | 0.95 | 3.69 | 1759 | 7 | 1626 | 17 |
| spot 55 | 98 | 970 | 522 | 0.54 | 0.10469 | 0.402 | 3.888 | 1.283 | 0.2693 | 1.219 | 0.95 | 4.91 | 1709 | 7 | 1537 | 17 |
| spot 56 | 46 | 654 | 55 | 0.08 | 0.10734 | 0.450 | 4.642 | 1.382 | 0.3134 | 1.307 | 0.95 | 0.06 | 1755 | 8 | 1757 | 20 |
| spot 57 | 553 | 1351 | 654 | 0.48 | 0.11154 | 0.380 | 4.707 | 1.213 | 0.3054 | 1.152 | 0.95 | 2.94 | 1825 | 7 | 1717 | 17 |
| spot 58 | 576 | 1411 | 672 | 0.48 | 0.11130 | 0.397 | 4.663 | 1.312 | 0.3038 | 1.251 | 0.95 | 2.98 | 1821 | 7 | 1710 | 19 |
| spot 59 | 738 | 1553 | 824 | 0.53 | 0.11247 | 0.401 | 4.768 | 1.300 | 0.3077 | 1.236 | 0.95 | 2.89 | 1840 | 7 | 1729 | 19 |
| spot 60 | 111 | 1235 | 148 | 0.12 | 0.10341 | 0.445 | 3.788 | 1.245 | 0.2657 | 1.162 | 0.93 | 4.68 | 1686 | 8 | 1518 | 16 |
| spot 61 | 150 | 1687 | 188 | 0.11 | 0.10533 | 0.377 | 3.899 | 1.351 | 0.2674 | 1.297 | 0.96 | 5.73 | 1720 | 7 | 1527 | 18 |
| spot 62 | 411 | 1391 | 532 | 0.38 | 0.10968 | 0.394 | 4.598 | 1.377 | 0.3022 | 1.320 | 0.96 | 2.34 | 1795 | 7 | 1707 | 20 |

**12TM14-10 zircon** (spot size: 24 µm, frequency: 4 Hz, 100 shot count, laser energy: 4 mJ at 75%)

| | | | | | ISOTOPIC RATIOS | | | | | | | | APPARENT AGES | | | |
|---|---|---|---|---|---|---|---|---|---|---|---|---|---|---|---|---|
| | Pb (ppm) | U (ppm) | Th (ppm) | Th/U | $^{207}Pb/^{206}Pb$ | 2σ % | $^{207}Pb/^{235}U$ | 2σ % | $^{206}Pb/^{238}U$ | 2σ % | Rho | % disc.* | $^{207}Pb/^{206}Pb$ | 2σ abs | $^{206}Pb/^{238}U$ | 2σ abs |
| spot 63 | 179 | 2759 | 250 | 0.09 | 0.10352 | 0.438 | 3.454 | 1.340 | 0.2414 | 1.266 | 0.95 | 8.90 | 1689 | 8 | 1393 | 16 |
| spot 64 | 1034 | 2124 | 1156 | 0.54 | 0.11382 | 0.423 | 4.772 | 1.537 | 0.3022 | 1.478 | 0.96 | 4.53 | 1861 | 8 | 1701 | 22 |
| spot 65 | 862 | 1842 | 964 | 0.52 | 0.11303 | 0.444 | 4.745 | 1.121 | 0.3059 | 1.029 | 0.92 | 3.28 | 1850 | 8 | 1720 | 16 |
| spot 66 | 222 | 3095 | 291 | 0.09 | 0.11064 | 0.463 | 3.965 | 1.310 | 0.2589 | 1.226 | 0.94 | 9.57 | 1810 | 8 | 1484 | 16 |
| spot 67 | 607 | 1379 | 699 | 0.51 | 0.10828 | 0.441 | 4.329 | 1.415 | 0.2883 | 1.344 | 0.95 | 4.10 | 1771 | 8 | 1633 | 20 |
| spot 68 | 89 | 1286 | 116 | 0.09 | 0.10437 | 0.378 | 3.807 | 1.437 | 0.2636 | 1.387 | 0.96 | 5.77 | 1703 | 7 | 1508 | 19 |
| spot 69 | 183 | 1369 | 220 | 0.16 | 0.10640 | 0.375 | 4.175 | 1.285 | 0.2839 | 1.229 | 0.96 | 3.69 | 1739 | 7 | 1611 | 17 |
| spot 70 | 178 | 1844 | 208 | 0.11 | 0.10819 | 0.462 | 4.150 | 1.499 | 0.2776 | 1.426 | 0.95 | 5.38 | 1769 | 8 | 1579 | 20 |
| spot 71 | 113 | 1840 | 140 | 0.08 | 0.10765 | 0.391 | 4.006 | 1.243 | 0.2704 | 1.179 | 0.95 | 6.00 | 1761 | 7 | 1543 | 16 |
| spot 72 | 133 | 1171 | 287 | 0.25 | 0.10670 | 0.418 | 4.017 | 1.372 | 0.2732 | 1.307 | 0.95 | 5.21 | 1744 | 7 | 1556 | 18 |
| spot 73 | 224 | 2193 | 260 | 0.12 | 0.10958 | 0.459 | 4.218 | 1.394 | 0.2791 | 1.316 | 0.94 | 5.74 | 1792 | 8 | 1586 | 19 |
| spot 74 | 258 | 2202 | 307 | 0.14 | 0.11020 | 0.393 | 4.207 | 1.322 | 0.2757 | 1.262 | 0.95 | 6.76 | 1803 | 7 | 1569 | 18 |
| spot 75 | 693 | 1839 | 811 | 0.44 | 0.11271 | 0.378 | 4.679 | 1.321 | 0.2998 | 1.266 | 0.96 | 4.26 | 1844 | 7 | 1690 | 19 |
| spot 76 | 602 | 1631 | 739 | 0.45 | 0.11120 | 0.518 | 4.424 | 1.599 | 0.2878 | 1.513 | 0.95 | 5.28 | 1819 | 9 | 1630 | 22 |
| spot 77 | 730 | 1586 | 914 | 0.58 | 0.11202 | 0.414 | 4.749 | 1.486 | 0.3065 | 1.427 | 0.96 | 3.02 | 1832 | 8 | 1723 | 22 |
| spot 78 | 65 | 935 | 51 | 0.05 | 0.10694 | 0.404 | 4.197 | 1.485 | 0.2844 | 1.428 | 0.96 | 3.66 | 1748 | 7 | 1613 | 21 |
| spot 79 | 108 | 1367 | 125 | 0.09 | 0.10620 | 0.406 | 4.100 | 1.441 | 0.2796 | 1.382 | 0.96 | 4.03 | 1735 | 7 | 1589 | 19 |
| spot 80 | 91 | 1395 | 121 | 0.09 | 0.10693 | 0.386 | 4.029 | 1.428 | 0.2737 | 1.375 | 0.96 | 5.20 | 1748 | 7 | 1559 | 19 |
| spot 81 | 276 | 854 | 332 | 0.39 | 0.11045 | 0.381 | 4.674 | 1.450 | 0.3058 | 1.399 | 0.96 | 2.32 | 1807 | 7 | 1722 | 21 |
| spot 82 | 205 | 630 | 242 | 0.38 | 0.10770 | 0.485 | 4.373 | 1.624 | 0.2939 | 1.550 | 0.95 | 2.71 | 1760 | 9 | 1660 | 23 |
| spot 83 | 392 | 1112 | 465 | 0.42 | 0.11145 | 0.386 | 4.715 | 1.300 | 0.3063 | 1.242 | 0.95 | 2.73 | 1824 | 7 | 1722 | 19 |
| spot 84 | 491 | 1675 | 599 | 0.36 | 0.11209 | 0.363 | 4.672 | 1.369 | 0.3020 | 1.320 | 0.96 | 3.53 | 1833 | 7 | 1701 | 20 |
| spot 85 | 75 | 695 | 85 | 0.12 | 0.10739 | 0.450 | 4.446 | 1.313 | 0.3000 | 1.233 | 0.94 | 1.83 | 1755 | 8 | 1691 | 18 |

**12TM13-03 zircon** (spot size: 24 µm, frequency: 4 Hz, 80 shot count, laser energy: 4 mJ at 75%)

| | | | | | ISOTOPIC RATIOS | | | | | | | | APPARENT AGES | | | |
|---|---|---|---|---|---|---|---|---|---|---|---|---|---|---|---|---|
| | Pb (ppm) | U (ppm) | Th (ppm) | Th/U | $^{207}Pb/^{206}Pb$ | 2σ % | $^{207}Pb/^{235}U$ | 2σ % | $^{206}Pb/^{238}U$ | 2σ % | Rho | % disc.* | $^{207}Pb/^{206}Pb$ | 2σ abs | $^{206}Pb/^{238}U$ | 2σ abs |
| spot 1 | 32 | 136 | 45 | 0.33 | 0.09866 | 0.570 | 3.638 | 1.000 | 0.2678 | 0.822 | 0.82 | 1.86 | 1600 | 10 | 1529 | 11 |
| spot 2 | 29 | 188 | 40 | 0.21 | 0.10091 | 0.545 | 3.794 | 0.887 | 0.2715 | 0.700 | 0.79 | 2.87 | 1642 | 9 | 1548 | 10 |
| spot 3 | 24 | 163 | 37 | 0.23 | 0.08825 | 0.555 | 2.897 | 0.840 | 0.2380 | 0.630 | 0.75 | 0.34 | 1388 | 9 | 1376 | 8 |
| spot 4 | 21 | 124 | 31 | 0.25 | 0.08840 | 0.585 | 2.979 | 0.880 | 0.2433 | 0.658 | 0.75 | 0.13 | 1391 | 10 | 1404 | 8 |
| spot 5 | 107 | 498 | 151 | 0.30 | 0.09991 | 0.534 | 3.677 | 0.922 | 0.2663 | 0.751 | 0.81 | 2.90 | 1622 | 9 | 1522 | 10 |
| spot 6 | 384 | 301 | 468 | 1.55 | 0.10113 | 0.503 | 4.053 | 0.969 | 0.2898 | 0.828 | 0.85 | 0.27 | 1645 | 9 | 1640 | 12 |
| spot 7 | 43 | 238 | 57 | 0.24 | 0.10172 | 0.492 | 3.839 | 0.821 | 0.2739 | 0.657 | 0.80 | 2.59 | 1656 | 8 | 1560 | 9 |
| spot 8 | 54 | 225 | 67 | 0.30 | 0.10372 | 0.533 | 4.210 | 0.836 | 0.2947 | 0.645 | 0.77 | 0.64 | 1692 | 9 | 1665 | 9 |
| spot 9 | 27 | 162 | 43 | 0.27 | 0.08882 | 0.576 | 2.780 | 0.909 | 0.2273 | 0.704 | 0.77 | 2.26 | 1400 | 10 | 1320 | 8 |
| spot 10 | 86 | 280 | 110 | 0.39 | 0.10477 | 0.531 | 4.210 | 0.892 | 0.2930 | 0.717 | 0.80 | 1.18 | 1710 | 9 | 1656 | 11 |
| spot 11 | 31 | 145 | 40 | 0.28 | 0.10299 | 0.579 | 4.005 | 1.086 | 0.2828 | 0.919 | 0.85 | 1.85 | 1678 | 10 | 1605 | 13 |
| spot 12 | 19 | 115 | 31 | 0.27 | 0.08906 | 0.683 | 2.841 | 1.101 | 0.2317 | 0.863 | 0.78 | 1.72 | 1405 | 12 | 1343 | 10 |
| spot 13 | 59 | 295 | 77 | 0.26 | 0.10423 | 0.499 | 4.096 | 0.830 | 0.2864 | 0.663 | 0.80 | 1.83 | 1701 | 9 | 1624 | 10 |
| spot 14 | 20 | 189 | 52 | 0.27 | 0.08568 | 0.691 | 1.699 | 0.979 | 0.1441 | 0.694 | 0.71 | 16.14 | 1330 | 12 | 868 | 6 |
| spot 15 | 53 | 165 | 77 | 0.47 | 0.09669 | 0.604 | 3.428 | 1.079 | 0.2574 | 0.894 | 0.83 | 2.33 | 1561 | 10 | 1476 | 12 |
| spot 16 | 38 | 205 | 49 | 0.24 | 0.10218 | 0.542 | 3.990 | 1.001 | 0.2851 | 0.842 | 0.84 | 0.97 | 1665 | 9 | 1617 | 12 |
| spot 17 | 22 | 182 | 35 | 0.19 | 0.08935 | 0.545 | 2.889 | 0.874 | 0.2340 | 0.684 | 0.78 | 1.73 | 1411 | 9 | 1355 | 8 |
| spot 18 | 21 | 156 | 31 | 0.20 | 0.08936 | 0.574 | 2.988 | 0.940 | 0.2420 | 0.744 | 0.79 | 0.51 | 1412 | 10 | 1397 | 9 |
| spot 19 | 77 | 410 | 117 | 0.28 | 0.09386 | 0.492 | 3.072 | 0.869 | 0.2371 | 0.717 | 0.82 | 3.93 | 1505 | 8 | 1371 | 9 |
| spot 20 | 48 | 286 | 61 | 0.21 | 0.10160 | 0.487 | 4.067 | 0.874 | 0.2895 | 0.725 | 0.83 | 0.57 | 1653 | 8 | 1639 | 10 |
| spot 21 | 28 | 154 | 48 | 0.31 | 0.08906 | 0.575 | 2.612 | 0.989 | 0.2113 | 0.805 | 0.81 | 5.58 | 1405 | 10 | 1236 | 9 |
| spot 22 | 27 | 221 | 44 | 0.20 | 0.08878 | 0.553 | 2.778 | 0.831 | 0.2260 | 0.619 | 0.75 | 2.73 | 1399 | 9 | 1314 | 7 |
| spot 23 | 25 | 205 | 38 | 0.19 | 0.08887 | 0.525 | 2.950 | 0.850 | 0.2394 | 0.668 | 0.79 | 0.85 | 1401 | 8 | 1384 | 8 |
| spot 24 | 35 | 147 | 49 | 0.33 | 0.09552 | 0.631 | 3.413 | 1.188 | 0.2583 | 1.007 | 0.85 | 1.76 | 1538 | 11 | 1481 | 13 |
| spot 25 | 19 | 159 | 40 | 0.25 | 0.08678 | 0.658 | 2.164 | 1.195 | 0.1805 | 0.997 | 0.83 | 9.35 | 1355 | 11 | 1069 | 10 |
| spot 26 | 52 | 223 | 66 | 0.30 | 0.10294 | 0.511 | 4.158 | 0.939 | 0.2922 | 0.787 | 0.84 | 0.82 | 1678 | 9 | 1652 | 11 |
| spot 27 | 33 | 180 | 42 | 0.24 | 0.10248 | 0.529 | 4.125 | 0.921 | 0.2921 | 0.753 | 0.82 | 0.42 | 1669 | 9 | 1652 | 11 |
| spot 28 | 24 | 179 | 37 | 0.21 | 0.08966 | 0.597 | 2.861 | 1.084 | 0.2321 | 0.905 | 0.83 | 2.03 | 1418 | 10 | 1345 | 11 |
| spot 29 | 25 | 134 | 43 | 0.32 | 0.08963 | 0.672 | 2.557 | 1.059 | 0.2076 | 0.819 | 0.77 | 5.95 | 1417 | 12 | 1216 | 9 |
| spot 30 | 95 | 263 | 147 | 0.56 | 0.09146 | 0.568 | 2.661 | 0.947 | 0.2113 | 0.757 | 0.80 | 6.52 | 1457 | 10 | 1237 | 8 |
| spot 31 | 31 | 204 | 58 | 0.28 | 0.09046 | 0.594 | 2.459 | 1.088 | 0.1976 | 0.911 | 0.84 | 8.38 | 1435 | 10 | 1162 | 10 |

**12TM13-03 zircon** (spot size: 24 µm, frequency: 4 Hz, 80 shot count, laser energy: 4 mJ at 75%)

| | | | | | ISOTOPIC RATIOS | | | | | | | | APPARENT AGES | | | |
|---|---|---|---|---|---|---|---|---|---|---|---|---|---|---|---|---|
| | Pb (ppm) | U (ppm) | Th (ppm) | Th/U | $^{207}Pb/^{206}Pb$ | 2σ % | $^{207}Pb/^{235}U$ | 2σ % | $^{206}Pb/^{238}U$ | 2σ % | Rho | % disc.* | $^{207}Pb/^{206}Pb$ | 2σ abs | $^{206}Pb/^{238}U$ | 2σ abs |
| spot 32 | 29 | 113 | 37 | 0.32 | 0.10239 | 0.594 | 4.133 | 1.039 | 0.2934 | 0.852 | 0.82 | 0.14 | 1668 | 10 | 1658 | 13 |
| spot 33 | 33 | 221 | 53 | 0.24 | 0.08812 | 0.507 | 2.676 | 1.040 | 0.2203 | 0.908 | 0.87 | 2.99 | 1385 | 8 | 1284 | 11 |
| spot 34 | 20 | 97 | 28 | 0.30 | 0.09302 | 0.825 | 3.284 | 1.366 | 0.2572 | 1.089 | 0.80 | 0.20 | 1487 | 14 | 1475 | 14 |
| spot 35 | 23 | 170 | 43 | 0.25 | 0.08879 | 0.650 | 2.520 | 1.127 | 0.2064 | 0.921 | 0.82 | 5.73 | 1399 | 11 | 1209 | 10 |
| spot 36 | 25 | 179 | 36 | 0.20 | 0.08813 | 0.563 | 2.971 | 0.893 | 0.2453 | 0.693 | 0.78 | 0.88 | 1386 | 9 | 1414 | 9 |
| spot 37 | 23 | 166 | 36 | 0.21 | 0.08834 | 0.547 | 2.874 | 0.935 | 0.2373 | 0.759 | 0.81 | 0.18 | 1390 | 9 | 1372 | 9 |
| spot 38 | 60 | 317 | 97 | 0.31 | 0.08818 | 0.513 | 2.753 | 1.056 | 0.2276 | 0.923 | 0.87 | 1.55 | 1386 | 8 | 1322 | 11 |
| spot 39 | 46 | 236 | 59 | 0.25 | 0.10049 | 0.527 | 3.956 | 0.904 | 0.2857 | 0.735 | 0.81 | 0.30 | 1633 | 9 | 1620 | 11 |
| spot 40 | 27 | 199 | 52 | 0.26 | 0.08701 | 0.558 | 2.320 | 1.038 | 0.1943 | 0.875 | 0.84 | 6.44 | 1360 | 9 | 1144 | 9 |
| spot 41 | 19 | 159 | 27 | 0.17 | 0.08870 | 0.600 | 2.960 | 1.019 | 0.2428 | 0.824 | 0.81 | 0.28 | 1397 | 10 | 1401 | 10 |
| spot 42 | 38 | 175 | 49 | 0.28 | 0.10173 | 0.556 | 4.011 | 1.033 | 0.2870 | 0.871 | 0.84 | 0.62 | 1656 | 10 | 1626 | 13 |
| spot 43 | 25 | 127 | 34 | 0.27 | 0.09616 | 0.710 | 3.513 | 1.177 | 0.2664 | 0.938 | 0.80 | 0.59 | 1550 | 13 | 1522 | 13 |
| spot 44 | 15 | 140 | 25 | 0.18 | 0.08855 | 0.592 | 2.711 | 1.267 | 0.2232 | 1.120 | 0.88 | 2.53 | 1394 | 10 | 1299 | 13 |
| spot 45 | 19 | 118 | 27 | 0.23 | 0.10083 | 0.613 | 3.515 | 1.123 | 0.2551 | 0.941 | 0.84 | 4.52 | 1639 | 11 | 1464 | 13 |
| spot 46 | 41 | 260 | 55 | 0.21 | 0.10173 | 0.549 | 3.834 | 0.972 | 0.2742 | 0.802 | 0.83 | 2.39 | 1656 | 10 | 1562 | 11 |
| spot 47 | 20 | 197 | 32 | 0.16 | 0.08897 | 0.553 | 2.927 | 1.110 | 0.2389 | 0.963 | 0.87 | 0.61 | 1403 | 9 | 1381 | 12 |
| spot 48 | 26 | 124 | 32 | 0.26 | 0.10248 | 0.615 | 4.178 | 1.070 | 0.2968 | 0.876 | 0.82 | 0.35 | 1669 | 11 | 1675 | 13 |
| spot 49 | 20 | 132 | 27 | 0.21 | 0.09845 | 0.599 | 3.601 | 1.051 | 0.2661 | 0.864 | 0.82 | 1.92 | 1595 | 11 | 1521 | 12 |
| spot 50 | 20 | 126 | 30 | 0.23 | 0.09019 | 0.750 | 3.007 | 1.241 | 0.2427 | 0.989 | 0.80 | 0.64 | 1429 | 13 | 1401 | 13 |
| spot 51 | 28 | 167 | 39 | 0.24 | 0.09654 | 0.562 | 3.397 | 0.993 | 0.2563 | 0.819 | 0.82 | 2.19 | 1558 | 10 | 1471 | 11 |
| spot 52 | 276 | 472 | 325 | 0.69 | 0.10238 | 0.472 | 3.972 | 0.972 | 0.2826 | 0.849 | 0.87 | 1.50 | 1668 | 8 | 1604 | 12 |
| spot 53 | 22 | 152 | 33 | 0.22 | 0.09574 | 0.592 | 3.281 | 1.134 | 0.2481 | 0.967 | 0.85 | 3.36 | 1542 | 10 | 1428 | 12 |
| spot 54 | 703 | 949 | 1024 | 1.08 | 0.09260 | 0.467 | 2.988 | 0.898 | 0.2346 | 0.767 | 0.85 | 3.35 | 1480 | 7 | 1359 | 9 |

**12TM15-14 zircon** (spot size: 19 µm, frequency: 4 Hz, 80 shot count, laser energy: 4 mJ at 75%)

| | | | | | ISOTOPIC RATIOS | | | | | | | | APPARENT AGES | | | |
|---|---|---|---|---|---|---|---|---|---|---|---|---|---|---|---|---|
| | Pb (ppm) | U (ppm) | Th (ppm) | Th/U | $^{207}Pb/^{206}Pb$ | 2σ % | $^{207}Pb/^{235}U$ | 2σ % | $^{206}Pb/^{238}U$ | 2σ % | Rho | % disc.* | $^{207}Pb/^{206}Pb$ | 2σ abs | $^{206}Pb/^{238}U$ | 2σ abs |
| spot 1 | 67 | 621 | 93 | 0.15 | 0.10211 | 0.980 | 3.876 | 1.406 | 0.2759 | 1.008 | 0.72 | 2.43 | 1663 | 16 | 1570 | 15 |
| spot 2 | 26 | 154 | 34 | 0.22 | 0.10459 | 1.081 | 4.223 | 1.688 | 0.2934 | 1.296 | 0.77 | 1.45 | 1707 | 19 | 1658 | 20 |
| spot 3 | 24 | 335 | 46 | 0.14 | 0.09051 | 1.039 | 2.536 | 1.534 | 0.2033 | 1.129 | 0.74 | 7.47 | 1437 | 16 | 1193 | 13 |
| spot 4 | 13 | 141 | 21 | 0.15 | 0.08879 | 1.107 | 2.829 | 1.547 | 0.2310 | 1.080 | 0.70 | 1.72 | 1399 | 17 | 1340 | 14 |
| spot 5 | 20 | 254 | 33 | 0.13 | 0.08847 | 1.086 | 2.740 | 1.545 | 0.2244 | 1.099 | 0.71 | 2.62 | 1394 | 16 | 1305 | 13 |
| spot 6 | 23 | 219 | 36 | 0.17 | 0.09293 | 1.039 | 3.003 | 1.644 | 0.2348 | 1.274 | 0.77 | 3.59 | 1486 | 16 | 1359 | 16 |
| spot 7 | 58 | 367 | 90 | 0.24 | 0.08883 | 1.010 | 2.879 | 1.495 | 0.2352 | 1.101 | 0.74 | 1.04 | 1400 | 15 | 1362 | 14 |
| spot 8 | 1001 | 458 | 1245 | 2.72 | 0.10623 | 0.998 | 4.482 | 1.468 | 0.3054 | 1.077 | 0.73 | 0.54 | 1736 | 17 | 1718 | 17 |
| spot 9 | 22 | 241 | 43 | 0.18 | 0.08782 | 1.094 | 2.510 | 1.538 | 0.2063 | 1.081 | 0.70 | 5.45 | 1378 | 17 | 1209 | 12 |
| spot 10 | 27 | 219 | 35 | 0.16 | 0.10069 | 1.072 | 3.928 | 1.808 | 0.2821 | 1.456 | 0.81 | 1.12 | 1637 | 18 | 1602 | 21 |
| spot 11 | 42 | 1170 | 66 | 0.06 | 0.09716 | 1.002 | 3.183 | 1.533 | 0.2378 | 1.160 | 0.76 | 5.64 | 1570 | 16 | 1375 | 15 |
| spot 12 | 10 | 122 | 19 | 0.15 | 0.09024 | 1.108 | 2.491 | 1.677 | 0.2007 | 1.259 | 0.75 | 7.63 | 1430 | 18 | 1179 | 14 |
| spot 13 | 109 | 2281 | 160 | 0.07 | 0.10045 | 0.972 | 3.352 | 1.478 | 0.2423 | 1.114 | 0.75 | 6.79 | 1632 | 16 | 1398 | 15 |
| spot 14 | 18 | 330 | 53 | 0.16 | 0.08065 | 1.086 | 1.495 | 1.708 | 0.1344 | 1.317 | 0.77 | 14.15 | 1214 | 15 | 813 | 10 |
| spot 15 | 42 | 1694 | 68 | 0.04 | 0.09983 | 0.975 | 3.295 | 1.439 | 0.2394 | 1.058 | 0.74 | 6.85 | 1621 | 16 | 1385 | 14 |
| spot 16 | 30 | 149 | 37 | 0.25 | 0.10452 | 1.068 | 4.261 | 1.651 | 0.2962 | 1.259 | 0.76 | 0.87 | 1706 | 18 | 1672 | 19 |
| spot 17 | 489 | 577 | 640 | 1.11 | 0.10254 | 1.004 | 3.869 | 1.505 | 0.2737 | 1.122 | 0.75 | 3.14 | 1670 | 17 | 1559 | 16 |
| spot 18 | 302 | 306 | 403 | 1.32 | 0.10208 | 1.010 | 3.777 | 1.497 | 0.2689 | 1.105 | 0.74 | 3.49 | 1662 | 17 | 1535 | 16 |
| spot 19 | 440 | 945 | 632 | 0.67 | 0.10407 | 0.987 | 3.789 | 1.447 | 0.2645 | 1.058 | 0.73 | 5.10 | 1698 | 17 | 1513 | 15 |
| spot 20 | 13 | 162 | 21 | 0.13 | 0.09632 | 1.101 | 3.241 | 1.562 | 0.2448 | 1.107 | 0.71 | 3.94 | 1553 | 18 | 1412 | 15 |
| spot 21 | 20 | 226 | 28 | 0.12 | 0.09729 | 1.022 | 3.527 | 1.454 | 0.2624 | 1.035 | 0.71 | 2.06 | 1573 | 16 | 1502 | 15 |
| spot 22 | 45 | 613 | 64 | 0.10 | 0.10256 | 0.982 | 3.749 | 1.421 | 0.2658 | 1.028 | 0.72 | 4.17 | 1671 | 16 | 1519 | 15 |
| spot 23 | 20 | 164 | 26 | 0.16 | 0.10297 | 1.063 | 4.183 | 1.586 | 0.2957 | 1.178 | 0.74 | 0.08 | 1679 | 18 | 1670 | 18 |
| spot 24 | 59 | 659 | 78 | 0.12 | 0.10317 | 0.986 | 3.957 | 1.485 | 0.2782 | 1.111 | 0.75 | 2.72 | 1682 | 17 | 1582 | 16 |
| spot 25 | 7 | 115 | 9 | 0.08 | 0.09870 | 1.136 | 3.642 | 1.695 | 0.2680 | 1.258 | 0.74 | 1.90 | 1600 | 19 | 1530 | 18 |
| spot 26 | 25 | 380 | 41 | 0.11 | 0.10372 | 1.050 | 3.668 | 1.594 | 0.2567 | 1.199 | 0.75 | 6.17 | 1691 | 18 | 1473 | 17 |
| spot 27 | 11 | 181 | 17 | 0.09 | 0.10093 | 1.063 | 3.724 | 1.624 | 0.2674 | 1.229 | 0.76 | 3.28 | 1641 | 18 | 1527 | 18 |
| spot 28 | 7 | 96 | 9 | 0.10 | 0.10173 | 1.142 | 4.027 | 1.723 | 0.2861 | 1.290 | 0.75 | 1.04 | 1655 | 19 | 1622 | 19 |
| spot 29 | 40 | 421 | 55 | 0.13 | 0.10213 | 1.007 | 3.790 | 1.473 | 0.2693 | 1.076 | 0.73 | 3.54 | 1663 | 17 | 1537 | 15 |
| spot 30 | 15 | 271 | 21 | 0.08 | 0.10051 | 1.015 | 3.959 | 1.577 | 0.2845 | 1.208 | 0.77 | 0.76 | 1633 | 17 | 1614 | 18 |
| spot 31 | 41 | 246 | 59 | 0.24 | 0.09652 | 1.046 | 3.401 | 1.547 | 0.2557 | 1.140 | 0.74 | 2.47 | 1558 | 17 | 1468 | 16 |

**12TM15-14 zircon** (spot size: 19 µm, frequency: 4 Hz, 80 shot count, laser energy: 4 mJ at 75%)

| | | | | | ISOTOPIC RATIOS | | | | | | | | APPARENT AGES | | | |
|---|---|---|---|---|---|---|---|---|---|---|---|---|---|---|---|---|
| | Pb (ppm) | U (ppm) | Th (ppm) | Th/U | $^{207}Pb/^{206}Pb$ | 2σ % | $^{207}Pb/^{235}U$ | 2σ % | $^{206}Pb/^{238}U$ | 2σ % | Rho | % disc.* | $^{207}Pb/^{206}Pb$ | 2σ abs | $^{206}Pb/^{238}U$ | 2σ abs |
| spot 32 | 16 | 152 | 25 | 0.17 | 0.09376 | 1.125 | 3.041 | 1.698 | 0.2355 | 1.272 | 0.75 | 3.98 | 1506 | 18 | 1363 | 16 |
| spot 33 | 359 | 748 | 557 | 0.74 | 0.09756 | 0.994 | 3.201 | 1.552 | 0.2383 | 1.192 | 0.77 | 5.81 | 1578 | 16 | 1377 | 15 |
| spot 34 | 19 | 226 | 43 | 0.19 | 0.08847 | 1.097 | 2.160 | 1.805 | 0.1760 | 1.433 | 0.79 | 11.73 | 1392 | 17 | 1045 | 14 |
| spot 35 | 19 | 783 | 26 | 0.03 | 0.10130 | 0.986 | 3.770 | 1.501 | 0.2699 | 1.132 | 0.75 | 2.98 | 1648 | 16 | 1540 | 16 |
| spot 36 | 10 | 143 | 13 | 0.09 | 0.10165 | 1.066 | 3.829 | 1.704 | 0.2742 | 1.330 | 0.78 | 2.41 | 1654 | 18 | 1562 | 19 |
| spot 37 | 36 | 146 | 48 | 0.33 | 0.10236 | 1.125 | 4.020 | 1.652 | 0.2837 | 1.210 | 0.73 | 1.59 | 1667 | 19 | 1612 | 18 |
| spot 38 | 24 | 290 | 34 | 0.12 | 0.10046 | 1.028 | 3.692 | 1.625 | 0.2677 | 1.259 | 0.77 | 2.68 | 1632 | 17 | 1529 | 18 |
| spot 39 | 308 | 1325 | 423 | 0.32 | 0.10021 | 0.977 | 3.431 | 1.425 | 0.2483 | 1.037 | 0.73 | 5.72 | 1628 | 16 | 1430 | 14 |
| spot 40 | 53 | 741 | 88 | 0.12 | 0.09705 | 0.989 | 3.165 | 1.609 | 0.2361 | 1.269 | 0.79 | 5.85 | 1568 | 16 | 1368 | 16 |
| spot 41 | 47 | 435 | 69 | 0.16 | 0.10092 | 0.997 | 3.651 | 1.643 | 0.2630 | 1.306 | 0.80 | 3.67 | 1641 | 17 | 1505 | 18 |
| spot 42 | 35 | 372 | 59 | 0.16 | 0.08867 | 1.018 | 2.593 | 1.523 | 0.2131 | 1.134 | 0.74 | 4.44 | 1397 | 15 | 1245 | 13 |
| spot 43 | 36 | 153 | 49 | 0.32 | 0.10243 | 1.064 | 3.920 | 1.760 | 0.2798 | 1.402 | 0.80 | 1.70 | 1668 | 18 | 1590 | 20 |
| spot 44 | 16 | 264 | 23 | 0.09 | 0.10209 | 1.023 | 3.736 | 1.581 | 0.2650 | 1.205 | 0.76 | 4.26 | 1662 | 17 | 1515 | 17 |
| spot 45 | 51 | 820 | 106 | 0.13 | 0.08795 | 1.001 | 2.205 | 1.444 | 0.1818 | 1.041 | 0.72 | 9.80 | 1381 | 14 | 1077 | 11 |
| spot 46 | 28 | 242 | 46 | 0.19 | 0.08877 | 1.047 | 2.764 | 1.641 | 0.2280 | 1.264 | 0.77 | 1.62 | 1399 | 16 | 1324 | 16 |
| spot 47 | 12 | 89 | 16 | 0.18 | 0.10015 | 1.255 | 3.590 | 1.841 | 0.2608 | 1.347 | 0.73 | 3.48 | 1626 | 22 | 1494 | 18 |
| spot 48 | 29 | 173 | 43 | 0.25 | 0.09886 | 1.071 | 3.866 | 1.592 | 0.2850 | 1.178 | 0.74 | 0.62 | 1602 | 18 | 1616 | 18 |
| spot 49 | 35 | 285 | 48 | 0.17 | 0.10189 | 1.016 | 3.697 | 1.534 | 0.2634 | 1.149 | 0.75 | 4.27 | 1659 | 17 | 1507 | 16 |
| spot 50 | 57 | 278 | 75 | 0.27 | 0.10072 | 1.051 | 3.828 | 1.714 | 0.2760 | 1.354 | 0.79 | 1.59 | 1637 | 18 | 1573 | 19 |
| spot 51 | 80 | 128 | 115 | 0.90 | 0.09237 | 1.113 | 3.177 | 2.011 | 0.2498 | 1.675 | 0.83 | 0.69 | 1475 | 18 | 1440 | 22 |
| spot 52 | 29 | 481 | 51 | 0.11 | 0.09024 | 1.023 | 2.676 | 1.665 | 0.2159 | 1.314 | 0.79 | 4.95 | 1430 | 15 | 1260 | 16 |
| spot 53 | 23 | 175 | 34 | 0.19 | 0.09564 | 1.083 | 3.291 | 1.658 | 0.2495 | 1.255 | 0.76 | 3.03 | 1542 | 18 | 1436 | 16 |
| spot 54 | 50 | 679 | 92 | 0.14 | 0.08913 | 1.000 | 2.349 | 1.575 | 0.1909 | 1.217 | 0.77 | 8.97 | 1407 | 15 | 1126 | 13 |
| spot 55 | 12 | 309 | 23 | 0.07 | 0.08780 | 1.044 | 2.479 | 1.686 | 0.2048 | 1.323 | 0.79 | 5.35 | 1378 | 15 | 1201 | 15 |

**13TM-05 zircon** (spot size: 24 µm, frequency: 4 Hz, 100 shot count, laser energy: 4 mJ at 75%)

| | | | | | ISOTOPIC RATIOS | | | | | | | | APPARENT AGES | | | |
|---|---|---|---|---|---|---|---|---|---|---|---|---|---|---|---|---|
| | Pb (ppm) | U (ppm) | Th (ppm) | Th/U | $^{207}Pb/^{206}Pb$ | 2σ % | $^{207}Pb/^{235}U$ | 2σ % | $^{206}Pb/^{238}U$ | 2σ % | Rho | % disc.* | $^{207}Pb/^{206}Pb$ | 2σ abs | $^{206}Pb/^{238}U$ | 2σ abs |
| spot 1 | 17 | 1142 | 174 | 0.15 | 0.05222 | 1.905 | 0.270 | 2.268 | 0.0374 | 1.230 | 0.54 | 2.32 | 302 | 24 | 237 | 3 |
| spot 2 | 21 | 1120 | 197 | 0.18 | 0.05240 | 1.807 | 0.269 | 2.062 | 0.0373 | 0.993 | 0.48 | 2.46 | 305 | 20 | 236 | 2 |
| spot 3 | 37 | 1876 | 361 | 0.19 | 0.06366 | 1.762 | 0.427 | 2.291 | 0.0485 | 1.465 | 0.64 | 18.19 | 730 | 20 | 305 | 4 |
| spot 4 | 10 | 503 | 13 | 0.02 | 0.09157 | 1.653 | 3.038 | 1.868 | 0.2415 | 0.870 | 0.47 | 1.69 | 1458 | 25 | 1394 | 11 |
| spot 5 | 263 | 488 | 339 | 0.69 | 0.10867 | 1.630 | 4.613 | 1.988 | 0.3078 | 1.137 | 0.57 | 1.24 | 1777 | 29 | 1729 | 17 |
| spot 6 | 32 | 1439 | 289 | 0.20 | 0.06674 | 1.748 | 0.505 | 2.050 | 0.0551 | 1.071 | 0.52 | 20.08 | 828 | 20 | 346 | 4 |
| spot 7 | 23 | 681 | 24 | 0.04 | 0.09973 | 1.630 | 3.651 | 1.900 | 0.2663 | 0.976 | 0.51 | 2.56 | 1619 | 27 | 1522 | 13 |
| spot 8 | 81 | 458 | 112 | 0.24 | 0.10339 | 1.640 | 4.138 | 2.186 | 0.2904 | 1.446 | 0.66 | 1.03 | 1686 | 28 | 1643 | 21 |
| spot 9 | 35 | 2100 | 367 | 0.17 | 0.05090 | 1.734 | 0.244 | 1.991 | 0.0347 | 0.979 | 0.49 | 0.95 | 235 | 15 | 220 | 2 |
| spot 10 | 121 | 4629 | 1229 | 0.27 | 0.05192 | 1.671 | 0.253 | 2.004 | 0.0352 | 1.107 | 0.55 | 2.60 | 281 | 12 | 223 | 2 |
| spot 11 | 194 | 380 | 251 | 0.66 | 0.10780 | 1.636 | 4.709 | 1.941 | 0.3164 | 1.043 | 0.54 | 0.24 | 1762 | 29 | 1772 | 16 |
| spot 12 | 42 | 2891 | 400 | 0.14 | 0.05184 | 1.760 | 0.254 | 2.030 | 0.0356 | 1.013 | 0.50 | 1.95 | 278 | 18 | 225 | 2 |
| spot 13 | 240 | 484 | 318 | 0.66 | 0.10585 | 1.636 | 4.398 | 1.915 | 0.3013 | 0.996 | 0.52 | 0.77 | 1729 | 28 | 1698 | 15 |
| spot 14 | 51 | 58 | 71 | 1.22 | 0.10240 | 1.983 | 4.170 | 2.591 | 0.2940 | 1.667 | 0.64 | 0.48 | 1667 | 34 | 1660 | 24 |
| spot 15 | 68 | 72 | 96 | 1.32 | 0.10320 | 1.871 | 4.216 | 2.249 | 0.2965 | 1.248 | 0.55 | 0.24 | 1685 | 33 | 1673 | 18 |
| spot 16 | 44 | 2050 | 435 | 0.21 | 0.05239 | 1.741 | 0.264 | 2.055 | 0.0366 | 1.092 | 0.53 | 2.41 | 304 | 17 | 232 | 3 |
| spot 17 | 39 | 1875 | 431 | 0.23 | 0.05066 | 1.735 | 0.242 | 2.021 | 0.0347 | 1.037 | 0.51 | 0.09 | 225 | 16 | 220 | 2 |
| spot 18 | 695 | 1873 | 985 | 0.53 | 0.10758 | 1.609 | 4.063 | 1.867 | 0.2742 | 0.948 | 0.51 | 5.45 | 1759 | 28 | 1562 | 13 |
| spot 19 | 42 | 1640 | 433 | 0.26 | 0.05051 | 1.728 | 0.248 | 2.125 | 0.0356 | 1.236 | 0.58 | 0.13 | 219 | 16 | 225 | 3 |
| spot 20 | 39 | 97 | 59 | 0.61 | 0.09091 | 1.790 | 3.046 | 2.196 | 0.2437 | 1.272 | 0.58 | 0.85 | 1443 | 28 | 1406 | 16 |
| spot 21 | 9 | 512 | 89 | 0.17 | 0.05069 | 2.038 | 0.260 | 2.283 | 0.0370 | 1.028 | 0.45 | 0.17 | 228 | 30 | 234 | 2 |
| spot 22 | 20 | 598 | 206 | 0.34 | 0.05016 | 1.928 | 0.245 | 2.310 | 0.0354 | 1.271 | 0.55 | 0.67 | 202 | 25 | 224 | 3 |
| spot 23 | 56 | 2156 | 531 | 0.25 | 0.05066 | 1.759 | 0.252 | 2.173 | 0.0361 | 1.276 | 0.59 | 0.13 | 225 | 17 | 228 | 3 |
| spot 24 | 18 | 1512 | 164 | 0.11 | 0.05045 | 1.752 | 0.251 | 2.167 | 0.0361 | 1.276 | 0.59 | 0.18 | 215 | 17 | 228 | 3 |
| spot 25 | 28 | 1641 | 260 | 0.16 | 0.05110 | 1.756 | 0.262 | 2.379 | 0.0374 | 1.605 | 0.67 | 0.08 | 245 | 16 | 237 | 4 |
| spot 26 | 66 | 73 | 89 | 1.23 | 0.10211 | 1.846 | 4.029 | 2.564 | 0.2865 | 1.780 | 0.69 | 0.99 | 1671 | 32 | 1623 | 26 |
| spot 27 | 6 | 542 | 10 | 0.02 | 0.10169 | 1.650 | 3.851 | 2.063 | 0.2744 | 1.239 | 0.60 | 2.56 | 1655 | 28 | 1563 | 17 |
| spot 28 | 70 | 557 | 94 | 0.17 | 0.10300 | 1.636 | 3.953 | 1.882 | 0.2795 | 0.930 | 0.49 | 2.25 | 1679 | 28 | 1588 | 13 |
| spot 29 | 24 | 1056 | 224 | 0.21 | 0.05742 | 1.847 | 0.326 | 2.281 | 0.0411 | 1.338 | 0.59 | 10.24 | 507 | 23 | 260 | 3 |
| spot 30 | 44 | 400 | 65 | 0.16 | 0.09318 | 1.662 | 3.116 | 2.044 | 0.2437 | 1.190 | 0.58 | 2.28 | 1491 | 25 | 1405 | 15 |
| spot 31 | 56 | 2373 | 548 | 0.23 | 0.05161 | 1.709 | 0.256 | 2.054 | 0.0360 | 1.140 | 0.55 | 1.58 | 267 | 15 | 228 | 3 |

**13TM-05 zircon** (spot size: 24 µm, frequency: 4 Hz, 100 shot count, laser energy: 4 mJ at 75%)

| | | | | | ISOTOPIC RATIOS | | | | | | | | APPARENT AGES | | | |
|---|---|---|---|---|---|---|---|---|---|---|---|---|---|---|---|---|
| | Pb (ppm) | U (ppm) | Th (ppm) | Th/U | $^{207}Pb/^{206}Pb$ | 2σ % | $^{207}Pb/^{235}U$ | 2σ % | $^{206}Pb/^{238}U$ | 2σ % | Rho | % disc.* | $^{207}Pb/^{206}Pb$ | 2σ abs | $^{206}Pb/^{238}U$ | 2σ abs |
| spot 32 | 30 | 824 | 304 | 0.37 | 0.05107 | 1.897 | 0.248 | 2.155 | 0.0352 | 1.023 | 0.47 | 0.81 | 242 | 24 | 223 | 2 |
| spot 33 | 39 | 222 | 70 | 0.32 | 0.09202 | 1.811 | 2.431 | 2.259 | 0.1926 | 1.350 | 0.60 | 10.31 | 1469 | 28 | 1135 | 14 |
| spot 34 | 84 | 2877 | 832 | 0.29 | 0.05092 | 1.726 | 0.252 | 2.024 | 0.0360 | 1.057 | 0.52 | 0.18 | 237 | 15 | 228 | 2 |
| spot 35 | 13 | 179 | 22 | 0.12 | 0.08921 | 1.736 | 2.857 | 2.264 | 0.2339 | 1.454 | 0.64 | 1.33 | 1407 | 26 | 1354 | 18 |
| spot 36 | 216 | 4347 | 2072 | 0.48 | 0.05110 | 1.673 | 0.253 | 2.038 | 0.0361 | 1.163 | 0.57 | 0.26 | 245 | 12 | 229 | 3 |
| spot 37 | 128 | 880 | 181 | 0.21 | 0.10139 | 1.625 | 3.891 | 2.056 | 0.2778 | 1.260 | 0.61 | 2.03 | 1649 | 27 | 1580 | 17 |
| spot 38 | 158 | 1204 | 209 | 0.17 | 0.10508 | 1.622 | 4.161 | 2.072 | 0.2869 | 1.290 | 0.62 | 2.46 | 1716 | 28 | 1626 | 18 |
| spot 39 | 175 | 1084 | 234 | 0.22 | 0.09707 | 1.616 | 3.399 | 1.934 | 0.2543 | 1.062 | 0.55 | 3.03 | 1568 | 25 | 1460 | 14 |
| spot 40 | 44 | 994 | 62 | 0.06 | 0.10200 | 1.625 | 3.748 | 1.977 | 0.2666 | 1.125 | 0.57 | 3.78 | 1661 | 27 | 1523 | 15 |
| spot 41 | 47 | 799 | 64 | 0.08 | 0.10111 | 1.627 | 3.751 | 1.949 | 0.2704 | 1.072 | 0.55 | 2.63 | 1645 | 27 | 1542 | 15 |
| spot 42 | 409 | 743 | 513 | 0.69 | 0.10847 | 1.621 | 4.461 | 1.978 | 0.2999 | 1.134 | 0.57 | 2.01 | 1774 | 29 | 1690 | 17 |
| spot 43 | 137 | 372 | 197 | 0.53 | 0.09752 | 1.687 | 3.646 | 2.057 | 0.2716 | 1.178 | 0.57 | 0.65 | 1576 | 27 | 1549 | 16 |
| spot 44 | 61 | 2388 | 591 | 0.25 | 0.05059 | 1.687 | 0.248 | 1.927 | 0.0354 | 0.931 | 0.48 | 0.09 | 222 | 13 | 224 | 2 |
| spot 45 | 84 | 2887 | 798 | 0.28 | 0.05154 | 1.661 | 0.255 | 1.997 | 0.0361 | 1.108 | 0.55 | 0.87 | 264 | 11 | 229 | 3 |
| spot 46 | 46 | 2146 | 410 | 0.19 | 0.05259 | 1.705 | 0.264 | 2.045 | 0.0363 | 1.129 | 0.55 | 3.57 | 310 | 15 | 230 | 3 |
| spot 47 | 48 | 395 | 64 | 0.16 | 0.09966 | 1.689 | 3.799 | 2.152 | 0.2776 | 1.333 | 0.62 | 0.76 | 1618 | 28 | 1579 | 19 |
| spot 48 | 48 | 2366 | 487 | 0.21 | 0.05077 | 1.699 | 0.245 | 2.099 | 0.0349 | 1.232 | 0.59 | 0.41 | 229 | 14 | 221 | 3 |
| spot 49 | 385 | 819 | 502 | 0.61 | 0.10492 | 1.622 | 4.087 | 1.920 | 0.2825 | 1.027 | 0.53 | 2.91 | 1713 | 28 | 1604 | 14 |
| spot 50 | 96 | 742 | 130 | 0.17 | 0.09724 | 1.640 | 3.345 | 2.154 | 0.2505 | 1.397 | 0.65 | 3.54 | 1572 | 26 | 1441 | 18 |
| spot 51 | 44 | 2015 | 418 | 0.21 | 0.05107 | 1.733 | 0.247 | 2.025 | 0.0353 | 1.047 | 0.52 | 0.09 | 242 | 15 | 224 | 2 |
| spot 52 | 386 | 1017 | 483 | 0.47 | 0.10749 | 1.618 | 4.336 | 1.862 | 0.2931 | 0.921 | 0.49 | 2.56 | 1758 | 28 | 1657 | 13 |
| spot 53 | 57 | 2243 | 534 | 0.24 | 0.05105 | 1.711 | 0.249 | 1.988 | 0.0356 | 1.012 | 0.51 | 0.13 | 242 | 15 | 226 | 2 |
| spot 54 | 36 | 1833 | 347 | 0.19 | 0.05078 | 1.742 | 0.244 | 2.067 | 0.0351 | 1.112 | 0.54 | 0.09 | 229 | 16 | 222 | 2 |
| spot 55 | 28 | 178 | 34 | 0.19 | 0.10417 | 1.751 | 3.304 | 2.229 | 0.2318 | 1.381 | 0.62 | 10.03 | 1698 | 30 | 1346 | 16 |
| spot 56 | 503 | 800 | 637 | 0.80 | 0.10407 | 1.619 | 4.060 | 1.973 | 0.2837 | 1.128 | 0.57 | 2.19 | 1698 | 28 | 1610 | 16 |
| spot 57 | 2 | 325 | 17 | 0.05 | 0.05176 | 2.349 | 0.250 | 2.612 | 0.0350 | 1.143 | 0.44 | 2.17 | 278 | 40 | 222 | 3 |
| spot 58 | 163 | 476 | 224 | 0.47 | 0.10202 | 1.641 | 3.753 | 1.987 | 0.2675 | 1.121 | 0.56 | 3.68 | 1662 | 27 | 1527 | 15 |
| spot 59 | 78 | 282 | 104 | 0.37 | 0.10260 | 1.662 | 3.964 | 1.995 | 0.2810 | 1.103 | 0.55 | 1.88 | 1671 | 28 | 1596 | 16 |
| spot 60 | 42 | 1738 | 399 | 0.23 | 0.05125 | 1.740 | 0.251 | 2.069 | 0.0357 | 1.120 | 0.54 | 0.44 | 250 | 16 | 226 | 3 |
| spot 61 | 22 | 210 | 31 | 0.15 | 0.09348 | 1.708 | 3.345 | 2.128 | 0.2600 | 1.269 | 0.60 | 0.20 | 1498 | 26 | 1489 | 17 |
| spot 62 | 48 | 2553 | 461 | 0.18 | 0.05162 | 1.723 | 0.254 | 1.928 | 0.0358 | 0.866 | 0.45 | 1.59 | 269 | 16 | 227 | 2 |

**13TM-05 zircon** (spot size: 24 µm, frequency: 4 Hz, 100 shot count, laser energy: 4 mJ at 75%)

| | | | | | ISOTOPIC RATIOS | | | | | | | | APPARENT AGES | | | |
|---|---|---|---|---|---|---|---|---|---|---|---|---|---|---|---|---|
| | Pb (ppm) | U (ppm) | Th (ppm) | Th/U | $^{207}Pb/^{206}Pb$ | 2σ % | $^{207}Pb/^{235}U$ | 2σ % | $^{206}Pb/^{238}U$ | 2σ % | Rho | % disc.* | $^{207}Pb/^{206}Pb$ | 2σ abs | $^{206}Pb/^{238}U$ | 2σ abs |
| spot 63 | 35 | 1127 | 417 | 0.37 | 0.05125 | 1.905 | 0.267 | 2.220 | 0.0377 | 1.140 | 0.51 | 0.50 | 249 | 24 | 239 | 3 |
| spot 64 | 42 | 2123 | 414 | 0.20 | 0.05194 | 1.744 | 0.251 | 1.997 | 0.0350 | 0.973 | 0.49 | 2.48 | 283 | 16 | 221 | 2 |
| spot 65 | 37 | 2035 | 372 | 0.18 | 0.05168 | 1.753 | 0.247 | 2.065 | 0.0348 | 1.091 | 0.53 | 1.27 | 271 | 18 | 221 | 2 |
| spot 66 | 21 | 1271 | 203 | 0.16 | 0.05156 | 1.778 | 0.253 | 2.071 | 0.0358 | 1.062 | 0.51 | 1.02 | 263 | 18 | 227 | 2 |
| spot 67 | 16 | 936 | 162 | 0.17 | 0.05095 | 1.964 | 0.250 | 2.375 | 0.0359 | 1.336 | 0.56 | 0.44 | 239 | 26 | 228 | 3 |
| spot 68 | 22 | 1298 | 202 | 0.16 | 0.05174 | 1.761 | 0.255 | 2.135 | 0.0356 | 1.208 | 0.57 | 2.22 | 278 | 18 | 226 | 3 |
| spot 69 | 24 | 1641 | 230 | 0.14 | 0.05143 | 1.796 | 0.262 | 2.018 | 0.0370 | 0.920 | 0.46 | 0.94 | 260 | 19 | 234 | 2 |
| spot 70 | 34 | 345 | 46 | 0.13 | 0.09731 | 1.697 | 3.475 | 2.099 | 0.2589 | 1.236 | 0.59 | 2.43 | 1574 | 27 | 1484 | 17 |
| spot 71 | 41 | 1804 | 404 | 0.22 | 0.05171 | 1.730 | 0.247 | 2.032 | 0.0347 | 1.065 | 0.52 | 1.73 | 273 | 16 | 220 | 2 |

**13TM-01 zircon** (spot size: 24 µm, frequency: 4 Hz, 100 shot count, laser energy: 4 mJ at 75%)

| | | | | | ISOTOPIC RATIOS | | | | | | | | APPARENT AGES | | | |
|---|---|---|---|---|---|---|---|---|---|---|---|---|---|---|---|---|
| | Pb (ppm) | U (ppm) | Th (ppm) | Th/U | $^{207}Pb/^{206}Pb$ | 2σ % | $^{207}Pb/^{235}U$ | 2σ % | $^{206}Pb/^{238}U$ | 2σ % | Rho | % disc.* | $^{207}Pb/^{206}Pb$ | 2σ abs | $^{206}Pb/^{238}U$ | 2σ abs |
| spot 1 | 127 | 5700 | 1563 | 0.27 | 0.05081 | 1.222 | 0.187 | 1.518 | 0.0266 | 0.901 | 0.59 | 2.71 | 231 | 12 | 170 | 2 |
| spot 2 | 110 | 4929 | 1287 | 0.26 | 0.04998 | 1.234 | 0.182 | 1.411 | 0.0264 | 0.683 | 0.48 | 1.31 | 194 | 13 | 168 | 1 |
| spot 3 | 146 | 6950 | 1676 | 0.24 | 0.05090 | 1.297 | 0.184 | 1.547 | 0.0261 | 0.842 | 0.54 | 2.89 | 234 | 16 | 166 | 1 |
| spot 4 | 210 | 10180 | 2451 | 0.24 | 0.05033 | 1.163 | 0.181 | 1.460 | 0.0261 | 0.883 | 0.60 | 1.93 | 210 | 9 | 166 | 2 |
| spot 5 | 153 | 7810 | 1672 | 0.21 | 0.05132 | 1.167 | 0.186 | 1.393 | 0.0263 | 0.761 | 0.55 | 3.89 | 254 | 10 | 167 | 1 |
| spot 6 | 263 | 12110 | 3188 | 0.26 | 0.05017 | 1.140 | 0.180 | 1.398 | 0.0259 | 0.810 | 0.58 | 1.64 | 203 | 7 | 165 | 1 |
| spot 7 | 56 | 2895 | 718 | 0.25 | 0.04992 | 1.273 | 0.188 | 1.570 | 0.0272 | 0.919 | 0.59 | 0.87 | 191 | 15 | 173 | 2 |
| spot 8 | 273 | 9450 | 3333 | 0.35 | 0.05040 | 1.163 | 0.182 | 1.436 | 0.0261 | 0.842 | 0.59 | 2.17 | 213 | 9 | 166 | 1 |
| spot 9 | 157 | 7270 | 1938 | 0.27 | 0.05007 | 1.170 | 0.181 | 1.443 | 0.0261 | 0.845 | 0.59 | 1.75 | 198 | 10 | 166 | 1 |
| spot 10 | 197 | 8250 | 2499 | 0.30 | 0.05002 | 1.164 | 0.180 | 1.485 | 0.0260 | 0.923 | 0.62 | 1.39 | 195 | 9 | 166 | 2 |
| spot 11 | 184 | 9744 | 2321 | 0.24 | 0.05007 | 1.145 | 0.181 | 1.516 | 0.0262 | 0.992 | 0.65 | 1.50 | 198 | 8 | 167 | 2 |
| spot 12 | 258 | 9420 | 3273 | 0.35 | 0.05033 | 1.145 | 0.181 | 1.539 | 0.0262 | 1.029 | 0.67 | 1.20 | 210 | 8 | 167 | 2 |
| spot 13 | 27 | 1824 | 337 | 0.18 | 0.04958 | 1.465 | 0.180 | 1.686 | 0.0264 | 0.834 | 0.49 | 0.06 | 174 | 23 | 168 | 1 |
| spot 14 | 39 | 2940 | 488 | 0.17 | 0.04970 | 1.255 | 0.182 | 1.485 | 0.0264 | 0.794 | 0.53 | 1.01 | 181 | 14 | 168 | 1 |
| spot 15 | 13 | 1013 | 173 | 0.17 | 0.04983 | 1.691 | 0.176 | 1.879 | 0.0257 | 0.819 | 0.44 | 0.98 | 180 | 29 | 163 | 1 |
| spot 16 | 124 | 6540 | 1613 | 0.25 | 0.05006 | 1.170 | 0.181 | 1.534 | 0.0262 | 0.992 | 0.65 | 1.32 | 198 | 10 | 167 | 2 |
| spot 17 | 108 | 5510 | 1407 | 0.26 | 0.04994 | 1.200 | 0.180 | 1.512 | 0.0261 | 0.920 | 0.61 | 1.08 | 193 | 11 | 166 | 2 |
| spot 18 | 53 | 4662 | 689 | 0.15 | 0.04979 | 1.226 | 0.182 | 1.572 | 0.0264 | 0.983 | 0.63 | 0.77 | 187 | 12 | 168 | 2 |
| spot 19 | 104 | 5340 | 1380 | 0.26 | 0.04998 | 1.178 | 0.180 | 1.448 | 0.0261 | 0.843 | 0.58 | 1.08 | 193 | 10 | 166 | 1 |
| spot 20 | 94 | 5180 | 1243 | 0.24 | 0.04992 | 1.200 | 0.180 | 1.466 | 0.0261 | 0.842 | 0.57 | 1.08 | 193 | 11 | 166 | 1 |
| spot 21 | 124 | 6109 | 1660 | 0.27 | 0.04976 | 1.171 | 0.179 | 1.589 | 0.0261 | 1.074 | 0.68 | 0.84 | 183 | 10 | 166 | 2 |
| spot 22 | 89 | 4276 | 1106 | 0.26 | 0.05070 | 1.222 | 0.190 | 1.597 | 0.0272 | 1.028 | 0.64 | 2.08 | 228 | 12 | 173 | 2 |
| spot 23 | 51 | 2185 | 686 | 0.31 | 0.05004 | 1.408 | 0.179 | 1.643 | 0.0260 | 0.846 | 0.52 | 1.21 | 196 | 21 | 165 | 1 |
| spot 24 | 297 | 12750 | 4024 | 0.32 | 0.05035 | 1.151 | 0.180 | 1.430 | 0.0259 | 0.850 | 0.59 | 2.00 | 211 | 8 | 165 | 1 |
| spot 25 | 277 | 11310 | 3650 | 0.32 | 0.05028 | 1.151 | 0.180 | 1.430 | 0.0259 | 0.848 | 0.59 | 1.94 | 208 | 8 | 165 | 1 |
| spot 26 | 58 | 13400 | 754 | 0.06 | 0.05038 | 1.145 | 0.180 | 1.629 | 0.0259 | 1.159 | 0.71 | 2.06 | 212 | 8 | 165 | 2 |
| spot 27 | 164 | 8270 | 2177 | 0.26 | 0.04998 | 1.171 | 0.180 | 1.564 | 0.0260 | 1.037 | 0.66 | 1.15 | 194 | 9 | 166 | 2 |
| spot 28 | 187 | 8460 | 2451 | 0.29 | 0.04996 | 1.178 | 0.180 | 1.593 | 0.0261 | 1.073 | 0.67 | 1.08 | 194 | 10 | 166 | 2 |
| spot 29 | 155 | 7190 | 2012 | 0.28 | 0.05000 | 1.151 | 0.180 | 1.577 | 0.0260 | 1.077 | 0.68 | 1.45 | 195 | 8 | 166 | 2 |
| spot 30 | 99 | 11000 | 1307 | 0.12 | 0.05034 | 1.145 | 0.180 | 1.547 | 0.0259 | 1.041 | 0.67 | 1.76 | 210 | 8 | 165 | 2 |
| spot 31 | 223 | 16740 | 2802 | 0.17 | 0.05060 | 1.139 | 0.182 | 1.486 | 0.0262 | 0.954 | 0.64 | 2.16 | 222 | 7 | 167 | 2 |

**13TM-01 zircon** (spot size: 24 µm, frequency: 4 Hz, 100 shot count, laser energy: 4 mJ at 75%)

| | | | | | ISOTOPIC RATIOS | | | | | | | | APPARENT AGES | | | |
|---|---|---|---|---|---|---|---|---|---|---|---|---|---|---|---|---|
| | Pb (ppm) | U (ppm) | Th (ppm) | Th/U | $^{207}Pb/^{206}Pb$ | 2σ % | $^{207}Pb/^{235}U$ | 2σ % | $^{206}Pb/^{238}U$ | 2σ % | Rho | % disc.* | $^{207}Pb/^{206}Pb$ | 2σ abs | $^{206}Pb/^{238}U$ | 2σ abs |
| spot 32 | 96 | 5500 | 1234 | 0.22 | 0.04991 | 1.217 | 0.179 | 1.529 | 0.0260 | 0.925 | 0.61 | 1.09 | 191 | 12 | 165 | 2 |
| spot 33 | 89 | 6320 | 1131 | 0.18 | 0.04985 | 1.209 | 0.178 | 1.546 | 0.0260 | 0.963 | 0.62 | 0.54 | 187 | 12 | 165 | 2 |
| spot 34 | 24 | 1334 | 314 | 0.24 | 0.04980 | 1.463 | 0.177 | 1.776 | 0.0258 | 1.007 | 0.57 | 0.85 | 183 | 22 | 164 | 2 |
| spot 35 | 34 | 1519 | 406 | 0.27 | 0.04942 | 1.441 | 0.177 | 1.672 | 0.0259 | 0.849 | 0.51 | 0.36 | 165 | 22 | 165 | 1 |
| spot 36 | 18 | 1094 | 231 | 0.21 | 0.04997 | 1.556 | 0.174 | 2.024 | 0.0255 | 1.294 | 0.64 | 0.12 | 190 | 25 | 162 | 2 |
| spot 37 | 94 | 4910 | 1208 | 0.25 | 0.05000 | 1.192 | 0.178 | 1.608 | 0.0259 | 1.079 | 0.67 | 0.73 | 195 | 11 | 165 | 2 |
| spot 38 | 51 | 4291 | 681 | 0.16 | 0.05009 | 1.234 | 0.178 | 1.697 | 0.0258 | 1.165 | 0.69 | 1.16 | 198 | 13 | 164 | 2 |
| spot 39 | 20 | 1164 | 276 | 0.24 | 0.05028 | 1.551 | 0.179 | 1.873 | 0.0257 | 1.049 | 0.56 | 2.01 | 207 | 25 | 164 | 2 |
| spot 40 | 178 | 7310 | 2316 | 0.32 | 0.04976 | 1.164 | 0.178 | 1.462 | 0.0260 | 0.885 | 0.60 | 0.36 | 183 | 9 | 165 | 2 |
| spot 41 | 181 | 7550 | 2283 | 0.30 | 0.05005 | 1.164 | 0.181 | 1.528 | 0.0262 | 0.991 | 0.65 | 0.84 | 197 | 9 | 167 | 2 |
| spot 42 | 165 | 7080 | 2074 | 0.29 | 0.05001 | 1.177 | 0.179 | 1.451 | 0.0259 | 0.848 | 0.58 | 1.39 | 196 | 10 | 165 | 1 |
| spot 43 | 28 | 1494 | 357 | 0.24 | 0.04947 | 1.480 | 0.176 | 1.836 | 0.0258 | 1.087 | 0.59 | 0.30 | 167 | 23 | 164 | 2 |
| spot 44 | 180 | 9160 | 2263 | 0.25 | 0.05012 | 1.163 | 0.179 | 1.536 | 0.0259 | 1.003 | 0.65 | 1.09 | 201 | 9 | 165 | 2 |
| spot 45 | 21 | 1444 | 282 | 0.20 | 0.05014 | 1.471 | 0.176 | 1.933 | 0.0255 | 1.254 | 0.65 | 1.23 | 201 | 23 | 163 | 2 |
| spot 46 | 34 | 1707 | 438 | 0.26 | 0.04964 | 1.478 | 0.175 | 1.915 | 0.0255 | 1.217 | 0.64 | 0.93 | 175 | 23 | 162 | 2 |
| spot 47 | 20 | 1085 | 248 | 0.23 | 0.04936 | 1.731 | 0.176 | 2.067 | 0.0257 | 1.129 | 0.55 | 0.73 | 163 | 30 | 164 | 2 |
| spot 48 | 13 | 881 | 153 | 0.17 | 0.05029 | 1.759 | 0.184 | 2.149 | 0.0267 | 1.236 | 0.58 | 0.88 | 199 | 32 | 170 | 2 |
| spot 49 | 25 | 1508 | 312 | 0.21 | 0.04939 | 1.428 | 0.173 | 1.729 | 0.0257 | 0.975 | 0.56 | 0.80 | 166 | 21 | 163 | 2 |
| spot 50 | 128 | 14050 | 1612 | 0.11 | 0.05048 | 1.130 | 0.179 | 1.464 | 0.0258 | 0.931 | 0.64 | 1.95 | 218 | 7 | 164 | 2 |
| spot 51 | 102 | 4358 | 1270 | 0.29 | 0.05005 | 1.208 | 0.178 | 1.647 | 0.0259 | 1.120 | 0.68 | 1.03 | 196 | 12 | 165 | 2 |
| spot 52 | 15 | 473 | 183 | 0.39 | 0.05007 | 2.006 | 0.184 | 2.283 | 0.0266 | 1.091 | 0.48 | 1.24 | 202 | 39 | 169 | 2 |
| spot 53 | 168 | 506 | 218 | 0.43 | 0.10223 | 1.158 | 3.664 | 1.504 | 0.2606 | 0.959 | 0.64 | 4.66 | 1666 | 19 | 1493 | 13 |
| spot 54 | 48 | 2118 | 628 | 0.30 | 0.04938 | 1.378 | 0.173 | 1.784 | 0.0256 | 1.132 | 0.63 | 0.37 | 166 | 20 | 163 | 2 |
| spot 55 | 41 | 1996 | 548 | 0.27 | 0.04964 | 1.364 | 0.175 | 1.679 | 0.0255 | 0.980 | 0.58 | 0.80 | 178 | 19 | 162 | 2 |
| spot 56 | 16 | 1020 | 214 | 0.21 | 0.04957 | 1.666 | 0.176 | 2.033 | 0.0257 | 1.166 | 0.57 | 0.49 | 174 | 29 | 164 | 2 |
| spot 57 | 51 | 2305 | 679 | 0.29 | 0.04997 | 1.273 | 0.175 | 1.538 | 0.0255 | 0.863 | 0.56 | 0.86 | 192 | 15 | 162 | 1 |
| spot 58 | 51 | 2041 | 702 | 0.34 | 0.04953 | 1.389 | 0.174 | 1.698 | 0.0256 | 0.977 | 0.58 | 0.25 | 170 | 19 | 163 | 2 |
| spot 59 | 19 | 586 | 255 | 0.44 | 0.04941 | 1.810 | 0.181 | 2.339 | 0.0263 | 1.481 | 0.63 | 0.90 | 165 | 32 | 168 | 3 |
| spot 60 | 200 | 334 | 303 | 0.91 | 0.10421 | 1.193 | 3.669 | 1.591 | 0.2564 | 1.053 | 0.66 | 6.23 | 1701 | 21 | 1473 | 14 |
| spot 61 | 365 | 485 | 528 | 1.09 | 0.10380 | 1.156 | 3.920 | 1.618 | 0.2738 | 1.132 | 0.70 | 3.65 | 1694 | 20 | 1560 | 16 |
| spot 62 | 27 | 1459 | 385 | 0.26 | 0.05253 | 1.480 | 0.192 | 1.928 | 0.0267 | 1.235 | 0.64 | 4.94 | 311 | 22 | 170 | 2 |

**13TM-01 zircon** (spot size: 24 µm, frequency: 4 Hz, 100 shot count, laser energy: 4 mJ at 75%)

| | | | | | ISOTOPIC RATIOS | | | | | | | | APPARENT AGES | | | |
|---|---|---|---|---|---|---|---|---|---|---|---|---|---|---|---|---|
| | Pb (ppm) | U (ppm) | Th (ppm) | Th/U | $^{207}Pb/^{206}Pb$ | 2σ % | $^{207}Pb/^{235}U$ | 2σ % | $^{206}Pb/^{238}U$ | 2σ % | Rho | % disc.* | $^{207}Pb/^{206}Pb$ | 2σ abs | $^{206}Pb/^{238}U$ | 2σ abs |
| spot 63 | 52 | 3712 | 723 | 0.19 | 0.05035 | 1.261 | 0.181 | 1.580 | 0.0262 | 0.953 | 0.60 | 0.96 | 211 | 15 | 167 | 2 |
| spot 64 | 219 | 9950 | 2952 | 0.30 | 0.05011 | 1.164 | 0.179 | 1.484 | 0.0261 | 0.921 | 0.62 | 1.02 | 200 | 9 | 166 | 2 |
| spot 65 | 302 | 11590 | 4170 | 0.36 | 0.05032 | 1.151 | 0.179 | 1.553 | 0.0259 | 1.043 | 0.67 | 1.46 | 209 | 8 | 165 | 2 |
| spot 66 | 39 | 1814 | 519 | 0.29 | 0.04991 | 1.422 | 0.176 | 1.662 | 0.0256 | 0.860 | 0.52 | 0.80 | 188 | 21 | 163 | 1 |
| spot 67 | 296 | 10260 | 3981 | 0.39 | 0.05019 | 1.170 | 0.179 | 1.516 | 0.0259 | 0.965 | 0.64 | 1.21 | 203 | 9 | 165 | 2 |
| spot 68 | 101 | 4940 | 1284 | 0.26 | 0.05014 | 1.225 | 0.179 | 1.682 | 0.0260 | 1.153 | 0.69 | 1.15 | 200 | 12 | 166 | 2 |
| spot 69 | 148 | 7110 | 1873 | 0.26 | 0.05000 | 1.200 | 0.177 | 1.409 | 0.0257 | 0.739 | 0.52 | 0.98 | 194 | 11 | 164 | 1 |
| spot 70 | 199 | 7250 | 2456 | 0.34 | 0.04969 | 1.193 | 0.177 | 1.468 | 0.0257 | 0.855 | 0.58 | 0.79 | 180 | 11 | 164 | 1 |
| spot 71 | 171 | 8260 | 2125 | 0.26 | 0.05023 | 1.177 | 0.178 | 1.524 | 0.0258 | 0.969 | 0.64 | 1.16 | 205 | 10 | 164 | 2 |
| spot 72 | 200 | 8670 | 2522 | 0.29 | 0.05014 | 1.145 | 0.179 | 1.521 | 0.0260 | 1.001 | 0.66 | 0.85 | 202 | 8 | 165 | 2 |

**12TM13-04 zircon** (spot size: 12 µm, frequency: 4 Hz, 100 shot count, laser energy: 3 mJ at 75%)

| | | | | | ISOTOPIC RATIOS | | | | | | | | APPARENT AGES | | | |
|---|---|---|---|---|---|---|---|---|---|---|---|---|---|---|---|---|
| | Pb (ppm) | U (ppm) | Th (ppm) | Th/U | $^{207}Pb/^{206}Pb$ | 2σ % | $^{207}Pb/^{235}U$ | 2σ % | $^{206}Pb/^{238}U$ | 2σ % | Rho | % disc.* | $^{207}Pb/^{206}Pb$ | 2σ abs | $^{206}Pb/^{238}U$ | 2σ abs |
| spot 1 | 42 | 3051 | 569 | 0.19 | 0.04891 | 1.653 | 0.177 | 1.910 | 0.0261 | 0.957 | 0.50 | 0.48 | 145 | 16 | 166 | 2 |
| spot 2 | 29 | 2128 | 385 | 0.18 | 0.04905 | 1.698 | 0.179 | 1.929 | 0.0262 | 0.916 | 0.47 | 0.06 | 149 | 19 | 167 | 2 |
| spot 3 | 54 | 3507 | 737 | 0.21 | 0.04880 | 1.585 | 0.176 | 2.968 | 0.0259 | 2.510 | 0.85 | 0.36 | 140 | 12 | 165 | 4 |
| spot 4 | 23 | 1599 | 298 | 0.19 | 0.04879 | 1.690 | 0.179 | 2.965 | 0.0263 | 2.436 | 0.82 | 0.00 | 137 | 18 | 167 | 4 |
| spot 5 | 38 | 1993 | 369 | 0.19 | 0.05424 | 2.003 | 0.197 | 2.925 | 0.0263 | 2.132 | 0.73 | 9.15 | 382 | 30 | 167 | 4 |
| spot 6 | 39 | 2926 | 533 | 0.18 | 0.04891 | 1.662 | 0.176 | 2.780 | 0.0260 | 2.228 | 0.80 | 0.54 | 143 | 17 | 166 | 4 |
| spot 7 | 114 | 2466 | 143 | 0.06 | 0.10347 | 1.510 | 4.083 | 2.910 | 0.2854 | 2.488 | 0.85 | 1.98 | 1687 | 26 | 1617 | 35 |
| spot 8 | 180 | 1171 | 292 | 0.25 | 0.09366 | 1.538 | 3.045 | 2.757 | 0.2360 | 2.288 | 0.83 | 3.81 | 1501 | 23 | 1365 | 28 |
| spot 9 | 84 | 1458 | 116 | 0.08 | 0.10029 | 1.516 | 3.950 | 2.978 | 0.2848 | 2.563 | 0.86 | 0.43 | 1630 | 25 | 1614 | 37 |
| spot 10 | 23 | 767 | 61 | 0.08 | 0.10074 | 1.544 | 3.869 | 2.683 | 0.2780 | 2.194 | 0.82 | 1.77 | 1638 | 26 | 1580 | 31 |
| spot 11 | 114 | 638 | 212 | 0.33 | 0.08890 | 1.537 | 2.515 | 2.370 | 0.2052 | 1.803 | 0.76 | 5.99 | 1402 | 22 | 1203 | 20 |
| spot 12 | 33 | 2466 | 444 | 0.18 | 0.04908 | 1.636 | 0.177 | 1.977 | 0.0261 | 1.111 | 0.56 | 0.54 | 153 | 15 | 166 | 2 |
| spot 13 | 56 | 8980 | 756 | 0.08 | 0.04939 | 1.530 | 0.180 | 1.903 | 0.0265 | 1.131 | 0.59 | 0.36 | 167 | 8 | 169 | 2 |
| spot 14 | 24 | 1897 | 330 | 0.17 | 0.04931 | 1.686 | 0.178 | 2.204 | 0.0261 | 1.420 | 0.64 | 0.24 | 162 | 18 | 166 | 2 |
| spot 15 | 23 | 2075 | 317 | 0.15 | 0.04932 | 1.686 | 0.176 | 2.188 | 0.0258 | 1.394 | 0.64 | 0.12 | 162 | 18 | 164 | 2 |
| spot 16 | 23 | 1801 | 304 | 0.17 | 0.05051 | 1.831 | 0.179 | 2.324 | 0.0259 | 1.431 | 0.62 | 1.64 | 216 | 24 | 165 | 2 |
| spot 17 | 37 | 200 | 56 | 0.28 | 0.09483 | 1.604 | 3.363 | 2.312 | 0.2583 | 1.665 | 0.72 | 0.95 | 1524 | 25 | 1481 | 22 |
| spot 18 | 32 | 160 | 41 | 0.25 | 0.10442 | 1.651 | 4.288 | 2.297 | 0.3006 | 1.597 | 0.70 | 0.24 | 1704 | 29 | 1694 | 24 |
| spot 19 | 334 | 395 | 468 | 1.18 | 0.10178 | 1.546 | 3.743 | 2.328 | 0.2701 | 1.740 | 0.75 | 2.66 | 1657 | 26 | 1541 | 24 |
| spot 20 | 29 | 119 | 39 | 0.33 | 0.10339 | 1.692 | 3.953 | 2.188 | 0.2811 | 1.387 | 0.63 | 1.69 | 1685 | 29 | 1597 | 20 |
| spot 21 | 17 | 65 | 20 | 0.30 | 0.10450 | 1.889 | 4.290 | 2.877 | 0.2995 | 2.170 | 0.75 | 0.06 | 1704 | 34 | 1688 | 32 |
| spot 22 | 46 | 197 | 70 | 0.35 | 0.10539 | 1.591 | 3.735 | 2.633 | 0.2575 | 2.097 | 0.80 | 6.84 | 1721 | 28 | 1476 | 28 |
| spot 23 | 1579 | 1672 | 2199 | 1.32 | 0.10346 | 1.515 | 3.752 | 2.450 | 0.2649 | 1.925 | 0.79 | 4.43 | 1687 | 26 | 1514 | 26 |
| spot 24 | 470 | 444 | 579 | 1.30 | 0.10272 | 1.552 | 4.096 | 2.447 | 0.2908 | 1.891 | 0.77 | 0.43 | 1674 | 26 | 1645 | 28 |
| spot 25 | 79 | 119 | 115 | 0.96 | 0.10170 | 1.727 | 3.406 | 2.271 | 0.2440 | 1.475 | 0.65 | 6.97 | 1655 | 30 | 1407 | 18 |
| spot 26 | 41 | 195 | 60 | 0.31 | 0.08915 | 1.673 | 3.033 | 2.386 | 0.2468 | 1.702 | 0.71 | 0.49 | 1407 | 25 | 1422 | 22 |
| spot 27 | 48 | 326 | 67 | 0.21 | 0.09922 | 1.570 | 3.489 | 2.359 | 0.2555 | 1.761 | 0.75 | 3.96 | 1609 | 26 | 1466 | 23 |
| spot 28 | 281 | 2246 | 3640 | 1.62 | 0.04949 | 1.633 | 0.177 | 2.374 | 0.0261 | 1.722 | 0.73 | 0.60 | 175 | 16 | 166 | 3 |
| spot 29 | 48 | 136 | 45 | 0.33 | 0.09933 | 1.727 | 4.049 | 2.426 | 0.2994 | 1.703 | 0.70 | 2.73 | 1611 | 29 | 1688 | 25 |
| spot 30 | 14 | 115 | 20 | 0.17 | 0.09315 | 1.808 | 3.035 | 2.415 | 0.2374 | 1.601 | 0.66 | 3.28 | 1493 | 29 | 1373 | 20 |
| spot 31 | 11 | 563 | 90 | 0.16 | 0.06477 | 1.993 | 0.336 | 3.540 | 0.0376 | 2.926 | 0.83 | 24.11 | 775 | 32 | 238 | 7 |

**12TM13-04 zircon** (spot size: 12 µm, frequency: 4 Hz, 100 shot count, laser energy: 3 mJ at 75%)

| | | | | | ISOTOPIC RATIOS | | | | | | | | APPARENT AGES | | | |
|---|---|---|---|---|---|---|---|---|---|---|---|---|---|---|---|---|
| | Pb (ppm) | U (ppm) | Th (ppm) | Th/U | $^{207}Pb/^{206}Pb$ | 2σ % | $^{207}Pb/^{235}U$ | 2σ % | $^{206}Pb/^{238}U$ | 2σ % | Rho | % disc.* | $^{207}Pb/^{206}Pb$ | 2σ abs | $^{206}Pb/^{238}U$ | 2σ abs |
| spot 32 | 44 | 185 | 63 | 0.34 | 0.10386 | 1.633 | 3.461 | 2.631 | 0.2424 | 2.063 | 0.78 | 8.43 | 1694 | 28 | 1399 | 26 |
| spot 33 | 45 | 13040 | 590 | 0.05 | 0.04945 | 1.523 | 0.179 | 1.977 | 0.0262 | 1.261 | 0.64 | 0.18 | 170 | 7 | 166 | 2 |
| spot 34 | 41 | 11720 | 527 | 0.04 | 0.04927 | 1.531 | 0.179 | 2.156 | 0.0263 | 1.519 | 0.70 | 0.12 | 161 | 7 | 168 | 3 |
| spot 35 | 51 | 12360 | 568 | 0.05 | 0.04974 | 1.538 | 0.181 | 2.139 | 0.0263 | 1.486 | 0.69 | 1.08 | 184 | 8 | 167 | 3 |
| spot 36 | 85 | 1660 | 118 | 0.07 | 0.09884 | 1.514 | 3.629 | 2.082 | 0.2658 | 1.430 | 0.69 | 2.37 | 1602 | 24 | 1519 | 19 |
| spot 37 | 70 | 1443 | 96 | 0.07 | 0.09870 | 1.539 | 3.727 | 2.387 | 0.2740 | 1.825 | 0.76 | 1.09 | 1600 | 25 | 1561 | 25 |
| spot 38 | 27 | 2029 | 359 | 0.18 | 0.04932 | 1.725 | 0.178 | 2.314 | 0.0259 | 1.542 | 0.67 | 0.67 | 162 | 20 | 165 | 3 |
| spot 39 | 35 | 2586 | 471 | 0.18 | 0.04964 | 1.641 | 0.178 | 2.299 | 0.0261 | 1.611 | 0.70 | 0.24 | 180 | 15 | 166 | 3 |
| spot 40 | 33 | 1020 | 92 | 0.09 | 0.08766 | 1.547 | 2.044 | 2.177 | 0.1697 | 1.532 | 0.70 | 11.88 | 1375 | 22 | 1010 | 14 |
| spot 41 | 12 | 1052 | 158 | 0.15 | 0.04884 | 2.118 | 0.173 | 2.968 | 0.0260 | 2.080 | 0.70 | 1.88 | 138 | 35 | 165 | 3 |
| spot 42 | 11 | 977 | 152 | 0.16 | 0.04931 | 1.970 | 0.176 | 2.572 | 0.0260 | 1.653 | 0.64 | 0.66 | 164 | 30 | 166 | 3 |
| spot 43 | 65 | 1478 | 83 | 0.06 | 0.10385 | 1.516 | 4.187 | 2.329 | 0.2942 | 1.768 | 0.76 | 0.18 | 1695 | 26 | 1667 | 27 |
| spot 44 | 91 | 1870 | 128 | 0.07 | 0.10536 | 1.508 | 4.154 | 2.339 | 0.2907 | 1.789 | 0.76 | 1.46 | 1721 | 26 | 1644 | 26 |
| spot 45 | 86 | 1206 | 127 | 0.11 | 0.09781 | 1.522 | 3.432 | 2.469 | 0.2572 | 1.944 | 0.79 | 2.58 | 1583 | 24 | 1475 | 26 |
| spot 46 | 37 | 1142 | 47 | 0.04 | 0.09787 | 1.662 | 3.750 | 2.536 | 0.2819 | 1.916 | 0.76 | 1.12 | 1583 | 27 | 1604 | 28 |
| spot 47 | 52 | 913 | 82 | 0.09 | 0.10283 | 1.518 | 3.309 | 2.538 | 0.2360 | 2.034 | 0.80 | 8.57 | 1676 | 26 | 1365 | 25 |
| spot 48 | 6 | 533 | 9 | 0.02 | 0.10134 | 1.549 | 3.869 | 2.358 | 0.2812 | 1.778 | 0.75 | 0.56 | 1649 | 26 | 1597 | 25 |
| spot 49 | 30 | 1056 | 43 | 0.04 | 0.09461 | 1.525 | 3.264 | 2.176 | 0.2512 | 1.553 | 0.71 | 1.94 | 1520 | 23 | 1444 | 20 |
| spot 50 | 104 | 1413 | 142 | 0.10 | 0.10163 | 1.514 | 3.576 | 2.533 | 0.2561 | 2.030 | 0.80 | 5.04 | 1654 | 25 | 1469 | 27 |
| spot 51 | 80 | 553 | 123 | 0.22 | 0.09007 | 1.530 | 2.994 | 2.405 | 0.2424 | 1.856 | 0.77 | 0.64 | 1427 | 22 | 1399 | 23 |
| spot 52 | 138 | 1735 | 187 | 0.11 | 0.10178 | 1.515 | 3.611 | 2.443 | 0.2557 | 1.916 | 0.78 | 5.66 | 1657 | 25 | 1467 | 25 |
| spot 53 | 85 | 2867 | 1126 | 0.39 | 0.04929 | 1.687 | 0.175 | 2.563 | 0.0259 | 1.930 | 0.75 | 0.55 | 160 | 18 | 165 | 3 |
| spot 54 | 81 | 2706 | 1085 | 0.40 | 0.04927 | 1.627 | 0.173 | 2.388 | 0.0257 | 1.748 | 0.73 | 0.85 | 163 | 15 | 164 | 3 |
| spot 55 | 91 | 2472 | 144 | 0.06 | 0.08869 | 1.510 | 2.899 | 2.461 | 0.2367 | 1.943 | 0.79 | 0.80 | 1398 | 21 | 1369 | 24 |
| spot 56 | 114 | 2359 | 154 | 0.07 | 0.10177 | 1.515 | 3.885 | 2.197 | 0.2766 | 1.591 | 0.72 | 2.41 | 1657 | 25 | 1574 | 22 |
| spot 57 | 36 | 1055 | 45 | 0.04 | 0.09918 | 1.528 | 3.902 | 2.225 | 0.2844 | 1.617 | 0.73 | 0.00 | 1609 | 25 | 1613 | 23 |
| spot 58 | 134 | 1748 | 190 | 0.11 | 0.10272 | 1.514 | 4.041 | 2.486 | 0.2839 | 1.973 | 0.79 | 1.93 | 1674 | 25 | 1610 | 28 |
| spot 59 | 71 | 1088 | 113 | 0.10 | 0.09777 | 1.535 | 2.982 | 2.513 | 0.2211 | 1.990 | 0.79 | 8.94 | 1582 | 24 | 1287 | 23 |
| spot 60 | 19 | 1444 | 247 | 0.17 | 0.04856 | 1.774 | 0.180 | 2.639 | 0.0266 | 1.953 | 0.74 | 0.95 | 125 | 22 | 169 | 3 |
| spot 61 | 48 | 3473 | 638 | 0.18 | 0.04925 | 1.643 | 0.178 | 2.306 | 0.0260 | 1.618 | 0.70 | 0.48 | 159 | 16 | 165 | 3 |
| spot 62 | 20 | 1602 | 273 | 0.17 | 0.04903 | 1.748 | 0.175 | 2.365 | 0.0257 | 1.593 | 0.67 | 0.00 | 148 | 21 | 164 | 3 |

**12TM13-04 zircon** (spot size: 12 µm, frequency: 4 Hz, 100 shot count, laser energy: 3 mJ at 75%)

| | | | | | ISOTOPIC RATIOS | | | | | | | | APPARENT AGES | | | |
|---|---|---|---|---|---|---|---|---|---|---|---|---|---|---|---|---|
| | Pb (ppm) | U (ppm) | Th (ppm) | Th/U | $^{207}Pb/^{206}Pb$ | 2σ % | $^{207}Pb/^{235}U$ | 2σ % | $^{206}Pb/^{238}U$ | 2σ % | Rho | % disc.* | $^{207}Pb/^{206}Pb$ | 2σ abs | $^{206}Pb/^{238}U$ | 2σ abs |
| spot 63 | 103 | 2053 | 132 | 0.06 | 0.10309 | 1.511 | 4.178 | 2.417 | 0.2916 | 1.886 | 0.78 | 1.15 | 1680 | 25 | 1649 | 28 |
| spot 64 | 103 | 2413 | 137 | 0.06 | 0.10393 | 1.510 | 4.080 | 2.247 | 0.2824 | 1.664 | 0.74 | 2.87 | 1695 | 26 | 1603 | 23 |
| spot 65 | 33 | 2484 | 440 | 0.18 | 0.04904 | 1.628 | 0.177 | 2.290 | 0.0261 | 1.610 | 0.70 | 0.12 | 149 | 15 | 166 | 3 |
| spot 66 | 88 | 1425 | 148 | 0.10 | 0.09016 | 1.520 | 2.852 | 2.876 | 0.2293 | 2.442 | 0.85 | 2.78 | 1430 | 22 | 1330 | 29 |
| spot 67 | 84 | 531 | 130 | 0.25 | 0.09647 | 1.546 | 3.319 | 3.231 | 0.2502 | 2.838 | 0.88 | 3.13 | 1558 | 24 | 1438 | 36 |
| spot 68 | 57 | 8500 | 780 | 0.09 | 0.05048 | 1.551 | 0.181 | 2.261 | 0.0261 | 1.645 | 0.73 | 1.50 | 217 | 10 | 166 | 3 |
| spot 69 | 112 | 2599 | 133 | 0.05 | 0.10490 | 1.015 | 4.336 | 2.251 | 0.3036 | 2.009 | 0.89 | 0.53 | 1712.5 | 17 | 1708 | 30 |
| spot 70 | 186 | 3488 | 230 | 0.07 | 0.10603 | 1.016 | 4.233 | 1.811 | 0.2935 | 1.499 | 0.83 | 1.27 | 1732.2 | 18 | 1659 | 22 |
| spot 71 | 19 | 1762 | 239 | 0.14 | 0.04985 | 1.489 | 0.178 | 2.251 | 0.0261 | 1.688 | 0.75 | 0.36 | 194 | 24 | 165.8 | 3 |
| spot 72 | 11 | 1050 | 142 | 0.13 | 0.04920 | 1.772 | 0.174 | 2.857 | 0.0259 | 2.241 | 0.78 | 1.09 | 155 | 34 | 164.7 | 4 |
| spot 73 | 159 | 3870 | 194 | 0.05 | 0.10559 | 1.032 | 4.350 | 2.019 | 0.2997 | 1.735 | 0.86 | 0.71 | 1725.3 | 18 | 1689 | 26 |
| spot 74 | 157 | 3212 | 199 | 0.06 | 0.10582 | 1.013 | 4.437 | 1.895 | 0.3059 | 1.602 | 0.85 | 0.12 | 1728.6 | 18 | 1720 | 24 |
| spot 75 | 187 | 3600 | 236 | 0.07 | 0.10552 | 1.013 | 4.490 | 2.304 | 0.3092 | 2.070 | 0.90 | 0.75 | 1723.3 | 17 | 1741 | 30 |
| spot 76 | 20 | 1619 | 280 | 0.17 | 0.04951 | 1.603 | 0.177 | 2.473 | 0.0260 | 1.883 | 0.76 | 0.06 | 170 | 29 | 165.6 | 3 |
| spot 77 | 198 | 3750 | 258 | 0.07 | 0.10611 | 1.014 | 4.510 | 2.529 | 0.3108 | 2.317 | 0.92 | 0.57 | 1733.5 | 18 | 1744 | 36 |
| spot 78 | 30 | 2334 | 417 | 0.18 | 0.04918 | 1.397 | 0.175 | 2.291 | 0.0259 | 1.815 | 0.79 | 0.49 | 155 | 23 | 164.8 | 3 |
| spot 79 | 31 | 2397 | 413 | 0.17 | 0.05020 | 1.254 | 0.180 | 2.481 | 0.0262 | 2.141 | 0.86 | 0.72 | 203 | 17 | 166.5 | 4 |
| spot 80 | 138 | 3344 | 173 | 0.05 | 0.10469 | 1.030 | 4.168 | 2.061 | 0.2913 | 1.785 | 0.87 | 1.09 | 1708.8 | 18 | 1648 | 26 |
| spot 81 | 7 | 676 | 92 | 0.14 | 0.04979 | 1.644 | 0.179 | 3.095 | 0.0259 | 2.622 | 0.85 | 1.15 | 182 | 30 | 165 | 4 |
| spot 82 | 9 | 915 | 135 | 0.15 | 0.04995 | 1.787 | 0.178 | 2.722 | 0.0258 | 2.053 | 0.75 | 0.97 | 189 | 34 | 164.3 | 3 |
| spot 83 | 132 | 1550 | 180 | 0.12 | 0.10208 | 1.042 | 4.120 | 2.962 | 0.2922 | 2.772 | 0.94 | 0.30 | 1662.1 | 18 | 1651 | 41 |
| spot 84 | 25 | 2172 | 352 | 0.16 | 0.04885 | 1.461 | 0.179 | 2.587 | 0.0262 | 2.135 | 0.83 | 0.18 | 139 | 25 | 166.9 | 4 |
| spot 85 | 149 | 3760 | 190 | 0.05 | 0.10470 | 1.013 | 4.434 | 2.355 | 0.3057 | 2.126 | 0.90 | 0.12 | 1709 | 17 | 1719 | 32 |
| spot 86 | 163 | 4160 | 210 | 0.05 | 0.10376 | 1.013 | 3.549 | 2.737 | 0.2478 | 2.542 | 0.93 | 7.71 | 1693 | 17 | 1426 | 33 |
| spot 87 | 158 | 2522 | 188 | 0.07 | 0.10493 | 1.015 | 4.323 | 2.250 | 0.2988 | 2.008 | 0.89 | 0.65 | 1713 | 17 | 1685 | 30 |
| spot 88 | 34 | 10840 | 438 | 0.04 | 0.04941 | 1.064 | 0.182 | 2.387 | 0.0267 | 2.136 | 0.90 | 0.06 | 167.2 | 9 | 169.7 | 4 |
| spot 89 | 40 | 847 | 78 | 0.09 | 0.09532 | 1.065 | 2.423 | 3.866 | 0.1830 | 3.716 | 0.96 | 15.90 | 1534.2 | 17 | 1082 | 37 |
| spot 90 | 102 | 1330 | 140 | 0.11 | 0.09931 | 1.034 | 3.950 | 3.694 | 0.2820 | 3.546 | 0.96 | 1.06 | 1611 | 17 | 1601 | 52 |
| spot 91 | 24 | 2437 | 313 | 0.13 | 0.04889 | 1.195 | 0.177 | 3.179 | 0.0258 | 2.946 | 0.93 | 0.43 | 142 | 15 | 164.2 | 5 |

**12TM15-12 zircon** (spot size: 15 µm, frequency: 4 Hz, 100 shot count, laser energy: 3 mJ at 75%)

| | | | | | ISOTOPIC RATIOS | | | | | | | | APPARENT AGES | | | |
|---|---|---|---|---|---|---|---|---|---|---|---|---|---|---|---|---|
| | Pb (ppm) | U (ppm) | Th (ppm) | Th/U | $^{207}Pb/^{206}Pb$ | 2σ % | $^{207}Pb/^{235}U$ | 2σ % | $^{206}Pb/^{238}U$ | 2σ % | Rho | % disc.* | $^{207}Pb/^{206}Pb$ | 2σ abs | $^{206}Pb/^{238}U$ | 2σ abs |
| spot 1 | 67 | 8000 | 839 | 0.10 | 0.04974 | 1.446 | 0.178 | 1.975 | 0.0260 | 1.345 | 0.68 | 0.18 | 183 | 9 | 166 | 2 |
| spot 2 | 48 | 6920 | 641 | 0.09 | 0.04901 | 1.453 | 0.174 | 1.930 | 0.0260 | 1.271 | 0.66 | 1.27 | 148 | 9 | 165 | 2 |
| spot 3 | 28 | 5320 | 366 | 0.07 | 0.04928 | 1.447 | 0.176 | 1.848 | 0.0261 | 1.150 | 0.62 | 0.78 | 162 | 9 | 166 | 2 |
| spot 4 | 27 | 5850 | 369 | 0.06 | 0.04918 | 1.458 | 0.174 | 1.935 | 0.0259 | 1.273 | 0.66 | 1.09 | 156 | 10 | 165 | 2 |
| spot 5 | 78 | 7270 | 1053 | 0.14 | 0.04919 | 1.442 | 0.177 | 1.989 | 0.0263 | 1.370 | 0.69 | 0.84 | 157 | 8 | 167 | 2 |
| spot 6 | 99 | 8930 | 1330 | 0.15 | 0.04930 | 1.433 | 0.179 | 1.978 | 0.0264 | 1.363 | 0.69 | 0.42 | 163 | 7 | 168 | 2 |
| spot 7 | 8 | 84 | 13 | 0.15 | 0.08880 | 1.869 | 2.870 | 2.531 | 0.2345 | 1.706 | 0.67 | 1.10 | 1402 | 32 | 1358 | 21 |
| spot 8 | 10 | 75 | 12 | 0.16 | 0.09995 | 1.633 | 3.683 | 2.633 | 0.2662 | 2.066 | 0.78 | 2.96 | 1622 | 28 | 1521 | 28 |
| spot 9 | 49 | 338 | 65 | 0.19 | 0.10279 | 1.464 | 4.415 | 2.077 | 0.3122 | 1.473 | 0.71 | 2.00 | 1675 | 25 | 1751 | 23 |
| spot 10 | 39 | 253 | 53 | 0.21 | 0.09396 | 1.487 | 3.415 | 2.479 | 0.2621 | 1.984 | 0.80 | 0.40 | 1509 | 23 | 1500 | 26 |
| spot 11 | 35 | 1222 | 40 | 0.03 | 0.10281 | 1.441 | 3.938 | 2.034 | 0.2785 | 1.436 | 0.71 | 2.40 | 1675 | 24 | 1583 | 20 |
| spot 12 | 37 | 1257 | 50 | 0.04 | 0.09893 | 1.423 | 3.469 | 2.198 | 0.2566 | 1.676 | 0.76 | 3.33 | 1604 | 23 | 1472 | 22 |
| spot 13 | 15 | 5010 | 185 | 0.04 | 0.04932 | 1.476 | 0.178 | 1.966 | 0.0262 | 1.299 | 0.66 | 0.24 | 163 | 11 | 167 | 2 |
| spot 14 | 18 | 5380 | 225 | 0.04 | 0.04923 | 1.482 | 0.176 | 2.082 | 0.0260 | 1.462 | 0.70 | 0.54 | 158 | 12 | 165 | 2 |
| spot 15 | 24 | 5830 | 312 | 0.05 | 0.04937 | 1.496 | 0.177 | 2.200 | 0.0260 | 1.613 | 0.73 | 0.12 | 167 | 12 | 166 | 3 |
| spot 16 | 21 | 5630 | 264 | 0.05 | 0.04947 | 1.452 | 0.175 | 2.068 | 0.0258 | 1.472 | 0.71 | 0.37 | 170 | 9 | 164 | 2 |
| spot 17 | 58 | 7510 | 694 | 0.09 | 0.04998 | 1.446 | 0.180 | 1.993 | 0.0262 | 1.372 | 0.69 | 0.54 | 194 | 9 | 167 | 2 |
| spot 18 | 114 | 1328 | 149 | 0.11 | 0.10438 | 1.411 | 3.963 | 2.154 | 0.2765 | 1.627 | 0.76 | 3.37 | 1703 | 24 | 1573 | 23 |
| spot 19 | 189 | 2041 | 255 | 0.12 | 0.10278 | 1.412 | 3.873 | 2.004 | 0.2743 | 1.422 | 0.71 | 2.88 | 1675 | 24 | 1562 | 20 |
| spot 20 | 99 | 1200 | 128 | 0.11 | 0.10284 | 1.416 | 3.965 | 2.198 | 0.2796 | 1.681 | 0.76 | 2.14 | 1676 | 24 | 1592 | 23 |
| spot 21 | 93 | 1216 | 124 | 0.10 | 0.10064 | 1.429 | 3.796 | 2.152 | 0.2735 | 1.609 | 0.75 | 2.12 | 1636 | 24 | 1558 | 22 |
| spot 22 | 142 | 1961 | 181 | 0.09 | 0.10376 | 1.413 | 3.970 | 1.965 | 0.2784 | 1.365 | 0.69 | 2.78 | 1692 | 24 | 1583 | 19 |
| spot 23 | 155 | 2270 | 217 | 0.10 | 0.10230 | 1.409 | 3.626 | 2.247 | 0.2571 | 1.750 | 0.78 | 5.36 | 1666 | 24 | 1475 | 23 |
| spot 24 | 135 | 1833 | 178 | 0.10 | 0.10268 | 1.413 | 3.901 | 1.853 | 0.2755 | 1.198 | 0.65 | 3.00 | 1674 | 24 | 1568 | 17 |
| spot 25 | 98 | 1372 | 127 | 0.09 | 0.10137 | 1.418 | 3.880 | 2.319 | 0.2779 | 1.835 | 0.79 | 1.90 | 1651 | 23 | 1580 | 26 |
| spot 26 | 90 | 1247 | 117 | 0.09 | 0.10015 | 1.416 | 3.752 | 2.382 | 0.2714 | 1.916 | 0.80 | 2.39 | 1627 | 23 | 1547 | 26 |
| spot 27 | 95 | 1218 | 123 | 0.10 | 0.10025 | 1.424 | 3.794 | 2.010 | 0.2748 | 1.419 | 0.71 | 1.79 | 1629 | 23 | 1565 | 20 |
| spot 28 | 110 | 1438 | 142 | 0.10 | 0.10091 | 1.414 | 3.884 | 2.122 | 0.2781 | 1.582 | 0.75 | 1.77 | 1641 | 23 | 1581 | 22 |
| spot 29 | 85 | 1151 | 111 | 0.10 | 0.10043 | 1.414 | 3.765 | 2.231 | 0.2723 | 1.726 | 0.77 | 2.26 | 1633 | 23 | 1552 | 24 |
| spot 30 | 88 | 1203 | 121 | 0.10 | 0.09813 | 1.423 | 3.680 | 2.182 | 0.2721 | 1.654 | 0.76 | 0.97 | 1589 | 23 | 1551 | 23 |
| spot 31 | 98 | 1328 | 136 | 0.10 | 0.09902 | 1.413 | 3.641 | 2.231 | 0.2664 | 1.727 | 0.77 | 2.03 | 1606 | 23 | 1526 | 24 |

**12TM15-12 zircon** (spot size: 15 µm, frequency: 4 Hz, 100 shot count, laser energy: 3 mJ at 75%)

| | | | | | ISOTOPIC RATIOS | | | | | | | | APPARENT AGES | | | |
|---|---|---|---|---|---|---|---|---|---|---|---|---|---|---|---|---|
| | Pb (ppm) | U (ppm) | Th (ppm) | Th/U | $^{207}Pb/^{206}Pb$ | 2σ % | $^{207}Pb/^{235}U$ | 2σ % | $^{206}Pb/^{238}U$ | 2σ % | Rho | % disc.* | $^{207}Pb/^{206}Pb$ | 2σ abs | $^{206}Pb/^{238}U$ | 2σ abs |
| spot 32 | 101 | 1314 | 133 | 0.10 | 0.09957 | 1.414 | 3.829 | 2.313 | 0.2787 | 1.830 | 0.79 | 0.88 | 1616 | 23 | 1584 | 26 |
| spot 33 | 140 | 257 | 164 | 0.64 | 0.10602 | 1.477 | 4.514 | 2.329 | 0.3110 | 1.801 | 0.77 | 0.57 | 1732 | 26 | 1745 | 28 |
| spot 34 | 124 | 281 | 150 | 0.53 | 0.10578 | 1.445 | 4.561 | 2.441 | 0.3152 | 1.967 | 0.81 | 1.42 | 1728 | 25 | 1766 | 30 |
| spot 35 | 36 | 5880 | 460 | 0.08 | 0.04959 | 1.457 | 0.177 | 2.263 | 0.0260 | 1.732 | 0.77 | 0.00 | 176 | 10 | 165 | 3 |
| spot 36 | 21 | 5720 | 278 | 0.05 | 0.04972 | 1.462 | 0.177 | 2.197 | 0.0262 | 1.640 | 0.75 | 0.66 | 182 | 10 | 167 | 3 |
| spot 37 | 18 | 6080 | 238 | 0.04 | 0.04930 | 1.458 | 0.176 | 2.377 | 0.0261 | 1.877 | 0.79 | 1.02 | 163 | 10 | 166 | 3 |
| spot 38 | 23 | 5620 | 301 | 0.05 | 0.04945 | 1.452 | 0.177 | 2.197 | 0.0261 | 1.649 | 0.75 | 0.30 | 169 | 9 | 166 | 3 |
| spot 39 | 18 | 5730 | 232 | 0.04 | 0.04936 | 1.452 | 0.177 | 2.106 | 0.0262 | 1.526 | 0.72 | 0.84 | 165 | 9 | 167 | 3 |
| spot 40 | 25 | 5730 | 324 | 0.06 | 0.04910 | 1.470 | 0.177 | 2.195 | 0.0264 | 1.631 | 0.74 | 1.49 | 152 | 10 | 168 | 3 |
| spot 41 | 21 | 5470 | 279 | 0.05 | 0.04918 | 1.447 | 0.176 | 2.334 | 0.0262 | 1.831 | 0.78 | 1.14 | 156 | 9 | 167 | 3 |
| spot 42 | 27 | 6030 | 360 | 0.06 | 0.04929 | 1.442 | 0.177 | 2.186 | 0.0262 | 1.643 | 0.75 | 0.48 | 162 | 8 | 167 | 3 |
| spot 43 | 381 | 335 | 470 | 1.40 | 0.10350 | 1.487 | 3.627 | 2.696 | 0.2535 | 2.249 | 0.83 | 6.94 | 1688 | 25 | 1456 | 29 |
| spot 44 | 205 | 195 | 262 | 1.35 | 0.10477 | 1.499 | 4.203 | 2.584 | 0.2897 | 2.106 | 0.81 | 1.95 | 1710 | 26 | 1644 | 30 |
| spot 45 | 219 | 451 | 271 | 0.60 | 0.10570 | 1.448 | 4.560 | 2.567 | 0.3113 | 2.120 | 0.83 | 0.34 | 1726 | 25 | 1746 | 32 |
| spot 46 | 151 | 508 | 183 | 0.36 | 0.10613 | 1.432 | 4.698 | 2.280 | 0.3213 | 1.774 | 0.78 | 1.50 | 1734 | 25 | 1795 | 28 |
| spot 47 | 13 | 5000 | 167 | 0.03 | 0.04907 | 1.490 | 0.175 | 2.410 | 0.0259 | 1.895 | 0.79 | 0.49 | 151 | 12 | 165 | 3 |
| spot 48 | 15 | 4780 | 194 | 0.04 | 0.04957 | 1.463 | 0.179 | 2.263 | 0.0261 | 1.726 | 0.76 | 0.48 | 175 | 10 | 166 | 3 |
| spot 49 | 22 | 5410 | 282 | 0.05 | 0.04910 | 1.464 | 0.175 | 2.130 | 0.0259 | 1.547 | 0.73 | 0.18 | 152 | 10 | 165 | 3 |
| spot 50 | 18 | 6200 | 233 | 0.04 | 0.04924 | 1.482 | 0.178 | 2.212 | 0.0262 | 1.641 | 0.74 | 0.54 | 159 | 11 | 167 | 3 |
| spot 51 | 19 | 5930 | 244 | 0.04 | 0.04936 | 1.457 | 0.179 | 2.028 | 0.0262 | 1.411 | 0.70 | 0.30 | 165 | 10 | 167 | 2 |
| spot 52 | 22 | 5668 | 277 | 0.05 | 0.04929 | 1.469 | 0.177 | 2.238 | 0.0261 | 1.688 | 0.75 | 0.30 | 161 | 10 | 166 | 3 |
| spot 53 | 20 | 5920 | 251 | 0.04 | 0.04943 | 1.447 | 0.177 | 2.345 | 0.0260 | 1.845 | 0.79 | 0.06 | 168 | 9 | 166 | 3 |
| spot 54 | 128 | 482 | 152 | 0.32 | 0.10359 | 1.434 | 4.108 | 2.582 | 0.2888 | 2.147 | 0.83 | 1.16 | 1689 | 24 | 1635 | 31 |
| spot 55 | 710 | 747 | 861 | 1.15 | 0.10366 | 1.422 | 4.290 | 2.786 | 0.3006 | 2.395 | 0.86 | 0.24 | 1691 | 24 | 1693 | 36 |
| spot 56 | 58 | 59 | 69 | 1.18 | 0.10460 | 1.810 | 4.193 | 2.699 | 0.2897 | 2.002 | 0.74 | 2.14 | 1705 | 32 | 1639 | 29 |
| spot 57 | 14 | 4000 | 176 | 0.04 | 0.05055 | 1.478 | 0.179 | 2.725 | 0.0258 | 2.289 | 0.84 | 1.89 | 220 | 11 | 164 | 4 |

**13TM-06 zircon** (spot size: 31 µm, frequency: 4 Hz, 100 shot count, laser energy: 4 mJ at 75%)

| | | | | | ISOTOPIC RATIOS | | | | | | | | APPARENT AGES | | | |
|---|---|---|---|---|---|---|---|---|---|---|---|---|---|---|---|---|
| | Pb (ppm) | U (ppm) | Th (ppm) | Th/U | $^{207}Pb/^{206}Pb$ | 2σ % | $^{207}Pb/^{235}U$ | 2σ % | $^{206}Pb/^{238}U$ | 2σ % | Rho | % disc.* | $^{207}Pb/^{206}Pb$ | 2σ abs | $^{206}Pb/^{238}U$ | 2σ abs |
| spot 1 | 14 | 101 | 176 | 1.75 | 0.04964 | 1.249 | 0.178 | 1.718 | 0.0260 | 1.180 | 0.69 | 0.18 | 175 | 28 | 166 | 2 |
| spot 2 | 13 | 112 | 164 | 1.47 | 0.04956 | 1.170 | 0.179 | 1.807 | 0.0261 | 1.376 | 0.76 | 0.54 | 175 | 27 | 166 | 2 |
| spot 3 | 11 | 91 | 137 | 1.50 | 0.05004 | 1.459 | 0.181 | 2.047 | 0.0261 | 1.437 | 0.70 | 1.93 | 193 | 34 | 166 | 2 |
| spot 4 | 11 | 87 | 132 | 1.51 | 0.04971 | 1.408 | 0.177 | 1.876 | 0.0257 | 1.240 | 0.66 | 0.73 | 181 | 32 | 164 | 2 |
| spot 5 | 18 | 98 | 235 | 2.39 | 0.05221 | 1.283 | 0.185 | 1.801 | 0.0259 | 1.264 | 0.70 | 4.67 | 296 | 29 | 165 | 2 |
| spot 6 | 26 | 175 | 315 | 1.80 | 0.05005 | 1.099 | 0.178 | 1.577 | 0.0259 | 1.131 | 0.72 | 0.85 | 194 | 25 | 165 | 2 |
| spot 7 | 25 | 174 | 308 | 1.77 | 0.04907 | 0.999 | 0.174 | 1.656 | 0.0259 | 1.321 | 0.80 | 1.09 | 149 | 23 | 165 | 2 |
| spot 8 | 26 | 174 | 316 | 1.82 | 0.04952 | 0.989 | 0.176 | 1.630 | 0.0258 | 1.296 | 0.79 | 0.37 | 170 | 23 | 164 | 2 |
| spot 9 | 22 | 154 | 276 | 1.80 | 0.04949 | 0.970 | 0.175 | 1.670 | 0.0256 | 1.360 | 0.81 | 0.12 | 168 | 22 | 163 | 2 |
| spot 10 | 21 | 149 | 268 | 1.80 | 0.04942 | 1.093 | 0.175 | 1.815 | 0.0257 | 1.449 | 0.80 | 0.00 | 162 | 25 | 164 | 2 |
| spot 11 | 35 | 169 | 449 | 2.66 | 0.04930 | 0.913 | 0.176 | 1.562 | 0.0258 | 1.267 | 0.81 | 0.24 | 157 | 21 | 164 | 2 |
| spot 12 | 31 | 158 | 402 | 2.54 | 0.04999 | 0.960 | 0.177 | 1.737 | 0.0258 | 1.447 | 0.83 | 0.85 | 192 | 22 | 164 | 2 |
| spot 13 | 24 | 125 | 302 | 2.42 | 0.05082 | 1.141 | 0.181 | 1.727 | 0.0258 | 1.296 | 0.75 | 2.86 | 228 | 26 | 164 | 2 |
| spot 14 | 35 | 1140 | 439 | 0.39 | 0.04992 | 0.361 | 0.180 | 1.285 | 0.0260 | 1.233 | 0.96 | 1.33 | 191 | 8 | 166 | 2 |
| spot 15 | 21 | 153 | 249 | 1.63 | 0.05088 | 0.884 | 0.181 | 1.593 | 0.0258 | 1.325 | 0.83 | 3.11 | 240 | 20 | 164 | 2 |
| spot 16 | 19 | 151 | 231 | 1.53 | 0.05252 | 1.066 | 0.188 | 1.748 | 0.0258 | 1.385 | 0.79 | 6.58 | 313 | 24 | 164 | 2 |
| spot 17 | 21 | 159 | 264 | 1.66 | 0.05070 | 1.006 | 0.182 | 1.639 | 0.0259 | 1.294 | 0.79 | 3.16 | 231 | 24 | 165 | 2 |
| spot 18 | 23 | 176 | 286 | 1.62 | 0.05038 | 0.774 | 0.180 | 1.559 | 0.0259 | 1.353 | 0.87 | 2.31 | 210 | 18 | 165 | 2 |
| spot 19 | 8 | 58 | 91 | 1.57 | 0.05126 | 1.853 | 0.183 | 2.309 | 0.0260 | 1.377 | 0.60 | 3.32 | 248 | 42 | 166 | 2 |
| spot 20 | 60 | 390 | 740 | 1.90 | 0.04950 | 0.646 | 0.177 | 1.499 | 0.0259 | 1.352 | 0.90 | 0.36 | 173 | 15 | 165 | 2 |
| spot 21 | 65 | 418 | 802 | 1.92 | 0.04950 | 0.626 | 0.177 | 1.363 | 0.0258 | 1.211 | 0.89 | 0.85 | 172 | 15 | 164 | 2 |
| spot 22 | 63 | 412 | 790 | 1.92 | 0.04955 | 0.565 | 0.178 | 1.463 | 0.0260 | 1.349 | 0.92 | 0.48 | 172 | 13 | 165 | 2 |
| spot 23 | 69 | 437 | 884 | 2.02 | 0.04959 | 0.665 | 0.179 | 1.421 | 0.0262 | 1.256 | 0.88 | 0.36 | 176 | 15 | 167 | 2 |
| spot 24 | 49 | 397 | 591 | 1.49 | 0.04941 | 0.668 | 0.178 | 1.560 | 0.0260 | 1.410 | 0.90 | 0.42 | 165 | 16 | 165 | 2 |
| spot 25 | 85 | 595 | 1061 | 1.78 | 0.04960 | 0.464 | 0.178 | 1.400 | 0.0259 | 1.321 | 0.94 | 0.61 | 175 | 11 | 165 | 2 |
| spot 26 | 107 | 689 | 1308 | 1.90 | 0.04961 | 0.403 | 0.178 | 1.379 | 0.0260 | 1.319 | 0.96 | 0.36 | 178 | 9 | 165 | 2 |
| spot 27 | 40 | 244 | 499 | 2.04 | 0.04954 | 0.828 | 0.182 | 1.597 | 0.0264 | 1.366 | 0.86 | 0.95 | 175 | 20 | 168 | 2 |
| spot 28 | 64 | 374 | 815 | 2.18 | 0.04945 | 0.566 | 0.178 | 1.408 | 0.0260 | 1.289 | 0.92 | 0.48 | 170 | 13 | 166 | 2 |
| spot 29 | 196 | 739 | 2641 | 3.57 | 0.04995 | 0.460 | 0.180 | 1.033 | 0.0261 | 0.925 | 0.90 | 0.98 | 193 | 11 | 166 | 1 |
| spot 30 | 97 | 465 | 1173 | 2.52 | 0.04956 | 0.504 | 0.180 | 1.060 | 0.0263 | 0.933 | 0.88 | 0.17 | 174 | 12 | 167 | 1 |
| spot 31 | 36 | 255 | 446 | 1.75 | 0.04939 | 0.891 | 0.178 | 1.282 | 0.0260 | 0.921 | 0.72 | 0.31 | 164 | 21 | 166 | 1 |

**13TM-06 zircon** (spot size: 31 µm, frequency: 4 Hz, 100 shot count, laser energy: 4 mJ at 75%)

| | | | | | ISOTOPIC RATIOS | | | | | | | | APPARENT AGES | | | |
|---|---|---|---|---|---|---|---|---|---|---|---|---|---|---|---|---|
| | Pb (ppm) | U (ppm) | Th (ppm) | Th/U | $^{207}Pb/^{206}Pb$ | 2σ % | $^{207}Pb/^{235}U$ | 2σ % | $^{206}Pb/^{238}U$ | 2σ % | Rho | % disc.* | $^{207}Pb/^{206}Pb$ | 2σ abs | $^{206}Pb/^{238}U$ | 2σ abs |
| spot 32 | 15 | 103 | 180 | 1.75 | 0.05269 | 1.366 | 0.191 | 1.689 | 0.0263 | 0.992 | 0.59 | 6.33 | 312 | 32 | 167 | 2 |
| spot 33 | 46 | 266 | 570 | 2.14 | 0.04964 | 0.745 | 0.178 | 1.199 | 0.0260 | 0.939 | 0.78 | 0.48 | 180 | 17 | 165 | 1 |
| spot 34 | 58 | 2704 | 704 | 0.26 | 0.05029 | 0.278 | 0.181 | 0.935 | 0.0261 | 0.892 | 0.95 | 1.70 | 208 | 7 | 166 | 1 |
| spot 35 | 22 | 133 | 254 | 1.91 | 0.04936 | 1.297 | 0.177 | 1.612 | 0.0261 | 0.958 | 0.59 | 0.30 | 155 | 30 | 166 | 2 |
| spot 36 | 36 | 170 | 427 | 2.52 | 0.05019 | 1.016 | 0.180 | 1.383 | 0.0261 | 0.938 | 0.68 | 1.27 | 202 | 24 | 166 | 1 |
| spot 37 | 32 | 316 | 362 | 1.15 | 0.05007 | 0.719 | 0.182 | 1.179 | 0.0263 | 0.935 | 0.79 | 1.39 | 200 | 17 | 167 | 1 |
| spot 38 | 39 | 335 | 463 | 1.38 | 0.04956 | 0.646 | 0.181 | 1.140 | 0.0265 | 0.939 | 0.82 | 0.29 | 175 | 15 | 168 | 2 |
| spot 39 | 21 | 135 | 259 | 1.91 | 0.04941 | 0.911 | 0.178 | 1.334 | 0.0262 | 0.974 | 0.73 | 0.41 | 167 | 21 | 167 | 2 |
| spot 40 | 84 | 371 | 989 | 2.67 | 0.04948 | 0.627 | 0.180 | 1.119 | 0.0264 | 0.927 | 0.83 | 0.15 | 173 | 15 | 168 | 1 |
| spot 41 | 24 | 116 | 278 | 2.39 | 0.05037 | 1.231 | 0.181 | 1.571 | 0.0260 | 0.976 | 0.62 | 1.75 | 207 | 28 | 166 | 2 |
| spot 42 | 32 | 185 | 395 | 2.13 | 0.04963 | 0.887 | 0.178 | 1.289 | 0.0260 | 0.936 | 0.73 | 0.72 | 179 | 21 | 165 | 1 |
| spot 43 | 16 | 118 | 190 | 1.61 | 0.04984 | 1.184 | 0.178 | 1.534 | 0.0261 | 0.975 | 0.64 | 0.22 | 186 | 28 | 166 | 2 |
| spot 44 | 18 | 124 | 208 | 1.69 | 0.04925 | 1.218 | 0.177 | 1.561 | 0.0261 | 0.975 | 0.62 | 0.42 | 157 | 28 | 166 | 2 |
| spot 45 | 73 | 563 | 876 | 1.56 | 0.04972 | 0.523 | 0.179 | 1.060 | 0.0261 | 0.922 | 0.87 | 0.53 | 181 | 12 | 166 | 1 |
| spot 46 | 14 | 122 | 167 | 1.37 | 0.04946 | 1.173 | 0.177 | 1.515 | 0.0259 | 0.959 | 0.63 | 0.21 | 169 | 27 | 165 | 2 |
| spot 47 | 14 | 116 | 169 | 1.46 | 0.04960 | 1.089 | 0.178 | 1.463 | 0.0259 | 0.977 | 0.67 | 0.90 | 170 | 25 | 165 | 2 |
| spot 48 | 212 | 709 | 2671 | 3.77 | 0.04971 | 0.422 | 0.178 | 1.012 | 0.0260 | 0.920 | 0.91 | 0.60 | 180 | 10 | 165 | 1 |
| spot 49 | 177 | 665 | 2320 | 3.49 | 0.04975 | 0.462 | 0.177 | 1.051 | 0.0258 | 0.943 | 0.90 | 1.02 | 183 | 11 | 164 | 1 |
| spot 50 | 8 | 168 | 96 | 0.57 | 0.05154 | 0.776 | 0.184 | 1.262 | 0.0259 | 0.996 | 0.79 | 3.98 | 265 | 18 | 165 | 2 |
| spot 51 | 363 | 3628 | 4660 | 1.28 | 0.05099 | 0.314 | 0.181 | 0.993 | 0.0257 | 0.942 | 0.95 | 3.27 | 240 | 7 | 164 | 1 |
| spot 52 | 179 | 729 | 2219 | 3.04 | 0.04950 | 0.404 | 0.177 | 1.410 | 0.0259 | 1.351 | 0.96 | 0.30 | 171 | 9 | 165 | 2 |
| spot 53 | 176 | 724 | 2146 | 2.96 | 0.04952 | 0.485 | 0.177 | 1.382 | 0.0258 | 1.294 | 0.94 | 0.55 | 171 | 11 | 164 | 2 |
| spot 54 | 166 | 682 | 2034 | 2.98 | 0.04940 | 0.466 | 0.176 | 1.404 | 0.0258 | 1.325 | 0.94 | 0.00 | 166 | 11 | 164 | 2 |
| spot 55 | 141 | 604 | 1690 | 2.80 | 0.04944 | 0.526 | 0.178 | 1.585 | 0.0262 | 1.495 | 0.94 | 0.30 | 169 | 12 | 167 | 2 |
| spot 56 | 192 | 795 | 2255 | 2.84 | 0.04962 | 0.464 | 0.178 | 1.516 | 0.0259 | 1.444 | 0.95 | 0.85 | 177 | 11 | 165 | 2 |
| spot 57 | 53 | 329 | 627 | 1.90 | 0.05047 | 0.753 | 0.182 | 1.549 | 0.0258 | 1.354 | 0.87 | 3.10 | 217 | 18 | 164 | 2 |
| spot 58 | 105 | 526 | 1260 | 2.40 | 0.04936 | 0.608 | 0.177 | 1.718 | 0.0258 | 1.607 | 0.94 | 0.61 | 165 | 14 | 164 | 3 |
| spot 59 | 117 | 567 | 1400 | 2.47 | 0.04984 | 0.522 | 0.177 | 1.601 | 0.0257 | 1.514 | 0.95 | 1.28 | 188 | 12 | 164 | 2 |
| spot 60 | 57 | 351 | 673 | 1.92 | 0.05021 | 0.717 | 0.179 | 1.613 | 0.0258 | 1.445 | 0.90 | 1.64 | 207 | 17 | 164 | 2 |

# Appendix F – Alteration Geochronology U-Pb and REE Data

**12TM3-01** monazite (M18) (spot size: 7 µm, frequency: 3 Hz, 75 shot count, laser energy: 3 mJ at 75%)

| | | | | | ISOTOPIC RATIOS | | | | | | | | APPARENT AGES (Ma) | | | |
|---|---|---|---|---|---|---|---|---|---|---|---|---|---|---|---|---|
| | Pb (ppm) | U (ppm) | Th (ppm) | Th/U | $^{207}Pb/^{206}Pb$ | 2σ % | $^{207}Pb/^{235}U$ | 2σ % | $^{206}Pb/^{238}U$ | 2σ % | Rho | % disc.* | $^{207}Pb/^{206}Pb$ | 2σ abs | $^{206}Pb/^{238}U$ | 2σ abs |
| spot 1 | 17930 | 10240 | 194600 | 19.00 | 0.10687 | 1.138 | 4.050 | 0.140 | 0.2763 | 3.261 | 0.84 | 4.78 | 1747 | 20 | 1570 | 47 |
| spot 2 | 14850 | 8040 | 189200 | 23.53 | 0.10503 | 1.155 | 3.747 | 0.114 | 0.2599 | 2.818 | 0.78 | 6.39 | 1715 | 20 | 1487 | 39 |
| spot 3 | 18570 | 9530 | 203400 | 21.34 | 0.10649 | 1.138 | 3.908 | 0.108 | 0.2710 | 2.524 | 0.73 | 5.12 | 1741 | 20 | 1544 | 36 |
| spot 4 | 2229 | 9170 | 192800 | 21.03 | 0.04906 | 1.738 | 0.180 | 0.006 | 0.0274 | 2.625 | 0.68 | 3.67 | 148 | 30 | 174 | 5 |
| spot 5 | 9010 | 7780 | 188500 | 24.23 | 0.10034 | 1.208 | 2.059 | 0.068 | 0.1536 | 3.062 | 0.81 | 23.26 | 1630 | 20 | 920 | 27 |

| | La | Ce | Pr | Nd | Sm | Eu | Gd | Tb | Dy | Ho | Y | Er | Tm | Yb | Lu |
|---|---|---|---|---|---|---|---|---|---|---|---|---|---|---|---|
| spot 1 | 34000 | 75700 | 9600 | 33200 | 7070 | 27 | 6140 | 717 | 3540 | 559 | 12400 | 717 | 39 | 70 | 9 |
| spot 2 | 34900 | 77300 | 9600 | 39600 | 7060 | 30 | 6460 | 688 | 3480 | 587 | 12700 | 698 | 33 | 84 | 10 |
| spot 3 | 31100 | 79500 | 9620 | 36300 | 7160 | 27 | 5950 | 705 | 3610 | 539 | 11990 | 744 | 37 | 81 | 9 |
| spot 4 | 34900 | 78000 | 10340 | 37600 | 8750 | 76 | 8380 | 930 | 4140 | 520 | 10400 | 613 | 23 | 46 | 4 |
| spot 5 | 36600 | 85100 | 10200 | 42100 | 7580 | 37 | 6490 | 707 | 3360 | 463 | 11000 | 690 | 32 | 77 | 9 |

**12TM3-01** xenotime (X27) (spot size: 7 µm, frequency: 3 Hz, 75 shot count, laser energy: 3 mJ at 75%)

| | | | | | ISOTOPIC RATIOS | | | | | | | | APPARENT AGES (Ma) | | | |
|---|---|---|---|---|---|---|---|---|---|---|---|---|---|---|---|---|
| | Pb (ppm) | U (ppm) | Th (ppm) | Th/U | $^{207}Pb/^{206}Pb$ | 2σ % | $^{207}Pb/^{235}U$ | 2σ % | $^{206}Pb/^{238}U$ | 2σ % | Rho | % disc.* | $^{207}Pb/^{206}Pb$ | 2σ abs | $^{206}Pb/^{238}U$ | 2σ abs |
| spot 1 | 582 | 4270 | 5760 | 1.35 | 0.09348 | 0.651 | 3.002 | 3.049 | 0.2350 | 2.979 | 0.98 | 3.46 | 1497 | 11 | 1358 | 36 |
| spot 2 | 461 | 3585 | 4550 | 1.27 | 0.09095 | 0.638 | 2.858 | 2.855 | 0.2300 | 2.783 | 0.97 | 2.40 | 1445 | 10 | 1336 | 33 |
| spot 3 | 477 | 3101 | 4930 | 1.59 | 0.09264 | 0.768 | 2.770 | 4.084 | 0.2219 | 4.011 | 0.98 | 5.12 | 1481 | 13 | 1290 | 47 |
| spot 4 | 438 | 3960 | 4500 | 1.14 | 0.09406 | 0.714 | 2.862 | 3.132 | 0.2230 | 3.049 | 0.97 | 5.31 | 1510 | 12 | 1300 | 37 |
| spot 5 | 456 | 3750 | 4520 | 1.21 | 0.09502 | 0.640 | 3.025 | 3.281 | 0.2331 | 3.218 | 0.98 | 4.82 | 1528 | 11 | 1348 | 39 |
| spot 6 | 527 | 4070 | 5190 | 1.28 | 0.09405 | 0.623 | 2.964 | 2.806 | 0.2303 | 2.736 | 0.98 | 4.65 | 1509 | 10 | 1334 | 33 |
| spot 7 | 8 | 930 | 370 | 0.40 | 0.05930 | 3.243 | 0.271 | 5.130 | 0.0327 | 3.976 | 0.77 | 17.28 | 551 | 73 | 207 | 8 |
| spot 8 | 11 | 1499 | 863 | 0.58 | 0.05030 | 3.024 | 0.179 | 4.635 | 0.0262 | 3.513 | 0.76 | 0.18 | 203 | 64 | 167 | 6 |

| | La | Ce | Pr | Nd | Sm | Eu | Gd | Tb | Dy | Ho | Y | Er | Tm | Yb | Lu |
|---|---|---|---|---|---|---|---|---|---|---|---|---|---|---|---|
| spot 1 | 34 | 249 | 104 | 1037 | 1200 | 23 | 4220 | 960 | 9700 | 2410 | 73500 | 5360 | 435 | 1410 | 229 |
| spot 2 | 33 | 306 | 114 | 1090 | 1076 | 28 | 4230 | 1010 | 10320 | 2410 | 80800 | 5340 | 446 | 1420 | 213 |
| spot 3 | 37 | 286 | 108 | 1130 | 1192 | 27 | 4180 | 970 | 10200 | 2200 | 77900 | 5310 | 431 | 1570 | 215 |
| spot 4 | 36 | 287 | 119 | 1262 | 1250 | 18 | 4890 | 1080 | 10220 | 2750 | 76600 | 6010 | 459 | 1580 | 207 |
| spot 5 | 35 | 295 | 116 | 1170 | 1250 | 26 | 4710 | 1020 | 10800 | 2590 | 87800 | 5600 | 530 | 1434 | 225 |
| spot 6 | 35 | 292 | 124 | 1190 | 1110 | 22 | 4130 | 1000 | 9670 | 2410 | 79800 | 5590 | 528 | 1510 | 221 |
| spot 7 | 1 | 32 | 40 | 758 | 1068 | 24 | 4480 | 997 | 9980 | 2450 | 76600 | 5290 | 515 | 1410 | 219 |
| spot 8 | 1 | 39 | 49 | 770 | 1160 | 22 | 3970 | 900 | 9000 | 2440 | 79000 | 4650 | 455 | 1270 | 175 |